EPA/635/R-09/011F www.epa.gov/iris

TOXICOLOGICAL REVIEW

OF

TRICHLOROETHYLENE

APPENDIX A

(CAS No. 79-01-6)

In Support of Summary Information on the Integrated Risk Information System (IRIS)

September 2011

A. PBPK MODELING OF TCE AND METABOLITES—DETAILED METHODS AND RESULTS

A.1. THE HIERARCHICAL BAYESIAN APPROACH TO CHARACTERIZING PBPK MODEL UNCERTAINTY AND VARIABILITY

The Bayesian approach for characterizing uncertainty and variability in PBPK model parameters, used previously for TCE in Bois (2000a, b) and Hack et al. (2006), is briefly described here as background. Once a PBPK model structure is specified, characterizing the model reduces to calibrating and making inferences about model parameters. The use of least-squares point estimators is limited by the large number of parameters and small amounts of data. The use of least-squares estimation is reported after imposing constraints for several parameters (Clewell et al., 2000; Fisher, 2000). This is reasonable for a first estimate, but it is important to follow-up with a more refined treatment. This is implemented by a Bayesian approach to estimate posterior distributions on the unknown parameters, a natural choice, and almost a compulsory consequence given the large number of parameters and relatively small amount of data, and given the difficulties of frequentist estimation in this setting.

As described by Gelman et al. (1996), the Bayesian approach to population PBPK modeling involves setting up the overall model in several stages. A nonlinear PBPK model, with predictions denoted *f*, describes the absorption, distribution, metabolism, and excretion of a compound and its metabolites in the body. This model depends on several, usually known, parameters such as measurement times *t*, exposure *E*, and measured covariates φ. Additionally, each subject *i* in a population has a set of unmeasured parameters θ_i. A random effects model describes their population variability $P(\theta_i \mid \mu, \Sigma^2)$, and a prior distribution $P(\mu, \Sigma^2)$ on the population mean μ and covariance Σ^2 (often assumed to be diagonal) incorporates existing scientific knowledge about them. Finally, a "measurement error" model $P(y \mid f[\theta, \varphi, E, t], \sigma^2)$ describes deviations (with variance σ^2) between the data *y* and model predictions *f* (which of course depends on the unmeasured parameters θ_i and the measured parameters *t*, *E*, and φ). This "measurement error" level of the hierarchical model typically also encompasses intrasubject variability as well as model misspecification, but for notational convenience we refer to it here as "measurement error." Because these other sources of variance are lumped into a single "measurement error," a prior distribution of its variance σ^2 must be specified even if the actual analytic measurement error is known. All of these components are illustrated graphically in Figure A-1.

EPA/635/R-09/011F www.epa.gov/iris

TOXICOLOGICAL REVIEW

OF

TRICHLOROETHYLENE

APPENDIX A

(CAS No. 79-01-6)

In Support of Summary Information on the Integrated Risk Information System (IRIS)

August 2011

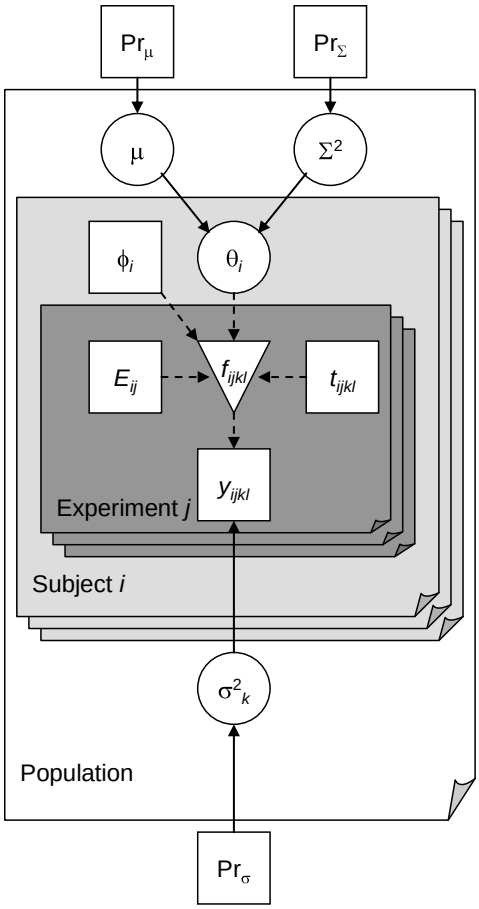

Square nodes denote fixed or observed quantities; circle notes represent uncertain or unobserved quantities, and the nonlinear model outputs are denoted by the inverted triangle. Solid arrows denote a stochastic relationship represented by a conditional distribution [$A \rightarrow B$ means $B \sim P(B|A)$], while dashed arrows represent a function relationship [$B = f(A)$]. The population consists of subjects i, each of which undergoes one or more experiments j with exposure parameters E_{ij} with data y_{ijkl} collected at times t_{ijkl}, where k denotes different types of outputs and l denotes the different time points. The PBPK model produces outputs f_{ijkl} for comparison with the data y_{ijkl}. The difference between them ("measurement error") has variance σ^2_k, with a fixed prior distribution Pr, which in this case is the same for the entire population. The PBPK model also depends on measured covariates ϕ_i (e.g., body weight) and unobserved model parameters θ_i (e.g., V_{MAX}). The parameters θ_i are drawn from a population with mean μ and variance Σ^2, each of which is uncertain and has a prior distribution assigned to it.

Source: Gelman et al. (1996).

Figure A-1. Hierarchical population statistical model for PBPK model parameter uncertainty and variability.

The posterior distribution for the unknown parameters is obtained in the usual manner by multiplying: (1) the prior distribution for the population mean and variance and the "measurement" error $P(\mu, \Sigma^2)\, P(\sigma^2)$; (2) the population distribution for the subject parameters $P(\theta \mid \mu, \Sigma^2)$; and (3) the likelihood $P(y \mid \theta, \sigma^2)$, where for notational convenience, the dependence on f, φ, E, and t (which are taken as fixed for a given data set) is dropped:

$$P(\theta, \mu, \Sigma^2, \sigma^2 \mid y) \propto P(\mu, \Sigma^2)\, P(\sigma^2)\, P(\theta \mid \mu, \Sigma^2)\, P(y \mid \theta, \sigma^2) \qquad \text{(Eq. A-1)}$$

Here, each subject's parameters θ_i have the same sampling distribution (i.e., they are independently and identically distributed), so their joint prior distribution is:

$$P(\theta \mid \mu, \Sigma^2) = \prod_{i=1\ldots n} P(\theta_i \mid \mu, \Sigma^2) \qquad \text{(Eq. A-2)}$$

Different experiments $j = 1\ldots n_j$ may have different exposure and different data collected and different time points. In addition, different types of measurements $k = 1\ldots n_k$ (e.g., TCE blood, TCE breath, TCA blood, etc.) may have different errors, but errors are otherwise assumed to be iid. Since the subjects are treated as independent given $\theta_{1\ldots n}$, the total likelihood function is simply

$$P(y \mid \theta, \sigma^2) = \prod_{I = 1\ldots n} \prod_{j = 1\ldots nij} \prod_{k = 1\ldots m} \prod_{l = 1\ldots Nijk} P(y_{ijkl} \mid \theta_i, \sigma_k^2, t_{ijkl}) \qquad \text{(Eq. A-3)}$$

where n is the number of subjects, n_{ij} is the number of experiments in that subject, m is the number of different types of measurements, N_{ijk} is the number (possibly 0) of measurements (e.g., time points) for subject i of type k in experiment j, and t_{ijkl} are the times at which measurements for subject i of type k were made in experiment j.

Given the large number of parameters, complex likelihood functions, and nonlinear PBPK model, Markov chain Monte Carlo (MCMC) simulation was used to generate samples from the posterior distribution. An important practical advantage of MCMC sampling is the ability to implement inference in nearly any probability model and the possibility to report inference on any event of interest. MCMC simulation was introduced by Gelfand and Smith (1990) as a generic tool for posterior inference. See Gilks et al. (1995) for a review. In addition, because many parameters are allowed to vary simultaneously, the local parameter sensitivity analyses often performed with PBPK models (in which the changes in model predictions are assessed with each parameter varied by a small amount) are unnecessary.[1] In the context of PBPK models, the MCMC simulation can be carried out as described by Hack et al. (2006). The

[1]In particular, local sensitivity analyses are typically used to assess the impact of alternative parameter estimates on model predictions, inform experimental design, or assist prioritizing risk assessment research. Only the first purpose is relevant here; however, the full uncertainty and variability analysis allows for a more comprehensive assessment than can be done with sensitivity analyses. Separately, such analyses could be done to design experiments and prioritize research that would be most likely to help reduce the remaining uncertainties in TCE toxicokinetics, but that is beyond the scope of this assessment.

simulation program MCSim (version 5.0.0) was used to implement MCMC posterior simulation, with analysis of the results performed using the *R* statistical package. Simulation-based parameter estimation with MCMC posterior simulation gives rise to an additional source of uncertainty. For instance, averages computed from the MCMC simulation output represent the desired posterior means only asymptotically, in the limit as the number of iterations goes to infinity. Any implementation needs to include a convergence diagnostic to judge practical convergence. The potential scale-reduction-factor convergence diagnostic *R* of Gelman et al. (1996) was used here, as it was in Hack et al. (2006).

A.2. EVALUATION OF THE HACK ET AL. (2006) PBPK MODEL

U.S. EPA obtained the original model code for the version of the TCE PBPK model published in Hack et al. (2006) and conducted a detailed evaluation of the model, focusing on the following areas: convergence, posterior estimates for model parameters, and comparison of model predictions with in vivo data.

A.2.1. Convergence

As noted in Hack et al. (2006), the diagnostics for the MCMC simulations (three chains of length 20,000–25,000 for each species) indicated that additional samples might further improve convergence. A recent analysis of tetrachloroethylene pharmacokinetics indicated the need to be especially careful in ensuring convergence (Chiu and Bois, 2007). Therefore, the number of MCMC samples per chain was increased to 75,000 for rats (first 25,000 discarded) and 175,000 for mice and humans (first 75,000 discarded). Using these chain lengths, the vast majority of the parameters had potential scale reduction factors $R \leq 1.01$, and all population parameters had $R \leq 1.05$, indicating that longer chains would be expected to reduce the SD (or other measure of scale, such as a CI) of the posterior distribution by less than this factor (Gelman et al., 2003).

In addition, analysis of autocorrelation within chains using the R-CODA package (Plummer et al., 2006) indicated that there was significant serial correlation, so additional "thinning" of the chains was performed in order to reduce serial correlations. In particular, for rats, for each of three chains, every 100th sample from the last 50,000 samples was used; and for mice and humans, for each of three chains, every 200th sample from the last 100,000 samples was used. This thinning resulted in a total of 1,500 samples for each species available for use for posterior inference.

Finally, an evaluation was made of the "convergence" of dose-metric predictions—that is, the extent to which the SD or CIs for these predictions would be reduced with additional samples. This is analogous to a "sensitivity analysis" performed so that most effort is spent on parameters that are most influential in the result. In this case, the purpose is to evaluate whether one can sample chains only long enough to ensure convergence of predictions of interest, even if

certain more poorly identified parameters take longer chains to converge. The motivation for this analysis is that for a more complex model, running chains until all parameters have $R \leq 1.01$ or 1.05 may be infeasible given the available time and resource. In addition, as some of the model parameters had prior distributions derived from "visual fitting" to the same data, replacing those distributions with less informative distributions (in order to reduce bias from "using the same data twice") may require even longer chains for convergence.

Indeed, it was found that *R*-values for dose-metric predictions approached one more quickly than PBPK model input parameters. The most informative simulations were for mice, which converged the slowest and, thus, had the most potential for convergence-related error. Results for rats could not be assessed because the model converged so rapidly, and results for humans were similar to those in mice, though the deviations were all less because of the more rapid convergence. In the mouse model, after 25,000 iterations, many PBPK model parameters had *R*-values >2, with >25% >1.2. However, all dose-metric predictions had $R < 1.4$, with the >96% of them <1.2 and the majority of them <1.01. In addition, when compared to the results of the last 100,000 iterations (after the total of 175,000 iterations), >90% of the medians estimates shifted by <20%, with the largest shifts <40% (for GSH metabolism dose-metrics, which had no relevant calibration data). Tail quantiles had somewhat larger shifts, which was expected given the limited number of samples in the tail, but still >90% of the 2.5 and 97.5 percentile quantiles had shifts of <40%. Again, the largest shifts, on the order of twofold, were for GSH-related dose-metrics that had high uncertainty, so the relative impact of limited sample size is small.

Therefore, the additional simulations performed in this evaluation, with three- to sevenfold longer chains, did not result in much change in risk assessment predictions from the original Hack et al. (2006) results. Thus, assessing prediction convergence appears sufficient for assessing convergence of the TCE PBPK model for the purposes of risk assessment prediction.

A.2.2. Evaluation of Posterior Distributions for Population Parameters

Posterior distributions for the population parameters were first checked for whether they appeared reasonable given the prior distributions. Inconsistency between the prior and posterior distributions may indicate an insufficiently broad prior distribution (i.e., overconfidence in their specification), a mis-specification of the model structure, or an error in the data. Parameters that were flagged for further investigation were those for which the interquartile ranges (intervals bounded by the 25^{th} and 75^{th} percentiles) of the prior and posterior distributions did not overlap. In addition, lumped metabolism and clearance parameters for TCA, TCOH, and TCOG were checked to make sure that they remained physiological—e.g., metabolic clearance was not more than hepatic blood flow and urinary clearance not more than kidney blood flow (constraints that were not present in the Hack et al. (2006) priors).

In mice, population mean parameters that had lack of overlap between priors and posteriors included the affinity of oxidative metabolism ($\ln K_M$), the TCA plasma-blood

concentration ratio (TCAPlas), the TCE stomach to duodenum transfer coefficient (lnKTSD), and the urinary excretion rates of TCA and TCOG (lnkUrnTCAC and lnkUrnTCOGC). For K_M, this is not unexpected, as previous investigators have noted inconsistency in the K_M values between in vitro values (upon which the prior distribution was based) and in vivo values derived from oral and inhalation exposures in mice (Greenberg et al., 1999; Abbas and Fisher, 1997). For the other mean parameters, the central estimates were based on visual fits, without any other a priori data, so it is reasonable to assume that the inconsistency is due to insufficiently broad prior distributions. In addition, the population variance for the TCE absorption coefficient from the duodenum (kAD) was rather large compared to the prior distribution, likely due to the fact that oral studies included TCE in both oil and aqueous solutions, which are known to have very different absorption properties. Thus, the larger population variance was required to accommodate both of them. Finally, the estimated clearance rate for glucuronidation of TCOH was substantially greater than hepatic blood flow. This is an artifact of the one-compartment model used for TCOH and TCOG, and suggests that first-pass effects are important for TCOH glucuronidation. Therefore, the model would benefit from the addition of a separate liver compartment so that first-pass effects can be accounted for, particularly when comparing across dose-routes.

In rats, the only population mean or variance parameter for which the posterior distribution was somewhat inconsistent with the prior distribution was the population mean for the lnK_M. While the interquartile regions did not overlap, the 95^{th} percentile regions did, so the discordance was relatively minor. However, as with mice, the estimated clearance rate for glucuronidation of TCOH was substantially greater than hepatic blood flow.

In humans, some of the chemical-specific parameters for which priors were established using visual fits had posterior distributions that were somewhat inconsistent, including the oxidative split between TCA and TCOH, biliary excretion of TCOG (lnkBileC), and the TCOH distribution volume (VBodC). More concerning was the fact that the posterior distributions for several physiological volumes and flows were rather strongly discordant with the priors and/or near their truncation limits, including gut, liver, and slowly perfused blood flow, the volumes of the liver and rapidly perfused compartments. In addition, a number of tissue partition coefficients were somewhat inconsistent with their priors, including those for TCE in the gut, rapidly perfused, and slowly perfused tissues, and TCA in the body and liver. Finally, a number of population variances (for TCOH clearance [lnClTCOHC], urinary excretion of TCOG [lnkUrnTCOGC], ventilation-perfusion ratio [lnVPRC], cardiac output [lnQCC], fat blood flow and volume [QFatC and VFatC], and TCE blood-air partition coefficient [PBC]) were somewhat high compared to their prior distributions, indicating much greater population variability than expected.

A.2.3. Comparison of Model Predictions With Data

A schematic of the comparisons between model predictions and data are shown in Figure A-2. In the hierarchical population model, subject-specific parameters were estimated for each data set used in calibrating the model (posterior subject-specific θ_i in Figure A-2). Because these parameters are in a sense "optimized" to the experimental data themselves, the subject-specific predictions (posterior subject-specific y_{ij} in Figure A-2) using these parameters should be accurate by design. Poor fits to the data using these subject-parameters may indicate a misspecification of the model structure, prior parameter distributions, or an error in the data. In addition, it is useful to generate "population-based" parameters (posterior population θ) using only the posterior distributions for the population means (μ) and variances (Σ^2), instead of the estimated subject-specific parameters. These population predictions provide a sense as to whether the model and the predicted degree of population uncertainty and variability adequately account for the range of heterogeneity in the experimental data. Furthermore, assuming the subject-specific predictions are accurate, the population-based predictions are useful to identify whether one or more if the data sets are "outliers" with respect to the predicted population. In addition, a substantial number of in vivo data sets was available in all three species that were not previously used for calibration. Thus, it is informative to compare the population-based model predictions, discussed above, to these additional "validation" data in order to assess the predictive power of the PBPK model.

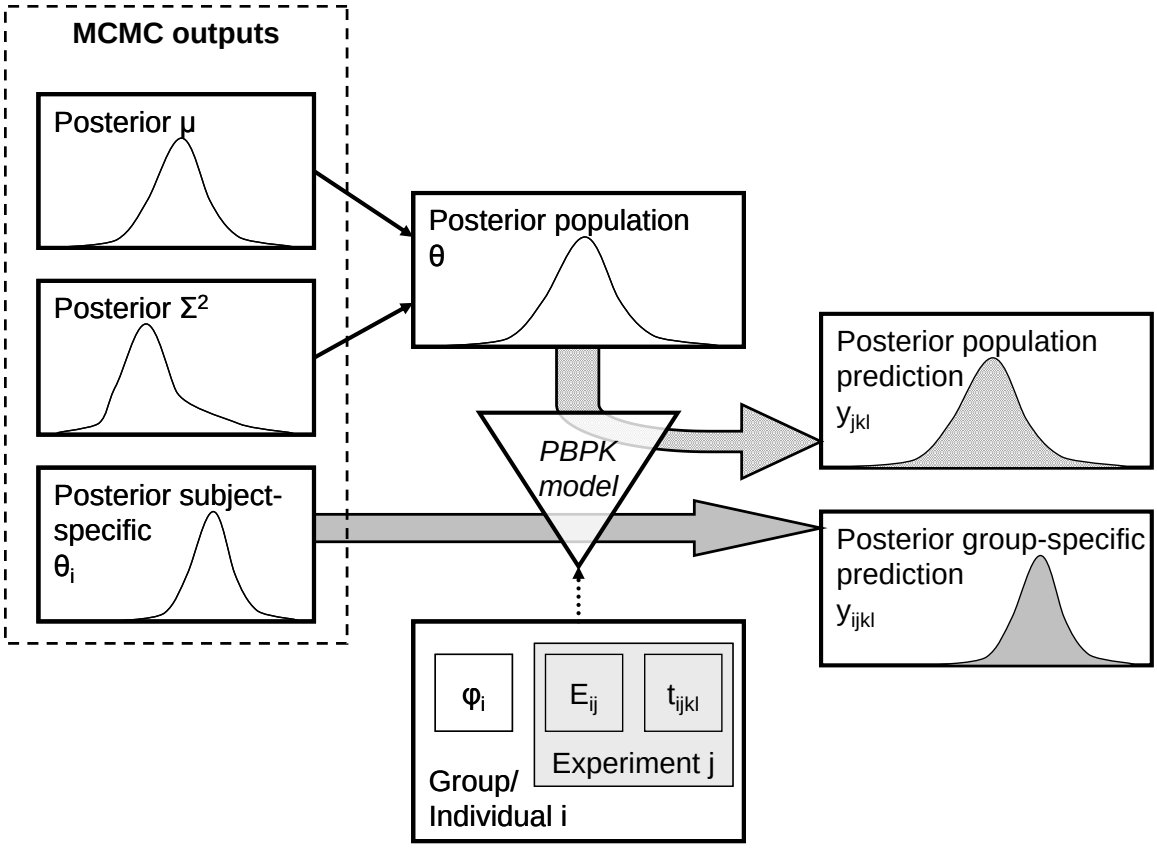

Two sets of posterior predictions were generated: population predictions (diagonal hashing) and subject-specific predictions (vertical hashing).

Figure A-2. Schematic of how posterior predictions were generated for comparison with experimental data.

A.2.3.1. Mouse Model

A.2.3.1.1. Subject-specific and population-based predictions

Initially, the sampled subject-specific parameters were used to generate predictions for comparison to the calibration data. Because these parameters were "optimized" for each subject, these "subject-specific" predictions should be accurate by design. However, unlike for the rat (see below), this was not the case for some experiments (this is partially responsible for the slower convergence). In particular, the predictions for TCE and TCOH concentrations for the Abbas and Fisher (1997) data were poor. In addition, TCE blood concentrations for the Greenberg et al. (1999) data were consistently overpredicted. These data are discussed further in Table A-1.

Table A-1. Evaluation of Hack et al. (2006) PBPK model predictions for in vivo data in mice

Reference	Simulation #	Calibration data	Discussion
Abbas et al. (1997)	41–42		These data are only published as an abstract. They consist of TCA and TCOH blood and urine data from TCA and TCOH i.v. dosing. Blood levels of TCA and TCOH are fairly accurately predicted. From TCOH dosing, urinary TCOG excretion is substantially overpredicted, and from TCA dosing, urinary TCA excretion is substantially overpredicted.
Abbas and Fisher (1997)	3–6	√	Results for these data were mixed. TCA levels were the best fit. The calibration data included TCA blood and liver data, which were well predicted except at the earliest time-point. In addition, TCA concentrations in the kidney were fairly consistent with the surrogate TCA body concentrations predicted by the model. Urinary TCA was well predicted at the lower two and highest doses, but somewhat underpredicted (though still in the 95% confidence region) at 1,200 mg/kg. TCE levels were in general not well fit. Calibration data included blood, fat, and liver concentrations, which were predicted poorly particularly at early and late times. One reason for this is probably the representation of oral uptake. Although both the current model and the original Abbas and Fisher (1997) model had two-compartments representing oral absorption, in the current model uptake can only occur from the second compartment. By contrast, the Abbas and Fisher (1997) model had uptake from both compartments, with the majority occurring from the first compartment. Thus, the explanation for the poor fit, particularly of blood and liver concentrations, at early times is probably simply due to differences in modeling oral uptake. This is also supported by the fact that the oral uptake parameters tended to be among those that took the longest to converge. Subject-specific blood TCOH predictions were poor, with underprediction at early times and overprediction at late times. Population-based blood TCOH predictions tended to be underpredicted, though generally within the 95% confidence region. Subject-specific urinary TCOG predictions were fairly accurate except at the highest dose. These predictions are also probably affected by the apparent misrepresentation of oral uptake. In addition, a problem as found in the calibration data in that data on free TCOH was calibrated against predictions of total TCOH (TCOH+TCOG). A number of TCOH and TCOG measurements were not included in the calibration—among them tissue concentrations of TCOH and tissue and blood concentrations of TCOG. Blood concentrations (the only available surrogate) were poor predictors of tissue concentrations of TCOH and TCOG (model generally underpredicted). For TCOG, this may be due in part to the model assumption that the distribution volume of TCOG is equal to that of TCOH.

Table A-1. Evaluation of Hack et al. (2006) PBPK model predictions for in vivo data in mice (continued)

Reference	Simulation #	Calibration data	Discussion
Fisher et al. (1991)	1–2 (open-chamber)	√	Venous blood TCE concentrations were somewhat underpredicted (a common issue with inhalation exposures in mice below) (Greenberg et al., 1999), but within the 95% confidence region of both subject-specific and population-based predictions. Plasma TCA levels were well predicted, with most of the data near the interquartile region of both subject-specific and population-based predictions (but with substantial scatter in the male mice). However, it should be noted that only a single exposure concentration for each sex was used in calibration, with six additional exposures (three for each sex) not included (see simulations 21–26, below).
	7–16 (closed-chamber)	√	Good posterior fits were obtained for these data—closed-chamber data with initial concentrations from 300 to 10,000 ppm. Some variability in V_{MAX}, however, was noted in the posterior distributions for that parameter. Using subject-specific V_{MAX} values resulted in better fits to these data. However, there appears to be a systematic trend of lower estimated apparent V_{MAX} at higher exposures. Similarly, posterior estimates of cardiac output and the ventilation-perfusion ratio declined (slightly) with higher exposures. These could be related to documented physiological changes (e.g., reduced ventilation rate and body temperature) in mice when exposed to some volatile organics.
	21–26 (open-chamber, additional exposures)		Data from three additional exposures for each sex were available for comparison to model predictions. Plasma TCA levels were generally well predicted, though the predictions for female mice data showed some systematic overprediction, particularly at late times (i.e., data showed shorter apparent half-life). Blood TCE concentrations were consistently overpredicted, sometimes by almost an order of magnitude, except in the case of female mice at 236 ppm, for which predictions were fairly accurate.
Fisher and Allen (1993)	31–36		Predictions for these gavage data were generally fairly accurate. There was a slight tendency to overpredict TCA plasma concentrations, with predictions tending to be worse in the female mice. Blood levels of TCE were adequately predicted, though there was some systematic underprediction at 2–6 hrs after dosing.
Green and Prout (1985)	40		This datum consists of a single measurement of urinary excretion of TCA at 24 hrs as a fraction of dose, from TCA i.v. dosing. The model substantially overpredicts the amount excreted. Whereas Green and Prout (1985) measured 35% excreted at 24 hrs, the model predicts virtually complete excretion at 24 hrs.
Greenberg et al. (1999)	17–18	√	The calibration data included blood TCE, TCOH, and TCA data. Fits to blood TCA and TCOH were adequate, but as with the Fisher et al. (1991) inhalation data, TCE levels were overpredicted (outside the 95% confidence region during and shortly after exposure). As with Abbas and Fisher (1997), there were additional data in the study that was not used in calibration, including blood levels of TCOG and tissue levels of TCE, TCA, TCOH, and TCOG. Tissue levels of TCE were somewhat overpredicted, but generally within the 95% confidence region. TCA levels were adequately predicted, and mostly in or near the interquartile region. TCOH levels were somewhat underpredicted, though within the 95% confidence region. TCOG levels, for which blood served as a surrogate for all tissues, were well predicted in blood and the lung, generally within the interquartile region. However, blood TCOG predictions underpredicted liver and kidney concentrations.

Table A-1. Evaluation of Hack et al. (2006) PBPK model predictions for in vivo data in mice (continued)

Reference	Simulation #	Calibration data	Discussion
Larson and Bull (1992a)	37–39		Blood TCA predictions were fairly accurate for these data. However, TCE and TCOH blood concentrations were underpredicted by up to an order of magnitude (outside the 95% confidence region). Part of this may be due to uncertain oral dosing parameters. Urinary TCA and TCOG were also generally underpredicted, in some cases outside of the 95% confidence region.
Prout et al. (1985)	19	√	Fits to these data were generally adequate—within or near the interquartile region.
	27–30 (urinary excretion at different doses)		These data consisted of mass balance studies of the amount excreted in urine and exhaled unchanged at doses from 10 to 2,000 mg/kg. TCA excretion was consistently overpredicted, except at the highest dose. TCOG excretion was generally well predicted—within the interquartile range. The amount exhaled was somewhat overpredicted, with a fourfold difference (but still within 95% confidence) at the highest dose.
Templin et al. (1993)	20	√	Blood TCA levels from these data were well predicted by the model. Blood TCE and TCOH levels were well predicted using subject-specific parameters, but did not appear representative using population-derived parameters. However, this is probably a result of the subject-specific oral absorption parameter, which was substantially different than the population mean.

Next, only samples of the population parameters (means and variances) were used, and "new subjects" were sampled from appropriate distributions using these population means and variances. These "new subjects" then represent the predicted population distribution, incorporating both variability in the population as well as uncertainty in the population means and variances. These "population-based" predictions were then compared to both the data used in calibration, as well as the additional data identified that was not used in calibration. The PBPK model was modified to accommodate some of the different outputs (e.g., tissue concentrations) and exposure routes (TCE, TCA, and TCOH i.v.) used in the "noncalibration" data, but otherwise it is unchanged.

A.2.3.1.1.1. Subject-specific predictions and calibration data

(See "Supplementary data for TCE assessment: Hack mouse subject calibration," 2011)

A.2.3.1.1.2. Population-based predictions and calibration and additional evaluation data

(See "Supplementary data for TCE assessment: Hack mouse population calibration evaluation," 2011)

A.2.3.1.2. Conclusions regarding mouse model

A.2.3.1.2.1. TCE concentrations in blood and tissues not well-predicted

The PBPK model for the parent compound does not appear to be robust. Even subject-specific fits to data sets used for calibration were not always accurate. For oral dosing data, there is clearly high variability in oral uptake parameters, and the addition of uptake through the first (stomach) compartment should improve the fit. Unfortunately, inaccurate TCE uptake parameters may lead to inaccurately estimated kinetic parameters for metabolites, TCA and TCOH, even if current fits are adequate.

The TCE data from inhalation experiments also are not well estimated, particularly blood levels of TCE. While fractional uptake has been hypothesized, direct evidence for this is lacking. In addition, physiologic responses to TCE vapors (reduced ventilation rates, lowered body temperature) are a possibility. These are weakly supported by the closed-chamber data, but the amount of the changes is not sufficient to account for the low blood levels of TCE observed in the open-chamber experiments. It is also not clear what role presystemic elimination due to local metabolism in the lung may play. It is known that the mouse lung has a high capacity to metabolize TCE (Green et al., 1997b). However, in the Hack et al. (2006) model, lung metabolism is limited by flow to the tracheobronchial region. An alternative formulation for lung metabolism in which TCE is available for metabolism directly from inhaled air (similar to that used for styrene) (Sarangapani et al., 2003), may allow for greater presystemic elimination of TCE, as well as for evaluating the possibility of wash-in/wash-out effects. Furthermore, the potential impact of other extrahepatic metabolism has not been evaluated. Curiously, predictions

for the tissue concentrations of TCE observed by Greenberg et al. (1999) were not as discrepant as those for blood. A number of these hypotheses could be tested; however, the existing data may not be sufficient to distinguish them. The Merdink et al. (1998) study, in which TCE was given by i.v. (thereby avoiding both first-pass in the liver and any fractional uptake issue in the lung), may be somewhat helpful, but unfortunately only oxidative metabolite concentrations were reported, not TCE concentrations.

A.2.3.1.2.2. TCA blood concentrations well predicted following TCE exposures, but TCA flux and disposition may not be accurate

TCA blood and plasma concentrations following TCE exposure are consistently well predicted. However, the total flux of TCA may not be correct, as evidenced by the varying degrees of consistency with urinary excretion data. Of particular importance are TCA dosing studies, none of which were included in the calibration. In these studies, total recovery of urinary TCA was found to be substantially less than the administered dose. However, the current model assumes that urinary excretion is the only source of clearance of TCA, leading to overestimation of urinary excretion. This fact, combined with the observation that under TCE dosing, the model appears to give accurate predictions of TCA urinary excretion for several data sets, strongly suggests a discrepancy in the amount of TCA formed from TCE. That is, since the model appears to overpredict the fraction of TCA that appears in urine, it may be reducing TCA production to compensate. Inclusion of the TCA dosing studies (including some oral dosing studies), along with inclusion of a nonrenal clearance pathway, would probably be helpful in reducing these discrepancies. Finally, improvements in the TCOH/TCOG submodel, below, should also help to ensure accurate estimates of TCA kinetics.

A.2.3.1.2.3. TCOH/TCOG submodel requires revision and recalibration

Blood levels of TCOH and TCOG were inconsistently predicted. Part of this is due to the problems with oral uptake, as discussed above. In addition, the problems identified with the use of the Abbas and Fisher (1997) data (i.e., free TCOH vs. total TCOH), mean that this submodel is not likely to be robust.

An additional concern is the overprediction of urinary TCOG from the Abbas et al. (1997) TCOH i.v. data. Like the case of TCA, this indicates that some other source of TCOH clearance (not to TCA or urine—e.g., to DCA or some other untracked metabolite) is possible. This pathway can be considered for inclusion, and limits can be placed on it using the available data.

Also, like for TCA, the fact that blood and urine are relatively well predicted from TCE dosing strongly suggests a discrepancy in the amount of TCOH formed from TCE. That is, since the model appears to overpredict the fraction of TCOH that appears in urine, it may be reducing

TCOH production to compensate. Including the TCOH dosing data would likely be helpful in reducing these discrepancies.

Finally, as with the rat, the model needs to ensure that any first-pass effect is accounted for appropriately. Importantly, the estimated clearance rate for glucuronidation of TCOH is substantially greater than hepatic blood flow. As was shown in Okino et al. (2005), in such a situation, the use of a single compartment model across dose routes will be misleading because it implies a substantial first-pass effect in the liver that cannot be modeled in a single compartment model. That is, since TCOH is formed in the liver from TCE, and TCOH is also glucuronidated in the liver to TCOG, a substantial portion of the TCOH may be glucuronidated before reaching systemic circulation. This suggests that a liver compartment for TCOH is necessary. Furthermore, because substantial TCOG can be excreted in bile from the liver prior to systemic circulation, a liver compartment for TCOG may also be necessary to address that first-pass effect.

The addition of the liver compartment will necessitate several changes to model parameters. The distribution volume for TCOH will be replaced by two parameters: the liver:blood and body:blood partition coefficients. Similarly for TCOG, liver:blood and body:blood partition coefficients will need to be added. Clearance of TCOH to TCA and TCOG can be redefined as occurring in the liver, and urinary clearance can be redefined as coming from the rest of the body. Fortunately, there are substantial data on circulating TCOG that has not been included in the calibration. These data should be extremely informative in better estimating the TCOH/TCOG submodel parameters.

A.2.3.1.2.4. Uncertainty in estimates of total metabolism

Closed-chamber data are generally thought to provide a good indicator of total metabolism. Both subject-specific and population-based predictions of the only available closed-chamber data (Fisher et al., 1991) were fairly accurate. Unfortunately, no additional closed-chamber data were available. In addition, the discrepancies in observed and predicted TCE blood concentrations following inhalation exposures remain unresolved. Hypothesized explanations such as fractional uptake or presystemic elimination could have a substantial impact on estimates of total metabolism.

In addition, no data are directly informative as to the fraction of total metabolism in the lung, the amount of "untracked" hepatic oxidative metabolism (parameterized as "FracDCA"), or any other extrahepatic metabolism. The lung metabolism as currently modeled could just as well be located in other extrahepatic tissues, with little change in calibration. In addition, it is difficult to distinguish between untracked hepatic oxidative metabolism and GSH conjugation, particularly at low doses.

A.2.3.2. Rat Model

A.2.3.2.1. Subject-specific and population-based predictions

As with the mouse mode, initially, the sampled subject-specific parameters were used to generate predictions for comparison to the calibration data. Because these parameters were "optimized" for each subject, these "subject-specific" predictions should be accurate by design, and indeed they were, as discussed in more detail in Table A-2.

Next, as with the mouse, only samples of the population parameters (means and variances) were used, and "new subjects" were sampled from appropriate distribution using these population means and variances. These "new subjects" then represent the predicted population distribution, incorporating both variability in the population as well as uncertainty in the population means and variances. These "population-based" predictions were then compared to both the data used in calibration, as well as the additional data identified that were not used in calibration. The Hack et al. (2006) PBPK model used for prediction was modified to accommodate some of the different outputs (e.g., tissue concentrations) and exposure routes (i.v., i.a., and p.v.) used in the "noncalibration" data, but otherwise unchanged.

Table A-2. Evaluation of Hack et al. (2006) PBPK model predictions for in vivo data in rats

Reference	Simulation #	Calibration data	Discussion
Andersen et al. (1987b)	7–11	√	Good posterior fits were obtained for these data—closed-chamber data with initial concentrations of 100–4,640 ppm.
Barton et al. (1995)	17–20		It was assumed that the closed-chamber volume was the same as for Andersen et al. (1987b). However, the initial chamber concentrations are not clear in the paper. The values that were used in the simulations do not appear to be correct, since in many cases the time-course is inaccurately predicted even at the earliest time-points. Conclusions as to these data need to await definitive values for the initial chamber concentrations, which were not available.
Bernauer et al. (1996)	1–3	√	Urinary time-course data (see Figure 6-7) for TCA, TCOG, and NAcDCVC was given in concentration units (mg/mg creat-hr), whereas total excretion at 48 hrs (see Table 2) was given in molar units (mmol excreted). In the original calibration files, the conversion from concentration to cumulative excretion was not consistent (i.e., the amount excreted at 48 hrs was different). The data were revised using a conversion that forced consistency. One concern, however, is that this conversion amounts to 6.2 mg creatinine over 48 hrs, or 1.14 micromol/hr. This seems very low for rats; Trevisan et al. (2001), in samples from 195 male control rats, found a median value of 4.95 micromol/hr, a mean of 5.39 micromol/hr, and a 1–99th percentile range of 2.56–10.46 micromol/hr. In addition, the NAcDCVC data were revised in include both 1,2- and 2,2-isomers, since the goal of the GSH pathway is primarily to constrain the total flux. Furthermore, because of the extensive interorgan processing of GSH conjugates, and the fact that excretion was still ongoing at the end of the study (48 hrs), the amount of NAcDCVC recovered can only be a lower bound on the amount ultimately excreted in urine. However, the model does not attempt to represent the excretion time-course of GSH conjugates—it merely models the total flux. This is evinced by the fact that the model predicts complete excretion by the first time point of 12 hrs, whereas in the data, there is still substantial excretion occurring at 48 hrs. Posterior fits to these data were poor in all cases except urinary TCA at the highest dose. In all other cases, TCOH/TCOG and TCA excretion was substantially overpredicted, though this is due to the revision of the data (i.e., the different assumptions about creatinine excretion). Unfortunately, of the original calibration data, this is the only one with TCA and TCOH/TCOG urinary excretion. Therefore, that part of the model is poorly calibrated. On the other hand, NAcDCVC was underpredicted for a number of reasons, as noted above. Because of the incomplete capture of NAcDCVC in urine, unless the model can accurately portray the time-course of NAcDCVC in urine, it should probably not be used for calibration of the GSH pathway, except perhaps as a lower bound.

Table A-2. Evaluation of Hack et al. (2006) PBPK model predictions for in vivo data in rats (continued)

Reference	Simulation #	Calibration data	Discussion
Birner et al. (1993)	21–22		These data only showed urine concentrations, so a conversion was made to cumulative excretion based on an assumed urine flow rate of 22.5 mL/d. Based on this, urinary NAcDCVC was underestimated by 100- to 1,000-fold. Urinary TCA was underestimated by about twofold in females (barely within the 95% CI), and was accurately estimated in males. Note that data on urinary flow rate from Trevisan et al. (2001) in samples from 195 male control rats showed high variability, with a GSD of 1.75, so this may explain the discrepancy in urinary TCA. However, the underestimation of urinary NAcDCVC cannot be explained this way.
Dallas et al. (1991)	23–24		At the lower (50 ppm) exposure, arterial blood concentrations were consistently overpredicted by about 2.5-fold, while at the higher (500 ppm) exposure, arterial blood was overpredicted by 1.5–2-fold, but within the range of variability. Exhaled breath concentrations were in the middle of the predicted range of variability at both exposure levels. The ratio of exhaled breath and arterial blood should depend largely on the blood-air partition coefficient, with minor dependence on the assumed dead space. This suggests the possibility of some unaccounted-for variability in the partition coefficient (e.g., posterior mean estimated to be 15.7; in vitro measured values from the literature are as follows: 25.82 (Sato et al., 1977), 21.9 (Gargas et al., 1989), 25.8 (Koizumi, 1989), 13.2 (Fisher et al., 1989), posterior). Alternatively, there may be a systematic error in these data, since, as discussed below, the fit of the model to the arterial blood data of Keys et al. (2003) was highly accurate.
Fisher et al. (1989)	25–28		Good posterior fits were obtained for these data (in females)—closed-chamber data with initial concentrations from 300 to 5,100 ppm. There was some slight overprediction of chamber concentrations (i.e., data showed more uptake/metabolism) at the lower doses, but still within the 95% CI.
Fisher et al. (1991)	4–6	√	Good posterior fits were obtained from these data—plasma levels of TCA and venous blood levels of TCE.
Green and Prout (1985)	29–30		In naive rats at 500 mg/kg, urinary excretion of TCOH/TCOG and TCA at 24 hrs was underpredicted (twofold), although within the 95% CI. With bile-cannulated rats at the same dose, the amount of TCOG in bile was well within the 95% CI. Urinary TCOH/TCOG was still underpredicted by about twofold, but again still within the 95% CI.
Jakobson et al. (1986)	31		The only data from the experiment (500 ppm in female rats) were venous blood concentrations during exposure. There were somewhat overpredicted at early times (outside of 95% CI for first 30 min) but was well predicted at the termination of exposure. This suggests some discrepancies in uptake to tissues that reach equilibrium quickly—the model approaches the peak concentration at a faster rate than the data suggest.

Table A-2. Evaluation of Hack et al. (2006) PBPK model predictions for in vivo data in rats (continued)

Reference	Simulation #	Calibration data	Discussion
Kaneko et al. (1994)	32–35		In these inhalation experiments (50–1,000 ppm), urinary excretion of TCOH/TCOG and TCA are consistently overpredicted, particularly at lower doses. The discrepancy decreases systematically as dose increases, with TCA excretion accurately predicted at 1,000 ppm (TCOH/TCOG excretion slightly below near the lower 95% CI at this dose). This suggests a discrepancy in the dose-dependence of TCOH, TCOG, and TCA formation and excretion. On the other hand, venous blood TCE concentrations postexposure are well predicted. TCE blood concentrations right at the end of the exposure are overpredicted; however, concentrations are rapidly declining at this point, so even a few minutes delay in obtaining the blood sample could explain the discrepancy.
Keys et al. (2003)	36–39		These experiments collected extensive data on TCE in blood and tissues following i.a., oral, and inhalation exposures. For the i.a. exposure, blood and tissue concentrations were very well predicted by the model, even with the use of the rapidly perfused tissue concentration as a surrogate for brain, heart, kidney, liver, lung, and spleen concentrations. Similarly accurate predictions were found with the higher (500 ppm) inhalation exposure. At the lower inhalation exposure (50 ppm), there was some minor overprediction of concentrations (twofold), particularly in fat, but values were still within the 95% CIs. For oral exposure, the GI absorption parameters needed to be revised substantially to obtain a good fit. When the values reported by Keys et al. (2003) were used, the model generally had accurate predictions. Two exceptions were the values in the gut and fat in the first 30 min after exposure. In addition, the liver concentration was overpredicted in the first 30 min, and underpredicted at 2–4 hrs, but still within the 95% CI during the entire period.
Kimmerle and Eben (1973b)	40–44		In these inhalation experiments (49–3,160 ppm), urinary excretion of TCOH/TCOG was systematically overpredicted (>twofold; outside 95% CI), while excretion of TCA was accurately predicted. In addition, elimination by exhaled breath was substantially overpredicted at the lowest exposure. Blood TCOH levels were accurately predicted, but blood TCE levels were overpredicted at the 55 ppm. Part of the discrepancies may be due to limited analytic sensitivities at the lower exposures.
Larson and Bull (1992a)	12–14	√	The digitization in the calibration file did not appear to be accurate, as there was a 10-fold discrepancy with the original paper in the TCOH data. The data were replaced this those used by Clewell et al. (2000) and Bois (2000b). Except for the TCOH data, differences between the digitizations were ≤20%. Adequate posterior predictions were obtained for these data (oral dosing from 200 to 3,000 mg/kg). All predictions were within the 95% CI of posterior predictions. Better fits were obtained using subject-specific posterior parameters, for which gut absorption and TCA urinary excretion parameters were more highly identified.

Table A-2. Evaluation of Hack et al. (2006) PBPK model predictions for in vivo data in rats (continued)

Reference	Simulation #	Calibration data	Discussion
Lash et al. (2006)	45–46		In these corn-oil gavage experiments, almost all of the measurements appeared to be systematically low, sometimes by many orders of magnitude. For example, at the lowest dose (263 mg/kg), urinary excretion of TCOH/TCOG and TCA, and blood concentrations of TCOH were overpredicted by the model by around $>10^5$-fold. TCE concentrations in blood and tissues at 2, 4, and 8 hrs were underpredicted by 10^3- to 10^4-fold. Many studies, including those using the corn oil gavage (Hissink et al., 2002; Green and Prout, 1985), with similar ranges of oral doses show good agreement with the model, it seems likely that these data are aberrant.
Lee et al. (1996)	47–61		This extensive set of experiments involved multiroute administration of TCE (oral, i.v., i.a., or portal vein), with serial measurements of arterial blood concentrations. For the oral route (8–64 mg/kg), the GI absorption parameters had to be modified. The values from Keys et al. (2003) were used, and the resulting predictions were quite accurate, albeit a more prominent peak was predicted. Predictions >30 min after dosing were highly accurate. For the i.v. route (0.71–64 mg/kg), predictions were also highly accurate in almost all cases. At the lower doses (0.71 and 2 mg/kg), there was slight overprediction in the first 30 min after dosing. At highest dose (64 mg/kg), there was slight underprediction between 1 and 2 hrs after dosing. In all cases, the values were within the 95% CI. For the i.a. route (0.71–16 mg/kg), all predictions were very accurate. For the p.v. route (0.7–64 mg/kg), predictions still remained in the 95% CI, although there was more variation. At the lowest dose, there was overprediction in the first 30 min after dosing. At the highest two doses (16 and 64 mg/kg), there was slight underprediction between 1 and 5 hrs after dosing. This may in part be because a pharmacodynamic change in metabolism (e.g., via direct solvent injury proposed by Lee et al., 2000a).
Lee et al. (2000a)	62–69		In the p.v. and i.v. exposures, blood and liver concentrations were accurately predicted. For oral exposures, the GI absorption parameters needed to be changed. While the values from Keys et al. (2003) led to accurate predictions for lower doses (2–16 mg/kg), at the higher doses (48–432 mg/kg), much slower absorption was evident. Comparisons at these higher dose are not meaningful without calibration of absorption parameters.
Prout et al. (1985)	15	√	Adequate posterior fits were obtained for these data—rat dosing at 1,000 mg/kg in corn oil. All predictions were within the 95% CI of posterior predictions. Better fits were obtained using subject-specific posterior parameters, for which gut absorption and TCA urinary excretion parameters were more highly identified.
Stenner et al. (1997)	70		As with other oral exposures, different GI absorption parameters were necessary. Again, the values from Keys et al. (2003) were used, with some success. Blood TCA levels were accurately predicted, while TCOH blood levels were systematically underpredicted (up to 10-fold). Additional data with TCOH and TCA dosing, including naive and bile-cannulated rats, can be added when those exposure routes are added to the model. These could be useful in better calibrating the enterohepatic recirculation parameters.

Table A-2. Evaluation of Hack et al. (2006) PBPK model predictions for in vivo data in rats (continued)

Reference	Simulation #	Calibration data	Discussion
Templin et al. (1995b)	16	√	Adequate posterior fits were obtained for blood TCA from these data—oral dosing at 100 mg/kg in Tween. Blood levels of TCOH were underpredicted, while the time-course of TCE in blood exhibited an earlier peak. Better fits were obtained using subject-specific posterior parameters, for which gut absorption and TCA urinary excretion parameters (and to a lesser extent glucuronidation of TCOH and biliary excretion of TCOG) were more highly identified.

NAc-1,2-DCVC = N-acetyl-S-(1,2-dichlrovinyl)-L-cysteine; NAc-2,2-DCVC = N-acetyl-S-(2,2-dichlrovinyl)-L-cysteine; NAcDCVC = NAc-1,2-DCVC and NAc-2,2-DCVC.

A.2.3.2.1.1. Subject-specific predictions and calibration data

(See "Supplementary data for TCE assessment: Hack mouse subject calibration," 2011)

A.2.3.2.1.2. Population-based predictions and calibration and additional evaluation data

(See "Supplementary data for TCE assessment: Hack mouse subject calibration," 2011)

A.2.3.2.2. Conclusions regarding rat model

A.2.3.2.2.1. TCE concentrations in blood and tissues generally well-predicted

The PBPK model for the parent compound appears to be robust. Multiple data sets not used for calibration with TCE measurements in blood and tissues were simulated, and overall the model gave very accurate predictions. A few data sets seemed somewhat anomalous—Dallas et al. (1991), Kimmerle and Eben (1973b), and Lash et al. (2006). However, data from Kaneko et al. (1994), Keys et al. (2003), and Lee et al. (2000a; 1996) were all well simulated, and corroborated the data used for calibration (Templin et al., 1995b; Larson and Bull, 1992a; Fisher et al., 1991; Prout et al., 1985). Particularly important is the fact that tissue concentrations from Keys et al. (2003) were well simulated.

A.2.3.2.2.2. Total metabolism probably well simulated, but ultimate disposition is less certain

Closed-chamber data are generally thought to provide a good indicator of total metabolism. Two closed-chamber studies not used for calibration were available—Barton et al. (1995) and Fisher et al. (1989). Additional experimental information is required to analyze the Barton et al. (1995) data, but the predictions for the Fisher et al. (1989) data were quite accurate.

However, the ultimate disposition of metabolized TCE is much less certain. Clearly, the flux through the GSH pathway is not well constrained, with apparent discrepancies between the N-acetyl-S-(1,2-dichlorovinyl)-L-cysteine (NAc-1,2-DCVC) data of Bernauer et al. (1996) and Birner et al. (1993). Moreover, each of these data has limitations—in particular, the Bernauer et al. (1996) data show that excretion is still substantial at the end of the reporting period, so that the total flux of mercapturates has not been collected. Moreover, there is some question as to the consistency of the Bernauer et al. (1996) data (see Table 2 vs. Figures 6 and 7), since a direct comparison seems to imply a very low creatinine excretion rate. The Birner et al. (1993) data only report concentrations—not total excretion—so a urinary flow rate needs to be assumed.

In addition, no data are directly informative as to the fraction of total metabolism in the lung or the amount of "untracked" hepatic oxidative metabolism (parameterized as "FracDCA"). The lung metabolism could just as well be located in other extrahepatic tissues, with little change in calibration. In addition, there is a degeneracy between untracked hepatic oxidative metabolism and GSH conjugation, particularly at low doses.

The ultimate disposition of TCE as excreted TCOH/TCOG or TCA is also poorly estimated in some cases, as discussed in more detail below.

A.2.3.2.2.3. TCOH/TCOG submodel requires revision and recalibration

TCOH blood levels of TCOH were inconsistently predicted in noncalibration data sets (well predicted for Larson and Bull (1992a); Kimmerle and Eben (1973b); but not Stenner et al. (1997)] or Lash et al. (2006), and the amount of TCE ultimately excreted as TCOG/TCOH also appeared to be poorly predicted. The model generally underpredicted TCOG/TCOH urinary excretion (underpredicted Green and Prout (1985), overpredicted Kaneko et al. (1994), Kimmerle and Eben (1973b), and Lash et al. (2006)). This may in part be due to discrepancies in the Bernauer et al. (1996) data as to the conversion of excretion relative to creatinine.

Moreover, there are relatively sparse data on TCOH in combination with a relatively complex model, so the identifiability of various pathways—conversion to TCA, enterohepatic recirculation, and excretion in urine—is questionable.

This could be improved by the ability to incorporate TCOH dosing data from Merdink et al. (1999) and Stenner et al. (1997), the latter of which included bile duct cannulation to better estimate enterohepatic recirculation parameters. However, the TCOH dosing in these studies is by the i.v. route, whereas with TCE dosing, TCOH first appears in the liver. Thus, the model needs to ensure that any first-pass effect is accounted for appropriately. Importantly, the estimated clearance rate for glucuronidation of TCOH is substantially greater than hepatic blood flow. That is, since TCOH is formed in the liver from TCE, and TCOH is also glucuronidated in the liver to TCOG, a substantial portion of the TCOH may be glucuronidated before reaching systemic circulation. Thus, suggests that a liver compartment for TCOH is necessary. Furthermore, because substantial TCOG can be excreted in bile from the liver prior to systemic circulation, a liver compartment for TCOG may also be necessary to address that first-pass effect.

The addition of the liver compartment will necessitate several changes to model parameters. The distribution volume for TCOH will be replaced by two parameters: the liver:blood and body:blood partition coefficients. Similarly for TCOG, liver:blood and body:blood partition coefficients will need to be added. Clearance of TCOH to TCA and TCOG can be redefined as occurring in the liver, and urinary clearance can be redefined as coming from the rest of the body.

Finally, additional clearance of TCOH (not to TCA or urine—e.g., to DCA or some other untracked metabolite) is possible. This may in part explain the discrepancy between the accurate predictions to blood data along with poor predictions to urinary excretion (i.e., there is a missing pathway). This pathway can be considered for inclusion, and limits can be placed on it using the available data.

A.2.3.2.2.4. TCA submodel would benefit from revised submodel and incorporating TCA dosing studies

While blood levels of TCA were well predicted in the one noncalibration data set (Stenner et al., 1997), the urinary excretion of TCA was inconsistently predicted (underpredicted in Green and Prout (1985); overpredicted in Kaneko et al. (1994) and Lash et al. (2006); accurately predicted in Kimmerle and Eben (1973b)]). Because TCA is, in part, derived from TCOH, a more accurate TCOH/TCOG submodel would probably improve the TCA submodel.

In addition, there are a number of TCA dosing studies that could be used to isolate the TCA kinetics from the complexities of TCE and TCOH. These could be readily incorporated into the TCA submodel.

Finally, as with TCOH, additional clearance of TCA (not to urine—e.g., to DCA or some other untracked metabolite) is possible. This may in part explain the discrepancy between the accurate predictions to blood data along with poor predictions to urinary excretion (i.e., there is a missing pathway). As with TCOH, this pathway can be considered for inclusion, and limits can be placed on it using the available data.

A.2.3.3. Human Model

A.2.3.3.1. Subject-specific and population-based predictions

As with the mouse and rat models, initially, the sampled subject-specific parameters were used to generate predictions for comparison to the calibration data. Because these parameters were "optimized" for each subject, these "subject-specific" predictions should be accurate by design. However, unlike for the rat, this was not the case for some experiments (this is partially responsible for the slower convergence), although the inaccuracies were generally less than those in the mouse. For example, alveolar air concentrations were systematically overpredicted for several data sets. There was also variability in the ability to predict the precise time-course of TCA and TCOH blood levels, with a few data sets more difficult for the model to accommodate. These data are discussed further in Table A-3. Next, only samples of the population parameters (means and variances) were used, and "new subjects" were sampled from appropriate distribution using these population means and variances. These "new subjects" then represent the predicted population distribution, incorporating both variability as well as uncertainty in the population means and variances. These "population-based" predictions were then compared to both the data used in calibration, as well as the additional data identified that was not used in calibration. The Hack et al. (2006) PBPK model was modified to accommodate some of the different outputs (e.g., arterial blood, intermittently collected urine, retained dose) and exposure routes (TCA i.v., oral TCA, and TCOH) used in the "noncalibration" data, but otherwise unchanged.

Table A-3. Evaluation of Hack et al. (2006) PBPK model predictions for in vivo data in humans

Reference	Simulation number	Calibration data	Discussion
Bartonicek (1962)	38–45		The measured minute-volume was multiplied by a factor of 0.7 to obtain an estimate for alveolar ventilation rate, which was fixed for each subject. These data are difficult to interpret because they consist of many single data points. It is easiest to go through the measurements one at a time: *Alveolar retention* (1—exhaled dose/inhaled dose during exposure) and *Retained dose* (inhaled dose—exhaled dose during exposure): Curiously, retention was generally underpredicted, which in many cases retained dose was accurately predicted. However, alveolar retention was an adjustment of the observed total retention: TotRet = (CInh – CExh)/CInh = QAlv × (CInh – CAlv)/(MV × CInh), so that AlvRet = TotRet × (QAlv/MV), with QAlv/MV assumed to be 0.7. Because retained dose is the more relevant quantity, and is less sensitive to assumptions about QAlv/MV, then this is the better quantity to use for calibration. *Urinary TCOG*: This was generally underpredicted, although generally within the 95% CI. Thus, these data will be informative as to intersubject variability. *Urinary TCA*: Total collection (at 528 hrs) was accurately predicted, although the amount collected at 72 hrs was generally underpredicted, sometimes substantially so. *Plasma TCA*: Generally well predicted.
Bernauer et al. (1996)	1–3	√	Subject-specific predictions were good for the time-courses of urinary TCOG and TCA, but poor for total urinary TCOG+TCA and for urinary NAc-1,2-DCVC. One reason for the discrepancy in urinary excretion of TCA and TCOG is that the urinary time-course data (see Figures 4-5 in the manuscript) for TCA, TCOG, and NAc-1,2-DCVC was given in concentration units (mg/mg creat-hr), whereas total excretion at 48 hrs (see Table 2 in the manuscript) was given in molar units (mmol excreted). In the original calibration files, the conversion from concentration to cumulative excretion was not consistent (i.e., the amount excreted at 48 hrs was different). For population-based predictions, the data were revised using a conversion that forced consistency. One concern, however, is that this conversion amounts to 400–500 mg creatinine over 48 hrs, or 200–250 mg/d, which seems rather low. For instance, Araki (1978) reported creatinine excretion of 11.5 ± 1.8 mmol/24 hrs (mean ± SD) in nine subjects, corresponding to 1,300 ± 200 mg/d. In addition, for population-based predictions, the data were revised include both the NAc-1,2-DCVC and the N acetyl-S-(2,2-dichlorovinyl)-L-cysteine isomer (the combination denoted NAcDCVC), since the goal of the GSH pathway is primarily to constrain the total flux. Furthermore, because of the extensive interorgan processing of GSH conjugates, and the fact that excretion was still ongoing at the end of the study (48 hrs), the amount of NAcDCVC recovered can only be a lower bound on the amount ultimately excreted in urine. However, the model does not attempt to represent the excretion time-course of GSH conjugates—it merely models the total flux. This is evinced by the fact that the model predicts complete excretion by the first time point of 12 hrs, whereas in the data, there is still substantial excretion occurring at 48 hrs.

Table A-3. Evaluation of Hack et al. (2006) PBPK model predictions for in vivo data in humans (continued)

Reference	Simulation number	Calibration data	Discussion
Bernauer et al. (1996) (continued)	1–3 (continued)		Population-based posterior fits to these data were quite good for urinary TCA and TCOH, but not for NAcDCVC in urine. Because of the incomplete capture of NAcDCVC in urine, unless the model can accurately portray the time-course of NAcDCVC in urine, it should probably not be used for calibration of the GSH pathway, except perhaps as a lower bound.
Bloemen et al. (2001)	72–75		Like Bartonicek (1962), these data are more difficult to interpret due to their being single data points for each subject and exposure. However, in general, posterior population-based estimates of retained dose, urinary TCOG, and urinary TCA were fairly accurate, staying within the 95% CI, and mostly inside the interquartile range. The data on GSH mercapturates are limited—first they are all nondetects. In addition, because of the 48–56 hrs collection period, excretion of GSH mercapturates is probably incomplete, as noted above in the discussion of Bernauer et al. (1996).
Chiu et al. (2007)	66–71		The measured minute-volume was multiplied by a factor of 0.7 to obtain an estimate for alveolar ventilation rate, which was fixed for each subject. Alveolar air concentrations of TCE were generally well predicted, especially during the exposure period. Postexposure, the initial drop in TCE concentration was generally further than predicted, but the slope of the terminal phase was similar. Blood concentrations of TCE were consistently overpredicted for all subjects and occasions. Blood concentrations of TCA were consistently overpredicted, though mostly staying in the lower 95% confidence region. Blood TCOH (free) levels were generally overpredicted, in many cases falling below the 95% confidence region, though in some cases the predictions were accurate. On the other hand, total TCOH (free+glucuronidated) was well predicted (or even underpredicted) in most cases—in the cases where free TCOH was accurately predicted, total TCOH was underpredicted. The free and total TCOH data reflect the higher fraction of TCOH as TCOG than previously reported (e.g., Fisher et al. (1998) reported no detectable TCOG in blood). Data on urinary TCA and TCOG were complicated by some measurements being saturated, as well as the intermittent nature of urine collection after d 3. Thus, only the nonsaturated measurements for which the time since the last voiding was known were included for direct comparison to the model predictions. Saturated measurements were kept track of separately for comparison, but were considered only rough lower bounds. TCA excretion was generally overpredicted, whether looking at unsaturated or saturated measurements (the latter, would of course, be expected). Urinary excretion of TCOG generally stayed within the 95% confidence range.
Fernandez et al. (1977)			Alveolar air concentrations are somewhat overestimated. Other measurements are fairly well predicted.

Table A-3. Evaluation of Hack et al. (2006) PBPK model predictions for in vivo data in humans (continued)

Reference	Simulation number	Calibration data	Discussion
Fisher et al. (1998)	13–33	√	The majority of the data used in the calibration (both in terms of experiments and data points) came from this study. In general, the subject-specific fits to these data were good, with the exception of alveolar air concentrations, which were consistently overpredicted. In addition, for some subjects, the shape of the TCOH time-course deviated from the predictions (#14, 24, 29, and 30)—the predicted peak was too "sharp," with underprediction at early times. Simulation #23 showed the most deviation from predictions, with substantial inaccuracies in blood TCA, TCOH, and urinary TCA. Interestingly, in the population-based predictions, in some cases the predictions were not very accurate—indicating that the full range of population variability is not accounted for in the posterior simulations. This is particularly the case with venous blood TCE concentrations, which are generally underpredicted in population estimates (although in some cases the predictions are accurate). One issue with the way in which these data were utilized in the calibration is that in some cases, the same subject was exposed to two different concentrations, but in the calibration, they were treated as separate "subjects." Thus, parameters were allowed to vary between exposures, mixing intersubject and interoccasion variability. It is recommended that in subsequent calibrations, the different occasions with the same subject be modeled together. This will also allow identification of any dose-related changes in parameters (e.g., saturation).
Kimmerle and Eben (1973a)	46–57		Blood TCE levels are generally overpredicted for both single and multiexposure experiments. However, levels at the end of exposure are rapidly changing, so some of those values may be better predicted if the "exact" time after cessation of exposure were known. Blood TCOH levels are fairly accurately predicted, although in some subjects in single exposure experiments, there is a tendency to overpredict at early times and underpredict at late times. In multiexposure experiments, the decline after the last exposure was somewhat steeper than predicted. Urinary excretion of TCA and TCOH was well predicted. Only grouped data on alveolar air concentrations were available, so they were not used.
Laparé et al. (1995)	34	√	Predictions for these data were not accurate. However, there was an error in some of the exposure concentrations used in the original calibration. In addition, the last exposure "occasion" in these experiments involved exercise/workload, and so should be excluded. Finally, subject data are available for these experiments.
	62–65 (individual data)		Taking into account these changes, population-based predictions were somewhat more accurate. However, alveolar air concentrations and venous blood TCE concentrations were still overpredicted.

Table A-3. Evaluation of Hack et al. (2006) PBPK model predictions for in vivo data in humans (continued)

Reference	Simulation number	Calibration data	Discussion
Monster et al. (1976)	5–6 (summary data)	√	Subject-specific predictions were quite good, except that for blood TCA concentrations exhibited a higher peak that predicted. However, TCOH values were entered as free TCOH, whereas the TCOH data were actually total (free + glucuronidated) TCOH. Therefore, for population-based predictions, this change was made. In addition, as with the Monster et al. (1979a) data, minute-volume and exhaled air concentrations were measured and incorporated for population-based predictions. Finally, subject-specific data are available, so, in this case, those data should replace the grouped data in any revised calibration. These individual data also included estimates of retained dose based on complete inhaled and exhaled air samples during exposure. For population-based predictions, as with the Monster et al. (1979a) data, grouped urinary and blood TCOH/TCOG was somewhat underpredicted in the population-based predictions, and grouped alveolar and blood TCE concentrations were somewhat overpredicted.
	58–61 (individual data)		The results for the individual data were similar, but exhibited substantially greater variability that predicted. For instance, in subject A, blood TCOH levels were generally greater than the 95% CI at both 70 and 140 ppm, whereas predictions for blood TCOH in subject D were quite good. In another example, for blood TCE levels, predictions for subject B were quite good, but those for subject D were poor (substantially overpredicted). Thus, it is anticipated that adding these individual data will be substantially informative as to intersubject variability, especially since all four individuals were exposed at two different doses.
Monster et al. (1979a)	4	√	Subject-specific predictions for these data were quite good. However, TCA values were entered as plasma, whereas the TCA data were actually in whole blood. Therefore, for population-based predictions, this change was made. In addition, two additional time-courses were available that were not used in calibration: exhaled air concentrations and total TCOH blood concentrations. These were added for population-based predictions. In addition, the original article had data on ventilation rate, which as incorporated into the model. The minute volume needed to be converted to alveolar ventilation rate for the model, but this required adjusted for an extra dead space volume of 0.15 L due to use of a mask, as suggested in the article. The measured mean minute volume was 11 L/min, and with a breathing rate of 14 breaths/min (assumed in the article), this corresponding to a total volume of 0.79 L. Subtracting the 0.15 L of mask dead space and 0.15 L of physiological dead space (suggested in the article) gives 0.49 L of total physiological dead space. Thus, the minute volume of 11 L/min was adjusted by the factor 0.49/0.79 to give an alveolar ventilation rate of 6.8 L/min, which is a reasonably typical value at rest. Due to extra nonphysiological dead space issue, some adjustment to the exhaled air predictions also needed to be made. The alveolar air concentration CAlv was, therefore, estimated based on the formula

Table A-3. Evaluation of Hack et al. (2006) PBPK model predictions for in vivo data in humans (continued)

Reference	Simulation number	Calibration data	Discussion
Monster et al. (1979a) (continued)	4 (continued)		CAlv = (CExh × VTot – CInh × VDs)/VAlv where CExh is the measured exhaled air concentration, VTot is the total volume (alveolar space VAlv of 0.49 L, physiological dead space of 0.15 L, and mask dead space of 0.15 L), VDs is the total dead space of 0.3 L, and CInh is the inhaled concentration. Population-based predictions for these data lead to slight underestimation urinary TCOG and blood TCOH levels, as well as some overprediction of alveolar air and venous blood concentrations by factors of 3~10-fold.
Muller et al. (1975; 1974, 1972)	7–10	√	Subject-specific predictions for these data were good, except for alveolar air concentrations. However, several problems were found with these data as utilized in the original calibration: • Digitization problems, particular with the time axis in the multiday exposure study (Simulation 9) that led to measurements taken prior to an exposure modeled as occurring during the exposure. The original digitization from Bois (2000b) and Clewell et al. (2000) was used for population-based estimates. • Original article showed TCA as measured in plasma, not blood as was assumed in the calibration. • Blood was taken from the earlobe, which is thought to be indicative of arterial blood concentrations, rather than venous blood concentrations. • TCOH in blood was free, not total, as Ertle et al. (1972) (cited in Methods) had no use of β-glucuronidase in analyzing blood samples. Separate free and total measurements were done in plasma (not whole blood), but these data were not included. • Simulation 9, contiguous data on urinary excretion were only available out to 6 d, so only that data should be included. • Simulation 10, is actually the same as the first day of simulation 9, from Muller et al. (1975; 1972) (the data were reported in both papers), and, thus, should be deleted. These were corrected in the population-based estimates. Alveolar air concentration measurements remained overpredicted, while the change to arterial blood led to overprediction of those measurements during exposure (but postexposure predictions were accurate).
Muller et al. (1974)	81–82 (TCA and TCOH dosing)		The experiment with TCA showed somewhat more rapid decline in plasma levels than predicted, but still well within the 95% confidence range. Urinary excretion was well predicted, but only accounted for 60% of the administered dose—this is not consistent with the rapid decline in TCA plasma levels (10-fold lower than peak at the end of exposure), which would seem to suggest the majority of TCA has been eliminated. With TCOH dosing, blood levels of TCOH were overpredicted in the first 5 hrs, perhaps due to slower oral absorption (the augmented model used instantaneous and complete absorption). TCA plasma and urinary excretion levels were fairly well predicted. However, urinary excretion of TCOG was near the bottom of the 95% CI; while, in the same individuals with TCE dosing (Simulation 7), urinary excretion of TCOG was substantially greater (near slightly above the interquartile region). Furthermore, total TCA and TCOG urinary excretion accounted for <40% of the administered dose.

Table A-3. Evaluation of Hack et al. (2006) PBPK model predictions for in vivo data in humans (continued)

Reference	Simulation number	Calibration data	Discussion
Paykoc and Powell (1945)	35–37		Population-based fits were good, within the inner quartile region.
Sato et al. (1977)	76		Both alveolar air and blood concentrations are overpredicted in this model. Urinary TCA and TCOG, on the other hand, are well predicted.
Stewart et al. (1970)	11	√	Subject-specific predictions for these data were good, except for some alveolar air concentrations. However, a couple of problems were found with these data as utilized in the original calibration: • The original article noted that individuals took a lunch break during which there was no exposure. This was not accounted for in the calibration runs, which a assumed a continuous 7-hr exposure. The exposures were, therefore, revised with a 3-hr morning exposure (9–12), a 1 hr lunch break (12–1), and 4-hr afternoon exposure (1–5), to mimic a typical workday. The times of the measurements had to be revised as well, since the article gave "relative" rather than "absolute" times (e.g., *x* hr postexposure). • Contiguous data on urinary excretion were only available out to 11 d, so only that data should be included (see Table 2). With these changes, population-based predictions of urinary TCA and TCOG were still accurate, but alveolar air concentrations were overpredicted.
Triebig et al. (1976)	12	√	Only two data points are available for alveolar air, and blood TCA and TCOH. Only one data point is available on blood TCE. Alveolar air was underpredicted at 24 hrs. Blood TCA and TCOH were within the 95% confidence ranges. Blood TCE was overpredicted substantially (outside 95% confidence range).

A.2.3.3.1.1. Subject-specific predictions and calibration data

(See "Supplementary data for TCE assessment: Hack mouse subject calibration," 2011)

A.2.3.3.1.2. Population-based predictions and calibration and additional evaluation data

(See "Supplementary data for TCE assessment: Hack mouse subject calibration," 2011)

A.2.3.3.2. Conclusions regarding human model

A.2.3.3.2.1. TCE concentrations in blood and air are often not well-predicted

Except for the Chiu et al. (2007) during exposure, TCE alveolar air levels were consistently overpredicted. Even in Chiu et al. (2007), TCE levels postexposure were overpredicted, as the drop-off after the end of exposure was further than predicted. Because predictions for retained dose appear to be fairly accurate, this implies that less clearance is occurring via exhalation than predicted by the model. This could be the result of additional metabolism or storage not accounted for by the model.

Except for the Fisher et al. (1998) data, TCE blood levels were consistently overpredicted. Because the majority of the data used for calibration was from Fisher et al. (1998), this implies that the Fisher et al. (1998) data had blood concentrations that were consistently higher than the other studies. This could be due to differences in metabolism and/or distribution among studies.

Interestingly, the mouse inhalation data also exhibited inaccurate prediction of blood TCE levels. Hypotheses such as fractional uptake or presystemic elimination due to local metabolism in the lung have not been tested experimentally, nor is it clear that they can explain the discrepancies.

Due to the difficulty in accurately predicted blood and air concentrations, there may be substantial uncertainty in tissue concentrations of TCE. However, such potential model errors can be characterized estimated and estimated as part of a revised calibration.

A.2.3.3.2.2. TCA blood concentrations well predicted following TCE exposures, but some uncertainty in TCA flux and disposition

TCA blood and plasma concentrations and urinary excretion, following TCE exposure, are generally well predicted. Even though the model's central estimates overpredicted the Chiu et al. (2007) TCA data, the CIs were still wide enough to encompass those data.

However, the total flux of TCA may not be correct, as evidenced by TCA dosing studies, none of which were included in the calibration. In these studies, total recovery of urinary TCA was found to be substantially less than the administered dose. However, the current model assumes that urinary excretion is the only source of clearance of TCA. This leads to overestimation of urinary excretion. This fact, combined with the observation that under TCE

dosing, the model appears to give accurate predictions of TCA urinary excretion for several data sets, strongly suggests a discrepancy in the amount of TCA formed from TCE. That is, since the model appears to overpredict the fraction of TCA that appears in urine, it may be reducing TCA production to compensate. Inclusion of the TCA dosing studies, along with inclusion of a nonrenal clearance pathway, would probably be helpful in reducing these discrepancies. Finally, improvements in the TCOH/TCOG submodel, below, should also help to insure accurate estimates of TCA kinetics.

A.2.3.3.2.3. TCOH/TCOG submodel requires revision and recalibration

Blood levels of TCOH and urinary excretion of TCOG were generally well predicted. Additional individual data show substantial intersubject variability than can be incorporated into the calibration. Several errors as to the measurement of free or total TCOH in blood need to be corrected.

A few inconsistencies with noncalibration data sets stand out. The presence of substantial TCOG in blood in the Chiu et al. (2007) data are not predicted by the model. Interestingly, only two studies that included measurements of TCOG in blood (rather than just total TCOH or just free TCOH)—Muller et al. (1975), which found about 17% of total TCOH to be TCOG, and Fisher et al. (1998), who could not detect TCOG. Both of these studies had exposures at 100 ppm. Interestingly, Muller et al. (1975) reported increased TCOG (as fraction of total TCOH) with ethanol consumption, hypothesizing the inhibition of a glucuronyl transferase that slowed glucuronidation. This also would result in a greater half-life for TCOH in blood with ethanol consumptions, which was observed.

An additional concern is the overprediction of urinary TCOG following TCOH administration from the Muller et al. (1974) data. Like the case of TCA, this indicates that some other source of TCOH clearance (not to TCA or urine—e.g., to DCA or some other untracked metabolite) is possible. This pathway can be considered for inclusion, and limits can be placed on it using the available data.

Also, as for TCA, the fact that blood and urine are relatively well predicted from TCE dosing strongly suggests a discrepancy in the amount of TCOH formed from TCE. That is, since the model appears to overpredict the fraction of TCOH that appears in urine, it may be reducing TCOH production to compensate.

Finally, as with the rat and mice, the model needs to ensure that any first-pass effect is accounted for appropriately. Particularly for the Chiu et al. (2007) data, in which substantial TCOG appears in blood, since TCOH is formed in the liver from TCE, and TCOH is also glucuronidated in the liver to TCOG, a substantial portion of the TCOH may be glucuronidated before reaching systemic circulation. Thus, suggests that a liver compartment for TCOH is necessary. Furthermore, because substantial TCOG can be excreted in bile from the liver prior to systemic circulation, a liver compartment for TCOG may also be necessary to address that

first-pass effect. In addition, in light of the Chiu et al. (2007) data, it may be useful to expand the prior range for the K_M of TCOH glucuronidation.

The addition of the liver compartment will necessitate several changes to model parameters. The distribution volume for TCOH will be replaced by two parameters: the liver:blood and body:blood partition coefficients. Similarly for TCOG, liver:blood and body:blood partition coefficients will need to be added. Clearance of TCOH to TCA and TCOG can be redefined as occurring in the liver, and urinary clearance can be redefined as coming from the rest of the body. Fortunately, there are in vitro partition coefficients for TCOH. It may be important to incorporate the fact that Fisher et al. (1998) found no TCOG in blood. This can be included by having the TCOH data be used for both free and total TCOH (particularly since that is how the estimation of TCOG was made—by taking the difference between total and free).

A.2.3.3.2.4. Uncertainty in estimates of total metabolism

Estimates of total recovery after TCE exposure (TCE in exhaled air, TCA and TCOG in urine) have been found to be only 60–70% (Chiu et al., 2007; Monster et al., 1979a, 1976). Even estimates of total recovery after TCA and TCOH dosing have found 25–50% unaccounted for in urinary excretion (Muller et al., 1974; Paykoc and Powell, 1945). Bartonicek (1962) found some TCOH and TCA in feces, but this was about 10-fold less than that found in urine, so this cannot account for the discrepancy. Therefore, it is likely that additional metabolism of TCE, TCOH, and/or TCA are occurring. Additional metabolism of TCE could account for the consistent overestimation of TCE in blood and exhaled breath found in many studies. However, no data are *directly* informative as to the fraction of total metabolism in the lung, the amount of "untracked" hepatic oxidative metabolism (parameterized as "FracDCA"), or any other extrahepatic metabolism. The lung metabolism as currently modeled could just as well be located in other extrahepatic tissues, with little change in calibration. In addition, it is difficult to distinguish between untracked hepatic oxidative metabolism and GSH conjugation, particularly at low doses.

A.3. PRELIMINARY ANALYSIS OF MOUSE GAS UPTAKE DATA: MOTIVATION FOR MODIFICATION OF RESPIRATORY METABOLISM

Potential different model structures can be investigated using the core PBPK model containing averaged input parameters, since this approach saves computational time and is more efficient when testing different structural hypotheses. This approach is particularly helpful for quick comparisons of data with model predictions. During the calibration process, this approach was used for different routes of exposure and across all three species. For both mice and rats, the closed-chamber inhalation data resulted in fits that were considered not optimal when visually examined. Although closed-chamber inhalation usually combines multiple animals per experiment, and may not be as useful in differentiating between individual and experimental

uncertainty (Hack et al., 2006), closed-chamber data do describe in vivo metabolism and have been historically used to quantify averaged in vivo Michaelis-Menten kinetics in rodents.

There are several assumptions used when combining PBPK modeling and closed-chamber data to estimate metabolism via regression. The key experimental principles require a tight, sealed, or air-closed system where all chamber variables are controlled to known set points or monitored, that is all except for metabolism. For example, the inhalation chamber is calibrated without an animal, to determine normal absorption to the empty system. This empty chamber calibration is then followed with a dead animal experiment, identical in every way to the in vivo exposure, and is meant to account for every factor other than metabolism, which is zero in the dead animal. When the live animal(s) are placed in the chamber, oxygen is provided for, and carbon dioxide accumulated during breathing is removed by absorption with a chemical scrubber. A bolus injection of the parent chemical, TCE, is given and this injection time starts the inhalation exposure. The chemical inside the chamber will decrease with time, as it is absorbed by the system and the metabolic process inside the rodent. Since all known processes contributing to the decline are quantified, except for metabolism, the metabolic parameters can be extracted from the total chamber concentration decline using regression techniques.

The basic structure for the PBPK model that is linked to closed-chamber inhalation data has the same basic structure as described before. The one major difference is the inclusion of one additional equation that accounts for mass balance changes inside the inhalation chamber or system, and connects the chamber with the inhaled and exhaled concentrations breathed in and out by the animal:

$$\frac{dA_{Ch}}{dt} = RATS \;\; Q_P \;\; (C_X - \frac{A_{Ch}}{V_{Ch}}) - K_{LOSS} A_{Ch} \qquad \text{(Eq. A-4)}$$

where

$RATS$ = number of animals in the chamber
Q_P = alveolar ventilation rate
C_X = exhaled concentration
A_{Ch} = net amount of chemical inside chamber
V_{Ch} = volume of chamber
K_{LOSS} = loss rate constant to glassware.

An updated model was developed that included updated physiological and chemical-specific parameters as well as GSH metabolism in the liver and kidney, as discussed in Chapter 3. The PBPK model code was translated from MCSim to use in Matlab© (version 7.2.0.232, R2006a, Natick, MA) using their m language. This PBPK model made use of fixed or constant, averaged values for physiological, chemical and other input parameters; there were no statistical distributions attached to each average value. As an additional step in quality

control, mass balance was checked for the MCSim code, and comparisons across both sets of code were made to ensure that both sets of predictions were the same.

The resulting simulations were compared to mice gas uptake data (Fisher et al., 1991) after some adjustments of the fat compartment volumes and flows based on visual fits, and limited least-squares optimization of just V_{MAX} (different for males and females) and K_M (same for males and females). The results are shown in the top panels of Figures A-3 and A-4, which showed poor fits particularly at lower chamber concentrations. In particular, metabolism is observed to be faster than predicted by simulation. This is directly related to metabolism of TCE being limited by hepatic blood flow at these exposures. Indeed, Fisher et al. (1991) was able to obtain adequate fits to these data by using cardiac output and ventilation rates that were about twofold higher than is typical for mice. Although their later publication reporting inhalation experiments (Greenberg et al., 1999) used the lower values from Brown et al. (1997) for these parameters, they did not revisit the Fisher et al. (1991) data with the updated model. In addition, the Hack et al. (2006) model estimated the cardiac output and ventilation rate and for these experiments to be about twofold higher than typical. However, it seems unlikely that cardiac output and ventilation rate were really as high as used in these models, since TCE and other solvents typically have CNS-depressing effects. In the mouse, after the liver, the lung has the highest rate of oxidative metabolism, as assessed by in vitro methods (see footnote in Section 3.5.4.2 for a discussion of why kidney oxidative metabolism is likely to be minor quantitatively). In addition, TCE administered via inhalation is available to the lung directly, as well as through blood flow. Therefore, it was hypothesized that a more refined treatment of respiratory metabolism may be necessary to account for the additional metabolism.

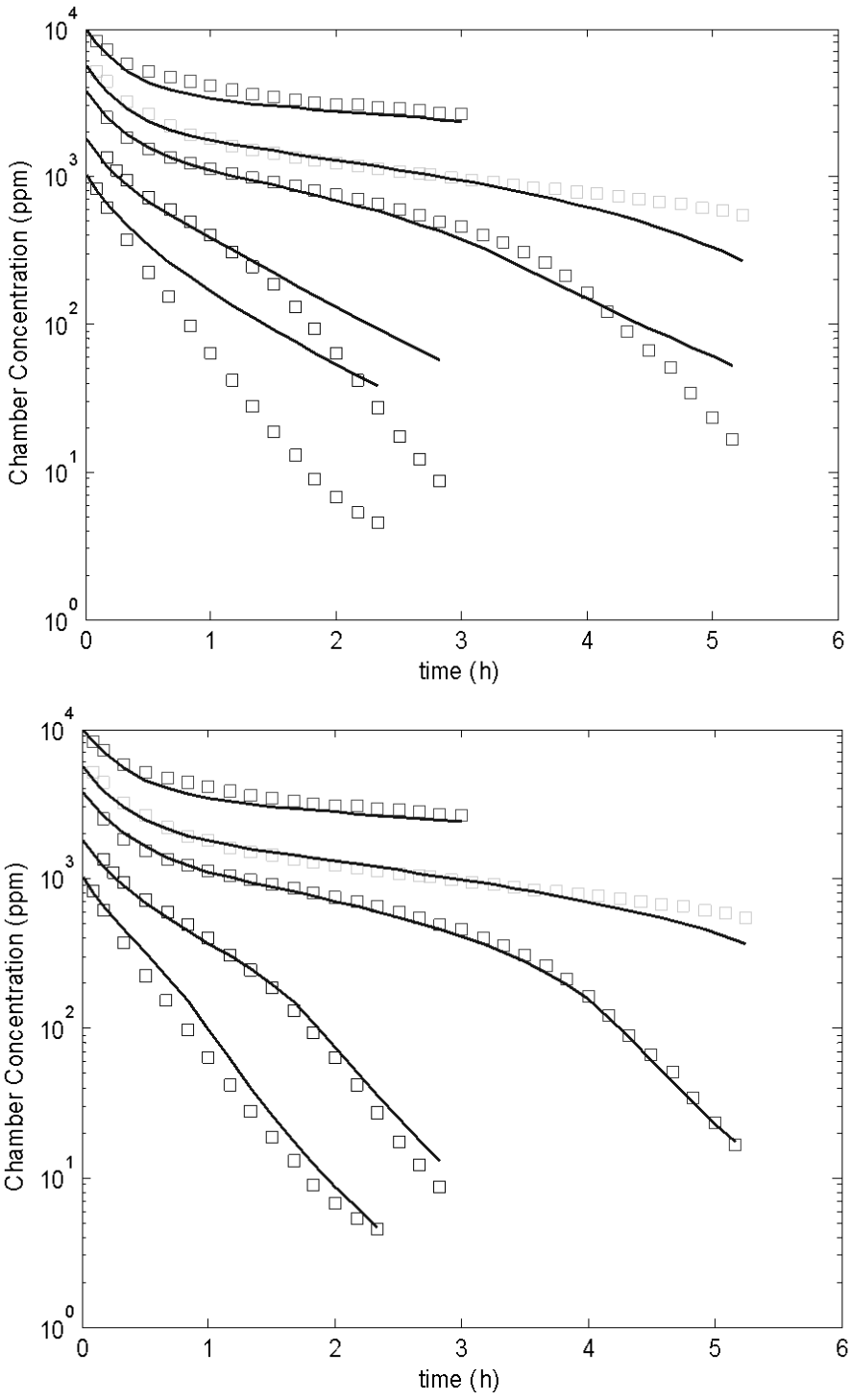

Figure A-3. Limited optimization results for male closed-chamber data from Fisher et al. (1991) without (top) and with (bottom) respiratory metabolism.

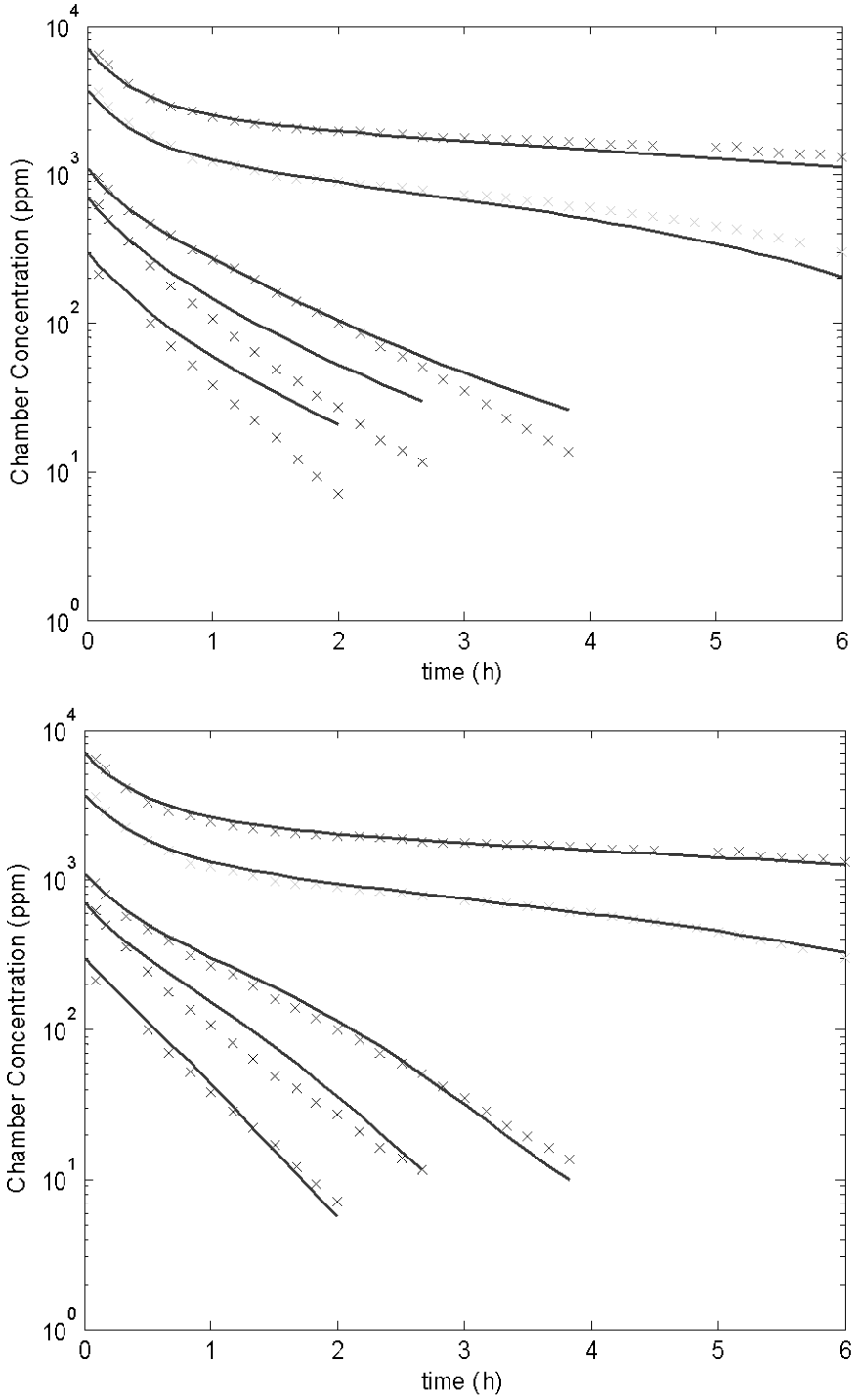

Figure A-4. Limited optimization results for female closed-chamber data from Fisher et al. (1991) without (top) and with (bottom) respiratory metabolism.

The structure of the updated respiratory metabolism model is shown in Figure A-5, with the mathematical formulation shown in the model code in Section A.6, where the "D" is the diffusion rate, "concentrations" and "amounts" are related by the compartment volume, and the other symbols have their standard meanings in the context of PBPK modeling. In brief, this is a more highly "lumped" version of the Sarangapani et al. (2003) respiratory metabolism model for styrene combined with a "continuous breathing" model to account for a possible wash-in/wash-out effect. In brief, upon inhalation (at a rate equal to the full minute volume, not just the alveolar ventilation), TCE can either: (1) diffuse between the respiratory tract lumen and the respiratory tract tissue; (2) remain in the dead space; or (3) enter the gas exchange region. In the respiratory tract tissue, TCE can either be "stored" temporarily until exhalation, during which it diffuses to the "exhalation" respiratory tract lumen, or be metabolized. In the dead space, TCE is transferred directly to the "exhalation" respiratory tract lumen at a rate equal to the minute-volume minus the alveolar ventilation rate, where it mixes with the other sources. In the gas exchange region, it undergoes transfer to and from blood, as is standard for PBPK models of volatile organics. Therefore, if respiratory metabolism is absent (V_{MAX}Clara = 0), then the model reduces to a wash-in/wash-out effect where TCE is temporarily adsorbed to the respiratory tract tissue, the amount of which depends on the diffusion rate, the volume of the tissue, and the partition coefficients.

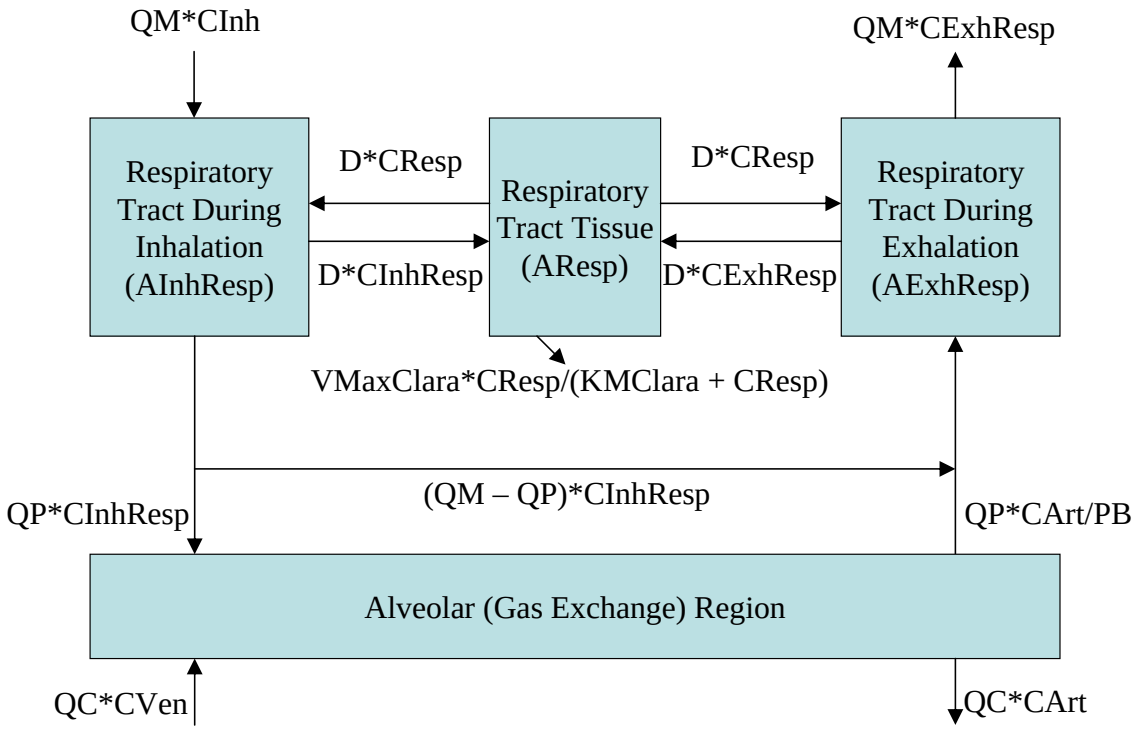

Figure A-5. Respiratory metabolism model for updated PBPK model.

The results of the same limited optimization, now with additional parameters V_{MAX}Clara, K_MClara, and D being estimated simultaneously with the hepatic V_{MAX} and K_M, are shown in the bottom panels of Figures A-2 and A-3. The improvement in the model fits is obvious, and these results served as a motivation to include this respiratory metabolism model for analysis by the more formal Bayesian methods.

A.4. DETAILS OF THE UPDATED PBPK MODEL FOR TCE AND ITS METABOLITES

The structure of the updated PBPK model and the statistical population model are shown graphically in Chapter 3, with the model code shown below in Section A.7. Details as to the model structure, equations, and parameter values and prior distributions are given below.

A.4.1. PBPK Model Structure and Equations

The equations below, along with the parameters defined in Table A-4, specify the PBPK model. The ordinary differential equations are shown in **bold**, with the remaining equations being algebraic definitions. The same equations are in the PBPK model code, with some additional provisions for unit conversions (e.g., ppm to mg/L) or numerical stability (e.g., truncating small values at 10^{-15}, so states are never negative). For reference, the stoichiometric adjustments for molecular weights are given by the following:

```
# Molecular Weights
        TCE:        MWTCE = 131.39
        DCVC:       MWDCVC = 216.1
        TCA:        MWTCA = 163.5
        TCOH:       MWTCOH = 149.5
        TCOG:       MWTCOHGluc = 325.53
        NAcDCVC:    MWNADCVC = 258.8
# Stoichiometry
        StochTCATCE = MWTCA/MWTCE;
        StochTCATCOH = MWTCA/MWTCOH;
        StochTCOHTCE = MWTCOH/MWTCE;
        StochGlucTCOH = MWTCOHGluc/MWTCOH;
        StochTCOHGluc = MWTCOH/MWTCOHGluc;
        StochTCEGluc = MWTCE/MWTCOHGluc;
        StochDCVCTCE = MWDCVC/MWTCE;
        StochN = MWNADCVC/MWDCVC;
```

Table A-4. PBPK model parameters, baseline values, and scaling relationships

Parameter	Description (units)	Formula	Baseline value or parameter	Description	Mouse	Rat	Human F/M	Scaling parameter	Sources(s)
Body weight	Body weight (kg)	-	Body weight$_0$	Standard body weight	0.03	0.3	60/70	–	[a]
Flows									
QC	Cardiac output (L/hr)	QC = QCC$_0$ × exp(lnQCC) × body weight$^{0.75}$	QCC$_0$	Cardiac output allometrically scaled	11.6	13.3	16/16	lnQCC	[b]
QP	Alveolar ventilation (L/hr)	QP = QC × VPR$_0$ × exp(lnVPR)	VPR$_0$	Ventilation-perfusion ratio	2.5	1.9	0.96/0.96	lnVPRC	[c]
DResp	Diffusion clearance rate (L/hr)	DResp = QP × exp(lnDRespC)	–	–	–	–	–	lnDRespC	[d]
Physiological blood flows to tissues									
QFat	Blood flow to fat (L/hr)	QFat = QC × QFatC$_0$ × QFatC	QFatC$_0$	Fraction of blood flow to fat	0.07	0.07	0.085/0.05	QFatC	[e]
QGut	Blood flow to gut (L/hr)	QGut = QC × QGutC$_0$ × QGutC	QGutC$_0$	Fraction of blood flow to gut	0.141	0.153	0.21/0.19	QGutC	[e]
QLiv	Hepatic artery blood flow (L/hr)	QLiv = QC × QLivC$_0$ × QLivC	QLivC$_0$	Fraction of blood flow to hepatic artery	0.02	0.021	0.065/0.065	QLivC	[e]
QSlw	Blood flow to slowly perfused tissues (L/hr)	QSlw = QC × QSlwC$_0$ × QSlwC	QSlwC$_0$	Fraction of blood flow to slowly perfused tissues	0.217	0.336	0.17/0.22	QSlwC	[e]
QKid	Blood flow to kidney (L/hr)	QKid = QC × QKidC$_0$ × QKidC	QKidC$_0$	Fraction of blood flow to kidney	0.091	0.141	0.085/0.05	QKidC	[e]
QRap	Blood flow to rapidly perfused tissues (L/hr)	QRap = QC–(QFat + QGut + QLiv + QSlw + QKid)	–	–	–	–	0.21/0.19	–	[e]
FracPlas	Fraction of blood that is plasma	FracPlas = FracPlas$_0$ × FracPlasC	FracPlas$_0$	Fraction of blood that is plasma	0.52	0.53	0.065/0.065	FracPlasC	[f]

Table A-4. PBPK model parameters, baseline values, and scaling relationships (continued)

Parameter	Description (units)	Formula	Baseline value or parameter	Description	Mouse	Rat	Human F/M	Scaling parameter	Sources(s)
Physiological volumes									
VFat	Volume of fat (L)	VFat = body weight × $VFatC_0$ × VFatC	$VFatC_0$	Fraction of body weight that is fat	0.07	0.07	0.317/0.199	VFatC	[g]
VGut	Volume of gut (L)	VGut = body weight × $VGutC_0$ × VGutC	$VGutC_0$	Fraction of body weight that is gut	0.049	0.032	0.022/0.02	VGutC	[g]
VLiv	Volume of liver (L)	VLiv = body weight × $VLivC_0$ × VLivC	$VLivC_0$	Fraction of body weight that is liver	0.055	0.034	0.023/0.025	VLivC	[g]
VRap	Volume of rapidly perfused tissues (L)	VRap = body weight × $VRapC_0$ × VRapC	$VRapC_0$	Fraction of body weight that is rapidly perfused	0.1	0.088	0.093/0.088	VRapC	[g]
VRespLum	Volume of respiratory tract lumen (L)	VRespLum = body weight × $VRespLumC_0$ × VRespLumC	$VRespLumC_0$	Respiratory lumen volume as fraction body weight	0.004667	0.004667	0.002386/0.002386	VRespLumC	[g]
VResp	Volume of respiratory tract tissue (L)	VResp = body weight × $VRespC_0$ × VRespC	$VRespC_0$	Fraction of body weight that is respiratory tract	0.0007	0.0005	0.00018/0.00018	VRespC	[g]
VRespEff	Effective air volume of respiratory tract tissue	VRespEff = VResp × PResp × PB	–	–	–	–	–	–	[g]
VKid	Volume of kidney (L)	VKid = body weight × $VKidC_0$ × VKidC	$VKidC_0$	Fraction of body weight that is kidney	0.017	0.007	0.0046/0.0043	VKidC	[g]
VBld	Volume of blood (L)	VBld = body weight × $VBldC_0$ × VBldC	$VBldC_0$	Fraction of body weight that is blood	0.049	0.074	0.068/0.077	VBldC	[g]
VSlw	Volume of slowly perfused tissue (L)	VSlw = body weight × $VperfC_0$ – (VFat + VGut + VLiv + VRap + VResp + VKid + VBld)	$VperfC_0$	Fraction of body weight that is blood perfused	0.8897	0.8995	0.85778/0.8560	–	[g]
VPlas	Volume of plasma (L)	VPlas = FracPlas × VBld	–	–	–	–	–	–	[h]

Table A-4. PBPK model parameters, baseline values, and scaling relationships (continued)

Parameter	Description (units)	Formula	Baseline value or parameter	Description	Mouse	Rat	Human F/M	Scaling parameter	Sources(s)
VBod	Volume body for TCA submodel (L)	VBod = VFat + VGut + VRap + VResp + VKid + VSlw	–	–	–	–	–	–	[i]
VBodTCOH	Volume body for TCOH and TCOG submodels (L)	VBodTCOH = VBod + VBld	–	–	–	–	–	–	[j]
TCE distribution/partitioning									
PB	TCE blood-air partition coefficient	$PB=PB_0 \times PBC$	PB_0	TCE blood-air partition coefficient	15	22	9.5	PBC	[k]
PFat	TCE fat-blood partition coefficient	$PFat=PFatC_0 \times \exp(PFatC)$	$PFatC_0$	TCE fat-blood partition coefficient	36	27	67	PFatC	[l]
PGut	TCE gut-blood partition coefficient	$PGut=(PGutC_0) \times \exp(lnPGutC)$	$PGutC_0$	TCE gut-blood partition coefficient	1.9	1.4	2.6	lnPGutC	[m]
PLiv	TCE liver-blood partition coefficient	$PLiv = (PLivC_0) \times \exp(lnPLivC)$	$PLivC_0$	TCE liver-blood partition coefficient	1.7	1.5	4.1	lnPLivC	[n]
PRap	TCE rapidly perfused-blood partition coefficient	$PRap = (PRapC_0) \times \exp(lnPRapC)$	$PRapC_0$	TCE rapidly perfused-blood partition coefficient	1.9	1.3	2.6	lnPRapC	[o]
PResp	TCE respiratory tract tissue-blood partition coefficient	$Presp = (PRespC_0) \times \exp(lnPRespC)$	$PRespC_0$	TCE respiratory tract tissue-blood partition coefficient	2.6	1.0	1.3	lnPRespC	[p]
PKid	TCE kidney-blood partition coefficient	$PKid = (PKidC_0) \times \exp(lnPKidC)$	$PKidC_0$	TCE kidney-blood partition coefficient	2.1	1.3	1.6	lnPKidC	[q]
PSlw	TCE slowly perfused-blood partition coefficient	$PSlw = (PSlwC_0) \times \exp(lnPSlwC)$	$PSlwC_0$	TCE slowly perfused-blood partition coefficient	2.4	0.58	2.1	lnPSlwC	[r]

Table A-4. PBPK model parameters, baseline values, and scaling relationships (continued)

Parameter	Description (units)	Formula	Baseline value or parameter	Description	Mouse	Rat	Human F/M	Scaling parameter	Sources(s)
TCA distribution/partitioning									
TCAPlas	TCA blood-plasma concentration ratio	TCAPlas = FracPlas + (1 – FracPlas) × $PRBCPlasTCA_0$ × exp(lnPRBCPlasTCAC)	$PRBCPlasTCA_0$	TCA red blood cell-plasma partition coefficient	0.5	0.5	0.5/0.5	lnPRBCPlasTCAC	[s]
PBodTCA	Free TCA body-plasma partition coefficient	PBodTCA = TCAPlas × $PBodTCAC_0$ × exp(lnPBodTCAC)	$PBodTCAC_0$	Free TCA body-blood partition coefficient	0.88	0.88	0.52	lnPBodTCAC	[t]
PLivTCA	Free TCA liver-plasma partition coefficient	PLivTCA = TCAPlas × $PLivTCAC_0$ × exp(lnPLivTCAC)	$PLivTCAC_0$	Free TCA liver-blood partition coefficient	1.18	1.18	0.66	lnPLivTCAC	[t]
TCA plasma binding									
kDissoc	Protein TCA dissociation constant (microM)	kDissoc = $kDissoc_0$ × exp(lnkDissocC)	$kDissoc_0$	Protein TCA dissociation constant (microM)	107	275	182	lnkDissocC	[u]
BMax	Protein concentration (microM)	BMax = $BMaxkD_0$ × kDissoc × exp(lnBMaxkDC)	$BMaxkD_0$	BMax/kDissoc ratio	0.88	1.22	4.62	lnBMaxkDC	[u]
TCOH and TCOG distribution/partitioning									
PBodTCOH	TCOH body-blood partition coefficient	PBodTCOH = $PBodTCOH_0$ × exp(lnPBodTCOHC)	$PBodTCOH_0$	TCOH body-blood partition coefficient	1.11	1.11	0.91	lnPBodTCOHC	[v]
PLivTCOH	TCOH liver-blood partition coefficient	PBodTCOH = $PLivTCOH_0$ × exp(lnPLivTCOHC)	$PLivTCOH_0$	TCOH liver-blood partition coefficient	1.3	1.3	0.59	lnPLivTCOHC	[v]
PBodTCOG	TCOG body-blood partition coefficient	PBodTCOG = $PBodTCOG_0$ × exp(lnPBodTCOGC)	$PBodTCOG_0$	TCOG body-blood partition coefficient	1.11	1.11	0.91	lnPBodTCOGC	[w]
PLivTCOG	TCOG liver-blood partition coefficient	PBodTCOG = $PLivTCOG_0$ × exp(lnPLivTCOGC)	$PLivTCOG_0$	TCOG liver-blood partition coefficient	1.3	1.3	0.59	lnPLivTCOGC	[w]
DCVG distribution/partitioning									
VDCVG	DCVG distribution volume (L)	VDCVG = VBld + (VBod+VLiv) × exp(lnPeffDCVG)	–	–	–	–	–	lnPeffDCVG	[x]

Table A-4. PBPK model parameters, baseline values, and scaling relationships (continued)

Parameter	Description (units)	Formula	Baseline value or parameter	Description	Mouse	Rat	Human F/M	Scaling parameter	Sources(s)
TCE metabolism									
V_{MAX}	V_{MAX} for TCE hepatic oxidation (mg/hr)	$V_{MAX} = V_{MAX0} \times VLiv \times \exp(lnV_{MAX}C)$	V_{MAX0}	V_{MAX} per kg liver for TCE hepatic oxidation (mg/hr/kg liver)	2,700	600	255	$lnV_{MAX}C$	[y]
KM	KM for TCE hepatic oxidation (mg/L blood)	$KM = KM_0 \times \exp(lnKMC)$ [Mouse and Rat]	KM_0	KM for TCE hepatic oxidation (mg/L)	36	21	–	lnKMC	[y]
		$KM = V_{MAX}/(ClC_0 \times VLiv \times \exp(lnClC))$ [Human]	ClC_0	V_{MAX}/KM per kg liver for TCE hepatic oxidation (L blood/hr/kg liver)	–	–	66	lnClC	[y]
FracOther	Fraction of TCE oxidation not to TCA or TCOH	FracOther = exp(lnFracOtherC)/ (1+exp(lnFracOtherC))	–	–	–	–	–	lnFracOtherC	[z]
FracTCA	Fraction of TCE oxidation to TCA	$FracTCA = (1\text{-}FracOther) \times logitFracTCA_0 \times \exp(lnFracTCAC)/ (1 + logitFracTCA_0 \times \exp(lnFracTCAC))$	$logitFracTCA_0$	Log of ratio of fraction to TCA to fraction not to TCA	0.32	0.32	0.32	lnFracTCAC	[aa]
V_{MAX}DCVG	V_{MAX} for TCE hepatic GSH conjugation (mg/hr)	$V_{MAX}DCVG = V_{MAX}DCVG_0 \times VLiv \times \exp(lnV_{MAX}DCVGC)$ [Mouse and Rat]	$V_{MAX}DCVG_0$	V_{MAX} per kg liver for TCE GSH conjugation (mg/hr/kg liver)	300	66	–	lnV_{MAX}DCVGC	[bb]
		$V_{MAX}DCVG = VLiv \times ClDCVG_0 \times \exp(lnClDCVGC) \times KMDCVG_0 \times \exp(lnKMDCVGC)$ [Human]	$ClDCVG_0$	V_{MAX}/KM per kg liver for TCE GSH conjugation (L blood/hr/kg liver)	–	–	19	lnClDCVGC	[bb]
			$KMDCVG_0$	KM for TCE GSH conjugation (mg/L blood)	–	–	2.9	lnKMDCVGC	[bb]

Table A-4. PBPK model parameters, baseline values, and scaling relationships (continued)

Parameter	Description (units)	Formula	Baseline value or parameter	Description	Mouse	Rat	Human F/M	Scaling parameter	Sources(s)
KMDCVG	KM for TCE hepatic GSH conjugation (mg/L blood)	KMDCVG = V_{MAX}DCVG/ ($ClDCVG_0$ × exp(lnClDCVGC) [Mouse and Rat]	$ClDCVG_0$	V_{MAX}/KM per kg liver for TCE hepatic GSH conjugation (L blood/hr/kg liver)	1.53	0.25	–	lnClDCVGC	[bb]
		KMDCVG = $KMDCVG_0$ × exp(lnKMDCVGC) [Human]	$KMDCVG_0$	KM for TCE GSH conjugation (mg/L blood)	–	–	2.9	lnKMDCVGC	[bb]
V_{MAX}KidDCVG	V_{MAX} for TCE kidney GSH conjugation (mg/hr)	V_{MAX}KidDCVG = $V_{MAX}KidDCVG_0$ × VKid × exp(lnV_{MAX}KidDCVGC) [Mouse and Rat]	$V_{MAX}KidDCVG_0$	V_{MAX} per kg kidney for TCE GSH conjugation (mg/hr/kg kidney)	60	6.0	–	lnV_{MAX}KidDCVGC	[bb]
		V_{MAX}KidDCVG = VKid × $ClKidDCVG_0$ × exp(lnClKidDCVGC) × $KMKidDCVG_0$ × exp(lnKMKidDCVGC) [Human]	$ClKidDCVG_0$	V_{MAX}/KM per kg kidney for TCE GSH conjugation (L blood/hr/kg liver)	–	–	230	lnClKidDCVGC	[bb]
			$KMKidDCVG_0$	KM for TCE GSH conjugation (mg/L blood)	–	–	2.7	lnKMKidDCVGC	[bb]
KMKidDCVG	KM for TCE kidney GSH conjugation (mg/L blood)	KMKidDCVG = V_{MAX}KidDCVG/ ($ClKidDCVG_0$ × exp(lnClKidDCVGC) [Mouse and Rat]	$ClKidDCVG_0$	V_{MAX}/KM per kg kidney for TCE kidney GSH conjugation (L blood/hr/kg liver)	0.34	0.026	–	lnClDCVGC	[bb]
		KMKidDCVG = $KMKidDCVG_0$ × exp(lnKMKidDCVGC) [Human]	$KMKidDCVG_0$	KM for TCE GSH conjugation (mg/L blood)	–	–	2.7	lnKMKidDCVGC	[bb]

Table A-4. PBPK model parameters, baseline values, and scaling relationships (continued)

Parameter	Description (units)	Formula	Baseline value or parameter	Description	Mouse	Rat	Human F/M	Scaling parameter	Sources(s)
TCE metabolism (respiratory tract)									
KMClara	KM for TCE lung oxidation (mg/L air)	KMClara = exp(lnKMClara)	–	–	–	–	–	–	[cc]
V_{MAX}Clara	V_{MAX} for TCE lung oxidation (mg/hr)	V_{MAX}Clara = V_{MAX} × V_{MAX}LungLiv$_0$ × exp(lnV_{MAX}LungLivC)	V_{MAX}LungLiv$_0$	Ratio of lung to liver total V_{MAX} (mg/hr per mg/hr)	0.07	0.0144	0.0138/ 0.0128	lnV_{MAX}LungLivC	[cc]
FracLungSys	Fraction of respiratory oxidation entering systemic circulation	FracLungSys = exp(lnFracLungSysC)/ (1+exp(lnFracLungSysC))	–	–	–	–	–	lnFracLungSysC	[dd]
TCOH metabolism									
V_{MAX}TCOH	V_{MAX} for TCOH oxidation to TCA (mg/hr)	V_{MAX}TCOH= body weight^{¾} × exp(lnV_{MAX}TCOHC) [Mouse and Rat]	–	–	–	–	–	lnV_{MAX}TCOHC	
		V_{MAX}TCOH = body weight^{¾} × exp(lnClTCOHC + lnKMTCOHC) [Human]	–	–	–	–	–	lnClTCOHC lnKMTCOHC	
KMTCOH	KM for TCOH oxidation to TCA (mg/L air)	KMTCOH = exp(lnKMTCOHC)	–	–	–	–	–	lnKMTCOHC	
V_{MAX}Gluc	V_{MAX} for TCOH glucuroni-dation (mg/hr)	V_{MAX}Gluc = body weight^{¾} × exp(lnV_{MAX}GlucC) [Mouse and Rat]	–	–	–	–	–	lnV_{MAX}GlucC	
		V_{MAX}Gluc = body weight^{¾} × exp(lnClGlucC + lnKMGlucC) [Human]	–	–	–	–	–	lnClGlucC lnKMGlucC	
KMGluc	KM for TCOH glucuroni-dation (mg/L air)	KMGluc = exp(lnKMGlucC)	–	–	–	–	–	lnKMGlucC	
kMetTCOH	Rate constant for TCOH other clearance	kMetTCOH = body weight$^{-¼}$ × exp(lnkMetTCOHC)	–	–	–	–	–	lnkMetTCOHC	

Table A-4. PBPK model parameters, baseline values, and scaling relationships (continued)

Parameter	Description (units)	Formula	Baseline value or parameter	Description	Mouse	Rat	Human F/M	Scaling parameter	Sources(s)
	(/hr)								
TCA metabolism/clearance									
kUrnTCA	Rate constant for TCA excretion to urine (/hr)	kUrnTCA = GFR_body weight exp(lnkUrnTCAC) × body weight /VPlas	GFR_body weight	Glomerular filtration rate per kg body weight (L/h/kg)	0.6	0.522	0.108	lnkUrnTCAC	[ee]
kMetTCA	Rate constant for other TCA clearance (/hr)	kMetTCA = body weight$^{-¼}$ × exp(lnkMetTCAC)	–	–	–	–	–	lnkMetTCAC	
TCOG metabolism/clearance									
kBile	Rate constant for other TCOG excretion to bile (/hr)	kBile = body weight$^{-¼}$ × exp(lnkBileC)	–	–	–	–	–	lnkBileC	
kEHR	Rate constant for other bile TCOG reaborption as TCOH (/hr)	kEHR = body weight$^{-¼}$ × exp(lnkEHRC)	–	–	–	–	–	lnkEHRC	
kUrnTCOG	Rate constant for TCOH excretion to urine (/hr)	kUrnTCOG = GFR_body weight exp(lnkUrnTCOGC) × body weight/(VBodTCOH × PBodTCOG)	GFR_body weight	Glomerular filtration rate per kg body weight (L/hr/kg)	0.6	0.522	0.108	lnkUrnTCOGC	[ee]
DCVG metabolism									
kDCVG	Rate constant for DCVC formation from DCVG (/hr)	kDCVG = body weight$^{-¼}$ × exp(lnkDCVGC)						lnkDCVGC	[ff]
kNAT	Rate constant for urinary excretion of NAcDCVC (/hr)	kNAT = body weight$^{-¼}$ × exp(lnkNATC)	–	–	–	–	–	lnkNATC	[gg]
kBioact	Rate constant for other bio-activation of DCVC (/hr)	kKidBioact = body weight$^{-¼}$ × exp(lnkKidBioactC)	–	–	–	–	–	lnkKidBioactC	[gg]

Table A-4. PBPK model parameters, baseline values, and scaling relationships (continued)

Parameter	Description (units)	Formula	Baseline value or parameter	Description	Mouse	Rat	Human F/M	Scaling parameter	Sources(s)
Oral uptake/transfer coefficients									
kTSD	TCE gavage stomach-duodenum transfer coefficient (/hr)	kTSD = exp(lnkTSD)	1.4	–	–	–	–	lnkTSD	[hh]
kAS	TCE gavage stomach-absorption coefficient (/hr)	kAS = exp(lnkAS)	1.4	–	–	–	–	lnkAS	[hh]
kAD	TCE gavage duodenum-absorption coefficient (/hr)	kAD = exp(lnkAD)	0.75	–	–	–	–	lnkAD	[hh]
kASTCA	TCA stomach absorption coefficient (/hr)	kASTCA = exp(lnkASTCA)	0.75	–	–	–	–	lnkASTCA	[hh]
kASTCOH	TCOH stomach absorption coefficient (/hr)	kASTCOH = exp(lnkASTCOH)	0.75	–	–	–	–	lnkASTCOH	[hh]

Explanatory note. Unless otherwise noted, the model parameter is obtained by multiplying: (1) the "baseline value" (equals one if not specified); (2) the scaling parameter (or for those beginning with "ln," which are natural-log transformed, exp[lnXX]); and (3) any additional scaling as noted in the second to last column. Unless otherwise noted, all log-transformed scaling parameters have baseline value of 0 (i.e., exp[lnXX] has baseline value of 1) and all other scaling parameters have baseline parameters of 1.

[a]Use measured value if available.
[b]If QP is measured, then scale by QP using VPR. Baseline values are from Brown et al. (1997) (mouse and rat) and International Commission on Radiological Protection (ICRP) Publication 89 (2003) (human).
[c]Use measured QP, if available; otherwise scale by QC using alveolar VPR. Baseline values are from Brown et al. (1997) (mouse and rat) and ICRP Publication 89 (2003) (human).
[d]Scaling parameter is relative to alveolar ventilation rate.
[e]Fat represents adipose tissue only. Gut is the GI tract, pancreas, and spleen (all drain to the portal vein). Slowly perfused tissue is the muscle and skin. Rapidly perfused tissue is the rest of the organs, plus the bone marrow and lymph nodes, the blood flow for which is calculated as the difference between the cardiac output (QC) and the sum of the other blood flows. Baseline values are from Brown et al. (1997) (mouse and rat) and ICRP Publication 89 (2003) (human).
[f]This is equal to 1 minus the hematocrit (measured value used if available). Baseline values from control animals in (Hejtmancik et al., 2002) (mouse and rat) and ICRP Publication 89 (2003) (human).

Table A-4. PBPK model parameters, baseline values, and scaling relationships (continued)

[g]Fat represents adipose tissue only, and the measured value is used, if available. Gut is the GI tract, pancreas, and spleen (all drain to the portal vein). Rapidly perfused tissue is the rest of the organs, plus the bone marrow and lymph nodes, minus the tracheobronchial region. The respiratory tissue volume is tracheobronchial region, with an effective air volume given by multiplying by its tissue:air partition coefficient (= tissue:blood times blood:air). The slowly perfused tissue is the muscle and skin. This leaves a small (10–15% of body weight) unperfused volume that consists mostly of bone (minus marrow) and the GI tract contents. Baseline values are from Brown et al. (1997) (mouse and rat) and ICRP Publication 89 (2003) (human), except for volumes of the respiratory lumen, which are from Sarangapani et al. (2003).

[h]Derived from blood volume using FracPlas.

[i]Sum of all compartments except the blood and liver.

[j]Sum of all compartments except the liver.

[k]Mouse value is from pooling Abbas and Fisher (1997) and Fisher et al. (1991). Rat value is from pooling Sato et al. (1977), Gargas et al. (1989), Barton et al. (1995), Simmons et al. (2002), Koizumi (1989), and Fisher et al. (1989). Human value is from pooling Sato and Nakajima (1979), Sato et al. (1977), Gargas et al. (1989), Fiserova-Bergerova et al. (1984), Fisher et al. (1998), and Koizumi (1989).

[l]Mouse value is from Abbas and Fisher (1997). Rat value is from pooling Barton et al. (1995), Sato et al. (1977), and Fisher et al. (1989). Human value is from pooling Fiserova-Bergerova et al. (1984), Fisher et al. (1998), and Sato et al. (1977).

[m]Value is the geometric mean of liver and kidney (relatively high uncertainty) values.

[n]Mouse value is from Fisher et al. (1991). Rat value is from pooling Barton et al. (1995), Sato et al. (1977), and Fisher et al. (1989). Human value is from pooling Fiserova-Bergerova et al. (1984) and Fisher et al. (1998).

[o]Mouse value is geometric mean of liver and kidney values. Rat value is the brain value from Sato et al. (1977). Human value is the brain value from Fiserova-Bergerova et al. (1984).

[p]Mouse value is the lung value from Abbas and Fisher (1997). Rat value is the lung value from Sato et al. (1977). Human value is from pooling lung values from Fiserova-Bergerova et al. (1984) and Fisher et al. (1998).

[q]Mouse value is from Abbas and Fisher (1997). Rat value is from pooling Barton et al. (1995) and Sato et al. (1977). Human value is from pooling Fiserova-Bergerova et al. (1984) and Fisher et al. (1998).

[r]Mouse value is the muscle value from Abbas and Fisher (1997). Rat value is the muscle value from pooling Barton et al. (1995), Sato et al. (1977), and Fisher et al. (1989). Human value is the muscle value from pooling Fiserova-Bergerova et al. (1984) and Fisher et al. (1998).

[s]Scaling parameter is the effective partition coefficient between red blood cells and plasma. Thus, the TCA blood-plasma concentration ratio depends on the plasma fraction. Baseline value is based on the blood-plasma concentration ratio of 0.76 in rats (Schultz et al., 1999).

[t]In vitro partition coefficients were determined at high concentration, when plasma binding is saturated, so should reflect the free blood:tissue partition coefficient. To get the plasma partition coefficient, the partition coefficient is multiplied by the blood:plasma concentration ratio (TCAPlas). In vitro values were from Abbas and Fisher (1997) in the mouse (used for both mouse and rat) and from Fisher et al. (1998). Body values based on measurements in muscle.

[u]Values are based on the geometric mean of estimates based on data from Lumpkin et al. (2003), Schultz et al. (1999), Templin et al. (1995b; 1993), and Yu et al. (2000). Scaling parameter for B_{MAX} is actually the ratio of B_{MAX}/kD, which determines the binding at low concentrations.

[v]Data are from Abbas and Fisher (1997) in the mouse (used for the mouse and rat) and Fisher et al. (1998) (human).

[w]Used in vitro measurements in TCOH as a proxy, but higher uncertainty is noted.

[x]The scaling parameter (only used in the human model) is the effective partition coefficient for the "body" (nonblood) compartment, so that the distribution volume VDCVG is given by VBld + exp(lnPeffDCVG) × (VBod + VLiv).

Table A-4. PBPK model parameters, baseline values, and scaling relationships (continued)

[y]Baseline values have the following units: for V_{MAX}, mg/hr/kg liver; for K_M, mg/L blood; and for clearance (Cl), L/hr/kg liver (in humans, K_M is calculated from $K_M = V_{MAX}/(\exp(\text{lnClC}) \times \text{Vliv})$. Values are based on in vitro (microsomal and hepatocellular preparations) from Elfarra et al. (1998), Lipscomb et al. (1998b; 1998c, 1997). Scaling from in vitro data based on 32 mg microsomal protein/g liver and 99 × 106 hepatocytes/g liver (Barter et al., 2007). Scaling of K_M from microsomes were based on two methods: (1) assuming microsomal concentrations equal to liver tissue concentrations and (2) using the measured microsome:air partition coefficient and a central estimate of the blood:air partition coefficient. For K_M from human hepatocyte preparations, the measured hepatocyte:air partition coefficient and a central estimate of the blood:air partition coefficient was used.

[z]Scaling parameter is ratio of "DCA" to "non-DCA" oxidative pathway (where DCA is a proxy for oxidative metabolism not producing TCA or TCOH). Fraction of "other" oxidation is $\exp(\text{lnFracOtherC})/(1 + \exp[\text{lnFracOtherC}])$.

[aa]Scaling parameter is ratio of TCA to TCOH pathways. Baseline value based on geometric mean of Lipscomb et al. (1998b) using fresh hepatocytes and Bronley-DeLancey et al. (2006) using cryogenically-preserved hepatocytes. Fraction of oxidation to TCA is $(1 - \text{FracOther}) \times \exp(\text{lnFracTCAC})/(1 + \exp[\text{lnFracTCAC}])$.

[bb]Baseline values are based on in vitro data. In the mouse and rat, the only in vitro data are at 1 or 2 mM (Lash et al., 1998b; Lash et al., 1995). In most cases, rates at 2 mM were increased over the same sex/species at 1 mM, indicating V_{MAX} has not yet been reached. These data therefore put lower bounds on both V_{MAX} (in units of mg/hr/kg tissue) and clearance (in units of L/hr/kg tissue), so those are the scaling parameters used, with those bounds used as baseline values. For humans, data from Lash et al. (1999a) in the liver (hepatocytes) and the kidney (cytosol) and Green et al. (1997b) (liver cytosol) was used to estimate the clearance in units of L/hr/kg tissue and K_M in units of mg/L in blood.

[cc]Scaling parameter is the ratio of the lung to liver V_{MAX} (each in units of mg/hr), with baseline values based on microsomal preparations (mg/hr/mg protein) assayed at ~1 mM (Green et al., 1997b), further adjusted by the ratio of lung to liver tissue masses (Publication 89, ICRP, 2003; Brown et al., 1997).

[dd]Scaling parameter is the ratio of respiratory oxidation entering systemic circulation (translocated to the liver) to that locally cleared in the lung. Fraction of respiratory oxidation entering systemic circulation is $\exp(\text{lnFracLungSysC})/(1 + \exp[\text{lnFracLungSysC}])$.

[ee]Baseline parameters for urinary clearance (L/hr) were based on glomular filtration rate per unit body weight (L/hr/kg body weight) from Lin (1995), multiplied by the body weights cited in the study. For TCA, these were scaled by plasma volume to obtain the rate constant (/hr), since the model clears TCA from plasma. For TCOG, these were scaled by the effective distribution volume of the body (VBodTCOH × PBodTCOG) to obtain the rate constant (/hr), since the model clears TCOG from the body compartment.

[ff]Human model only.

[gg]Rat and human models only.

[hh]Baseline value for oral absorption scaling parameter are as follows: kTSD and kAS, 1.4/hr, based on human stomach half time of 0.5 hr; kAD, kASTCA, and kASTCOH, 0.75/hr, based on human small intestine transit time of 4 hrs (Publication 89, ICRP, 2003). These are noted to have very high uncertainty.

A.4.1.1. TCE Submodel

The TCE submodel is a whole-body, flow-limited PBPK model, with gas respiratory exchange, oral absorption, and metabolizing and nonmetabolizing tissues (see Figures A-6 and A-7).

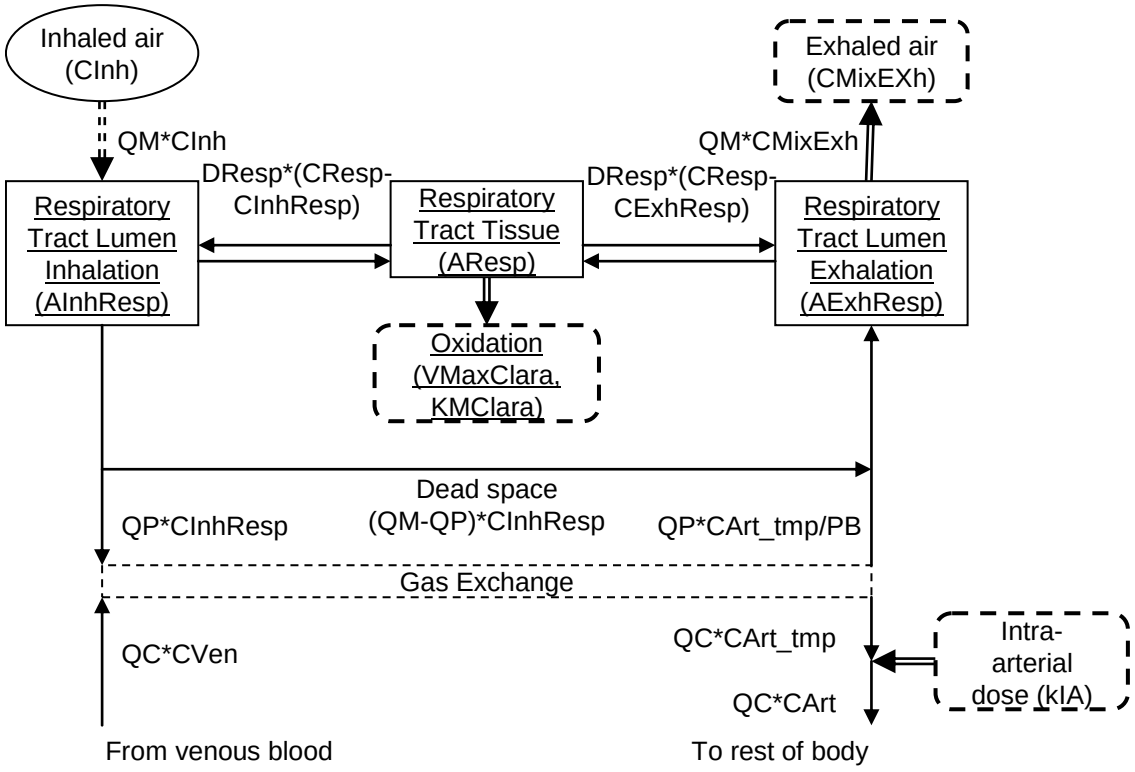

Figure A-6. Submodel for TCE gas exchange, respiratory metabolism, and arterial blood concentration.

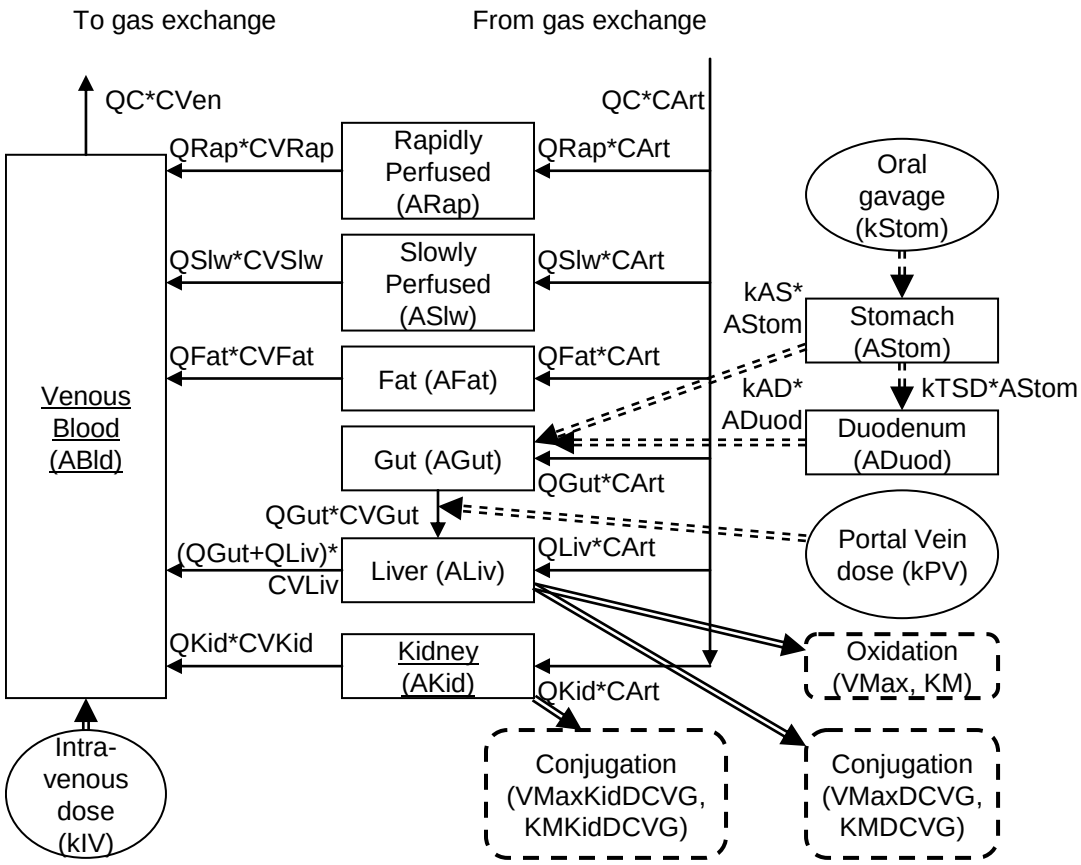

Figure A-7 Submodel for TCE oral absorption, tissue distribution, and metabolism.

A.4.1.1.1. Gas exchange, respiratory metabolism, arterial blood concentration, and closed-chamber concentrations

For an open-chamber concentration and a closed-chamber concentration of ACh/VCh, the rates of change for the amount in the respiratory lumen during inhalation (AInhResp, in mg), the amount in the respiratory tract tissue (AResp, in mg), and the respiratory lumen during exhalation (AExhResp, in mg) are given by the following:

$$d(AInhResp)/dt = (QM \times CInh + DResp \times (CResp - CInhResp) - QM \times CInhResp) \quad \text{(Eq. A-5)}$$

$$d(AResp)/dt = (DResp \times (CInhResp + CExhResp - 2 \times CResp) - RAMetLng) \quad \text{(Eq. A-6)}$$

$$d(AExhResp)/dt = (QM \times (CInhResp - CExhResp) + QP \times (CArt\_tmp/PB-CInhResp) + DResp \times (CResp-CExhResp)) \quad \text{(Eq. A-7)}$$

where

CInh = inhaled concentration (mg/L) = ACh/VCh + Conc
QM = minute volume (L/hour) = QP/0.7
CInhResp = concentration in respiratory lumen during inhalation (mg/L)
= AInhResp/VRespLum
CResp = concentration in respiratory tract tissue (mg/L)
= AResp/VRespEff
CExhResp = concentration in respiratory lumen during exhalation (mg/L)
= AExhResp/VRespLum
RAMetLng = rate of metabolism in respiratory tract tissue
= (V_{MAX}Clara × CResp)/(KMClara + CResp)
CArt_tmp = arterial blood concentration after gas exchange
= (QC × CVen + QP × CInhResp)/(QC + (QP/PB))

Because alveolar breath concentrations can include desorption from the respiratory tract tissue, the concentration at the alveolae (CArt_tmp/PB) may not equal the measured concentration in end-exhaled breath. It is therefore assumed that the ratio of the measured end-exhaled breath concentration to the concentration in the absence of desorption is the same as the ratio of the rate of TCE leaving the lumen to the rate of TCE entering the lumen:

$$CAlv/(CArt\_tmp/PB) = (QM \times CMixExh)/\{(QP \times CArt\_tmp/PB + (QM-QP) \times CInhResp)\} \quad \text{(Eq. A-8)}$$

That is, it is assumed that desorption occurs proportionally throughout the "breath." The concentration of arterial blood entering circulation needs to add the contribution from the i.a. dose (IADose in mg/kg, infused over a time period TChng):

$$CArt = CArt\_tmp + kIA/QC \quad \text{(Eq. A-9)}$$

where

kIA = (IADose × body weight)/TChng

For closed-chamber experiments, the additional differential equation for the amount in the chamber (ACh, in mg) is:

$$\mathbf{d(ACh)/dt = Rodents \times (QM \times CMixExh - QM \times ACh/VCh) - kLoss \times Ach} \quad \textbf{(Eq. A-10)}$$

where rodents is the number of animals in the chamber, and kLoss is the chamber loss rate (per hour).

A.4.1.1.2. Oral absorption to gut compartment

For oil-based gavage, the dose PDose is defined in terms of units of mg/kg, entering the stomach during a time TChng, with rates of change in the stomach (AStom, in mg) and duodenum (ADuod, in mg):

$$\mathbf{d(AStom)/dt = kStom - AStom \times (kAS + kTSD)} \qquad \textbf{(Eq. A-11)}$$

$$\mathbf{d(ADuod)/dt = (kTSD \times AStom) - kAD \times ADuod} \qquad \textbf{(Eq. A-12)}$$

where

kStom = rate of TCE entering stomach (mg/hour) = (PDose × body weight)/TChng

Note that there is absorption to the gut from both the stomach and duodenal compartments. Analogous equations are defined for aqueous gavage, with the expectation that absorption and transfer coefficients would differ with the different vehicle. In particular, the aqueous gavage dose PDoseAq is defined in terms of units of mg/kg, entering the stomach during a time TChng, with rates of change in the stomach (AStomAq, in mg) and duodenum (ADuodAq, in mg):

$$\mathbf{d(AStomAq)/dt = kStomAq - AStomAq \times (kASAq + kTSDAq)} \qquad \textbf{(Eq. A-13)}$$

$$\mathbf{d(ADuodAq)/dt = (kTSDAq \times AStomAq) - kADAq \times ADuodAq} \qquad \textbf{(Eq. A-14)}$$

where

kStomAq = rate of TCE entering stomach (mg/hour) = (PDoseAq × body weight)/TChng

For drinking water, the rate Drink is defined in terms of mg/kg-day, and it is assumed that absorption is direct to the gut:

$$kDrink = (Drink \times body\ weight)/24.0 \qquad \text{(Eq. A-15)}$$

Therefore, the total rate of absorption to the gut via oral exposure (RAO, in mg/hour) is:

$$RAO = kDrink + (kAS \times AStom) + (kAD \times ADuod) + (kASAq \times AStomAq) + (kADAq \times ADuodAq) \qquad \text{(Eq. A-16)}$$

The differential equation for the gut compartment (AGut, in mg) is, therefore, given by:

$$\mathbf{d(AGut)/dt = QGut \times (CArt - CVGut) + RAO} \qquad \textbf{(Eq. A-17)}$$

where

CVGut = concentration in the gut (mg/L) = AGut/VGut/PGut

A.4.1.1.3. Nonmetabolizing tissues

The differential equations for nonmetabolizing tissues (rapidly perfused, ARap, in mg; slowly perfused, ASlw, in mg; and fat, AFat, in mg) follow the standard flow-limited form:

$$\mathbf{d(ARap)/dt = QRap \times (CArt - CVRap)} \qquad \textbf{(Eq. A-18)}$$

$$\mathbf{d(ASlw)/dt = QSlw \times (CArt - CVSlw)} \qquad \textbf{(Eq. A-19)}$$

$$\mathbf{d(AFat)/dt = QFat \times (CArt - CVFat)} \qquad \textbf{(Eq. A-20)}$$

where

CVRap = venous blood concentration leaving rapidly perfused issues
= ARap/VRap/PRap

CVSlw = venous blood concentration leaving slowly perfused issues
= ASlw/VSlw/PSlw

CVFat = venous blood concentration leaving fat
= AFat/VFat/PFat

A.4.1.1.4. Liver compartment

The liver has two metabolizing pathways:

RAMetLiv1 = Rate of TCE oxidation by P450 in liver (mg/hour) (Eq. A-21)
$= (V_{MAX} \times CVLiv)/(KM + CVLiv)$

RAMetLiv2 = Rate of TCE metabolized to S-dichlorovinyl glutathione (DCVG_ in liver (mg/hour)
$= (V_{MAX}DCVG \times CVLiv)\ (KMDCVG + CVLiv)$ (Eq. A-22)

Some experiments also had portal vein dosing (PVDose in mg/kg, infused over a time period TChng), with a rate entering the liver of:

$$kPV = (PVDose \times body\ weight)/TChng \qquad \text{(Eq. A-23)}$$

The differential equation for TCE in liver (ALiv, in mg) is thus:

$$\mathbf{d(ALiv)/dt = (QLiv \times (CArt - CVLiv)) + (QGut \times (CVGut - CVLiv)) - RAMetLiv1 - RAMetLiv2 + kPV} \qquad \textbf{(Eq. A-24)}$$

where

CVLiv = venous blood concentration leaving liver
= ALiv/VLiv/PLiv

A.4.1.1.5. Kidney compartment

The kidney has one metabolizing pathway, GSH conjugation:

RAMetKid = Rate of TCE metabolized to DCVG in kidney (mg/hour) (Eq. A-25)
$= (V_{MAX}KidDCVG \times CVKid)/(KMKidDCVG + CVKid)$

The differential equation for TCE in kidney (AKid, in mg) is thus:

$$\mathbf{d(AKid)/dt = (QKid \times (CArt - CVKid)) - RAMetKid} \qquad \textbf{(Eq. A-26)}$$

where

CVKid = venous blood concentration leaving kidney = AKid/VKid/PKid

A.4.1.1.6. Venous blood compartment

The venous blood compartment (ABld, in mg) has inputs both from the venous blood exiting tissues as well as from an IV dose (IVDose in mg/kg infused during a time TChng), and output to the gas exchange region:

$$\mathbf{d(ABld)/dt = (QFat \times CVFat + QGutLiv \times CVLiv + QSlw \times CVSlw + QRap \times CVRap + QKid \times CVKid) + kIV - CVen \times QC} \quad \textbf{(Eq. A-27)}$$

where

kIV = IV infusion rate
= (IVDose × body weight)/TChng

CVen = concentration in mixed venous blood
= ABld/VBld

A.4.1.2. TCOH Submodel

The TCOH submodel is a simplified whole-body, flow-limited PBPK model, with only a body (ABodTCOH, in mg) and liver (ALivTCOH, in mg) compartment (see Figure A-8).

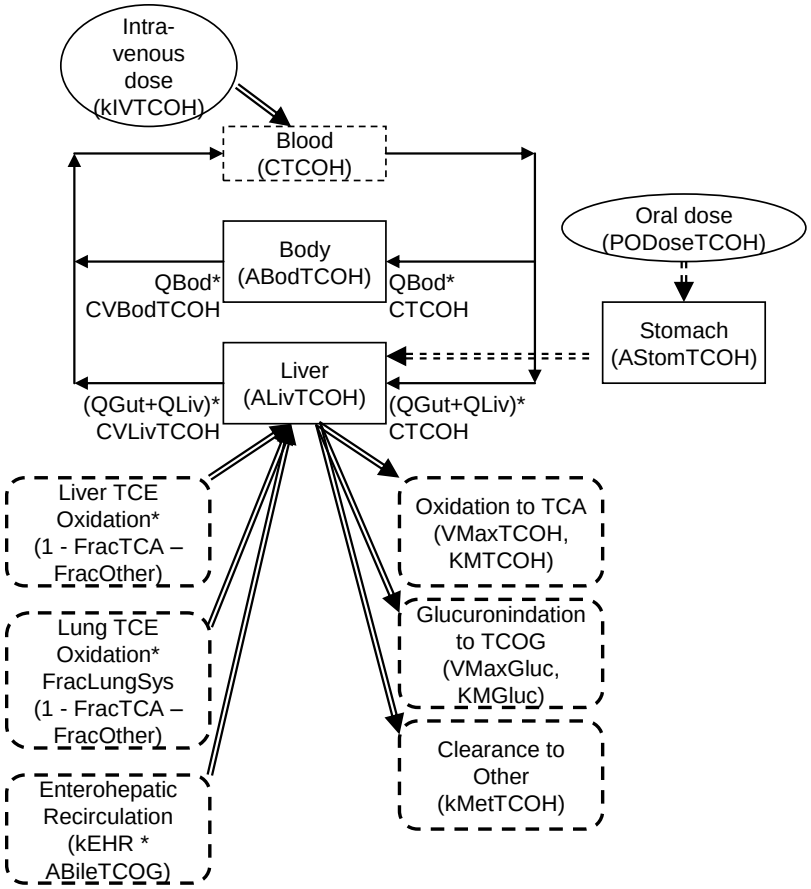

Figure A-8. Submodel for TCOH.

A.4.1.2.1. Blood concentration

The venous blood concentration, including an IV dose (IVDoseTCOH in mg/kg infused during a time TChng), is given by

$$CTCOH = (QBod \times CVBodTCOH + QGutLiv \times CVLivTCOH + kIVTCOH)/QC \quad \text{(Eq. A-28)}$$

where

CVBodTCOH = ABodTCOH/VBodTCOH/PBodTCOH
CVLivTCOH = ALivTCOH/VLiv/PLivTCOH
kIVTCOH = IV infusion rate
= (IVDoseTCOH × body weight)/TChng

and the partition coefficients for the body:blood and liver:blood are PBodTCOH and PLivTCOH, respectively, QGutLiv is the sum of the portal vein and hepatic artery blood flows, QBod is the remaining blood flow, VLiv is the liver volume, and VBodTCOH is the remaining perfused volume.

A.4.1.2.2. Body compartment

The rate of change of the amount of TCOH in the body compartment is

$$\mathbf{d(ABodTCOH)/dt = QBod \times (CTCOH - CVBodTCOH)} \quad \textbf{(Eq. A-29)}$$

A.4.1.2.3. Liver compartment

The liver has three metabolizing pathways:

$$RAMetTCOHTCA = \text{Rate of oxidation of TCOH to TCA (mg/hour)} = (V_{MAX}TCOH \times CVLivTCOH)/(KMTCOH + CVLivTCOH) \quad \text{(Eq. A-30)}$$

$$RAMetTCOHGluc = \text{Amount of glucuronidation to TCOG (mg/hour)} = (V_{MAX}Gluc \times CVLivTCOH)/(KMGluc + CVLivTCOH) \quad \text{(Eq. A-31)}$$

$$RAMetTCOH = \text{Amount of TCOH metabolized to other (e.g., DCA)} = kMetTCOH \times ALivTCOH \quad \text{(Eq. A-32)}$$

Some experiments also had oral dosing (PODoseTCOH in mg/kg, entering the stomach over a time TChng):

$$\mathbf{d(AStomTCOH)/dt = kStomTCOH - AStomTCOH \times kASTCOH} \quad \textbf{(Eq. A-33)}$$

$$kStomTCOH = (PODoseTCOH \times body\ weight)/TChng; \quad \text{(Eq. A-34)}$$

TCOH PO dose rate into stomach

kPOTCOH = AStomTCOH × kASTCOH; # TCOH oral absorption rate (mg/hour) (Eq. A-35)

In addition, there are three additional sources of TCOH:

Production in the liver from TCE (a fraction of hepatic oxidation) = (1.0 – FracOther – FracTCA) × StochTCOHTCE × RAMetLiv1 (Eq. A-36)

Production in the lung from TCE (a fraction of lung oxidation) = (1.0 – FracOther – FracTCA) × StochTCOHTCE × FracLungSys × RAMetLng (Eq. A-37)

Enterohepatic recirculation (rate kEHR) from TCOG in the bile (amount ABileTCOG) = StochTCOHGluc × RARecircTCOG = StochTCOHGluc × kEHR × ABileTCOG (Eq. A-38)

Note that StochTCOHTCE is the ratio of molecular weights of TCOH and TCE, StochTCOHGluc is the ratio of molecular weights of TCOH and TCOG, FracOther is the fraction of TCE oxidation not producing TCA or TCOH, FracTCA is the fraction of TCE oxidation producing TCA, and FracLungSys is the fraction of lung TCE oxidation that is translocated to the liver and not locally cleared.

The differential equation for TCOH in liver (ALivTCOH, in mg) is thus:

d(ALivTCOH)/dt = kPOTCOH + QGutLiv × (CTCOH – CVLivTCOH) (Eq. A-39)
- RAMetTCOH – RAMetTCOHTCA – RAMetTCOHGluc
+ ((1.0 – FracOther – FracTCA) × StochTCOHTCE
× (RAMetLiv1 + FracLungSys × RAMetLng))
+ (StochTCOHGluc × RARecircTCOG)

A.4.1.3. TCOG Submodel

The TCOG submodel is a simplified whole-body, flow-limited PBPK model, with body (ABodTCOG, in mg), liver (ALivTCOG, in mg), and bile (ABileTCOG) compartments (see Figure A-9).

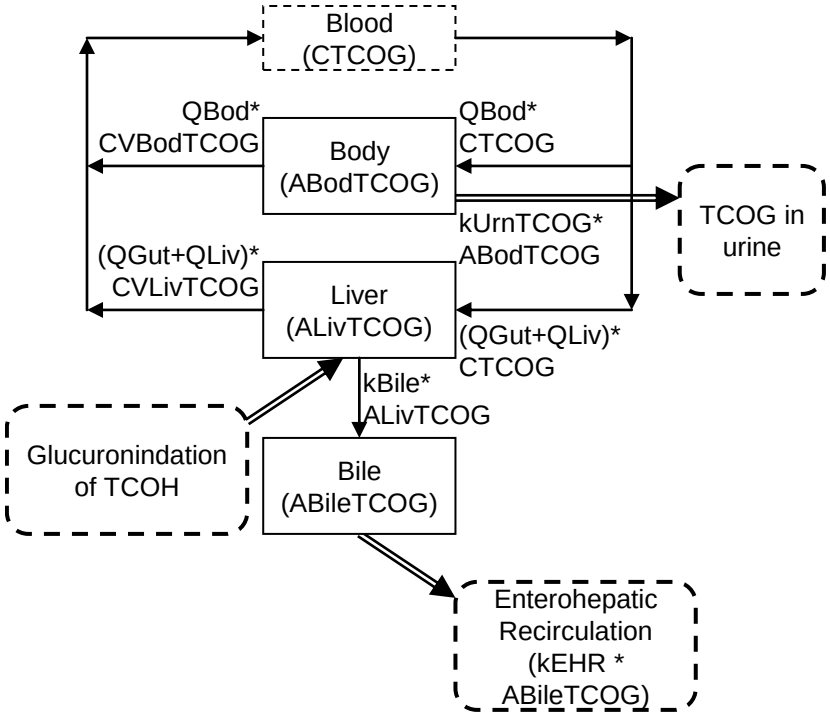

Figure A-9. Submodel for TCOG.

A.4.1.3.1. Blood concentration

The venous blood concentration is given by:

$$CTCOG = (QBod \times CVBodTCOG + QGutLiv \times CVLivTCOG)/QC \quad \text{(Eq. A-40)}$$

where

$CVBodTCOG = ABodTCOG/VBodTCOH/PBodTCOG$
$CVLivTCOG = ALivTCOG/VLiv/PLivTCOG$

and the partition coefficients for the body:blood and liver:blood are PBodTCOG and PLivTCOG, respectively, QGutLiv is the sum of the portal vein and hepatic artery blood flows, QBod is the remaining blood flow, VLiv is the liver volume, and VBodTCOH is the remaining perfused volume.

A.4.1.3.2. Body compartment

The body compartment is flow limited, with urinary excretion rate (mg/hour):

$$RUrnTCOG = kUrnTCOG \times ABodTCOG \quad \text{(Eq. A-41)}$$

So the rate of change of the amount of TCOG in the body compartment is:

$$\mathbf{d(ABodTCOG)/dt = QBod \times (CTCOG - CVBodTCOG) - RUrnTCOG} \quad \textbf{(Eq. A-42)}$$

Thus, the amount excreted in urine (AUrnTCOG, mg) is given by:

$$\mathbf{d(AUrnTCOG)/dt = RUrnTCOG} \qquad \textbf{(Eq. A-43)}$$

A.4.1.3.3. Liver compartment

The liver is flow limited, with one input, glucuronidation of TCOH (defined above in the TCOH submodel):

$$\text{StochGlucTCOH} \times \text{RAMetTCOHGluc} \qquad \text{(Eq. A-44)}$$

and one additional output, excretion in bile:

$$\text{RBileTCOG} = \text{rate of excretion in bile (mg/hour)} = \text{kBile} \times \text{ALivTCOG} \qquad \text{(Eq. A-45)}$$

The rate of change of the amount of TCOG in the liver is, therefore:

$$\mathbf{d(ALivTCOG)/dt = QGutLiv \times (CTCOG - CVLivTCOG) + (StochGlucTCOH \times RAMetTCOHGluc) - RBileTCOG} \qquad \textbf{(Eq. A-46)}$$

A.4.1.3.4. Bile compartment

The bile compartment has one input, excretion of TCOG in bile from the liver (defined above) and one output, enterohepatic recirculation to TCOH in the liver (defined above in the TCOH submodel), with rate of change:

$$\mathbf{d(ABileTCOG)/dt = RBileTCOG - RARecircTCOG} \qquad \textbf{(Eq. A-47)}$$

A.4.1.4. TCA Submodel

The TCA submodel is the same as that in Hack et al. (2006), with an error in the plasma flow to the liver corrected (see Figure A-10). In brief, TCA in plasma is assumed to undergo saturable plasma protein binding. TCA in tissues is assumed to be flow limited, but with the tissue partition coefficient reflecting equilibrium with the free concentration of TCA in plasma.

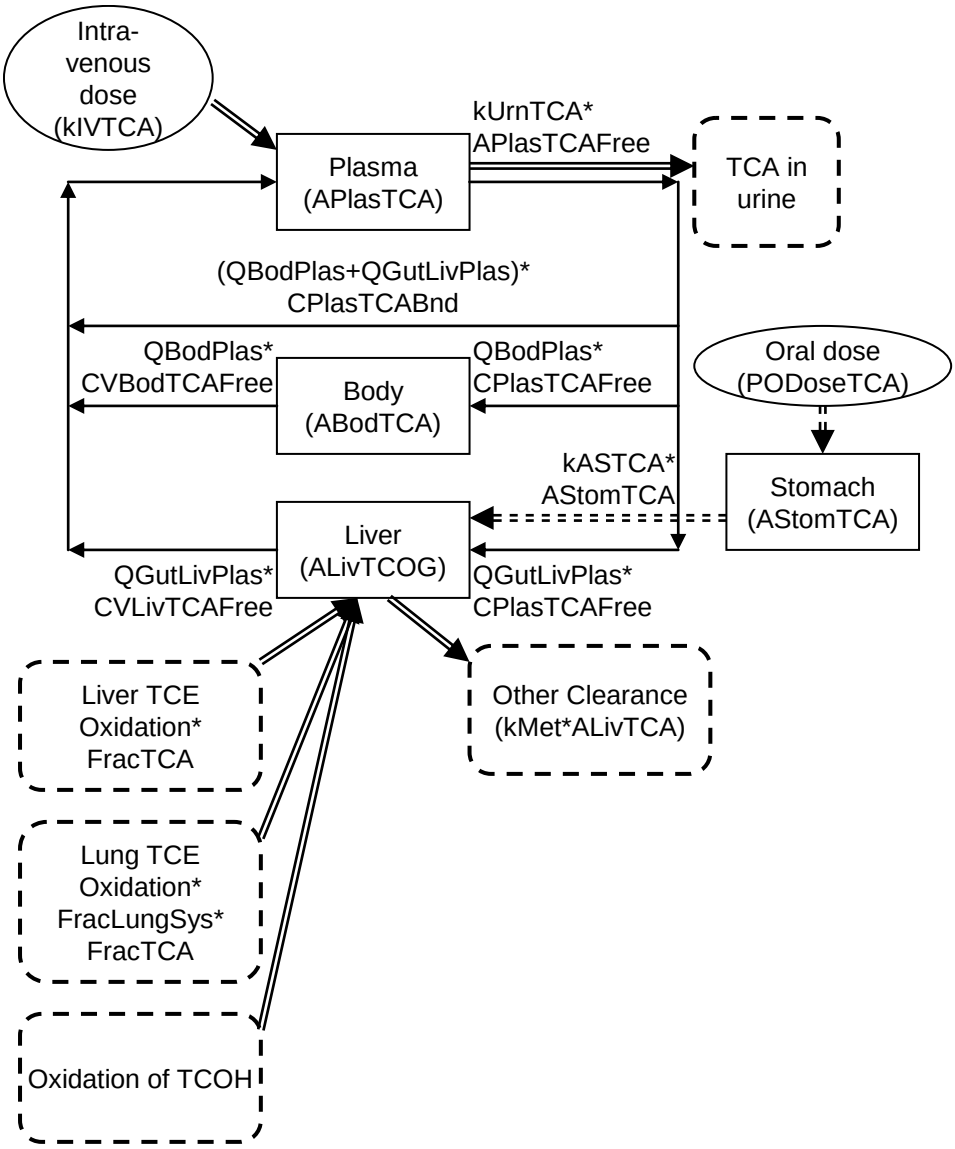

Figure A-10. **Submodel for TCA.**

A.4.1.4.1. Plasma binding and concentrations

For an i.v. dose of TCA given by IVDoseTCA (mg/kg during an infusion period of TChng), the rate of the change of the amount of total TCA in plasma (APlasTCA, in mg) is:

$$\mathbf{d(APlasTCA)/dt = kIVTCA + (QBodPlas \times CVBodTCA) + (QGutLivPlas \times CVLivTCA) - (QCPlas \times CPlasTCA) - RUrnTCAplas} \quad \textbf{(Eq. A-48)}$$

where

kIVTCA	= rate of IV infusion of TCA = (IVDoseTCA × body weight)/TChng
QBodPlas	= plasma flow from body = QBod × FracPlas
QGutLivPlas	= plasma flow from liver = (QGut + QLiv) × FracPlas
CVBodTCA	= venous concentration leaving body = CPlasTCABnd + CVBodTCAFree

CVBodTCAFree = free venous concentration leaving body
= (ABodTCA/VBod/PBodTCA)
CVLivTCA = venous concentration leaving liver
= CPlasTCABnd + CVLivTCAFree
CVLivTCAFree = free venous concentration leaving liver
= (ALivTCA/VLiv/PLivTCA)
QCPlas = total plasma flow
= QC × FracPlas
RUrnTCAplas = rate of urinary excretion of TCA from plasma
= kUrnTCA × APlasTCAFree

The free (CPlasTCAFree) and bound (CPlasTCABnd) concentrations are calculated from the total concentration (CPlasTCA = APlasTCA/VPlas) by solving the equations:

CPlasTCABndMole = BMax × CPlasTCAFreeMole/(kDissoc + CPlasTCAFreeMole) (Eq. A-49)

CPlasTCABndMole = CPlasTCAMole – CPlasTCAFreeMole (Eq. A-50)

Here the suffix "Mole" means that all concentrations are in micromole/L, because BMax and kDissoc in Table A-4 are given in those units. These lead to explicit solutions of:

CPlasTCAFreeMole = (sqrt(a × a + b) – a)/2 (Eq. A-51)

where
a = kDissoc + BMax – CPlasTCAMole
b = 4.0 × kDissoc × CPlasTCAMole
CPlasTCABlasTCAMoleCPlasTCAFreeMole

These concentrations are converted to mg/L (CPlasTCABnd, CPlasTCAFree) by multiplying by the molecular weight in mg/μmoles. The amount of free TCA in plasma is, thus:

APlasTCAFree = CPlasTCAFree × VPlas. (Eq. A-52)

Here, VPlas is derived from the blood volume and hematocrit (see Table A-4).

A.4.1.4.2. Urinary excretion

Urinary excretion is modeled as coming from the plasma compartment, so the rate of change of TCA in urine (AUrnTCA, in mg) is:

d(AUrnTCA)/dt = RUrnTCA **(Eq. A-53)**

where
RUrnTCA = RUrnTCAplas

For some human data (Chiu et al., 2007), urinary excretion was only collected during certain time periods, with data missing in other time periods. Thus, a switch UrnMissing was defined, which equals 0 during times of urine collection and 1 when urinary data are missing. The total amount of urinary TCA "collected" (AUrnTCA_collect, in mg) is, thus, given by:

$$\mathbf{d(AUrnTCA\_collect)/dt = (1\text{-}UrnMissing) \times RUrnTCA} \qquad \textbf{(Eq. A-54)}$$

A.4.1.4.3. Body compartment

The body compartment is flow limited, with the rate of change for the amount of TCA in the body (ABodTCA, in mg) given by:

$$\mathbf{d(ABodTCA)/dt = QBodPlas \times (CPlasTCAFree - CVBodTCAFree)} \qquad \textbf{(Eq. A-55)}$$

A.4.1.4.4. Liver compartment

The rate of change for the amount of TCA in the liver (ALivTCA, in mg) is given by:

$$\begin{aligned}\mathbf{d(ALivTCA)/dt} &= \mathbf{QGutLivPlas \times (CPlasTCAFree - CVLivTCAFree)} \qquad \textbf{(Eq. A-56)}\\ &+ \mathbf{(FracTCA \times StochTCATCE \times (RAMetLiv1 + FracLungSys \times RAMetLng))}\\ &+ \mathbf{(StochTCATCOH \times RAMetTCOHTCA) - RAMetTCA + kPOTCA}\end{aligned}$$

The first term reflects the free TCA in plasma flowing into and out of the liver compartment, the second term reflects production of TCA from liver (adjusted for molecular weights and fractional yield of TCA) and lung (adjusted for molecular weights, fraction of lung metabolism translocated to the liver, and fractional yield of TCA) metabolism of TCE, the third term reflects production of TCA from TCOH, the fourth term reflects other clearance of TCA from the liver, and the fifth term reflects absorption from the stomach of TCA. The contribution from liver metabolism of TCE is adjusted for molecular weights and production of oxidative metabolites other than TCA. The rate of clearance of TCA is given by:

$$\text{RAMetTCA} = \text{kMetTCA} \times \text{ALivTCA} \qquad \text{(Eq. A-57)}$$

The oral intake rate of TCA (mg/hour) includes a one-compartment stomach. So for an oral dose of PODoseTCA (in mg/kg), occurring over a time TChng, the rate of change of TCA in the stomach (AStomTCA, in mg) is given by:

$$\mathbf{d(AStomTCA)/dt = kStomTCA - AStomTCA \times kASTCA} \qquad \textbf{(Eq. A-58)}$$

where

kStomTCA = rate of input into stomach
= (PODoseTCA × body weight)/TChng

The rate of absorption into the liver is, thus,

$$kPOTCA = AStomTCA \times kASTCA \quad \text{(Eq. A-59)}$$

A.4.1.5. GSH Conjugation Submodel

The GSH conjugation submodel only tracks DCVG, DCVC, and urinary excretion of NAc-DCVC (see Figure A-11).

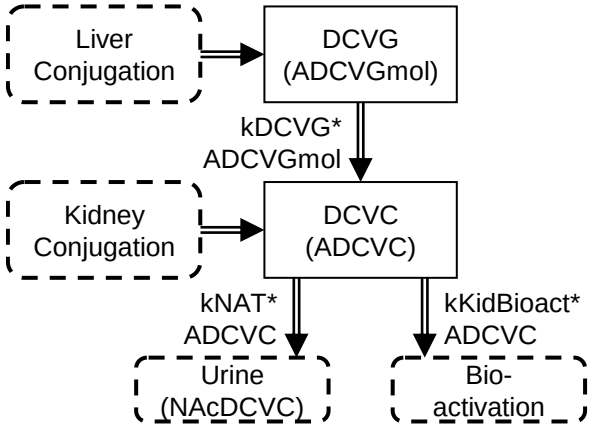

Figure A-11. Submodel for TCE GSH conjugation metabolites.

The rate of change for DCVG (ADCVGmol, in mmoles) depends on production from TCE in the liver and metabolism to DCVC:

$$\mathbf{d(ADCVGmol)/dt = RAMetLiv2/MWTCE - RAMetDCVGmol} \quad \textbf{(Eq. A-60)}$$

where

RAMetDCVGmol = rate of metabolism of DCVG to DCVC
= kDCVG × ADCVGmol

The rate of change of DCVC (ADCVC, in mg) depends on the production from TCE in the kidney (adjusted for molecular weights), production from DCVG, urinary excretion as NAc-DCVC (rate constant kNAT), and other bioactivation (rate constant kKidBioact):

$$\mathbf{d(ADCVC)/dt = RAMetDCVGmol \times MWDCVC + RAMetKid \times StochDCVCTCE - ((kNAT + kKidBioact) \times ADCVC)} \quad \textbf{(Eq. A-61)}$$

where

RAUrnDCVC = Rate of NAcDCVC excretion into urine
= kNAT × ADCVC

The rate of change of the amount of NAc-DCVC excreted (AUrnNDCVC, in mg) is given (adjusted for molecular weights) by:

$$\mathbf{d(AUrnNDCVC)/dt = StochN \times RAUrnDCVC} \qquad \textbf{(Eq. A-62)}$$

For the rat model, the DCVG compartment is "turned off" by setting kDCVG to an arbitrarily high value.

A.4.2. Model Parameters and Baseline Values

The multipage Table A-4 describes all the parameters of the updated PBPK model, their baseline values (which are used as central estimates in the prior distributions for the Bayesian analysis), and any scaling relationship used in their calculation. More detailed notes are included in the comments of the model code (see Section A.7).

A.4.3. Statistical Distributions for Parameter Uncertainty and Variability

A.4.3.1. Initial Prior Uncertainty in Population Mean Parameters

The following multipage Table A-5 describes the initial prior distributions for the population mean of the PBPK model parameters. For selected parameters, rat prior distributions were subsequently updated using the mouse posterior distributions, and human prior distributions were then updated using mouse and rat posterior distributions (see Section A.4.3.2).

A.4.3.2. Interspecies Scaling to Update Selected Prior Distributions in the Rat and Human

As shown in Table A-5, for several parameters, there is little or no in vitro or other prior information available to develop informative prior distributions, so many parameters had lognormal or log-uniform priors that spanned a wide range. Initially, the PBPK model for each species was run with the initial prior distributions in Table A-5, but, in the time available for analysis (up to about 100,000 iterations), only for the mouse did all of these parameters achieve adequate convergence. Additional preliminary runs indicated replacing the log-uniform priors with lognormal priors and/or requiring more consistency between species could lead to adequate convergence. However, an objective method of "centering" the lognormal distributions that did not rely on the in vivo data (e.g., via visual fitting or limited optimization) being calibrated against was necessary in order to minimize potential bias.

Therefore, the approach taken was to consider three species sequentially, from mouse to rat to human, and to use a model for interspecies scaling to update the prior distributions across species (the original prior distributions define the prior bounds). This sequence was chosen because the models are essentially "nested" in this order—the rat model adds to the mouse model the "downstream" GSH conjugation pathways, and the human model adds to the rat model the intermediary DCVG compartment. Therefore, for those parameters with little or no independent

data *only*, the mouse posteriors were used to update the rat priors, and both the mouse and rat posteriors were used to update the human priors. A list of the parameters for which this scaling was used to update prior distributions is contained in Table A-6, with the updated prior distributions. The correspondence between the "scaling parameters" and the physical parameters generally follows standard practice, and were explicitly described in Table A-4. For instance, V_{MAX} and clearance rates are scaled by body weight to the ¾ power, whereas K_M values are assumed to have no scaling, and rate constants (inverse time units) are scaled by body weight to the -¼ power.

Table A-5. Uncertainty distributions for the population mean of the PBPK model parameters

Scaling (sampled) parameter	Mouse			Rat			Human			Notes/ Source
	Distribution[a]	*SD or Min*	*Truncation (± nxSD) or Max*	Distribution	*SD or Min*	*Truncation (± nxSD) or Max*	Distribution	*SD or Min*	*Truncation (± nxSD) or Max*	
Flows										
lnQCC	TruncNormal	0.2	4	TruncNormal	0.14	4	TruncNormal	0.2	4	[a]
lnVPRC	TruncNormal	0.2	4	TruncNormal	0.3	4	TruncNormal	0.2	4	[a]
lnDRespC	Uniform	-11.513	2.303	Uniform	-11.513	2.303	Uniform	-11.513	2.303	[b]
Physiological blood flows to tissues										
QFatC	TruncNormal	0.46	2	TruncNormal	0.46	2	TruncNormal	0.46	2	[a]
QGutC	TruncNormal	0.17	2	TruncNormal	0.17	2	TruncNormal	0.18	2	[a]
QLivC	TruncNormal	0.17	2	TruncNormal	0.17	2	TruncNormal	0.45	2	[a]
QSlwC	TruncNormal	0.29	2	TruncNormal	0.3	2	TruncNormal	0.32	2	[a]
QKidC	TruncNormal	0.32	2	TruncNormal	0.13	2	TruncNormal	0.12	2	[a]
FracPlasC	TruncNormal	0.2	3	TruncNormal	0.2	3	TruncNormal	0.05	3	[c]
Physiological volumes										
VFatC	TruncNormal	0.45	2	TruncNormal	0.45	2	TruncNormal	0.45	2	[a]
VGutC	TruncNormal	0.13	2	TruncNormal	0.13	2	TruncNormal	0.08	2	[a]
VLivC	TruncNormal	0.24	2	TruncNormal	0.18	2	TruncNormal	0.23	2	[a]
VRapC	TruncNormal	0.1	2	TruncNormal	0.12	2	TruncNormal	0.08	2	[a]
VRespLumC	TruncNormal	0.11	2	TruncNormal	0.18	2	TruncNormal	0.2	2	[a]
VRespEffC	TruncNormal	0.11	2	TruncNormal	0.18	2	TruncNormal	0.2	2	[a]
VKidC	TruncNormal	0.1	2	TruncNormal	0.15	2	TruncNormal	0.17	2	[a]
VBldC	TruncNormal	0.12	2	TruncNormal	0.12	2	TruncNormal	0.12	2	[a]

Table A-5. Uncertainty distributions for the population mean of the PBPK model parameters (continued)

Scaling (sampled) parameter	Mouse			Rat			Human			Notes/ Source
	Distribution[a]	*SD or Min*	*Truncation (± nxSD) or Max*	Distribution	*SD or Min*	*Truncation (± nxSD) or Max*	Distribution	*SD or Min*	*Truncation (± nxSD) or Max*	
TCE distribution/partitioning										
lnPBC	TruncNormal	0.25	3	TruncNormal	0.25	3	TruncNormal	0.2	3	[d]
lnPFatC	TruncNormal	0.3	3	TruncNormal	0.3	3	TruncNormal	0.2	3	
lnPGutC	TruncNormal	0.4	3	TruncNormal	0.4	3	TruncNormal	0.4	3	
lnPLivC	TruncNormal	0.4	3	TruncNormal	0.15	3	TruncNormal	0.4	3	
lnPRapC	TruncNormal	0.4	3	TruncNormal	0.4	3	TruncNormal	0.4	3	
lnPRespC	TruncNormal	0.4	3	TruncNormal	0.4	3	TruncNormal	0.4	3	
lnPKidC	TruncNormal	0.4	3	TruncNormal	0.3	3	TruncNormal	0.2	3	
lnPSlwC	TruncNormal	0.4	3	TruncNormal	0.3	3	TruncNormal	0.3	3	
TCA distribution/partitioning										
lnPRBCPlasTCAC	Uniform	-4.605	4.605	TruncNormal	0.336	3	Uniform	-4.605	4.605	[e]
lnPBodTCAC	TruncNormal	0.336	3	TruncNormal	0.693	3	TruncNormal	0.336	3	[f]
lnPLivTCAC	TruncNormal	0.336	3	TruncNormal	0.693	3	TruncNormal	0.336	3	
TCA plasma binding										
lnkDissocC	TruncNormal	1.191	3	TruncNormal	0.61	3	TruncNormal	0.06	3	[g]
lnBMaxkDC	TruncNormal	0.495	3	TruncNormal	0.47	3	TruncNormal	0.182	3	
TCOH and TCOG distribution/partitioning										
lnPBodTCOHC	TruncNormal	0.336	3	TruncNormal	0.693	3	TruncNormal	0.336	3	
lnPLivTCOHC	TruncNormal	0.336	3	TruncNormal	0.693	3	TruncNormal	0.336	3	
lnPBodTCOGC	Uniform	-4.605	4.605	Uniform	-4.605	4.605	Uniform	-4.605	4.605	
lnPLivTCOGC	Uniform	-4.605	4.605	Uniform	-4.605	4.605	Uniform	-4.605	4.605	
DCVG distribution/partitioning										
lnPeffDCVG	Uniform	-6.908	6.908	Uniform	-6.908	6.908	Uniform	-6.908	6.908	[h]
TCE Metabolism										
lnV_{MAX}C	TruncNormal	0.693	3	TruncNormal	0.693	3	TruncNormal	0.693	3	[i]
lnK_MC	TruncNormal	1.386	3	TruncNormal	1.386	3				[i]
lnClC							TruncNormal	1.386	3	[i]
lnFracOtherC	Uniform	-6.908	6.908	Uniform	-6.908	6.908	Uniform	-6.908	6.908	[h]

Table A-5. Uncertainty distributions for the population mean of the PBPK model parameters (continued)

Scaling (sampled) parameter	Mouse			Rat			Human			Notes/ Source
	Distribution[a]	*SD or Min*	*Truncation (± nxSD) or Max*	Distribution	*SD or Min*	*Truncation (± nxSD) or Max*	Distribution	*SD or Min*	*Truncation (± nxSD) or Max*	
lnFracTCAC	TruncNormal	1.163	3	TruncNormal	1.163	3	TruncNormal	1.163	3	[j]
lnV_{MAX}DCVGC	Uniform	-4.605	9.21	Uniform	-4.605	9.21				[k]
lnClDCVGC	Uniform	-4.605	9.21	Uniform	-4.605	9.21	TruncNormal	4.605	3	[k]
lnK_MDCVGC							TruncNormal	1.386	3	[k]
lnV_{MAX}KidDCVGC	Uniform	-4.605	9.21	Uniform	-4.605	9.21				[k]
lnClKidDCVGC	Uniform	-4.605	9.21	Uniform	-4.605	9.21	TruncNormal	4.605	3	[k]
lnK_MKidDCVGC							TruncNormal	1.386	3	[k]
lnV_{MAX}LungLivC	TruncNormal	1.099	3	TruncNormal	1.099	3	TruncNormal	1.099	3	[l]
lnK_MClara	Uniform	-6.908	6.908	Uniform	-6.908	6.908	Uniform	-6.908	6.908	[h]
lnFracLungSysC	Uniform	-6.908	6.908	Uniform	-6.908	6.908	Uniform	-6.908	6.908	[h]
TCOH metabolism										
lnV_{MAX}TCOHC	Uniform	-9.21	9.21	Uniform	-9.21	9.21				[h]
lnClTCOHC							Uniform	-11.513	6.908	
lnK_MTCOH	Uniform	-9.21	9.21	Uniform	-9.21	9.21	Uniform	-9.21	9.21	
lnV_{MAX}GlucC	Uniform	-9.21	9.21	Uniform	-9.21	9.21				
lnClGlucC							Uniform	-9.21	4.605	
lnK_MGluc	Uniform	-6.908	6.908	Uniform	-6.908	6.908	Uniform	-6.908	6.908	[h]
lnkMetTCOHC	Uniform	-11.513	6.908	Uniform	-11.513	6.908	Uniform	-11.513	6.908	
TCA metabolism/clearance										
lnkUrnTCAC	Uniform	-4.605	4.605	Uniform	-4.605	4.605	Uniform	-4.605	4.605	[h]
lnkMetTCAC	Uniform	-9.21	4.605	Uniform	-9.21	4.605	Uniform	-9.21	4.605	
TCOG metabolism/clearance										
lnkBileC	Uniform	-9.21	4.605	Uniform	-9.21	4.605	Uniform	-9.21	4.605	[h]
lnkEHRC	Uniform	-9.21	4.605	Uniform	-9.21	4.605	Uniform	-9.21	4.605	
lnkUrnTCOGC	Uniform	-6.908	6.908	Uniform	-6.908	6.908	Uniform	-6.908	6.908	
DCVG metabolism										
lnFracKidDCVCC	Uniform	-6.908	6.908	Uniform	-6.908	6.908	Uniform	-6.908	6.908	[h]
lnkDCVGC	Uniform	-9.21	4.605	Uniform	-9.21	4.605	Uniform	-9.21	4.605	

Table A-5. Uncertainty distributions for the population mean of the PBPK model parameters (continued)

Scaling (sampled) parameter	Mouse			Rat			Human			Notes/ Source
	Distribution[a]	***SD or Min***	***Truncation (± nxSD) or Max***	**Distribution**	***SD or Min***	***Truncation (± nxSD) or Max***	**Distribution**	***SD or Min***	***Truncation (± nxSD) or Max***	
DCVC metabolism/clearance										
lnkNATC	Uniform	-9.21	4.605	Uniform	-9.21	4.605	Uniform	-9.21	4.605	[h]
lnkKidBioactC	Uniform	-9.21	4.605	Uniform	-9.21	4.605	Uniform	-9.21	4.605	
Oral uptake/transfer coefficients										
lnkTSD	Uniform	-4.269	4.942	Uniform	-4.269	4.942	Uniform	-4.269	4.942	[h]
lnkAS	Uniform	-6.571	7.244	Uniform	-6.571	7.244	Uniform	-6.571	7.244	
lnkTD	Uniform	-4.605	0	Uniform	-4.605	0	Uniform	-4.605	0	
lnkAD	Uniform	-7.195	6.62	Uniform	-7.195	6.62	Uniform	-7.195	6.62	
lnkASTCA	Uniform	-7.195	6.62	Uniform	-7.195	6.62	Uniform	-7.195	6.62	[h]
lnkASTCOH	Uniform	-7.195	6.62	Uniform	-7.195	6.62	Uniform	-7.195	6.62	

Explanatory note. All population mean parameters have either truncated normal (TruncNormal) or uniform distributions. For those with TruncNormal distributions, the mean for the population mean is 0 for natural-log transformed parameters (parameter name starting with "ln") and one for untransformed parameters, with the truncation at the specified number (n) of SDs. All uniformly distributed parameters are natural-log transformed, so their untransformed minimum and maximum are exp(Min) and exp(Max), respectively.

[a]Uncertainty based on coefficient of variation (CV) or range of values in Brown et al. (1997) (mouse and rat) and a comparison of values from ICRP Publication 89 (2003), Brown et al. (1997), and Price et al. (2003) (human).

[b]Noninformative prior distribution intended to span a wide range of possibilities because no independent data are available on these parameters. These priors for the rat and human were subsequently updated (see Section A.4.3.2).

[c]Because of potential strain differences, uncertainty in mice and rat assumed to be 20%. In humans, Price et al. (2003) reported variability of about 5%, and this is also used for the uncertainty in the mean.

[d]For partition coefficients, it is not clear whether interstudy variability is due to intersubject or assay variability, so uncertainty in the mean is based on interstudy variability among in vitro measurements. For single measurements, uncertainty SD of 0.3 was used for fat (mouse) and 0.4 for other tissues was used. In addition, where measurements were from a surrogate tissue (e.g., gut was based on liver and kidney), an uncertainty SD 0.4 was used.

[e]Single in vitro data point available in rats, so a GSD of 1.4 was used. In mice and humans, where no in vitro data was available, a noninformative prior was used.

[f]Single in vitro data points available in mice and humans, so a GSD of 1.4 was used. In rats, where the mouse data was used as a surrogate, a GSD of 2.0 was used, based on the difference between mice and rats in vitro.

[g]GSD for uncertainty based on different estimates from different in vitro studies.

[h]Noninformative prior distribution.

Table A-5. Uncertainty distributions for the population mean of the PBPK model parameters (continued)

[i]Assume twofold uncertainty GSD in V_{MAX}, based on observed variability and uncertainties of in vitro-to-in vivo scaling. For K_M and ClC, the uncertainty is assumed to be fourfold, due to the different methods for scaling of concentrations from TCE in the in vitro medium to TCE in blood.
[j]Uncertainty GSD of 3.2-fold reflects difference between in vitro measurements from Lipscomb et al. (1998b) and Bronley-DeLancey et al. (2006).
[k]In mice and rats, the baseline values are notional lower-limits on V_{MAX} and clearance, however, the lower bound of the prior distribution is set to 100-fold less because of uncertainty in in vitro-in vivo extrapolation, and because Green et al. (1997b) reported values 100-fold smaller than Lash et al. (1998b; 1995). In humans, the uncertainty GSD in clearance is assumed to be 100-fold, due to the difference between Lash et al. (1998b) and Green et al. (1997b). For K_M, the uncertainty GSD of fourfold is based on differences between concentrations in cells and cytosol.
[l]Uncertainty GSD of threefold was assumed due to possible differences in microsomal protein content, the fact that measurements were at a single concentration, and the fact that the human baseline values was based on the limit of detection.

Table A-6. Updated prior distributions for selected parameters in the rat and human

Scaling parameter	Initial prior bounds		Updated rat prior		Updated human prior	
	exp(min)	exp(max)	exp(μ)	exp(σ)	exp(μ)	exp(σ)
lnDRespC	1.0×10^{-5}	1.0×10^{1}	1.22	5.21	1.84	4.18
lnPBodTCOGC	1.0×10^{-2}	1.0×10^{2}	0.42	5.47	0.81	5.10
lnPLivTCOGC	1.0×10^{-2}	1.0×10^{2}	1.01	5.31	2.92	4.31
lnFracOtherC	1.0×10^{-3}	1.0×10^{3}	0.02	6.82	0.14	4.76
lnV_{MAX}DCVGC	1.0×10^{-2}	1.0×10^{4}	2.61	42.52		
lnClDCVGC	1.0×10^{-2}	1.0×10^{4}	0.36	15.03		
lnV_{MAX}KidDCVGC	1.0×10^{-2}	1.0×10^{4}	2.56	22.65		
lnClKidDCVGC	1.0×10^{-2}	1.0×10^{4}	1.22	15.03		
lnV_{MAX}LungLivC	3.7×10^{-2}	2.7×10^{1}	2.77	6.17	2.80	4.71
lnK_MClara	1.0×10^{-3}	1.0×10^{3}	0.01	6.69	0.02	4.85
lnFracLungSysC	1.0×10^{-3}	1.0×10^{3}	4.39	11.13	3.10	8.08
lnV_{MAX}TCOHC	1.0×10^{-4}	1.0×10^{4}	1.65	5.42		
lnClTCOHC	1.0×10^{-5}	1.0×10^{3}			0.37	4.44
lnK_MTCOH	1.0×10^{-4}	1.0×10^{4}	0.93	5.64	4.81	4.53
lnV_{MAX}GlucC	1.0×10^{-4}	1.0×10^{4}	69.41	5.58		
lnClGlucC	1.0×10^{-4}	1.0×10^{2}			3.39	4.35
lnK_MGluc	1.0×10^{-3}	1.0×10^{3}	30.57	6.11	11.13	4.57
lnkMetTCOHC	1.0×10^{-5}	1.0×10^{3}	3.35	5.87	2.39	4.62
lnkUrnTCAC	1.0×10^{-2}	1.0×10^{2}	0.11	5.42	0.09	4.22
lnkMetTCAC	1.0×10^{-4}	1.0×10^{2}	0.61	5.37	0.45	4.26
lnkBileC	1.0×10^{-4}	1.0×10^{2}	1.01	5.70	3.39	4.44
lnkEHRC	1.0×10^{-4}	1.0×10^{2}	0.01	6.62	0.22	4.71
lnkUrnTCOGC	1.0×10^{-3}	1.0×10^{3}	8.58	6.05	16.12	4.81
lnkNATC	1.0×10^{-4}	1.0×10^{2}			0.00	6.11
lnkKidBioactC	1.0×10^{-4}	1.0×10^{2}			0.01	6.49

Notes: updated rat prior is based on the mouse posterior; and the updated human priors are based on combining the mouse and rat posteriors, except in the case of lnkNATC and lnkKidBioactC, which are unidentified in the mouse model. Columns labeled exp(min) and exp(max) are the exponentiated prior bounds; columns labeled exp(μ) and exp(σ) are the exponentiated mean and SD of the updated prior distributions, which are normal distributions truncated at the prior bounds.

The scaling model is given explicitly as follows. If θ_i are the "scaling" parameters (usually also natural-log-transformed) that are actually estimated, and A is the "universal" (species-independent) parameter, then $\theta_i = A + \varepsilon_I$, where ε_i is the species-specific "departure" from the scaling relationship, assumed to be normally distributed with variance σ_ε^2. This "scatter" in the interspecies scaling relationship is assumed to have a SD of 1.15 = ln(3.16), so that the unlogarithmically transformed 95% CI spans about 100-fold (i.e., $\exp(2\sigma) = 10$). This implies that 95% of the time, the species-specific scaling parameter is assumed be within 10-fold higher or lower than the "species-independent" value. However, the prior bounds, which

generally span a wider range, are maintained so that if the data strongly imply an extreme species-specific value, they can be accommodated. In addition, the model transfers the marginal distributions for each parameter across species, so correlations between parameters are not retained. This is a restriction on the software used for conducting MCMC analyses, however, assuming independence will lead to a "broader" joint distribution, given the same marginal distributions. Thus, this assumption tends to reduce the weight of the interspecies scaling as compared to the species-specific calibration data.

Therefore, the mouse model gives an initial estimate of "A," which is used to update the prior distribution for $\theta_r = A + \varepsilon_r$ in the rat (alternatively, since there is only one species at this stage, one could think of this as estimating the rat parameter using the mouse parameter, but with a cross-species variance is twice the allometric scatter variance). The rat and mouse together then give a "better" estimate of A, which is used to update the prior distribution for $\theta_h = A + \varepsilon_h$ in the human, with the assumed distribution for ε_h. This approach is implemented by approximating the posterior distributions by normal distributions, deriving heuristic "data" for the specific-specific parameters, and then using these pseudo-data to derive updated prior distributions for the other species parameters. Specifically, the procedure is as follows:

1. Run the mouse model.
2. Use the mouse posterior to derive the mouse "pseudo-data" D_m (equal to the posterior mean) and its uncertainty σ_m^2 (equal to the posterior variance).
3. Use the D_m as the prior mean for the rat. The prior variance for the rat is $2\sigma_\varepsilon^2 + \sigma_m^2$, which accounts for two components of species-specific departure from "species-independence" (one each for mouse and rat), and the mouse posterior uncertainty.
4. Match the rat posterior mean and variance to the values derived from the normal approximation (posterior mean = $\{D_m/(2\sigma_\varepsilon^2 + \sigma_m^2) + D_r/\sigma_r^2\}/\{1/(2\sigma_\varepsilon^2 + \sigma_m^2) + 1/\sigma_r^2\}$; posterior variance = $\{1/(2\sigma_\varepsilon^2 + \sigma_m^2) + 1/\sigma_r^2\}^{-1}$), and solve for the rat "data" D_r and its uncertainty σ_r^2.
5. Use, σ_m^2, and σ_r^2 to derive the updated prior mean and variance for the human model. For the mean ($=\{D_m/(\sigma_\varepsilon^2 + \sigma_m^2) + D_r/(\sigma_\varepsilon^2 + \sigma_r^2)\}/\{1/(\sigma_\varepsilon^2 + \sigma_m^2) + 1/(\sigma_\varepsilon^2 + \sigma_r^2)\}$), it is the weighted average of the mouse and rat, with each weight including both posterior uncertainty and departure from "species-independence." For the variance ($=\{1/(\sigma_\varepsilon^2 + \sigma_m^2) + 1/(\sigma_\varepsilon^2 + \sigma_r^2)\}^{-1} + \sigma_\varepsilon^2$), it is the variance in the weighted average of the mouse and rat plus an additional component of species-specific departure from "species-independence."

Formally, then, the probability of θ_i given A can be written as:

$$P(\theta_i \mid A) = \varphi(\theta_i - A, \sigma_\varepsilon^2) \qquad \text{(Eq. A-63)}$$

where $\varphi(x, \sigma^2)$ is the normal density centered on 0 with variance σ^2. Let D_i be a heuristic "datum" for species *i*, so the likelihood given θ_i is adequately approximated by:

$$P(D_i \mid \theta_i) = \varphi(D_i - \theta_i, \sigma_i^2) \qquad \text{(Eq. A-64)}$$

Therefore, considering A to have a uniform prior distribution, then running the mouse model gives a posterior of the form:

$$P(A, \theta_m \mid D_m) \propto P(A)\, P(\theta_m \mid A)\, P(D_m \mid \theta_m) \propto \varphi(\theta_m - A, \sigma_\varepsilon^2)\, \varphi(D_m - \theta_m, \sigma_m^2) \qquad \text{(Eq. A-65)}$$

From the MCMC posterior, the values of D_m and σ_m^2 are simply the mean and variance of the scaled parameter θ_m.

Now, adding the rat data gives:

$$P(A, \theta_m, \theta_r \mid D_m, D_r) \propto P(A)\, P(\theta_m \mid A)\, P(D_m \mid \theta_m)\, P(\theta_r \mid A)\, P(D_r \mid \theta_r) \qquad \text{(Eq. A-66)}$$
$$\propto \varphi(\theta_m - A, \sigma_\varepsilon^2)\, \varphi(D_m - \theta_m, \sigma_m^2)\, \varphi(\theta_r - A, \sigma_\varepsilon^2)\, \varphi(D_r - \theta_r, \sigma_r^2)$$

D_r and σ_r^2 can be derived by marginalizing first over θ_m and then over *A*:

$$\int P(A, \theta_m, \theta_r \mid D_m, D_r)\, d\theta_m\, dA \qquad \text{(Eq. A-67)}$$
$$\propto [\int P(A)\, \{\int P(\theta_m \mid A)\, P(D_m \mid \theta_m)\, d\theta_m\}\, P(\theta_r \mid A)\, dA\,] P(D_r \mid \theta_r)$$
$$= [\int P(A)\, P(D_m \mid A)\, P(\theta_r \mid A)\, dA]\, P(D_r \mid \theta_r)$$
$$\propto [\int P(A \mid D_m)\, P(\theta_r \mid A)\, dA]\, P(D_r \mid \theta_r)$$
$$= P(\theta_r \mid D_m)\, P(D_r \mid \theta_r)$$

So $P(\theta_r \mid D_m)$ can be identified as the prior for θ_r based on the mouse data, and $P(D_r \mid \theta_r)$ as the rat-specific likelihood. The updated prior for the rats is then:

$$P(\theta_r \mid D_m) \propto \int \varphi(\theta_m - A, \sigma_\varepsilon^2)\, \varphi(D_m - \theta_m, \sigma_m^2)\, \varphi(\theta_r - A, \sigma_\varepsilon^2)\, d\theta_m\, dA \qquad \text{(Eq. A-68)}$$
$$= \int \varphi(D_m - A, \sigma_\varepsilon^2 + \sigma_m^2)\, \varphi(\theta_r - A, \sigma_\varepsilon^2)\, dA$$
$$= \varphi(D_m - \theta_r, 2\sigma_\varepsilon^2 + \sigma_m^2)$$

Therefore, for the "mouse-based" prior, use the mean D_m from the mouse, and then the variance from the mouse σ_m^2 plus twice the "allometric scatter" variance σ_ε^2.

The rat "data" and variance, assuming conditional independence of the rat and mouse "pseudo-data," is thus:

$$P(\theta_r \mid D_m, D_r) \propto P(\theta_r \mid D_m)\, P(D_r \mid \theta_r) \qquad \text{(Eq. A-69)}$$
$$\propto \varphi(D_m - \theta_r, 2\sigma_\varepsilon^2 + \sigma_m^2)\, \varphi(D_r - \theta_r, \sigma_r^2)$$

This distribution is also normal with:

$$E(\theta_r) = \{D_m/(2\sigma_\varepsilon^2 + \sigma_m^2) + D_r/\sigma_r^2\}/\{1/(2\sigma_\varepsilon^2 + \sigma_m^2) + 1/\sigma_r^2\} \quad \text{(Eq. A-70)}$$

= weighted mean of D_r

$$\mathrm{VAR}(\theta_r) = \{1/(2\sigma_\varepsilon^2 + \sigma_m^2) + 1/\sigma_r^2\}^{-1} \quad \text{(Eq. A-71)}$$

= harmonic mean of variances

Thus, using the mean and variance of the posterior distribution from the MCMC analysis, D_r and σ_r^2 can be derived.

Now, D_m, σ_m^2, D_r, and σ_r^2 are known, so the analogous "mouse + rat" based prior used in the human model can be derived. As with the rat prior, the human prior is based on a normal approximation of the posterior for *A*, and then incorporates a random term for cross-species variation (allometric scatter):

$$P(A, \theta_m, \theta_r, \theta_h \mid D_m, D_r, D_h) \quad \text{(Eq. A-72)}$$
$$\propto P(A)\, P(\theta_m \mid A)\, P(D_m \mid \theta_m)\, P(\theta_r \mid A)\, P(D_r \mid \theta_r)\, P(\theta_h \mid A)\, P(D_h \mid \theta_h)$$
$$\propto \varphi(\theta_m - A, \sigma_\varepsilon^2)\, \varphi(D_m - \theta_m, \sigma_m^2)\, \varphi(\theta_r - A, \sigma_\varepsilon^2)\, \varphi(D_r - \theta_r, \sigma_r^2)$$
$$\varphi(\theta_h - A, \sigma_\varepsilon^2)\, \varphi(D_h - \theta_h, \sigma_h^2)$$

Consider marginalizing first over θ_m, then over θ_r, and then over A:

$$\int P(A, \theta_m, \theta_r, \theta_h \mid D_m, D_r, D_h)\, d\theta_m\, d\theta_r\, dA \quad \text{(Eq. A-73)}$$
$$\propto [\int P(A)\, \{\int P(\theta_m \mid A)\, P(D_m \mid \theta_m)\, d\theta_m\}\, \{\int P(\theta_r \mid A)\, P(D_r \mid \theta_r)\, d\theta_r\}\, P(\theta_h \mid A)\, dA$$
$$P(D_h \mid \theta_h)$$
$$= [\int P(A)\, P(D_m \mid A)\, P(D_r \mid A)\, P(\theta_h \mid A)\, dA\,]\, P(D_h \mid \theta_h)$$
$$\propto [\int P(A \mid D_m D_r)\, P(\theta_h \mid A)\, dA]\, P(D_h \mid \theta_h)$$
$$= P(\theta_h \mid D_m D_r)\, P(D_h \mid \theta_h)$$

So $P(\theta_h \mid D_m D_r)$ is the prior for θ_h based on the mouse and rat data, and $P(D_h \mid \theta_h)$ as the human-specific likelihood. The prior is used in the MCMC analysis for the humans, and it is derived to be:

$$P(\theta_h \mid D_m D_r) \propto \int \varphi(\theta_m - A, \sigma_\varepsilon^2)\, \varphi(D_m - \theta_m, \sigma_m^2)\, \varphi(\theta_r - A, \sigma_\varepsilon^2)\, \varphi(D_r - \theta_r, \sigma_r^2) \quad \text{(Eq. A-74)}$$
$$\varphi(\theta_h - A, \sigma_\varepsilon^2)\, d\theta_m\, d\theta_r\, dA$$
$$= \int [\varphi(D_m - A, \sigma_\varepsilon^2 + \sigma_m^2)\, \varphi(D_r - A, \sigma_\varepsilon^2 + \sigma_r^2)]\, \varphi(\theta_h - A, \sigma_\varepsilon^2)\, dA$$
$$\propto \int \varphi(D_{m+r} - A, \sigma_{m+r}^2)\, \varphi(\theta_h - A, \sigma_\varepsilon^2)\, dA$$
$$= \varphi(D_{m+r} - \theta_h, \sigma_{m+r}^2 + \sigma_\varepsilon^2)$$

where D_{m+r} and σ_{m+r}^2 are the weighted mean and variances of *A* under the density:

$$[\varphi(D_m - A, \sigma_\varepsilon^2 + \sigma_m^2)\, \varphi(D_r - A, \sigma_\varepsilon^2 + \sigma_r^2)] \quad \text{(Eq. A-75)}$$

which is given by:

$$D_{m+r} = E(A|\, D_m\, D_r) = \{D_m/(\sigma_\varepsilon^2 + \sigma_m^2) + D_r/(\sigma_\varepsilon^2 + \sigma_r^2)\}/\{1/(\sigma_\varepsilon^2 + \sigma_m^2) + 1/(\sigma_\varepsilon^2 + \sigma_r^2)\}$$
$$= \text{weighted mean of } D_m \text{ and } D_r$$
$$\sigma_{m+r}^2 = \text{VAR}(A|\, D_m\, D_r) = \{1/(\sigma_\varepsilon^2 + \sigma_m^2) + 1/(\sigma_\varepsilon^2 + \sigma_r^2)\}^{-1}$$
$$= \text{harmonic mean of variances}$$

At this point, these values are used in the normal approximation of the combined rodent posterior, which will be incorporated into the cross-species extrapolation as described in Step 5 above.

The results of these calculations for the updated prior distributions, are shown in Table A-6. With this methodology for updating the prior distributions, adequate convergence was achieved for the rat and human after 110,000~140,000 iterations.

A.4.3.3. Population Variance: Prior Central Estimates and Uncertainty

The following multipage Table A-7 describes the uncertainty distributions used for the population variability in the PBPK model parameters.

Table A-7. Uncertainty distributions for the population variance of the PBPK model parameters

Scaling (sampled) parameter	Mouse		Rat		Human		Notes/source
	CV	CU	CV	CU	CV	CU	
Flows							
lnQCC	0.2	2	0.14	2	0.2	2	[a]
lnVPRC	0.2	2	0.3	2	0.2	2	
lnDRespC	0.2	0.5	0.2	0.5	0.2	0.5	
Physiological blood flows to tissues							
QFatC	0.46	0.5	0.46	0.5	0.46	0.5	[a]
QGutC	0.17	0.5	0.17	0.5	0.18	0.5	
QLivC	0.17	0.5	0.17	0.5	0.45	0.5	
QSlwC	0.29	0.5	0.3	0.5	0.32	0.5	
QKidC	0.32	0.5	0.13	0.5	0.12	0.5	
FracPlasC	0.2	0.5	0.2	0.5	0.05	0.5	
Physiological volumes							
VFatC	0.45	0.5	0.45	0.5	0.45	0.5	[a]
VGutC	0.13	0.5	0.13	0.5	0.08	0.5	
VLivC	0.24	0.5	0.18	0.5	0.23	0.5	
VRapC	0.1	0.5	0.12	0.5	0.08	0.5	
VRespLumC	0.11	0.5	0.18	0.5	0.2	0.5	
VRespEffC	0.11	0.5	0.18	0.5	0.2	0.5	
VKidC	0.1	0.5	0.15	0.5	0.17	0.5	
VBldC	0.12	0.5	0.12	0.5	0.12	0.5	

Table A-7. Uncertainty distributions for the population variance of the PBPK model parameters (continued)

Scaling (sampled) parameter	Mouse		Rat		Human		Notes/source
	CV	CU	CV	CU	CV	CU	
TCE distribution/partitioning							
lnPBC	0.25	2	0.25	0.333	0.185	0.333	[b]
lnPFatC	0.3	2	0.3	0.333	0.2	1	
lnPGutC	0.4	2	0.4	2	0.4	2	
lnPLivC	0.4	2	0.15	0.333	0.4	1.414	
lnPRapC	0.4	2	0.4	2	0.4	2	
lnPRespC	0.4	2	0.4	2	0.4	2	
lnPKidC	0.4	2	0.3	0.577	0.2	1.414	
lnPSlwC	0.4	2	0.3	0.333	0.3	1.414	
TCA distribution/partitioning							
lnPRBCPlasTCAC	0.336	2	0.336	2	0.336	2	[c]
lnPBodTCAC	0.336	2	0.693	2	0.336	2	[b]
lnPLivTCAC	0.336	2	0.693	2	0.336	2	
TCA plasma binding							
lnkDissocC	1.191	2	0.61	2	0.06	2	[b]
lnBMaxkDC	0.495	2	0.47	2	0.182	2	
TCOH and TCOG distribution/partitioning							
lnPBodTCOHC	0.336	2	0.693	2	0.336	2	[b]
lnPLivTCOHC	0.336	2	0.693	2	0.336	2	[b]
lnPBodTCOGC	0.4	2	0.4	2	0.4	2	[d]
lnPLivTCOGC	0.4	2	0.4	2	0.4	2	[d]
DCVG distribution/partitioning							
lnPeffDCVG	0.4	2	0.4	2	0.4	2	[b]
TCE metabolism							
lnV_{MAX}C	0.824	1	0.806	1	0.708	0.26	[e]
lnK_MC	0.270	1	1.200	1			
lnClC					0.944	1.41	
lnFracOtherC	0.5	2	0.5	2	0.5	2	[f]
lnFracTCAC	0.5	2	0.5	2	1.8	2	[g]
lnV_{MAX}DCVGC	0.5	2	0.5	2			[f]
lnClDCVGC	0.5	2	0.5	2	0.5	2	
lnK_MDCVGC					0.5	2	
lnV_{MAX}KidDCVGC	0.5	2	0.5	2			
lnClKidDCVGC	0.5	2	0.5	2	0.5	2	
lnK_MKidDCVGC					0.5	2	
lnV_{MAX}LungLivC	0.5	2	0.5	2	0.5	2	
lnK_MClara	0.5	2	0.5	2	0.5	2	
lnFracLungSysC	0.5	2	0.5	2	0.5	2	

Table A-7. Uncertainty distributions for the population variance of the PBPK model parameters (continued)

Scaling (sampled) parameter	Mouse		Rat		Human		Notes/source
	CV	CU	CV	CU	CV	CU	
TCOH metabolism							
lnV_{MAX}TCOHC	0.5	2	0.5	2			[f]
lnClTCOHC					0.5	2	
lnK_MTCOH	0.5	2	0.5	2	0.5	2	
lnV_{MAX}GlucC	0.5	2	0.5	2			
lnClGlucC					0.5	2	
lnK_MGluc	0.5	2	0.5	2	0.5	2	
lnkMetTCOHC	0.5	2	0.5	2	0.5	2	
TCA metabolism/clearance							
lnkUrnTCAC	0.5	2	0.5	2	0.5	2	[f]
lnkMetTCAC	0.5	2	0.5	2	0.5	2	
TCOG metabolism/clearance							
lnkBileC	0.5	2	0.5	2	0.5	2	[f]
lnkEHRC	0.5	2	0.5	2	0.5	2	
lnkUrnTCOGC	0.5	2	0.5	2	0.5	2	[f]
DCVG metabolism/clearance							
lnFracKidDCVCC	0.5	2	0.5	2	0.5	2	[f]
lnkDCVGC	0.5	2	0.5	2	0.5	2	
DCVC metabolism/clearance							
lnkNATC	0.5	2	0.5	2	0.5	2	[f]
lnkKidBioactC	0.5	2	0.5	2	0.5	2	
Oral uptake/transfer coefficients							
lnkTSD	2	2	2	2	2	2	[h]
lnkAS	2	2	2	2	2	2	
lnkTD	2	2	2	2	2	2	
lnkAD	2	2	2	2	2	2	
lnkASTCA	2	2	2	2	2	2	
lnkASTCOH	2	2	2	2	2	2	

Explanatory note. All population variance parameters (V_pname, for parameter "pname") have Inverse-Gamma distributions, with the expected value given by CV and coefficient of uncertainty given by CU (i.e., SD of V_pname divided by expected value of V_pname) (notation the same as Hack et al. (2006)). Under these conditions, the Inverse-Gamma distribution has a shape parameter is given by $\alpha = 2 + 1/CU^2$ and scale parameter $\beta = (\alpha I - 1)\ CV^2$. In addition, it should be noted that, under a normal distribution and a uniform prior distribution on the population variance, the posterior distribution for the variance given n data points with a sample variance s^2 is given by and Inverse-Gamma distribution with $\alpha = (n - 1)/2$ and $\beta = \alpha\ s^2$. Therefore, the "effective" number of data points is given by $n = 5 + 2/CU^2$ and the "effective" sample variance is $s^2 = CV^2\ \alpha\omega\eta\alpha\tau/(\alpha - 1)$.

[a]For physiological parameters, CV values generally taken to be equal to the uncertainty SD in the population mean, most of which were based on variability between studies (i.e., not clear whether variability represents uncertainty or variability). Given this uncertainty, CU of 2 assigned to cardiac output and ventilation-perfusion, while CU of 0.5 assigned to the remaining physiological parameters.

Table A-7. Uncertainty distributions for the population variance of the PBPK model parameters (continued)

[b]As discussed above, it is not clear whether interstudy variability is due to intersubject or assay variability, so the same central were assigned to the uncertainty in the population mean as to the central estimate of the population variance. In the cases where direct measurements were available, the CU for the uncertainty in the population variance is based on the actual sample n, with the derivation discussed in the notes preceding this table. Otherwise, a CU of 2 was assigned, reflecting high uncertainty.
[c]Used value from uncertainty in population in mean in rats for all species with high uncertainty.
[d]No data, so assumed CV of 0.4 with high uncertainty.
[e]For mice and rats, based on variability in results from Lipscomb et al. (1998c) and Elfarra et al. (1998) in microsomes. Since only pooled or mean values are available, CU of one was assigned (moderate uncertainty). For humans, based on variability in *individual* samples from Lipscomb et al. (1997) (microsomes), Elfarra et al. (1998) (microsomes), and Lipscomb et al. (1998c) (freshly isolated hepatocytes). High uncertainty in clearance (lnClC) reflects two different methods for scaling concentrations in microsomal preparations to blood concentrations: (1) assuming microsomal concentration equals liver concentration and then using the measured liver:blood partition coefficient to convert to blood and (2) using the measured microsome:air partition coefficient and then using the measured blood:air partition coefficient to convert to blood.
[f]No data on variability, so a CV of 0.5 was assigned, with a CU of 2.
[g]For mice and rats, no data on variability, so a CV of 0.5 was assigned, with a CU of 2. For humans, sixfold variability based on in vitro data from Bronley-DeLancy et al. (2006), but with high uncertainty.
[h]No data on variability, so a CV of 2 was assigned (larger than assumed for metabolism due to possible vehicle effects), with a CU of 2.

A.4.3.4. Likelihood Function and Prior distributions for Residual Error Estimates

From Equation A-3 for the total likelihood function, different measurement types may have different partial likelihoods. In all cases except one, the likelihood was assumed to be lognormal, with probability density for a particular measurement y_{ijkl} at time t_{ijkl} given by:

$$P(y_{ijkl} \mid \theta_i, \sigma_{ijk}^2, t_{ijkl}) = (2\pi\sigma^2)^{-½} \exp[\{-\ln y_{ijkl} - \ln f_{ijkl}(\theta_i, t_{ijkl})\}^2/(2\sigma_{ijk}^2)] \quad \text{(Eq. A-76)}$$

As before, the subject is labeled *i*, the study is labeled *j*, the type of measurement is labeled *k*, and the different time points are labeled *l*. The parameters θ_i are the "scaling parameters" at the subject-level, shown in Table A-4, whereas the parameters σ_{ijk}^2 represent the "residual error" variance σ^2. This error term may include variability due to measurement error, intrasubject and intrastudy heterogeneity, as well as model misspecification. The available in vivo measurements to which the model was calibrated are listed in Table A-8. The variances for each of the corresponding residual errors were given log-uniform distributions. For all measurements, the bounds on the log-uniform distribution were 0.01 and 3.3, corresponding to GSDs bounded by 1.11 and 6.15. The lower bound was set to prevent "over-fitting," as was done in Bois (2000a) and Hack et al. (2006).

Table A-8. Measurements used for calibration

Measurement abbreviation	Mouse	Rat	Human	Measurement description
RetDose			√	Retained TCE dose (mg)
CAlvPPM			√	TCE concentration in alveolar air (ppm)
CInhPPM	√	√		TCE concentration in closed-chamber (ppm)
Cart		√		TCE concentration in arterial blood (mg/L)
CVen	√	√	√	TCE concentration in venous blood (mg/L)
CBldMix	√	√		TCE concentration in mixed arterial and venous blood (mg/L)
CFat	√	√		TCE concentration in fat (mg/L)
CGut		√		TCE concentration in gut (mg/L)
CKid	√	√		TCE concentration in kidney (mg/L)
CLiv	√	√		TCE concentration in liver (mg/L)
CMus		√		TCE concentration in muscle (mg/L)
AExhpost	√	√		Amount of TCE exhaled postexposure (mg)
CTCOH	√	√	√	Free TCOH concentration in blood (mg/L)
CLivTCOH	√			Free TCOH concentration in liver (mg/L)
CPlasTCA	√	√	√	TCA concentration in plasma (mg/L)
CBldTCA	√	√	√	TCA concentration in blood (mg/L)
CLivTCA	√	√		TCA concentration in liver (mg/L)
AUrnTCA	√	√	√	Cumulative amount of TCA excreted in urine (mg)
AUrnTCA_collect			√	Cumulative amount of TCA collected in urine (noncontinuous sampling) (mg)
ABileTCOG		√		Cumulative amount of bound TCOH excreted in bile (mg)
CTCOG		√		Bound TCOH concentration in blood (mg/L)
CTCOGTCOH	√			Bound TCOH concentration in blood in free TCOH equivalents (mg/L)
CLivTCOGTCOH	√			Bound TCOH concentration in liver in free TCOH equivalents (mg/L)
AUrnTCOGTCOH	√	√	√	Cumulative amount of total TCOH excreted in urine (mg)
AUrnTCOGTCOH_collect			√	Cumulative amount of total TCOH collected in urine (noncontinuous sampling) (mg)
CDCVGmol			√	DCVG concentration in blood (mmol/L)
CDCVG_ND			√	DCVG nondetects from Lash et al. (1999b)
AUrnNDCVC		√	√	Cumulative amount of NAcDCVC excreted in urine (mg)
AUrnTCTotMole		√		Cumulative amount of TCA+total TCOH excreted in urine (mmol)
TotCTCOH	√	√	√	Total TCOH concentration in blood (mg/L)

where:

$\Phi(y)$ is the cumulative standard normal distribution.

Nondetects (ND) of DCVG from Lash et al. (1999b) were also included in the data, at it was found that these data were needed to place constraints on the clearance rate of DCVG from blood. The detection limit reported in the study was LD = 0.05 pmol/mL= 5×10^{-5} mmol/L. It

was assumed, as is standard in analytical chemistry, that the detection limit represents a response from a blank sample at 3 SDs. Because detector responses near the detection limit are generally normally distributed, the likelihood for observing a nondetect given a model-predicted value of $f_{ijkl}(\theta_i, t_{ijkl})$ is equal to:

$$P(= \text{ND}| \theta_i, t_{ijkl}) = \Phi(3 \times \{1 - f_{ijkl}(\theta_i, t_{ijkl})/\text{L}\square), \qquad \text{(Eq. A-77)}$$

The rat and human models differed from the mouse model in terms of the hierarchical structure of the residual errors. In the mouse model, all of the studies were assumed to have the same residual error, as shown in Figure A-1, so that the residual error is only indexed by *k*, the type of measurement: σ_k^2. This appeared reasonable because there were fewer studies, and there appeared to be less variation between studies. In the rat and human models, each of which used a much larger database of in vivo studies, residual errors were assumed to be the same within a study, but may differ between studies, and so are labeled by study *j* and the type of measurement *k*: σ_{jk}^2. The updated hierarchical structures are shown in Figure A-12. Initial attempts to use a single set of residual errors led to large residual errors for some measurements, even though fits to many studies appeared reasonable. Residual errors were generally reduced when study-specific errors were used, except for some data sets that appeared to be outliers (discussed below).

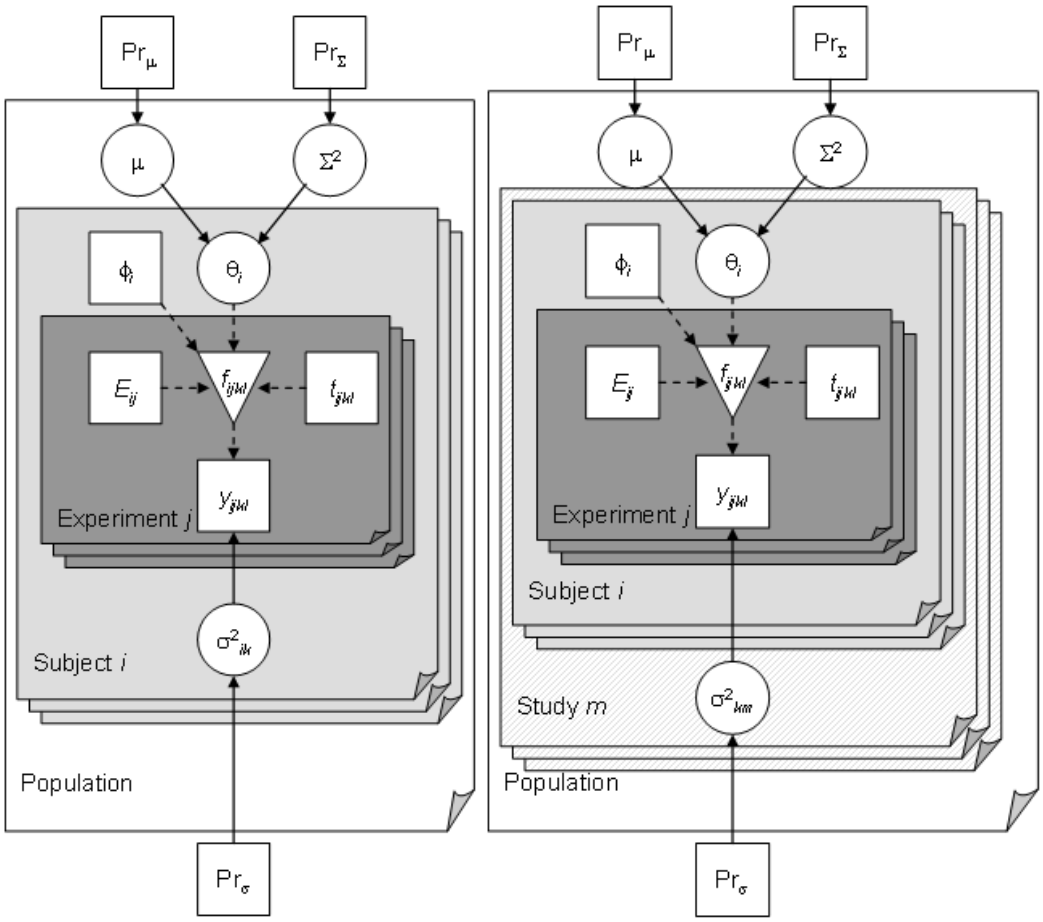

Symbols have the same meaning as Figure A-1, with modifications for the rat and human. In particular, in the rat, each "subject" consists of animals (usually comprising multiple dose groups) of the same sex, species, and strain within a study (possibly reported in more than one publication, but reasonably presumed to be of animals in the same "lot"). Animals within each subject are presumed to be "identical," with the same PBPK model parameters, and each such subject is assigned its own set of "residual" error variances σ^2_{ik}. In humans, each "subject" is a single person, possibly exposed in multiple experiments, and each subject is assigned a set of PBPK model parameters drawn from the population. However, in humans, "residual" error variances are assigned at an intermediate level of the hierarchy—the "study" level, σ^2_{km}—rather than the subject or the population level.

Figure A-12. Updated hierarchical structure for rat and human models.

A.4.4. Summary of Bayesian Posterior Distribution Function

As described in Section A.1, the posterior distribution for the unknown parameters is obtained in the usual Bayesian manner by multiplying:

(1) The prior distributions for the population mean of the scaling parameter(μ) (see Sections A.4.3.1–A.4.3.2), the population variance of the scaling parameters(Σ^2) (see Section A.4.3.3), and the "residual" error (σ^2) (see Section A.4.3.4);

(2) The population distribution, assumed to be a truncated normal distribution, for the subject parameters $(\theta \mid \mu, \Sigma^2)$; and

(3) The likelihood functions $(y \mid \theta, \sigma^2)$, (see Section A.4.3.4)

as follows:

$$(\theta, \mu, \Sigma^2, \sigma^2 \mid y) \propto (\mu)(\Sigma^2)\,(\sigma^2)\,(\theta \mid \mu, \Sigma^2)\,(y \mid \theta, \sigma^2) \qquad \text{(Eq. A-78)}$$

Each subject's parameters θ_i have the same sampling distribution (i.e., they are independently and identically distributed), so their joint prior distribution is:

$$(\theta \mid \mu, \Sigma^2) = \prod_{i=1\ldots n} (\theta_i \mid \mu, \Sigma^2) \qquad \text{(Eq. A-79)}$$

Different experiments $j = 1\ldots n_j$ may have different exposure and different data collected and different time points. In addition, different types of measurements $k = 1\ldots n_k$ (e.g., TCE blood, TCE breath, TCA blood, etc.) may have different errors, but errors are otherwise assumed to be independently and identically distributed. Because the subjects are treated as independent given $\theta_{1\ldots n}$, the likelihood function is simply:

$$y \mid \theta, \sigma^2) = \prod_{i=1\ldots n} \prod_{j=1\ldots nij} \prod_{k=1\ldots m} \prod_{l=1\ldots Nijk} (y_{ijkl} \mid \theta_i, \sigma_{ijk}{}^2, t_{ijkl}) \qquad \text{(Eq. A-80)}$$

where n is the number of subjects, n_{ij} is the number of experiments in that subject, m is the number of different types of measurements, N_{ijk} is the number (possibly 0) of measurements (e.g., time points) for subject i of type k in experiment j, and t_{ijkl} are the times at which measurements for subject i of type k were made in experiment j.

The MCSim software (version 5.0.0) was used to sample from this distribution.

A.5. RESULTS OF UPDATED PBPK MODEL

The evaluation of the updated PBPK model was discussed in Chapter 3. Detailed results in the form of tables and figures are provided in this section.

A.5.1. Convergence and Posterior Distributions of Sampled Parameters

For each sampled parameter (population mean and variance and the variance for residual errors), summary statistics (median, [2.5, 97.5%] CI) for the posterior distribution are tabulated in Tables A-9, A-10, A-12, A-13, A-15, and A-16 below. In addition, the potential scale reduction factor R, calculated from comparing four independent chains, is given. For each species, graphs of the prior and posterior distributions for the population mean and variance parameters are shown in Figures A-13 to A-18 for mice, A-19 to A-24 for rats, and A-25 to A-30

for humans. Finally, posterior correlations between population mean parameters are given in Tables A-11, A-14, and A-17, which show parameter pairs with correlation coefficients ≥0.25.

In addition, posterior distributions for the subject-specific parameters are summarized in supplementary figures accessible here:

- **Mouse:** (Supplementary data for TCE assessment: Mouse posterior by subject, 2011)
- **Rat:** (Supplementary data for TCE assessment: Rat posterior by subject, 2011)
- **Human**: (Supplementary data for TCE assessment: Human posterior by subject, 2011)

Table A-9. Posterior distributions for mouse PBPK model population parameters

Sampled parameter[a]	Posterior distributions reflecting uncertainty in population distribution			
	Population (geometric) mean		Population GSD	
	Median (2.5, 97.5%)	*R*	Median (2.5, 97.5%)	*R*
lnQCC	1.237 (0.8972, 1.602)	1	1.402 (1.183, 2.283)	1
lnVPRC	0.8076 (0.6434, 1.022)	1	1.224 (1.108, 1.63)	1.001
QFatC	1.034 (0.5235, 1.55)	1	0.436 (0.3057, 0.6935)	1
QGutC	1.183 (1.002, 1.322)	1	0.1548 (0.1101, 0.2421)	1
QLivC	1.035 (0.8002, 1.256)	1	0.1593 (0.1107, 0.2581)	1
QSlwC	0.9828 (0.6043, 1.378)	1	0.275 (0.1915, 0.4425)	1
lnDRespC	1.214 (0.7167, 2.149)	1.002	1.215 (1.143, 1.375)	1
QKidC	0.995 (0.5642, 1.425)	1	0.3001 (0.21, 0.48)	1
FracPlasC	0.8707 (0.5979, 1.152)	1.001	0.1903 (0.1327, 0.3039)	1
VFatC	1.329 (0.8537, 1.784)	1.002	0.4123 (0.2928, 0.6414)	1
VGutC	0.9871 (0.817, 1.162)	1	0.1219 (0.085, 0.1965)	1
VLivC	0.8035 (0.5609, 1.093)	1.013	0.2216 (0.1552, 0.3488)	1
VRapC	0.997 (0.8627, 1.131)	1	0.09384 (0.06519, 0.1512)	1
VRespLumC	0.9995 (0.8536, 1.145)	1	0.1027 (0.07172, 0.1639)	1
VRespEffC	1 (0.8537, 1.148)	1.001	0.1032 (0.07176, 0.1652)	1
VKidC	1.001 (0.8676, 1.134)	1	0.09365 (0.06523, 0.1494)	1
VBldC	0.9916 (0.8341, 1.153)	1.001	0.1126 (0.07835, 0.1817)	1
lnPBC	0.9259 (0.647, 1.369)	1	1.644 (1.278, 3.682)	1
lnPFatC	0.9828 (0.7039, 1.431)	1.001	1.321 (1.16, 2.002)	1.001
lnPGutC	0.805 (0.4735, 1.418)	1	1.375 (1.198, 2.062)	1
lnPLivC	1.297 (0.7687, 2.039)	1	1.415 (1.21, 2.342)	1
lnPRapC	0.9529 (0.5336, 1.721)	1	1.378 (1.203, 2.141)	1
lnPRespC	0.9918 (0.5566, 1.773)	1.001	1.378 (1.2, 2.066)	1
lnPKidC	1.277 (0.7274, 2.089)	1	1.554 (1.265, 2.872)	1
lnPSlwC	0.92 (0.5585, 1.586)	1.001	1.411 (1.209, 2.3)	1.001
lnPRBCPlasTCAC	2.495 (1.144, 5.138)	1.001	1.398 (1.178, 2.623)	1.001
lnPBodTCAC	0.8816 (0.6219, 1.29)	1.003	1.27 (1.158, 1.609)	1
lnPLivTCAC	0.8003 (0.5696, 1.15)	1.003	1.278 (1.157, 1.641)	1.001
lnkDissocC	1.214 (0.2527, 4.896)	1.003	2.71 (1.765, 8.973)	1

Table A-9. Posterior distributions for mouse PBPK model population parameters (continued)

Sampled parameter[a]	Posterior distributions reflecting uncertainty in population distribution			
	Population (geometric) mean		Population GSD	
	Median (2.5, 97.5%)	*R*	Median (2.5, 97.5%)	*R*
lnBMaxkDC	1.25 (0.6793, 2.162)	1.002	1.474 (1.253, 2.383)	1
lnPBodTCOHC	0.8025 (0.5607, 1.174)	1	1.314 (1.17, 1.85)	1.001
lnPLivTCOHC	1.526 (0.9099, 2.245)	1	1.399 (1.194, 2.352)	1
lnPBodTCOGC	0.4241 (0.1555, 1.053)	1.004	1.398 (1.207, 2.156)	1
lnPLivTCOGC	1.013 (0.492, 2.025)	1.002	1.554 (1.279, 2.526)	1
lnPeffDCVG	0.9807 (0.008098, 149.6)	1.041	1.406 (1.206, 2.379)	1
lnkTSD	5.187 (0.3909, 69.34)	1.001	5.858 (2.614, 80)	1
lnkAS	1.711 (0.3729, 11.23)	1.001	4.203 (2.379, 18.15)	1
lnkTD	0.1002 (0.01304, 0.7688)	1	5.16 (2.478, 60.24)	1
lnkAD	0.2665 (0.05143, 1.483)	1.003	4.282 (2.378, 20.21)	1
lnkASTCA	3.986 (0.1048, 141.9)	1	5.187 (2.516, 58.72)	1
lnkASTCOH	0.7308 (0.006338, 89.75)	1.001	5.047 (2.496, 54.8)	1
$lnV_{MAX}C$	0.6693 (0.4093, 1.106)	1.005	1.793 (1.49, 2.675)	1
lnK_MC	0.07148 (0.0323, 0.1882)	1	2.203 (1.535, 4.536)	1.001
lnFracOtherC	0.02384 (0.003244, 0.1611)	1.006	1.532 (1.265, 2.971)	1
lnFracTCAC	0.4875 (0.2764, 0.8444)	1.002	1.474 (1.258, 2.111)	1
lnV_{MAX}DCVGC	1.517 (0.02376, 1,421)	1.001	1.53 (1.263, 2.795)	1
lnClDCVGC	0.1794 (0.02333, 79.69)	1.013	1.528 (1.261, 2.922)	1
lnV_{MAX}KidDCVGC	1.424 (0.04313, 704.9)	1.014	1.533 (1.262, 2.854)	1
lnClKidDCVGC	0.827 (0.04059, 167.2)	1.019	1.527 (1.263, 2.874)	1
lnV_{MAX}LungLivC	2.903 (0.487, 12.1)	1.001	4.157 (1.778, 29.01)	1.018
lnK_MClara	0.01123 (0.001983, 0.09537)	1.012	1.629 (1.278, 5.955)	1.003
lnFracLungSysC	3.304 (0.2619, 182.1)	1.011	1.543 (1.266, 3.102)	1.001
lnV_{MAX}TCOHC	1.645 (0.6986, 3.915)	1.005	1.603 (1.28, 2.918)	1
lnK_MTCOH	0.9594 (0.2867, 2.778)	1.007	1.521 (1.264, 2.626)	1
lnV_{MAX}GlucC	65.59 (27.58, 232.5)	1.018	1.487 (1.254, 2.335)	1
lnK_MGluc	31.16 (6.122, 137.3)	1.015	1.781 (1.299, 5.667)	1.002
lnkMetTCOHC	3.629 (0.7248, 9.535)	1.009	1.527 (1.265, 2.626)	1
lnkUrnTCAC	0.1126 (0.04083, 0.2423)	1.012	1.757 (1.318, 3.281)	1.003
lnkMetTCAC	0.6175 (0.2702, 1.305)	1.027	1.508 (1.262, 2.352)	1.002
lnkBileC	0.9954 (0.316, 3.952)	1.003	1.502 (1.26, 2.453)	1
lnkEHRC	0.01553 (0.001001, 0.0432)	1.008	1.534 (1.264, 2.767)	1
lnkUrnTCOGC	7.874 (2.408, 50.28)	1	3.156 (1.783, 12.18)	1.001
lnFracKidDCVCC	1.931 (0.01084, 113.7)	1.018	1.53 (1.264, 2.77)	1
lnkDCVGC	0.2266 (0.001104, 16.46)	1.011	1.525 (1.263, 2.855)	1
lnkNATC	0.1175 (0.0008506, 14.34)	1.024	1.528 (1.264, 2.851)	1
lnkKidBioactC	0.07506 (0.0009418, 12.35)	1.035	1.527 (1.263, 2.84)	1.001

[a]These "sampled parameters" are scaled one or more times (see Table A-4) to obtain a biologically-meaningful parameter, posterior distributions of which are summarized in Tables 3-36 through 3-40). For natural log transformed parameters (name starting with "ln"), values are for the population geometric means and SDs.

Table A-10. Posterior distributions for mouse residual errors

Measurement	Residual error GSD	
	Median (2.5, 97.5%)	***R***
CInhPPM	1.177 (1.16, 1.198)	1.001
CVen	2.678 (2.354, 3.146)	1.001
CBldMix	1.606 (1.415, 1.96)	1.001
CFat	2.486 (2.08, 3.195)	1
CKid	2.23 (1.908, 2.796)	1
CLiv	1.712 (1.543, 1.993)	1
AExhpost	1.234 (1.159, 1.359)	1
CTCOH	1.543 (1.424, 1.725)	1
CLivTCOH	1.591 (1.454, 1.818)	1
CPlasTCA	1.396 (1.338, 1.467)	1.001
CBldTCA	1.488 (1.423, 1.572)	1.001
CLivTCA	1.337 (1.271, 1.43)	1
AUrnTCA	1.338 (1.259, 1.467)	1
CTCOGTCOH	1.493 (1.38, 1.674)	1.001
CLivTCOGTCOH	1.63 (1.457, 1.924)	1
AUrnTCOGTCOH	1.263 (1.203, 1.355)	1
TotCTCOH	1.846 (1.506, 2.509)	1.002

Note: the hierarchical statistical model for residual errors did not separate by subject.

Table A-11. Posterior correlations for mouse population mean parameters

Mouse		
Parameter 1	**Parameter 2**	**Correlation coefficient.**
lnKMGluc	lnV_{MAX}GlucC	0.765
lnClDCVGC	lnV_{MAX}DCVGC	-0.553
lnkMetTCAC	lnkUrnTCAC	-0.488
lnKMTCOH	lnV_{MAX}TCOHC	0.464
lnClKidDCVGC	lnV_{MAX}KidDCVGC	-0.394
lnkUrnTCAC	lnPRBCPlasTCAC	0.358
lnkDissocC	lnPBodTCAC	0.328
lnkEHRC	lnkMetTCOHC	0.314
lnV_{MAX}C	VLivC	-0.305
lnKMClara	lnV_{MAX}LungLivC	0.302
lnBMaxkDC	lnPLivTCAC	0.299
lnKMGluc	lnKMTCOH	0.293
lnkBileC	lnkEHRC	-0.280
lnkEHRC	lnKMTCOH	-0.273
lnPBodTCOGC	lnV_{MAX}GlucC	0.269
lnFracTCAC	lnV_{MAX}TCOHC	-0.267
lnkMetTCAC	lnPBodTCAC	0.264
lnkDissocC	lnPLivTCAC	0.253
lnPSlwC	QFatC	-0.252

Note: only parameter pairs with correlation coefficient ≥0.25 are listed.

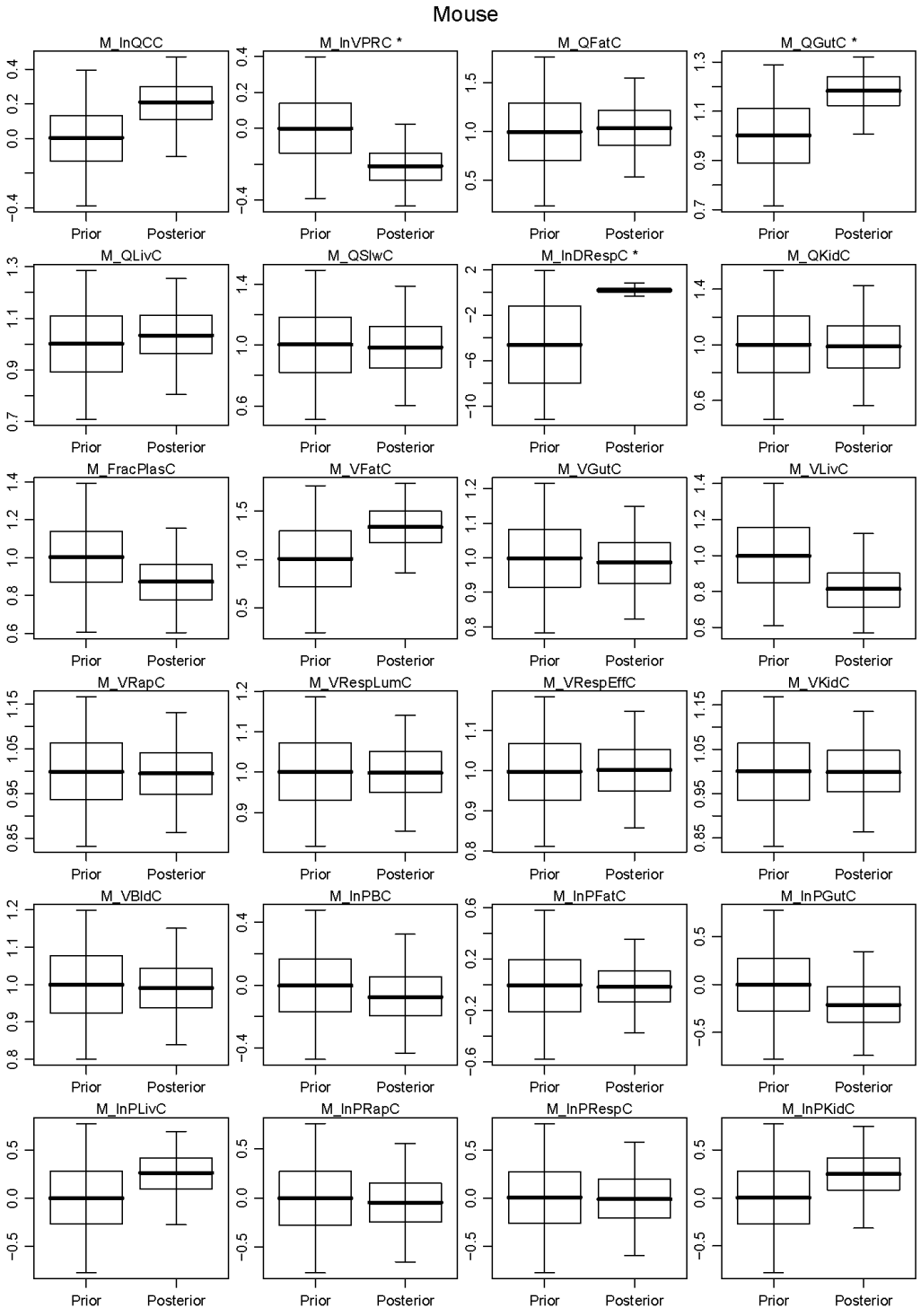

Thick lines are medians, boxes are interquartile regions, and error bars are (2.5, 97.5%) CIs. Parameters labeled with "*" have nonoverlapping interquartile regions.

Figure A-13. Prior and posterior mouse population mean parameters (Part 1).

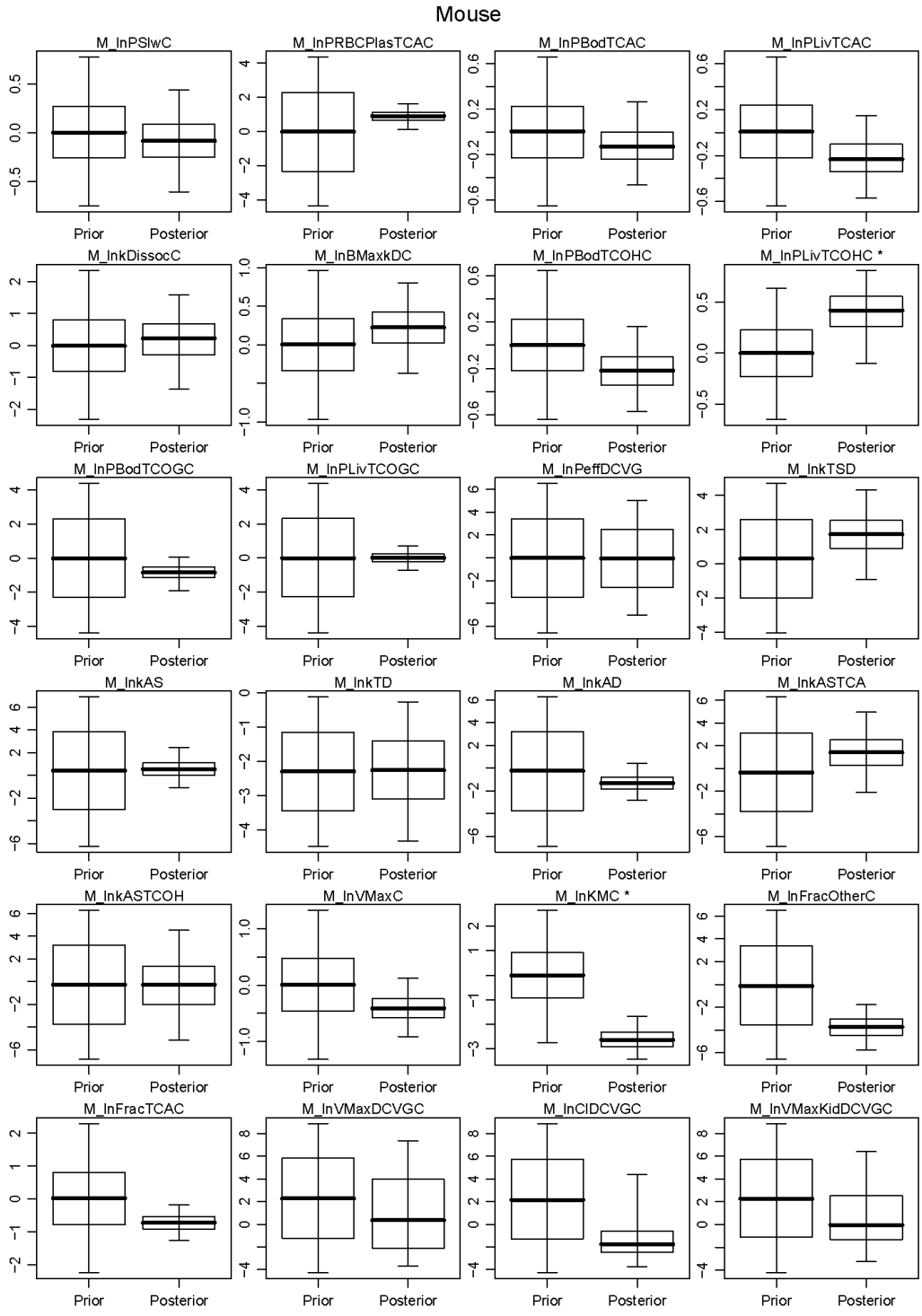

Thick lines are medians, boxes are interquartile regions, and error bars are (2.5, 97.5%) CIs. Parameters labeled with "*" have nonoverlapping interquartile regions.

Figure A-14. Prior and posterior mouse population mean parameters (Part 2).

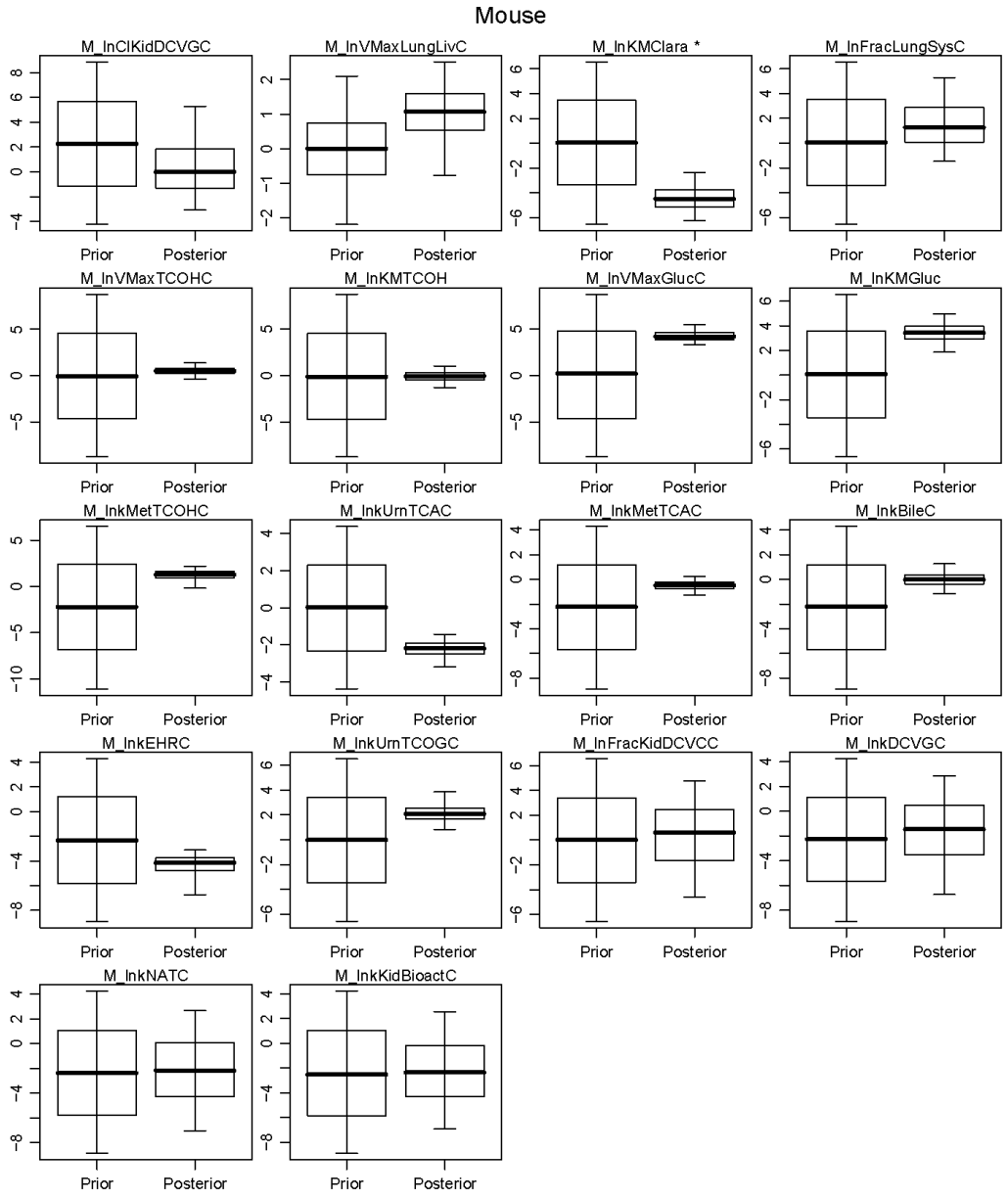

Thick lines are medians, boxes are interquartile regions, and error bars are (2.5, 97.5%) CIs. Parameters labeled with "*" have nonoverlapping interquartile regions.

Figure A-15. Prior and posterior mouse population mean parameters (Part 3).

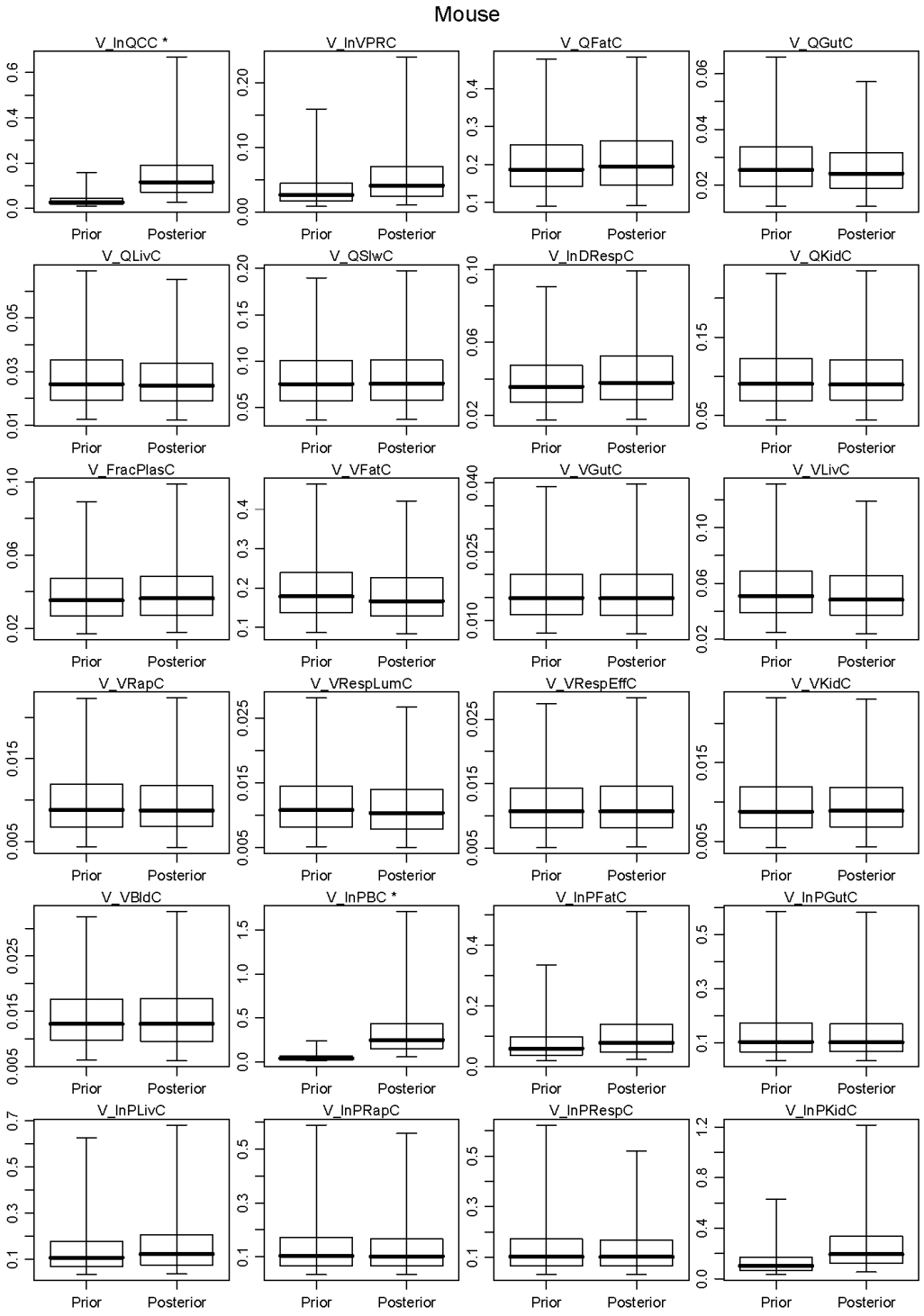

Thick lines are medians, boxes are interquartile regions, and error bars are (2.5, 97.5%) CIs. Parameters labeled with "*" have nonoverlapping interquartile regions.

Figure A-16. Prior and posterior mouse population variance parameters (Part 1).

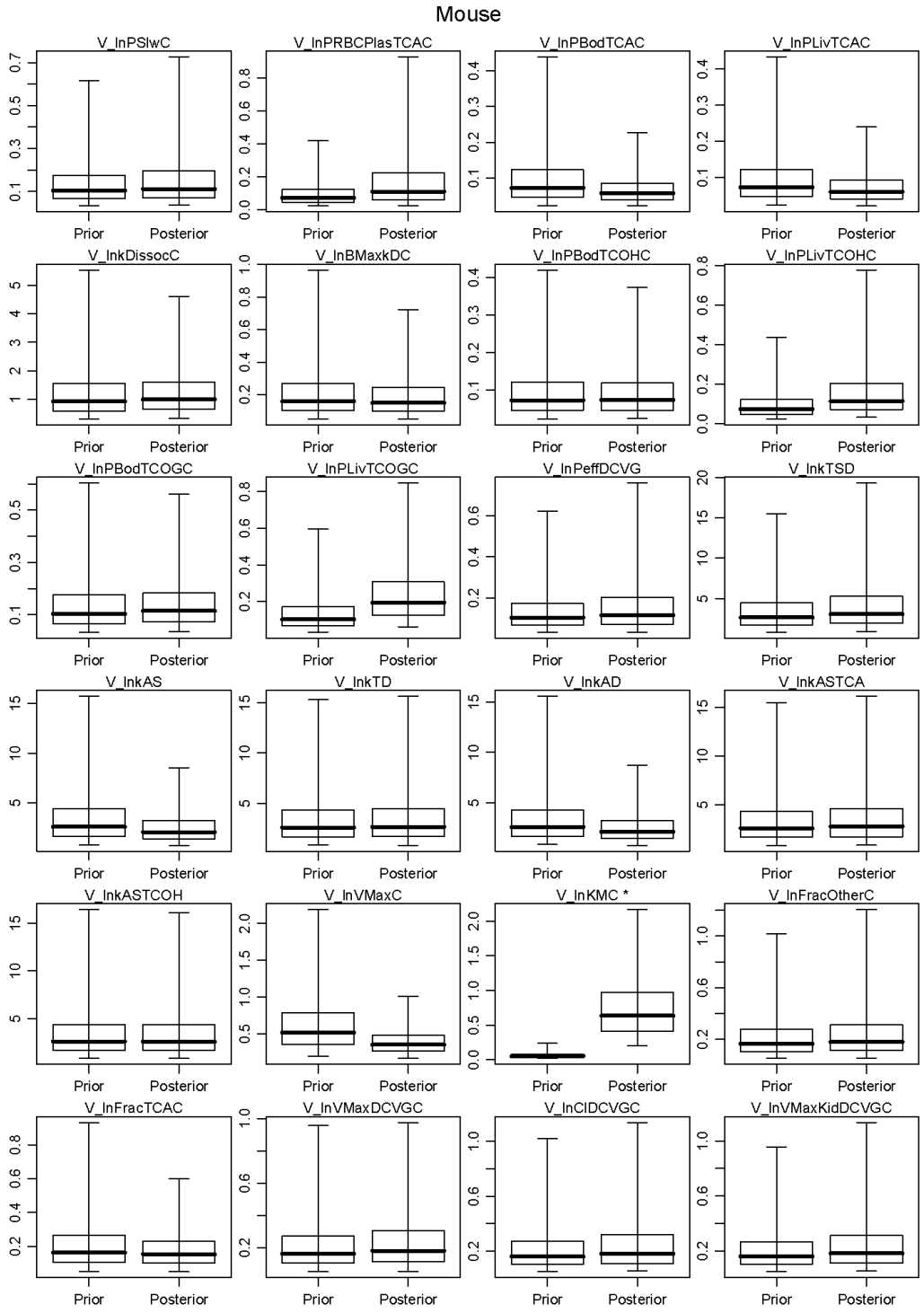

Thick lines are medians, boxes are interquartile regions, and error bars are (2.5, 97.5%) CIs. Parameters labeled with "*" have nonoverlapping interquartile regions.

Figure A-17. Prior and posterior mouse population variance parameters (Part 2).

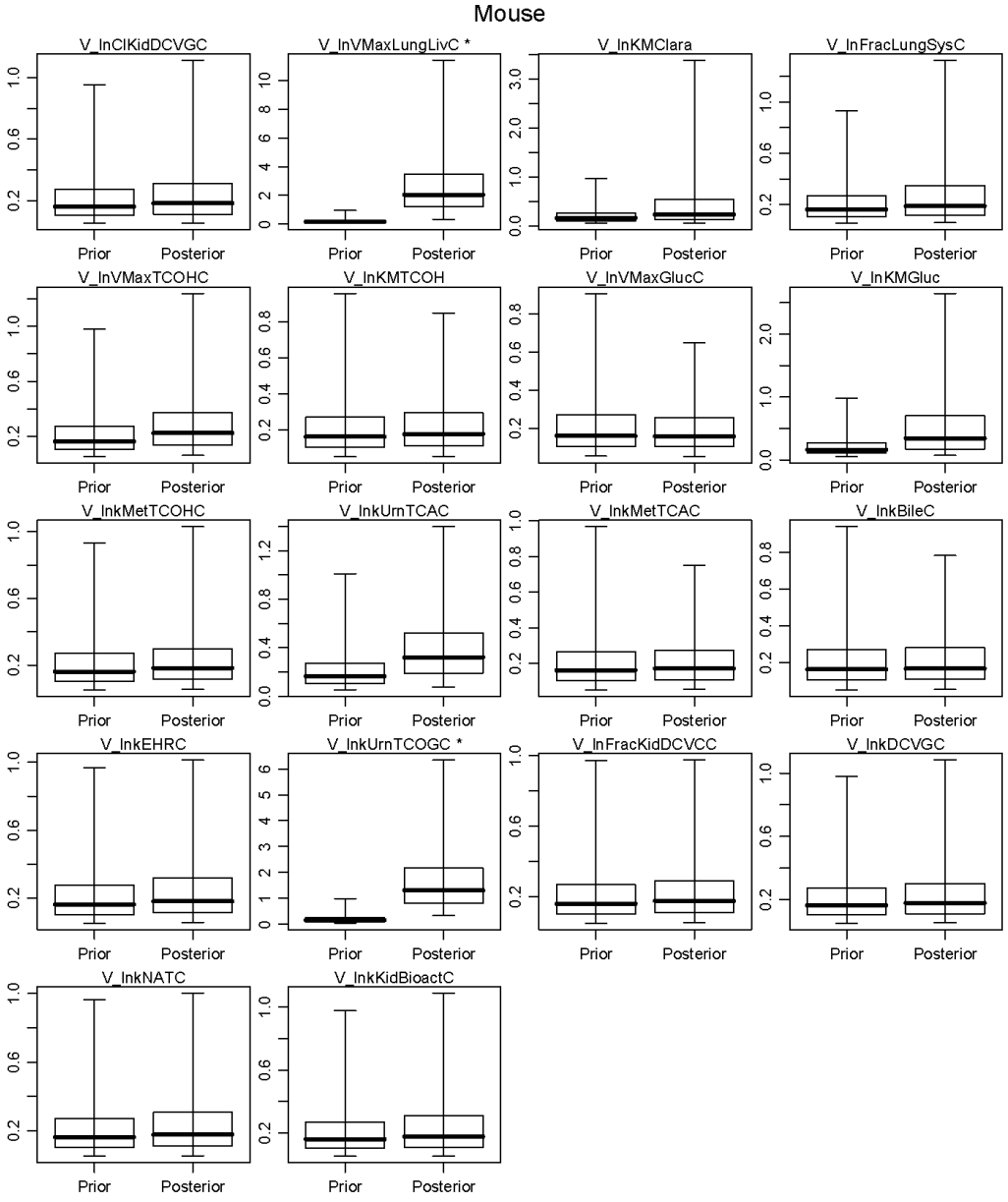

Thick lines are medians, boxes are interquartile regions, and error bars are (2.5, 97.5%) CIs. Parameters labeled with "*" have nonoverlapping interquartile regions.

Figure A-18. Prior and posterior mouse population variance parameters (Part 3).

Table A-12. Posterior distributions for rat PBPK model population parameters

	Posterior distributions reflecting uncertainty in population distribution			
	Population (geometric) mean		Population GSD	
Sampled parameter	Median (2.5, 97.5%)	*R*	Median (2.5, 97.5%)	*R*
lnQCC	1.195 (0.9285, 1.448)	1.034	1.298 (1.123, 2.041)	1.031
lnVPRC	0.6304 (0.4788, 0.8607)	1.012	1.446 (1.247, 2.011)	1.005
QFatC	1.167 (0.8321, 1.561)	1	0.4119 (0.2934, 0.6438)	1
QGutC	1.154 (0.988, 1.306)	1	0.1613 (0.1132, 0.2542)	1
QLivC	1.029 (0.8322, 1.223)	1.002	0.1551 (0.1092, 0.2483)	1
QSlwC	0.9086 (0.5738, 1.251)	1.001	0.2817 (0.1968, 0.4493)	1
lnDRespC	2.765 (1.391, 5.262)	1.018	1.21 (1.142, 1.358)	1.001
QKidC	1.002 (0.8519, 1.152)	1.001	0.1185 (0.08284, 0.1871)	1
FracPlasC	1.037 (0.8071, 1.259)	1.002	0.1785 (0.1272, 0.2723)	1
VFatC	0.9728 (0.593, 1.378)	1	0.4139 (0.2924, 0.6552)	1.002
VGutC	0.9826 (0.8321, 1.137)	1	0.1187 (0.08296, 0.1873)	1
VLivC	0.9608 (0.7493, 1.19)	1.015	0.1682 (0.1168, 0.2718)	1.001
VRapC	0.9929 (0.8563, 1.133)	1.001	0.1093 (0.07693, 0.175)	1
VRespLumC	1.001 (0.7924, 1.21)	1	0.1636 (0.116, 0.2601)	1
VRespEffC	0.999 (0.7921, 1.208)	1.001	0.1635 (0.1161, 0.2598)	1
VKidC	0.999 (0.8263, 1.169)	1	0.1361 (0.09617, 0.2167)	1
VBldC	1.002 (0.8617, 1.141)	1	0.1096 (0.07755, 0.176)	1
lnPBC	0.8551 (0.6854, 1.065)	1.001	1.317 (1.232, 1.462)	1.001
lnPFatC	1.17 (0.8705, 1.595)	1.003	1.333 (1.247, 1.481)	1.001
lnPGutC	0.8197 (0.5649, 1.227)	1	1.362 (1.198, 1.895)	1
lnPLivC	1.046 (0.8886, 1.234)	1.001	1.152 (1.115, 1.214)	1
lnPRapC	1.021 (0.6239, 1.675)	1.002	1.373 (1.201, 1.988)	1
lnPRespC	0.993 (0.5964, 1.645)	1.001	1.356 (1.197, 1.948)	1
lnPKidC	0.9209 (0.6728, 1.281)	1	1.304 (1.201, 1.536)	1
lnPSlwC	1.258 (0.9228, 1.711)	1.001	1.364 (1.263, 1.544)	1
lnPRBCPlasTCAC	0.9763 (0.6761, 1.353)	1	1.276 (1.159, 1.634)	1
lnPBodTCAC	1.136 (0.6737, 1.953)	1.008	1.631 (1.364, 2.351)	1.003
lnPLivTCAC	1.283 (0.6425, 2.491)	1.008	1.651 (1.356, 2.658)	1
lnkDissocC	1.01 (0.5052, 2.017)	1.002	1.596 (1.315, 2.774)	1
lnBMaxkDC	0.9654 (0.5716, 1.733)	1.02	1.412 (1.234, 2.01)	1
lnPBodTCOHC	0.9454 (0.4533, 1.884)	1.045	1.734 (1.39, 3.151)	1.002
lnPLivTCOHC	0.926 (0.3916, 2.196)	1.013	1.785 (1.382, 4.142)	1.003
lnPBodTCOGC	1.968 (0.09185, 14.44)	1.031	1.414 (1.208, 2.571)	1
lnPLivTCOGC	7.484 (2.389, 26.92)	1.017	1.41 (1.208, 2.108)	1
lnkTSD	3.747 (0.2263, 62.58)	1.01	6.777 (2.844, 87.29)	1
lnkAS	2.474 (0.2542, 28.35)	1.004	10.16 (4.085, 143.7)	1
lnkAD	0.1731 (0.04001, 0.7841)	1.018	4.069 (2.373, 14.19)	1.009
lnkASTCA	1.513 (0.1401, 17.19)	1.002	4.376 (2.43, 22.83)	1
lnkASTCOH	0.6896 (0.01534, 25.81)	1.001	4.734 (2.444, 35.2)	1.001
lnV_{MAX}C	0.8948 (0.6377, 1.293)	1.028	1.646 (1.424, 2.146)	1.021

Table A-12. Posterior distributions for rat PBPK model population parameters (continued)

	Posterior distributions reflecting uncertainty in population distribution			
	Population (geometric) mean		Population GSD	
Sampled parameter	Median (2.5, 97.5%)	*R*	Median (2.5, 97.5%)	*R*
lnK_MC	0.0239 (0.01602, 0.04993)	1.001	2.402 (1.812, 4.056)	1.001
lnFracOtherC	0.344 (0.0206, 1.228)	1.442	3 (1.332, 10.04)	1.353
lnFracTCAC	0.2348 (0.122, 0.4616)	1.028	1.517 (1.264, 2.393)	1.001
lnV_{MAX}DCVGC	7.749 (0.2332, 458.8)	1.088	1.534 (1.262, 2.804)	1.001
lnClDCVGC	0.3556 (0.06631, 2.242)	1.018	1.509 (1.261, 2.553)	1
lnV_{MAX}KidDCVGC	0.2089 (0.04229, 1.14)	1.011	1.542 (1.263, 2.923)	1.001
lnClKidDCVGC	184 (26.29, 1312)	1.02	1.527 (1.265, 2.873)	1.001
lnV_{MAX}LungLivC	2.673 (0.4019, 14.16)	1.002	4.833 (1.599, 48.32)	1.002
lnK_MClara	0.02563 (0.005231, 0.197)	1.01	1.66 (1.279, 18.74)	1.002
lnFracLungSysC	2.729 (0.04124, 63.27)	1.027	1.536 (1.267, 2.868)	1.001
lnV_{MAX}TCOHC	1.832 (0.6673, 6.885)	1.041	1.667 (1.292, 3.148)	1.002
lnK_MTCOH	22.09 (3.075, 131.9)	1.186	1.629 (1.276, 3.773)	1.017
lnV_{MAX}GlucC	28.72 (10.02, 86.33)	1.225	2.331 (1.364, 5.891)	1.126
lnK_MGluc	6.579 (1.378, 23.57)	1.119	2.046 (1.309, 10.3)	1.125
lnkMetTCOHC	2.354 (0.3445, 15.83)	1.287	1.876 (1.283, 11.82)	1.182
lnkUrnTCAC	0.07112 (0.03934, 0.1329)	1.076	1.513 (1.27, 2.327)	1.003
lnkMetTCAC	0.3554 (0.1195, 0.8715)	1.036	1.528 (1.263, 2.444)	1.001
lnkBileC	8.7 (1.939, 26.71)	1.05	1.65 (1.282, 5.494)	1.017
lnkEHRC	1.396 (0.2711, 6.624)	1.091	1.647 (1.277, 5.582)	1.005
lnkUrnTCOGC	20.65 (2.437, 138)	1.041	1.595 (1.269, 5.257)	1.026
lnkNATC	0.002035 (0.0004799, 0.01019)	1.01	1.523 (1.261, 2.593)	1.001
lnkKidBioactC	0.006618 (0.0009409, 0.0367)	1.039	1.52 (1.261, 2.674)	1

Table A-13. Posterior distributions for rat residual errors

Measurement	Subject[a]	Residual error GSD	
		Median (2.5, 97.5%)	*R*
CInhPPM	Subject 3	1.124 (1.108, 1.147)	1
	Subject 16	1.106 (1.105, 1.111)	1
CMixExh	Subject 2	1.501 (1.398, 1.65)	1
Cart	Subject 2	1.174 (1.142, 1.222)	1
	Subject 6	1.523 (1.321, 1.918)	1.002
CVen	Subject 4	1.22 (1.111, 1.877)	1
	Subject 7	1.668 (1.489, 1.986)	1.001
	Subject 8	1.45 (1.234, 2.065)	1.014
	Subject 9	1.571 (1.426, 1.811)	1
	Subject 10	4.459 (2.754, 6.009)	1
	Subject 11	1.587 (1.347, 2.296)	1.002
	Subject 16	1.874 (1.466, 2.964)	1.011
	Subject 18	1.676 (1.188, 3.486)	1.003
CBldMix	Subject 12	1.498 (1.268, 2.189)	1
CFat	Subject 9	1.846 (1.635, 2.184)	1
	Subject 16	2.658 (1.861, 4.728)	1.001
CGut	Subject 9	1.855 (1.622, 2.243)	1
CKid	Subject 9	1.469 (1.354, 1.648)	1
CLiv	Subject 9	1.783 (1.554, 2.157)	1
	Subject 12	1.744 (1.401, 2.892)	1
	Subject 16	1.665 (1.376, 2.411)	1.001
CMus	Subject 9	1.653 (1.494, 1.919)	1
AExhpost	Subject 6	1.142 (1.108, 1.239)	1.003
	Subject 10	1.117 (1.106, 1.184)	1.004
	Subject 14	1.166 (1.107, 1.475)	1
	Subject 15	1.125 (1.106, 1.237)	1
CTCOH	Subject 6	1.635 (1.455, 1.983)	1.002
	Subject 10	1.259 (1.122, 1.868)	1.009
	Subject 11	1.497 (1.299, 1.923)	1.01
	Subject 13	1.611 (1.216, 3.556)	1.001
	Subject 17	1.45 (1.213, 2.208)	1.004
	Subject 18	1.142 (1.107, 1.268)	1
CPlasTCA	Subject 4	1.134 (1.106, 1.254)	1
	Subject 5	1.141 (1.107, 1.291)	1
	Subject 11	1.213 (1.136, 1.381)	1
	Subject 19	1.201 (1.145, 1.305)	1

Table A-13. Posterior distributions for rat residual errors (continued)

Measurement	Subject[a]	Residual error GSD	
		Median (2.5, 97.5%)	*R*
CBldTCA	Subject 4	1.134 (1.106, 1.258)	1
	Subject 5	1.14 (1.107, 1.289)	1
	Subject 6	1.59 (1.431, 1.878)	1.001
	Subject 11	1.429 (1.292, 1.701)	1.001
	Subject 17	1.432 (1.282, 1.675)	1.03
	Subject 18	1.193 (1.12, 1.358)	1.004
	Subject 19	1.214 (1.153, 1.327)	1
CLivTCA	Subject 19	1.666 (1.443, 2.104)	1
AUrnTCA	Subject 1	1.498 (1.125, 2.18)	1.135
	Subject 6	1.95 (1.124, 5.264)	1.003
	Subject 8	1.221 (1.146, 1.375)	1.003
	Subject 10	1.18 (1.108, 1.444)	1.007
	Subject 17	1.753 (1.163, 4.337)	1.001
	Subject 19	1.333 (1.201, 1.707)	1
ABileTCOG	Subject 6	2.129 (1.128, 5.363)	1.003
CTCOG	Subject 17	2.758 (1.664, 5.734)	1.028
AUrnTCOGTCOH	Subject 1	1.129 (1.106, 1.232)	1.004
	Subject 6	1.483 (1.113, 4.791)	1.002
	Subject 8	1.115 (1.106, 1.162)	1
	Subject 10	1.145 (1.107, 1.305)	1
	Subject 17	2.27 (1.53, 4.956)	1.009
AUrnNDCVC	Subject 1	1.168 (1.11, 1.33)	1.002
AUrnTCTotMole	Subject 6	1.538 (1.182, 3.868)	1.002
	Subject 7	1.117 (1.106, 1.153)	1.001
	Subject 14	1.121 (1.106, 1.207)	1
	Subject 15	1.162 (1.108, 1.358)	1
TotCTCOH	Subject 17	1.488 (1.172, 2.366)	1.015

[a]The nineteen subjects are: (1) Bernauer et al. (1996); (2) Dallas et al. (1991); (3) Fisher et al. (1989) females; (4) Fisher et al. (1991) females; (5) Fisher et al. (1991) males; (6) Green and Prout (1985), Prout et al. (1985), male OA rats; (7) Hissink et al. (2002); (8) Kaneko et al. (1994) (9) Keys et al. (2003); (10) Kimmerle and Eben (1973b); (11) Larson and Bull (1992b, a); (12) Lee et al. (2000a); (13) Merdink et al. (1999); (14) Prout et al. (1985) AP rats; (15) Prout et al. (1985) OM rats; (16) Simmons et al. (2002); (17) Stenner et al. (1997); (18) Templin et al. (1995b); and (19) Yu et al. (2000).

Table A-14. Posterior correlations for rat population mean parameters

Rat		
Parameter 1	**Parameter 2**	**Correlation coefficient**
lnkNATC	lnV_{MAX}KidDCVGC	-0.599
lnkBileC	lnPLivTCOGC	-0.587
lnKMTCOH	lnV_{MAX}TCOHC	0.567
lnKMGluc	lnV_{MAX}GlucC	0.506
lnClKidDCVGC	lnkNATC	-0.497
lnkUrnTCAC	lnPBodTCAC	0.421
lnV_{MAX}C	VLivC	-0.417
lnBMaxkDC	lnkUrnTCAC	0.397
lnkUrnTCOGC	lnPBodTCOGC	-0.389
lnPFatC	VFatC	-0.385
lnClKidDCVGC	lnV_{MAX}KidDCVGC	0.384
lnKMGluc	lnKMTCOH	0.383
lnPLivTCOGC	lnV_{MAX}GlucC	0.358
lnBMaxkDC	lnPBodTCAC	0.352
lnClDCVGC	lnClKidDCVGC	0.343
FracPlasC	lnPRBCPlasTCAC	-0.337
lnClDCVGC	lnkNATC	-0.331
lnkEHRC	lnV_{MAX}GlucC	0.322
lnkBileC	lnkUrnTCOGC	0.307
lnFracLungSysC	lnFracOtherC	0.304
lnFracOtherC	lnkMetTCOHC	-0.296
lnFracLungSysC	lnKMTCOH	-0.271
lnkMetTCAC	lnPBodTCAC	0.264
lnkMetTCAC	VLivC	-0.261
lnKMTCOH	lnPBodTCOGC	-0.260
lnFracTCAC	lnKMTCOH	0.258
lnDRespC	lnVPRC	0.254
lnFracOtherC	lnKMTCOH	-0.252

Note: only parameter pairs with correlation coefficient ≥0.25 are listed.

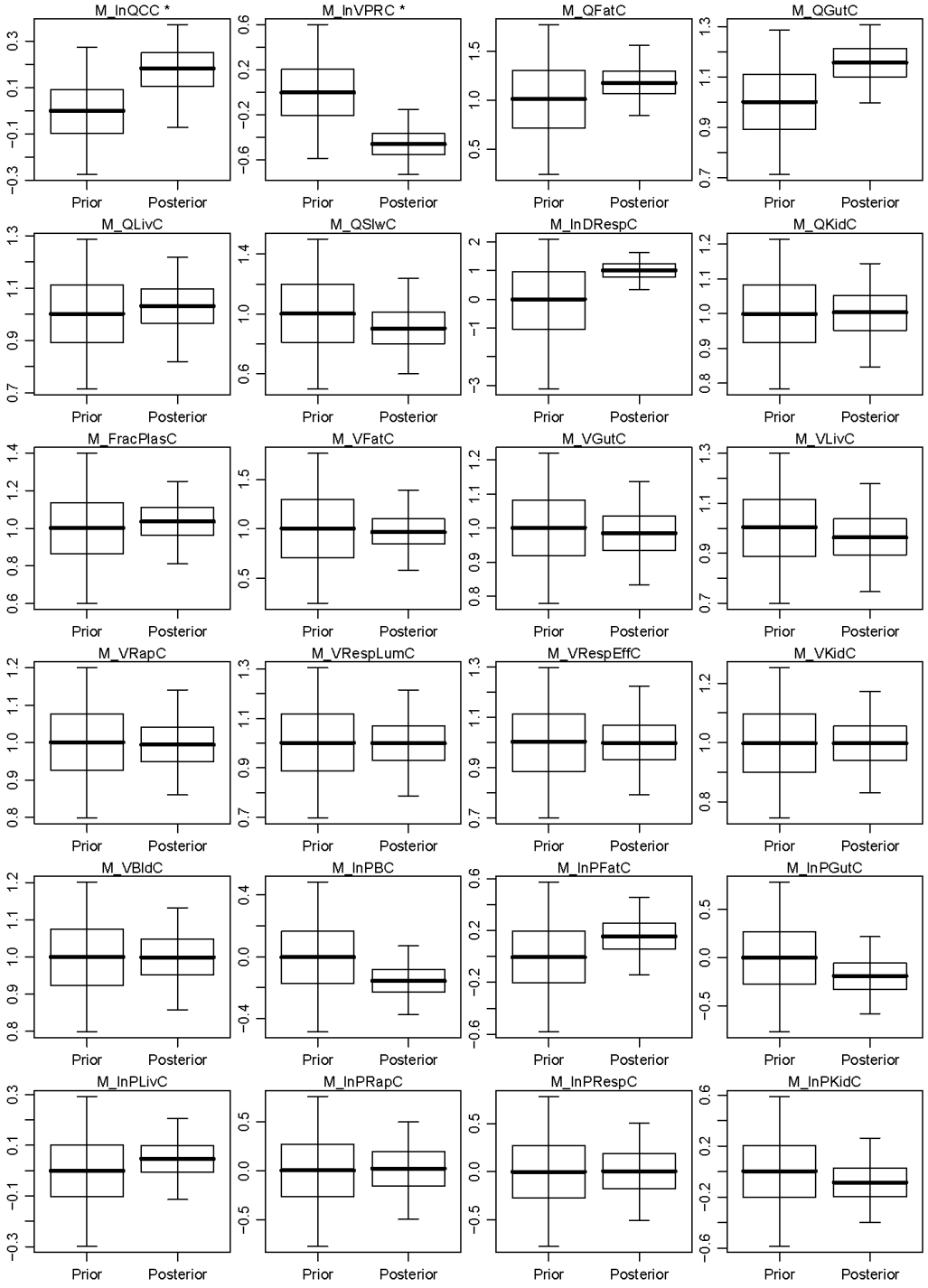

Thick lines are medians, boxes are interquartile regions, and error bars are (2.5, 97.5%) CIs. Parameters labeled with "*" have nonoverlapping interquartile regions.

Figure A-19. Prior and posterior rat population mean parameters (Part 1).

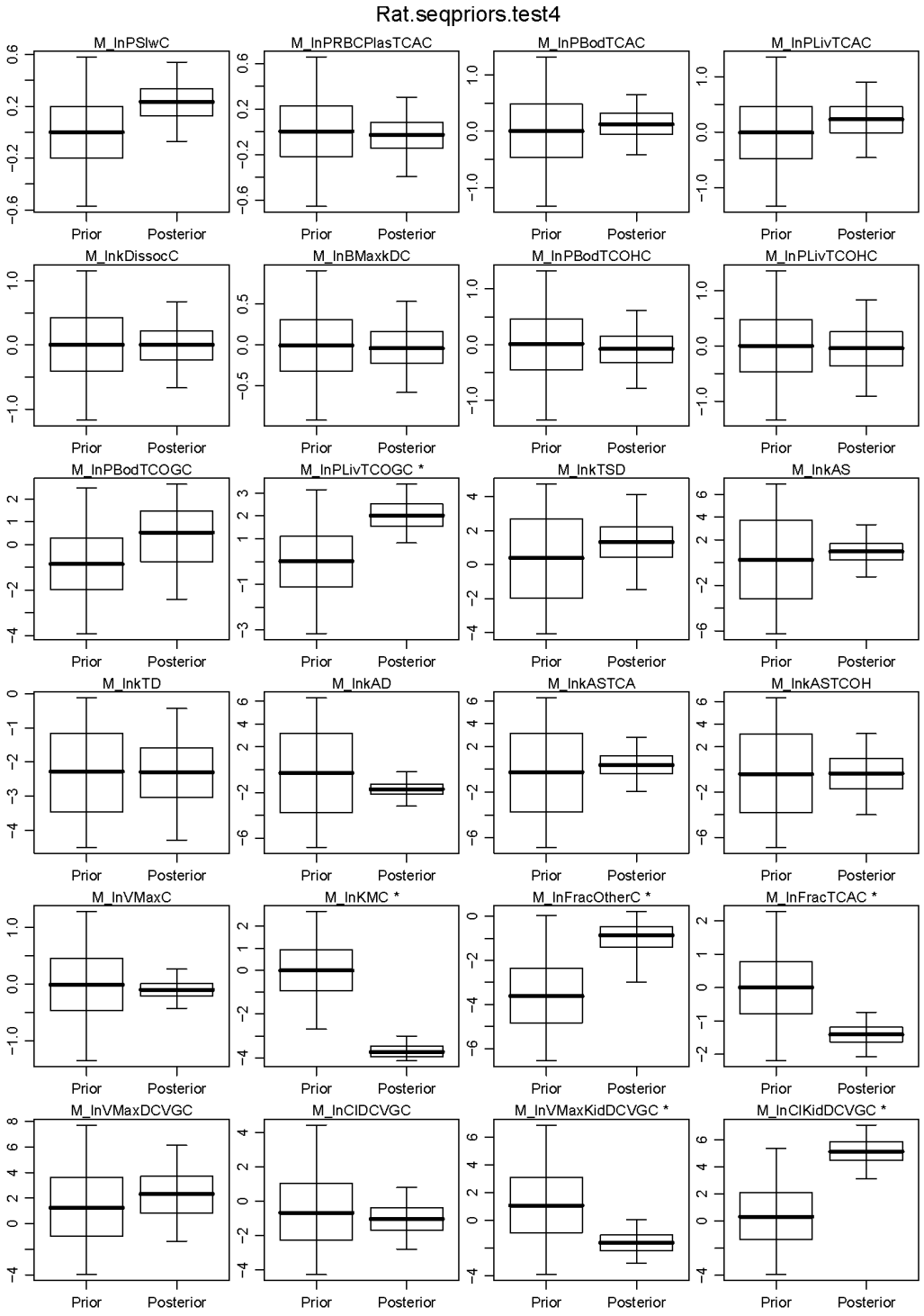

Thick lines are medians, boxes are interquartile regions, and error bars are (2.5, 97.5%) CIs. Parameters labeled with "*" have nonoverlapping interquartile regions.

Figure A-20. Prior and posterior rat population mean parameters (Part 2).

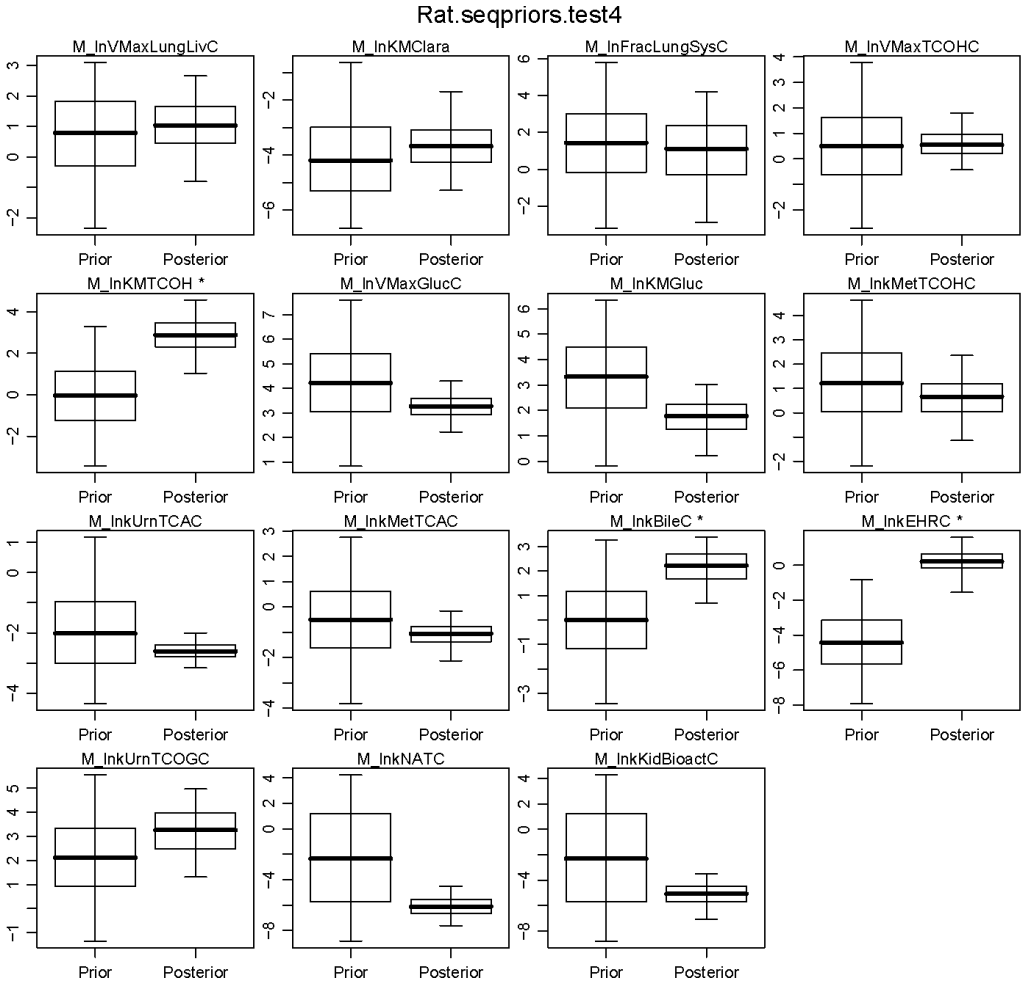

Thick lines are medians, boxes are interquartile regions, and error bars are (2.5, 97.5%) CIs. Parameters labeled with "*" have nonoverlapping interquartile regions.

Figure A-21. Prior and posterior rat population mean parameters (Part 3).

Thick lines are medians, boxes are interquartile regions, and error bars are (2.5, 97.5%) CIs. Parameters labeled with "*" have nonoverlapping interquartile regions.

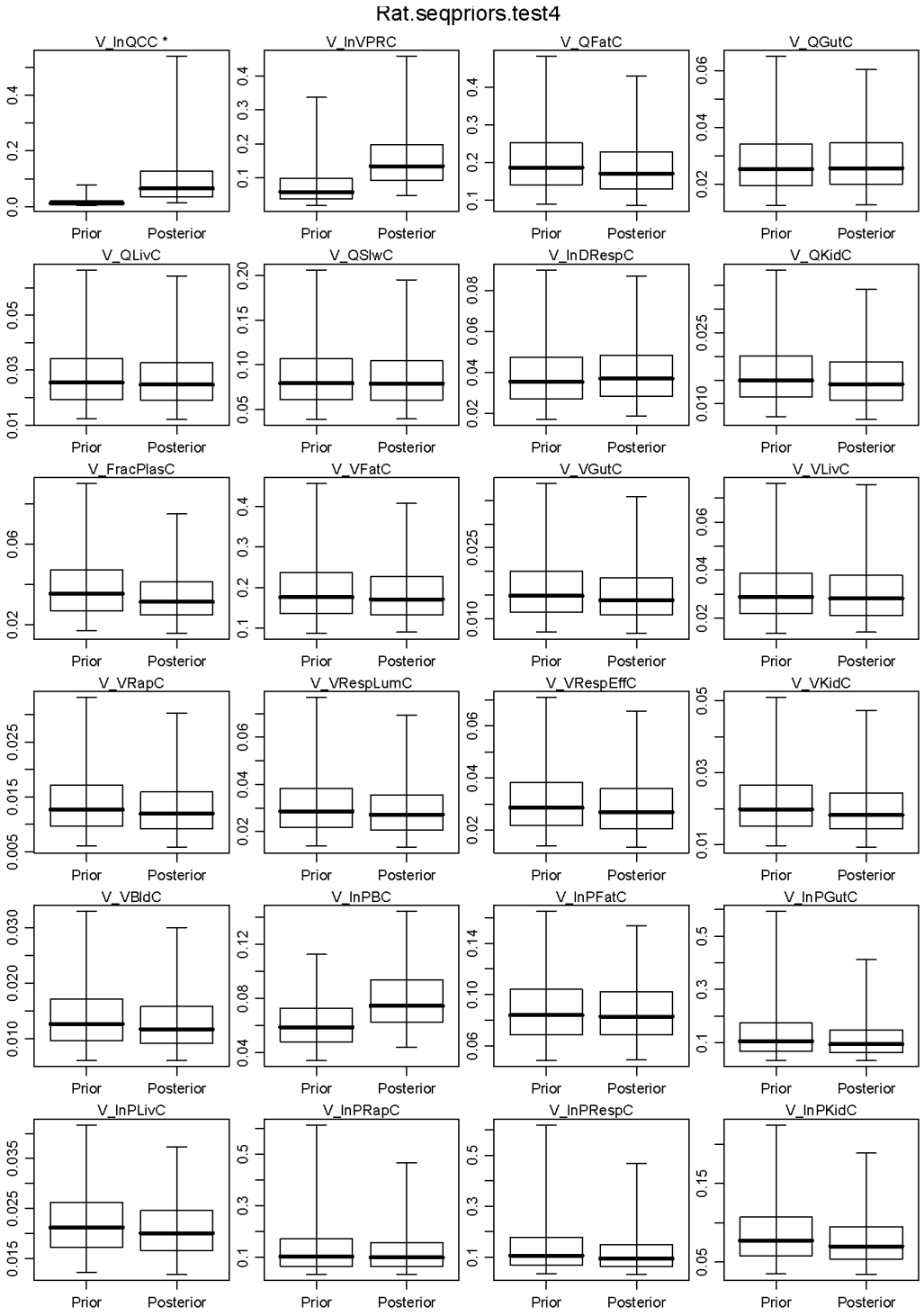

Figure A-22. Prior and posterior rat population variance parameters (Part 1).

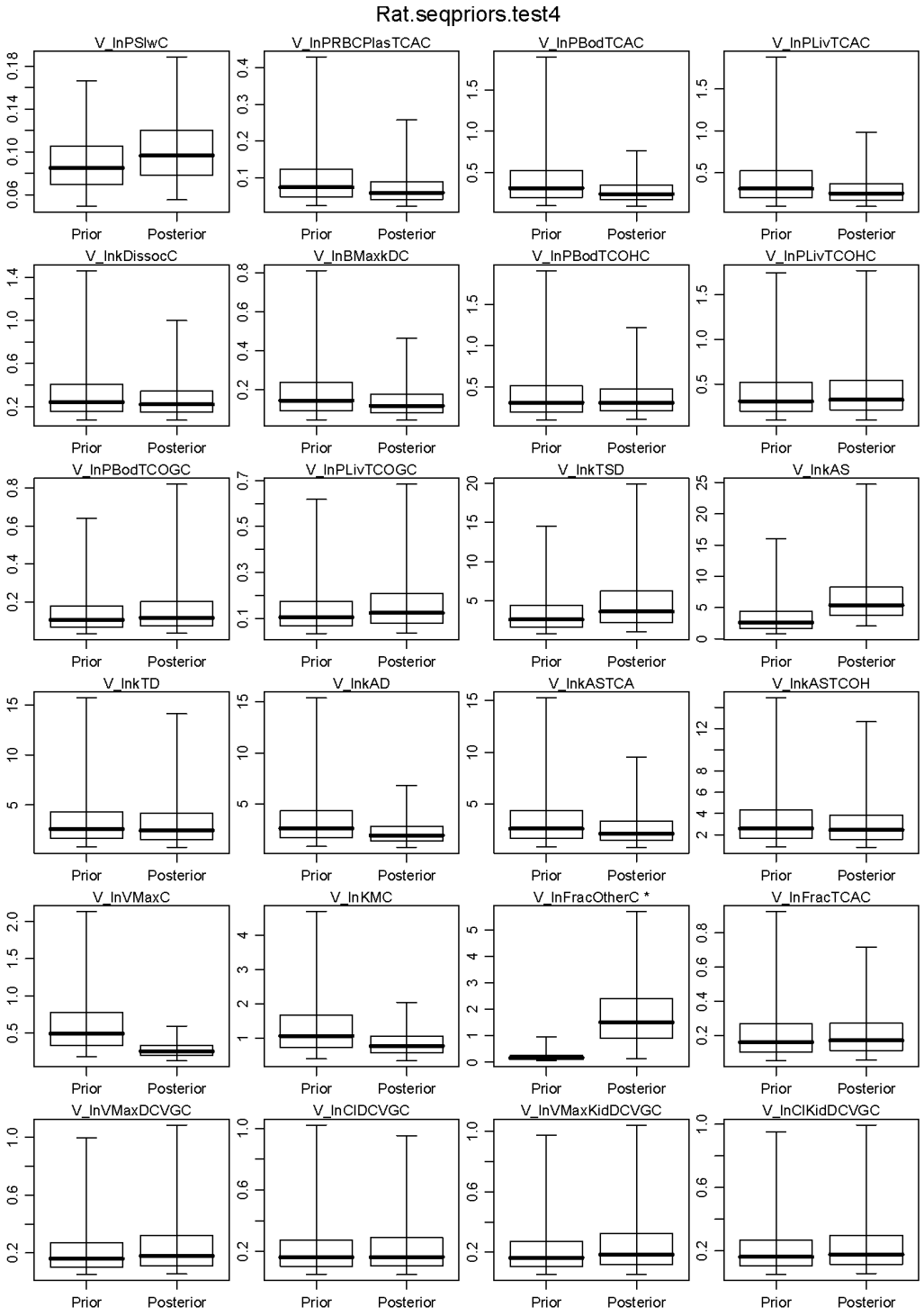

Thick lines are medians, boxes are interquartile regions, and error bars are (2.5, 97.5%) CIs. Parameters labeled with "*" have nonoverlapping interquartile regions.

Figure A-23. Prior and posterior rat population variance parameters (Part 2).

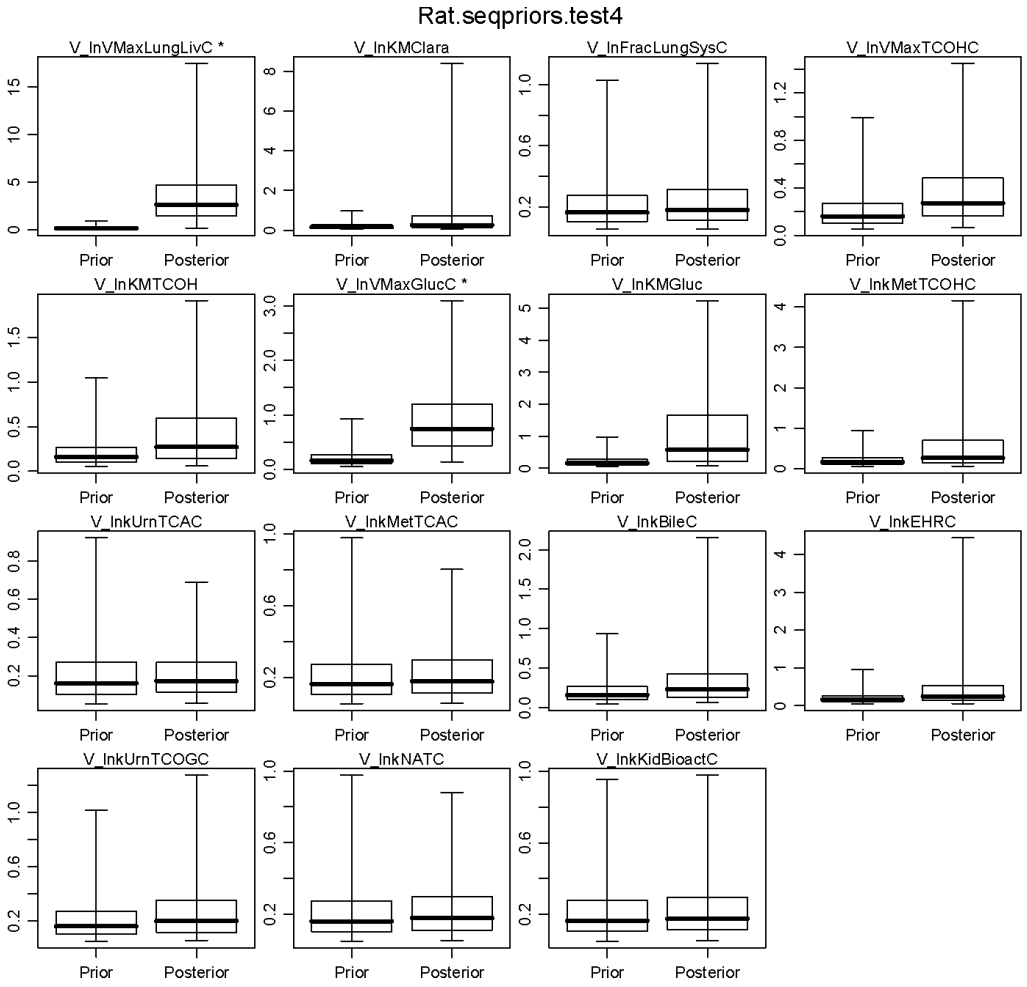

Thick lines are medians, boxes are interquartile regions, and error bars are (2.5, 97.5%) CIs. Parameters labeled with "*" have nonoverlapping interquartile regions.

Figure A-24. Prior and posterior rat population variance parameters (Part 3).

Table A-15. Posterior distributions for human PBPK model population parameters

Sampled parameter	Posterior distributions reflecting uncertainty in population distribution			
	Population (geometric) mean		Population GSD	
	Median (2.5, 97.5%)	*R*	Median (2.5, 97.5%)	*R*
lnQCC	0.837 (0.6761, 1.022)	1.038	1.457 (1.271, 1.996)	1.036
lnVPRC	1.519 (1.261, 1.884)	1.007	1.497 (1.317, 1.851)	1.008
QFatC	0.7781 (0.405, 1.143)	1.014	0.6272 (0.4431, 0.9773)	1
QGutC	0.7917 (0.6631, 0.925)	1.017	0.1693 (0.1199, 0.2559)	1.019
QLivC	0.5099 (0.1737, 0.8386)	1.031	0.4167 (0.2943, 0.6324)	1.009
QSlwC	0.7261 (0.4864, 0.9234)	1.011	0.3166 (0.2254, 0.4802)	1.005
lnDRespC	0.626 (0.3063, 1.013)	1.197	1.291 (1.158, 2.006)	1.083
QKidC	1.007 (0.9137, 1.103)	1.009	0.1004 (0.07307, 0.1545)	1
FracPlasC	1.001 (0.9544, 1.047)	1.01	0.04275 (0.03155, 0.06305)	1
VFatC	0.788 (0.48, 1.056)	1.005	0.3666 (0.2696, 0.5542)	1
VGutC	1 (0.937, 1.067)	1.007	0.06745 (0.04923, 0.1038)	1
VLivC	1.043 (0.8683, 1.23)	1.047	0.1959 (0.1424, 0.3017)	1.003
VRapC	0.9959 (0.9311, 1.06)	1.006	0.06692 (0.04843, 0.1027)	1
VRespLumC	1.003 (0.8461, 1.164)	1.001	0.1671 (0.1209, 0.255)	1
VRespEffC	1 (0.8383, 1.159)	1.001	0.1672 (0.1215, 0.259)	1
VKidC	0.9965 (0.8551, 1.14)	1.007	0.1425 (0.1037, 0.2183)	1
VBldC	1.013 (0.9177, 1.108)	1.003	0.1005 (0.07265, 0.1564)	1
lnPBC	0.9704 (0.8529, 1.101)	1.001	1.216 (1.161, 1.307)	1.002
lnPFatC	0.8498 (0.7334, 0.9976)	1.002	1.188 (1.113, 1.366)	1.002
lnPGutC	1.095 (0.7377, 1.585)	1.029	1.413 (1.214, 2.05)	1.002
lnPLivC	0.9907 (0.6679, 1.441)	1.01	1.338 (1.203, 1.683)	1
lnPRapC	0.93 (0.6589, 1.28)	1.003	1.528 (1.248, 2.472)	1.001
lnPRespC	1.018 (0.6773, 1.5)	1.015	1.32 (1.192, 1.656)	1
lnPKidC	0.9993 (0.8236, 1.219)	1.003	1.155 (1.097, 1.287)	1
lnPSlwC	1.157 (0.8468, 1.59)	1.018	1.69 (1.383, 3.157)	1.008
lnPRBCPlasTCAC	0.3223 (0.04876, 0.8378)	1.007	5.507 (3.047, 19.88)	1.003
lnPBodTCAC	1.194 (0.929, 1.481)	1.043	1.327 (1.185, 1.67)	1.018
lnPLivTCAC	1.202 (0.8429, 1.634)	1.046	1.285 (1.162, 1.648)	1.007
lnkDissocC	0.9932 (0.9387, 1.053)	1.012	1.043 (1.026, 1.076)	1.003
lnBMaxkDC	0.8806 (0.7492, 1.047)	1.038	1.157 (1.085, 1.37)	1.012
lnPBodTCOHC	1.703 (1.439, 2.172)	1.019	1.409 (1.267, 1.678)	1.011
lnPLivTCOHC	1.069 (0.7643, 1.485)	1.028	1.288 (1.165, 1.629)	1.002
lnPBodTCOGC	0.7264 (0.1237, 2.54)	1.003	11.98 (5.037, 185.3)	1.017
lnPLivTCOGC	6.671 (1.545, 24.87)	1.225	5.954 (2.653, 23.68)	1.052
lnPeffDCVG	0.01007 (0.003264, 0.03264)	1.004	1.385 (1.201, 2.03)	1.001
lnkASTCA	4.511 (0.04731, 465.7)	1	5.467 (2.523, 71.06)	1
lnkASTCOH	8.262 (0.0677, 347.9)	1	5.481 (2.513, 67.86)	1
lnV_{MAX}C	0.3759 (0.2218, 0.5882)	1.026	2.21 (1.862, 2.848)	1.003
lnClC	12.64 (5.207, 39.96)	1.028	4.325 (2.672, 9.003)	1.016

Table A-15. Posterior distributions for human PBPK model population parameters (continued)

Sampled parameter	Posterior distributions reflecting uncertainty in population distribution			
	Population (geometric) mean		Population GSD	
	Median (2.5, 97.5%)	*R*	Median (2.5, 97.5%)	*R*
lnFracOtherC	0.1186 (0.02298, 0.2989)	1.061	3.449 (1.392, 9.146)	1.102
lnFracTCAC	0.1315 (0.07115, 0.197)	1.026	2.467 (1.916, 3.778)	1.01
lnClDCVGC	2.786 (1.326, 5.769)	1.08	2.789 (1.867, 4.877)	1.02
lnK_MDCVGC	1.213 (0.3908, 4.707)	1.029	4.43 (2.396, 18.56)	1.035
lnClKidDCVGC	0.04538 (0.001311, 0.1945)	1.204	3.338 (1.295, 30.46)	1.095
lnK_MKidDCVGC	0.2802 (0.1096, 1.778)	1.097	1.496 (1.263, 2.317)	1.001
lnV_{MAX}LungLivC	3.772 (0.8319, 9.157)	1.035	2.228 (1.335, 21.89)	1.014
lnK_MClara	0.2726 (0.02144, 1.411)	1.041	11.63 (1.877, 682.7)	1.041
lnFracLungSysC	24.08 (6.276, 81.14)	1.016	1.496 (1.263, 2.439)	1.001
lnClTCOHC	0.1767 (0.1374, 0.2257)	1.011	1.888 (1.624, 2.307)	1.01
lnK_MTCOH	2.221 (1.296, 4.575)	1.02	2.578 (1.782, 4.584)	1.015
lnClGlucC	0.2796 (0.2132, 0.3807)	1.056	1.955 (1.583, 2.418)	1.079
lnK_MGluc	133.4 (51.56, 277.2)	1.02	1.573 (1.266, 4.968)	1.011
lnkMetTCOHC	0.7546 (0.1427, 2.13)	1.007	5.011 (2.668, 15.71)	1.002
lnkUrnTCAC	0.04565 (0.0324, 0.06029)	1.005	1.878 (1.589, 2.48)	1.006
lnkMetTCAC	0.2812 (0.1293, 0.5359)	1.004	2.529 (1.78, 4.211)	1.002
lnkBileC	6.855 (3.016, 20.69)	1.464	1.589 (1.27, 3.358)	1.015
lnkEHRC	0.1561 (0.09511, 0.2608)	1.1	1.699 (1.348, 2.498)	1.015
lnkUrnTCOGC	15.78 (6.135, 72.5)	1.007	9.351 (4.93, 29.96)	1.003
lnkDCVGC	7.123 (5.429, 9.702)	1.026	1.507 (1.311, 1.897)	1.008
lnkNATC	0.0003157 (0.0001087, 0.002305)	1.008	1.54 (1.261, 3.306)	1
lnkKidBioactC	0.06516 (0.01763, 0.1743)	1.001	1.523 (1.262, 2.987)	1

Table A-16. Posterior distributions for human residual errors

Measurement	Subject[a]	Residual error GSD	
		Median (2.5, 97.5%)	*R*
RetDose	Subject 4	1.131 (1.106, 1.25)	1.001
CAlvPPM	Subject 1	1.832 (1.509, 2.376)	1.015
	Subject 4	1.515 (1.378, 1.738)	1
	Subject 5	1.44 (1.413, 1.471)	1
CVen	Subject 1	1.875 (1.683, 2.129)	1.018
	Subject 3	1.618 (1.462, 1.862)	1
	Subject 4	1.716 (1.513, 2.057)	1.001
	Subject 5	2.948 (2.423, 3.8)	1.007
CTCOH	Subject 1	1.205 (1.185, 1.227)	1.012
	Subject 3	1.213 (1.187, 1.247)	1
	Subject 5	2.101 (1.826, 2.571)	1.001
	Subject 7	1.144 (1.106, 2.887)	1.123
CPlasTCA	Subject 2	1.117 (1.106, 1.17)	1.001
	Subject 7	1.168 (1.123, 1.242)	1
CBldTCA	Subject 1	1.138 (1.126, 1.152)	1.003
	Subject 2	1.119 (1.106, 1.178)	1
	Subject 4	1.488 (1.351, 1.646)	1.018
	Subject 5	1.438 (1.367, 1.537)	1.002
zAUrnTCA	Subject 1	1.448 (1.414, 1.485)	1.001
	Subject 2	1.113 (1.105, 1.149)	1.001
	Subject 3	1.242 (1.197, 1.301)	1.001
	Subject 4	1.538 (1.441, 1.67)	1
	Subject 6	1.158 (1.118, 1.228)	1
	Subject 7	1.119 (1.106, 1.181)	1
zAUrnTCA_collect	Subject 3	1.999 (1.178, 3.903)	1.003
	Subject 5	2.787 (2.134, 4.23)	1.001
AUrnTCOGTCOH	Subject 1	1.106 (1.105, 1.112)	1.001
	Subject 3	1.11 (1.105, 1.125)	1
	Subject 4	1.124 (1.107, 1.151)	1.001
	Subject 6	1.117 (1.106, 1.157)	1.001
	Subject 7	1.134 (1.106, 1.348)	1.003
AUrnTCOGTCOH_collect	Subject 3	1.3 (1.111, 2.333)	1.004
	Subject 5	1.626 (1.524, 1.767)	1
CDCVGmol	Subject 1	1.53 (1.436, 1.656)	1.009
zAUrnNDCVC	Subject 6	1.167 (1.124, 1.244)	1
TotCTCOH	Subject 1	1.204 (1.185, 1.226)	1.011
	Subject 4	1.247 (1.177, 1.366)	1.009
	Subject 5	1.689 (1.552, 1.9)	1.001

[a]The seven subjects are: (1) Fisher et al. (1998); (2) Paycok and Powell (1945); (3) Kimmerle and Eben (1973a); (4) Monster et al. (1976); (5) Chiu et al. (2007); (6) Bernauer et al. (1996); and (7) Muller et al. (1974).

Table A-17. Posterior correlations for human population mean parameters

Human		
Parameter 1	**Parameter 2**	**Correlation coefficient**
lnkBileC	lnPLivTCOGC	-0.649
lnClKidDCVGC	lnKMKidDCVGC	-0.567
lnClGlucC	lnkEHRC	0.438
lnkMetTCAC	lnPLivTCAC	-0.392
lnClKidDCVGC	lnDRespC	-0.324
lnClKidDCVGC	lnkEHRC	-0.301
lnKMTCOH	lnPBodTCAC	0.289
lnkMetTCAC	lnPBodTCAC	0.283
lnClKidDCVGC	lnkBileC	-0.277
lnkEHRC	lnPBodTCOHC	-0.277
lnClDCVGC	lnkDCVGC	0.269
lnBMaxkDC	lnPBodTCAC	0.267
lnFracOtherC	lnQCC	0.260
lnFracOtherC	lnkDCVGC	-0.258
lnFracOtherC	VLivC	0.257
lnFracOtherC	lnPLivTCOGC	-0.256
lnClDCVGC	lnFracOtherC	-0.256
lnClDCVGC	VLivC	-0.252

Note: only parameter pairs with correlation coefficient ≥0.25 are listed.

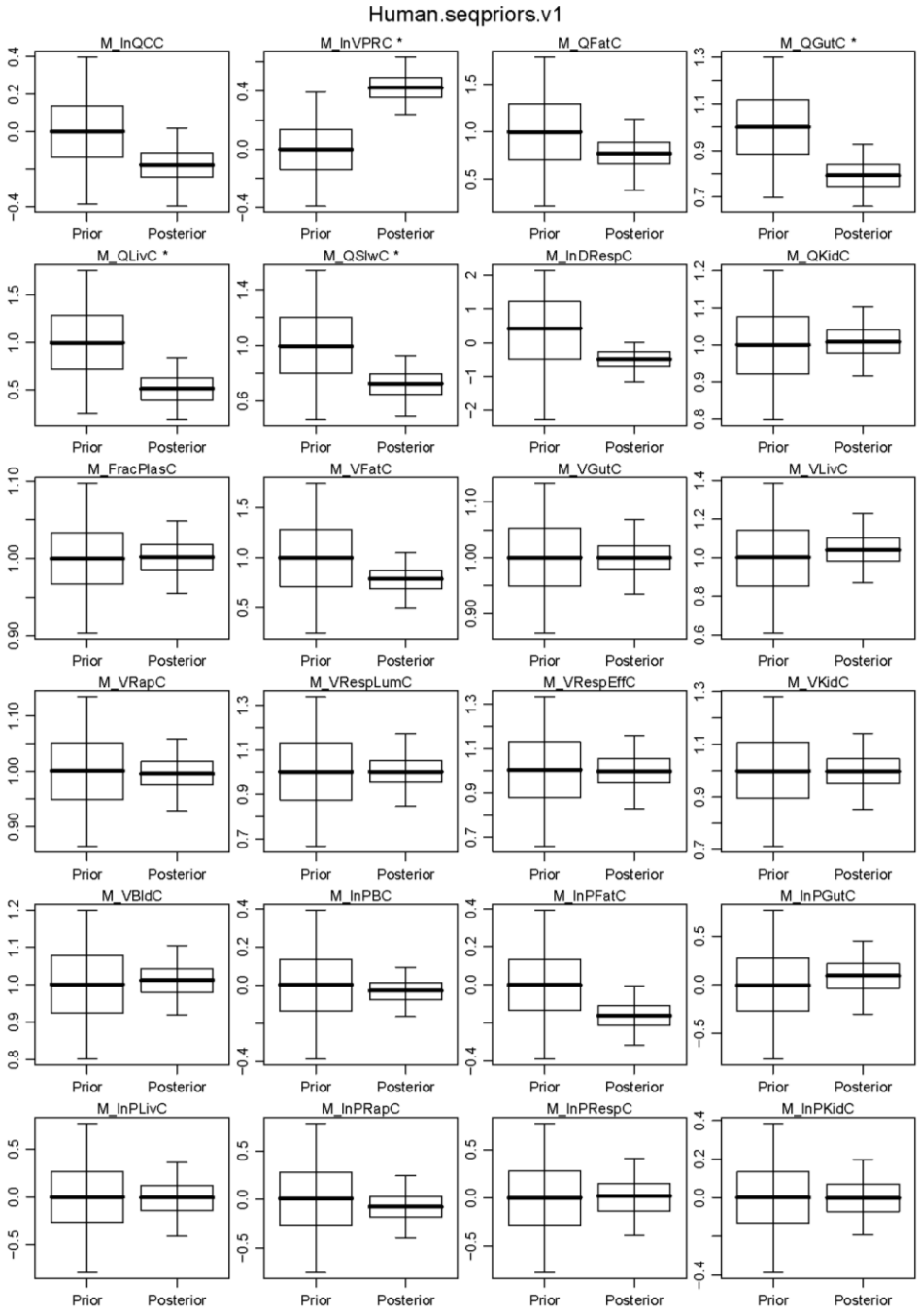

Thick lines are medians, boxes are interquartile regions, and error bars are (2.5, 97.5%) CIs. Parameters labeled with "*" have nonoverlapping interquartile regions.

Figure A-25. Prior and posterior human population mean parameters (Part 1).

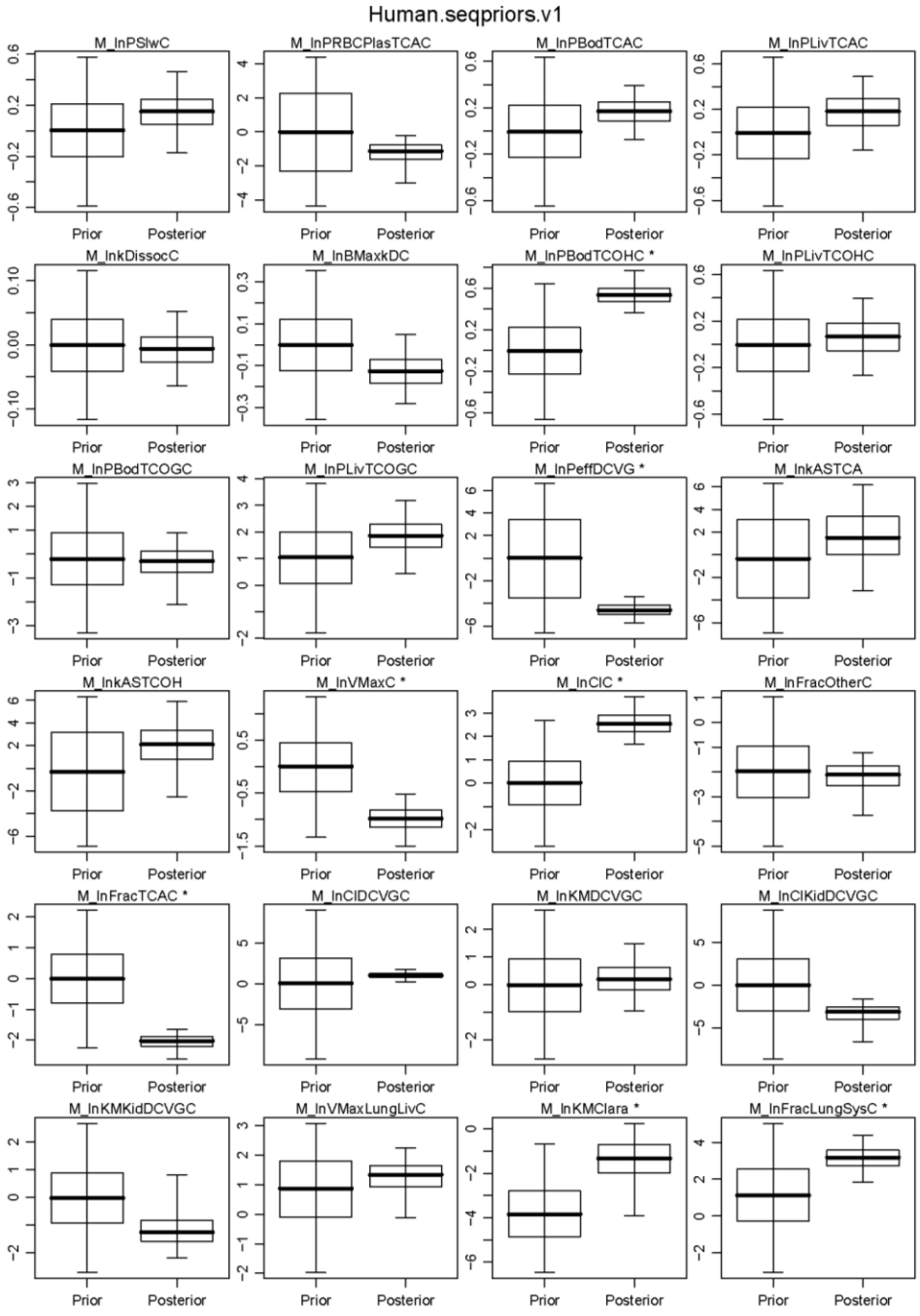

Thick lines are medians, boxes are interquartile regions, and error bars are (2.5, 97.5%) CIs. Parameters labeled with "*" have nonoverlapping interquartile regions.

Figure A-26. Prior and posterior human population mean parameters (Part 2).

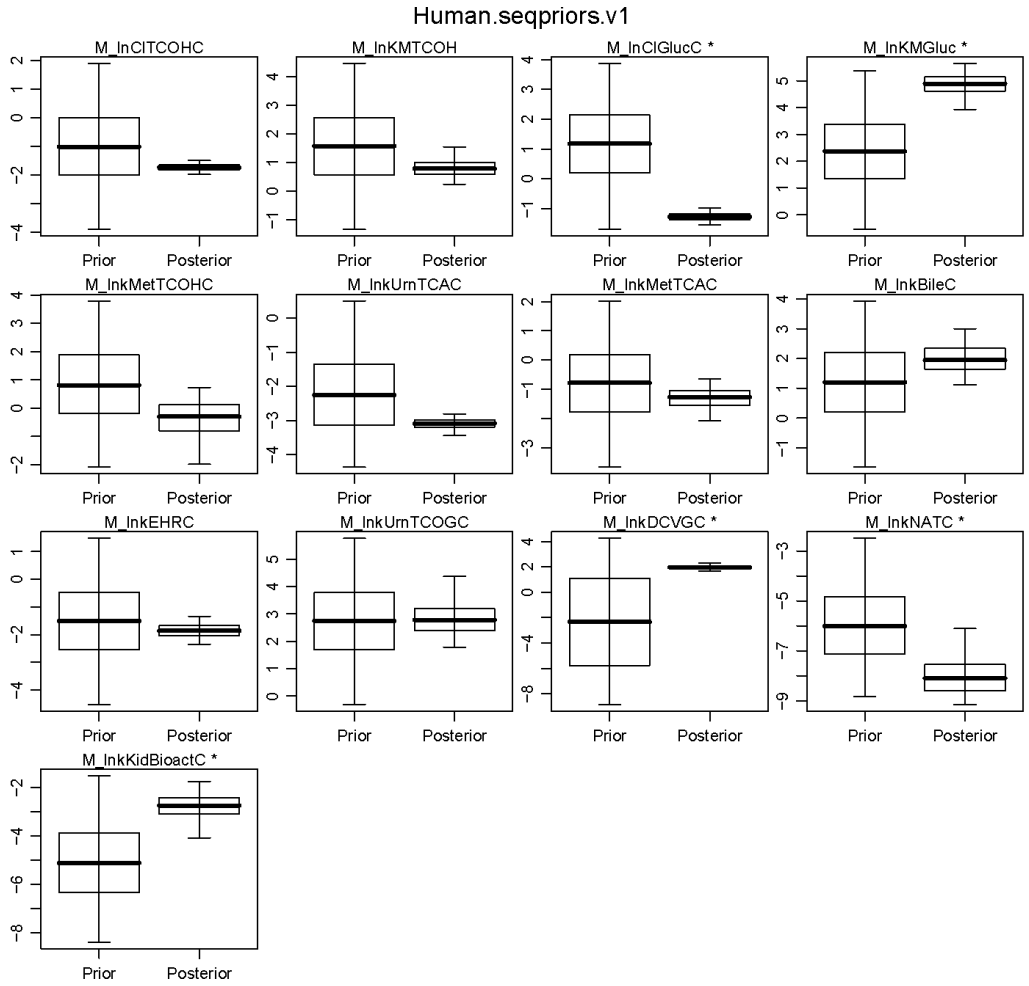

Thick lines are medians, boxes are interquartile regions, and error bars are (2.5, 97.5%) CIs. Parameters labeled with "*" have nonoverlapping interquartile regions.

Figure A-27. Prior and posterior human population mean parameters (Part 3).

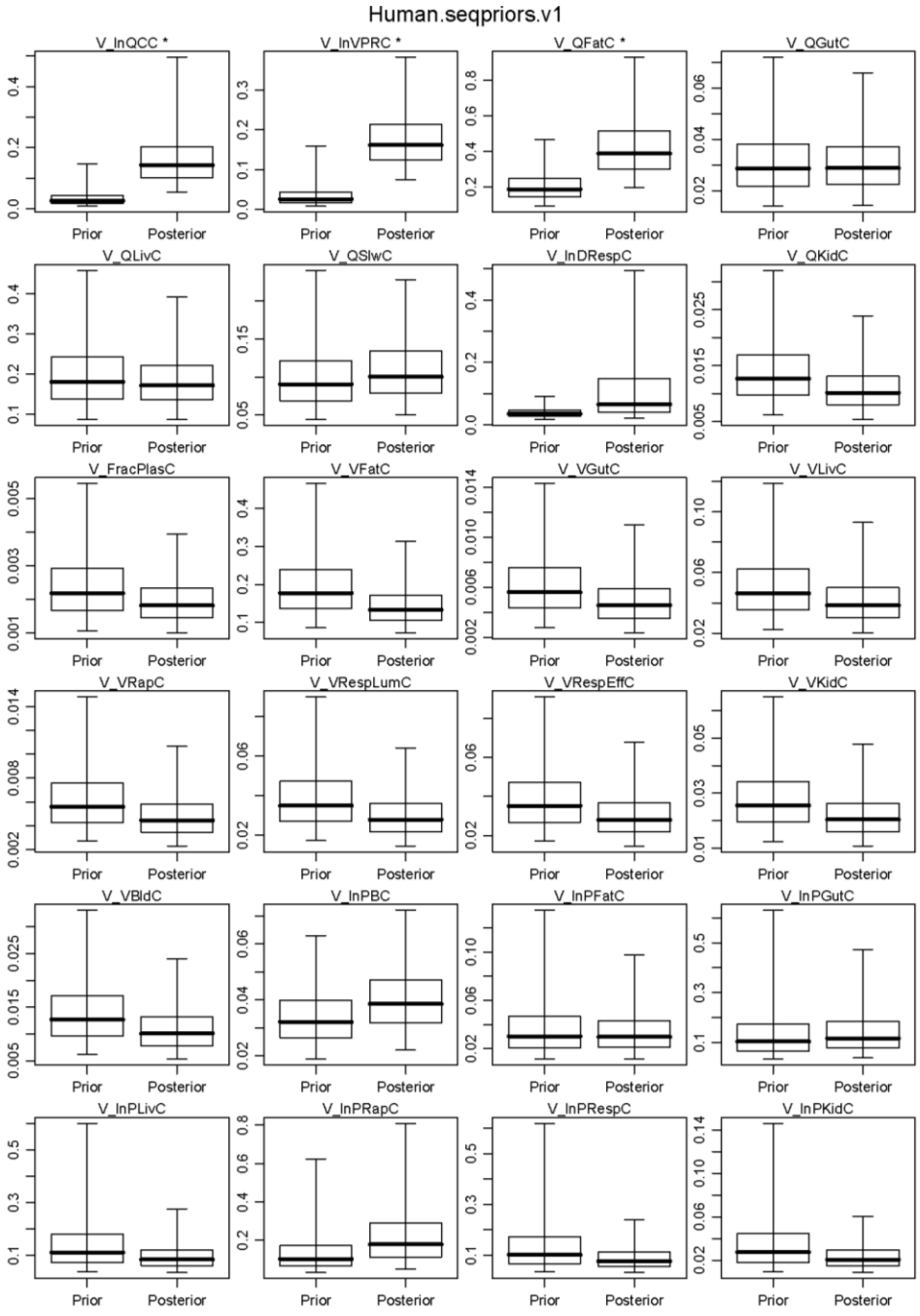

Thick lines are medians, boxes are interquartile regions, and error bars are (2.5, 97.5%) CIs. Parameters labeled with "*" have nonoverlapping interquartile regions.

Figure A-28. Prior and posterior human population variance parameters (Part 1).

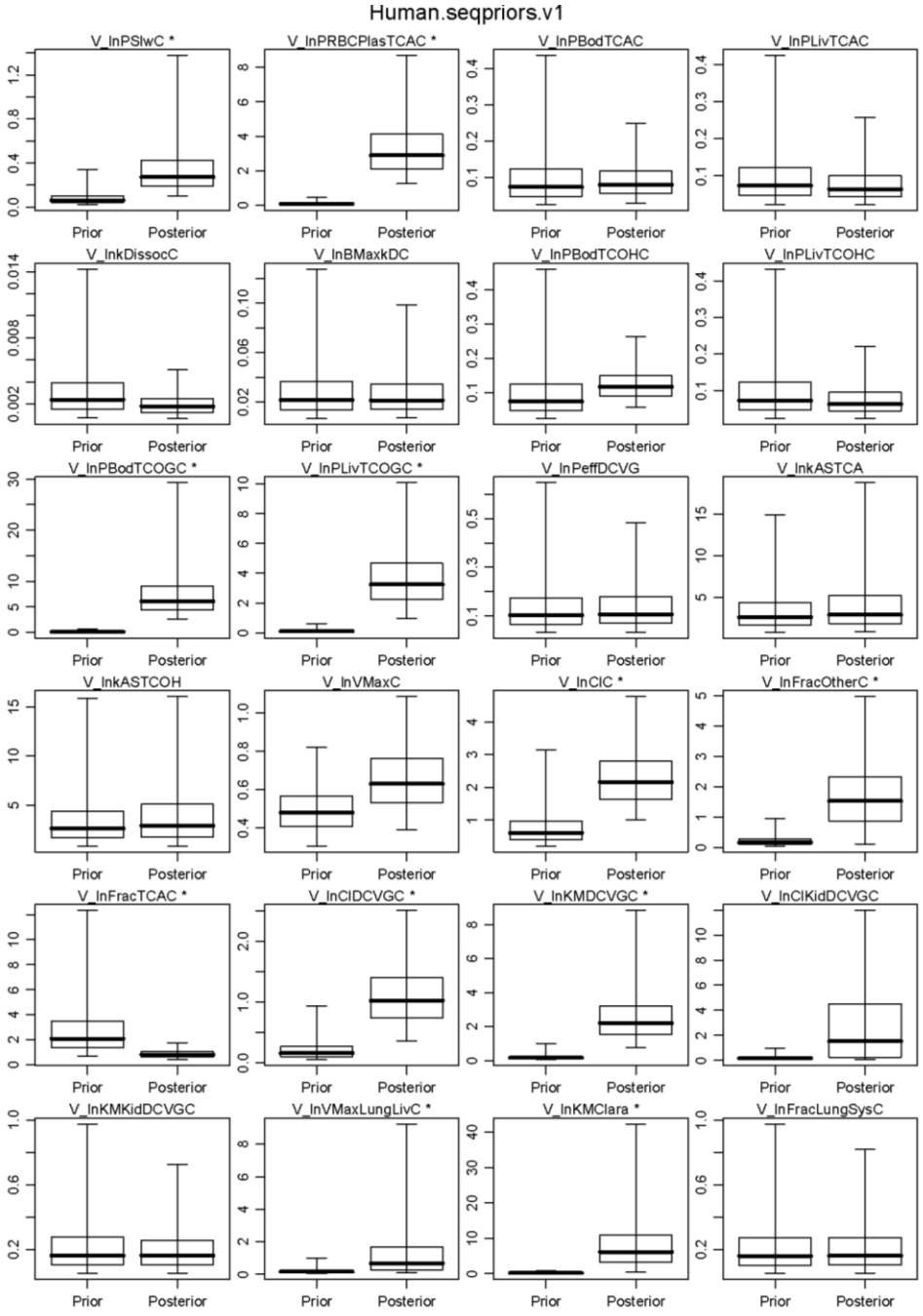

Thick lines are medians, boxes are interquartile regions, and error bars are (2.5, 97.5%) CIs. Parameters labeled with "*" have nonoverlapping interquartile regions.

Figure A-29. Prior and posterior human population variance parameters (Part 2).

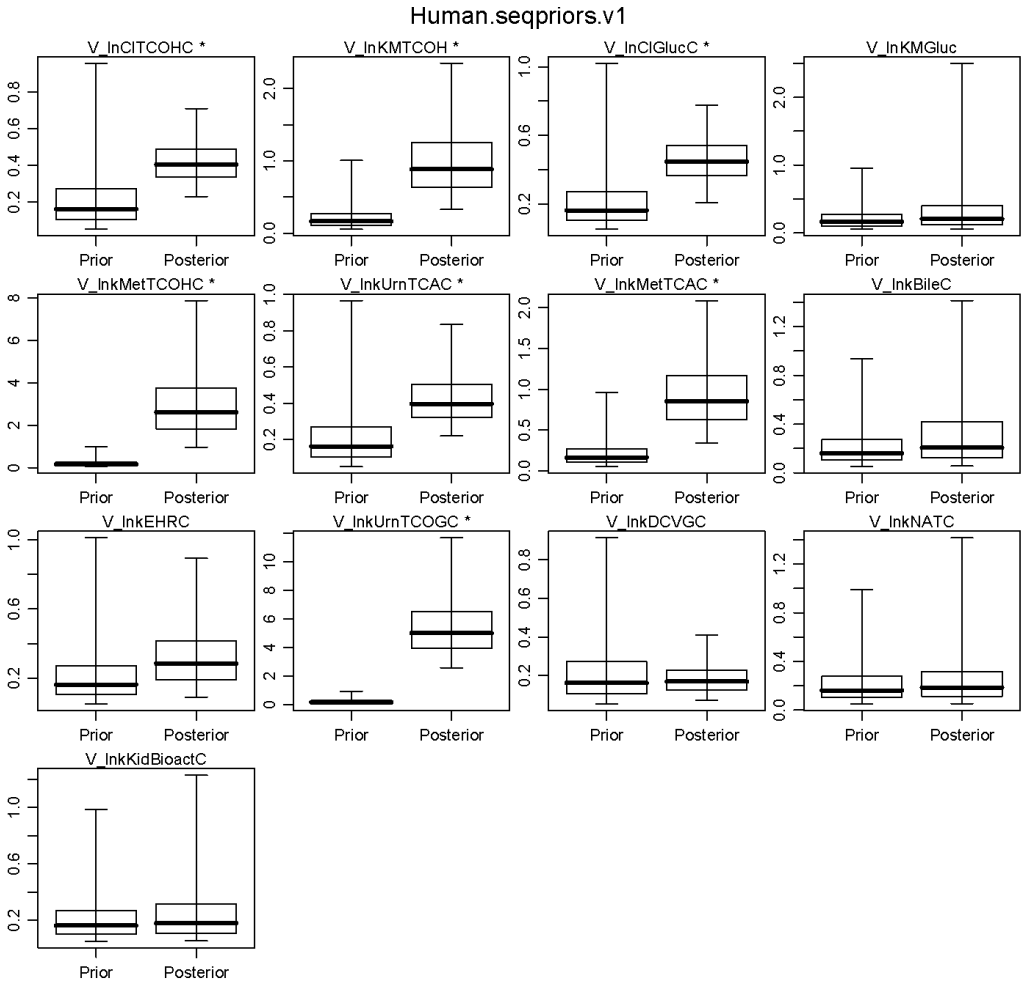

Thick lines are medians, boxes are interquartile regions, and error bars are (2.5, 97.5%) CIs. Parameters labeled with "*" have nonoverlapping interquartile regions.

Figure A-30. Prior and posterior human population variance parameters (Part 3).

A.5.2. Comparison of Model Predictions with Data

Time-course graphs of calibration and evaluation data compared to posterior predictions are shown in Figures A-31 to A-35. For each panel, the boxes are the experimental data, the solid red line is the prediction using the posterior mean of the subject-specific parameters (only shown for calibration data), and the shaded regions (or + with error bars, for single data points) are bounded by the 2.5, 25, 50, 75, and 97.5% population-based predictions.

A.5.2.1. Mouse Data and Model Predictions

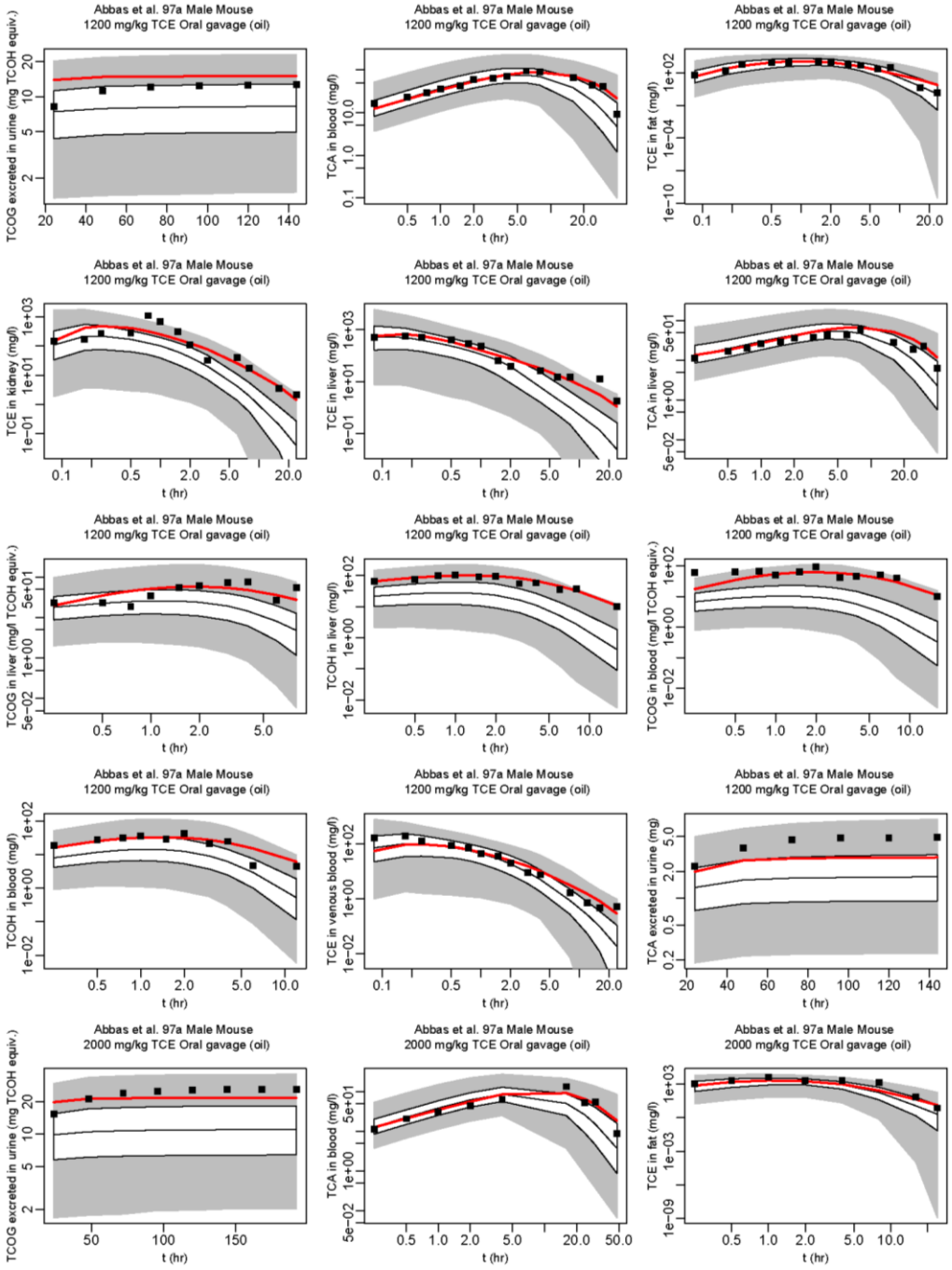

Figure A-31. Comparison of mouse calibration data (boxes) and PBPK model predictions (red line: using the posterior mean of the subject-specific parameters; + with error bars: single data points; or shaded regions: 2.5, 25, 50, 75, and 97.5% population-based predictions).

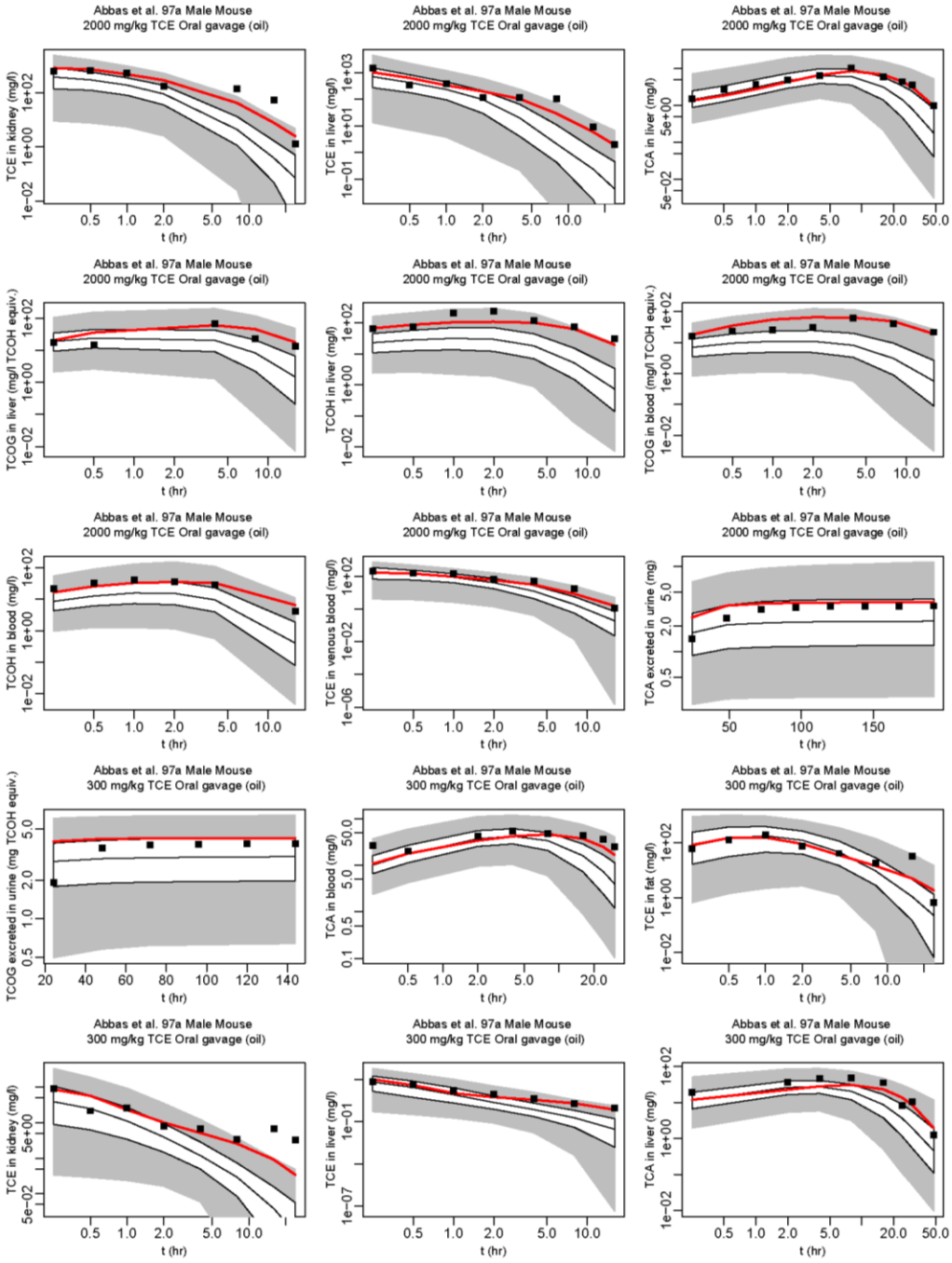

Figure A-31. Comparison of mouse calibration data (boxes) and PBPK model predictions (red line: using the posterior mean of the subject-specific parameters; + with error bars: single data points; or shaded regions: 2.5, 25, 50, 75, and 97.5% population-based predictions) (continued).

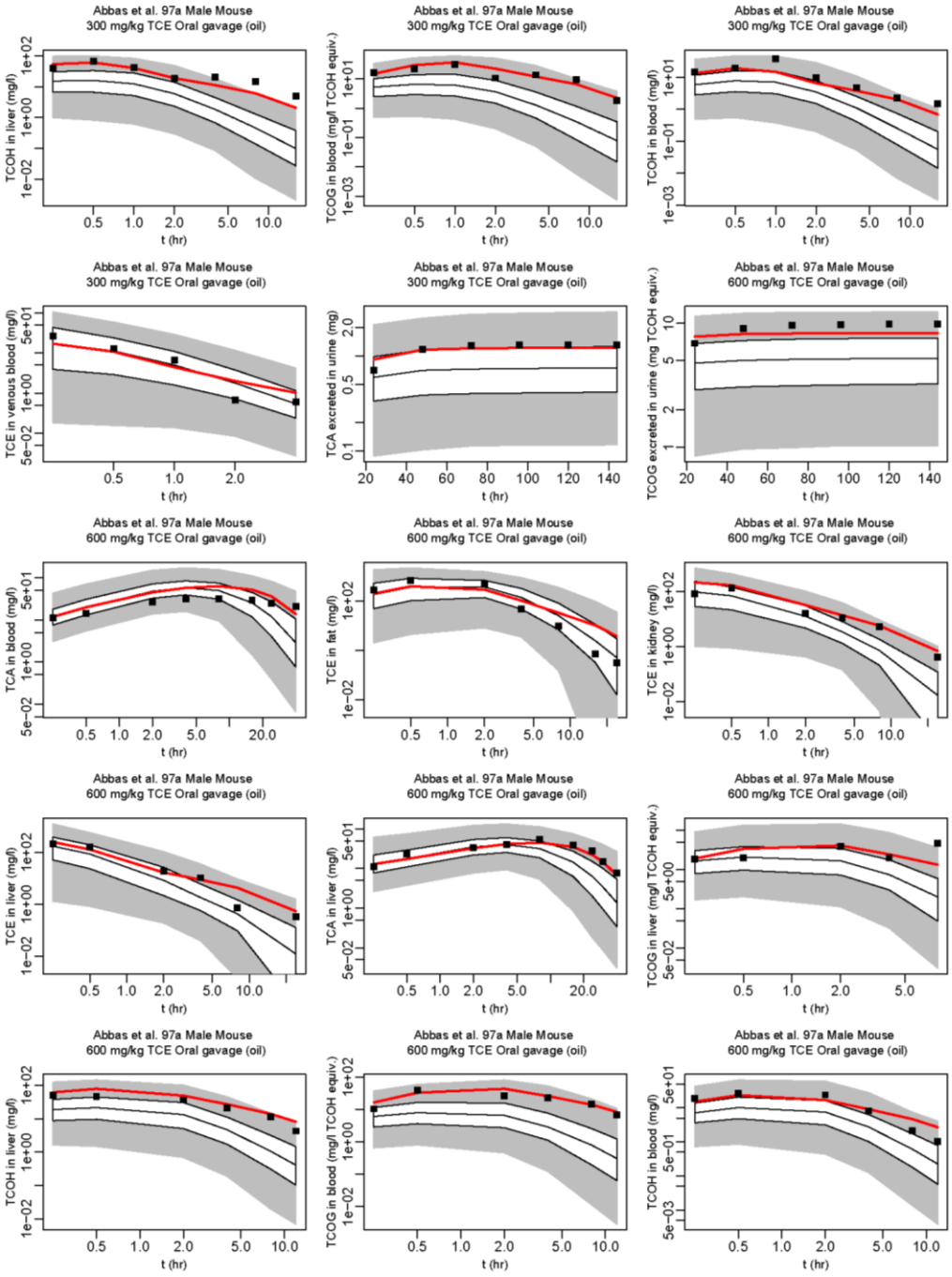

Figure A-31. Comparison of mouse calibration data (boxes) and PBPK model predictions (red line: using the posterior mean of the subject-specific parameters; + with error bars: single data points; or shaded regions: 2.5, 25, 50, 75, and 97.5% population-based predictions) (continued).

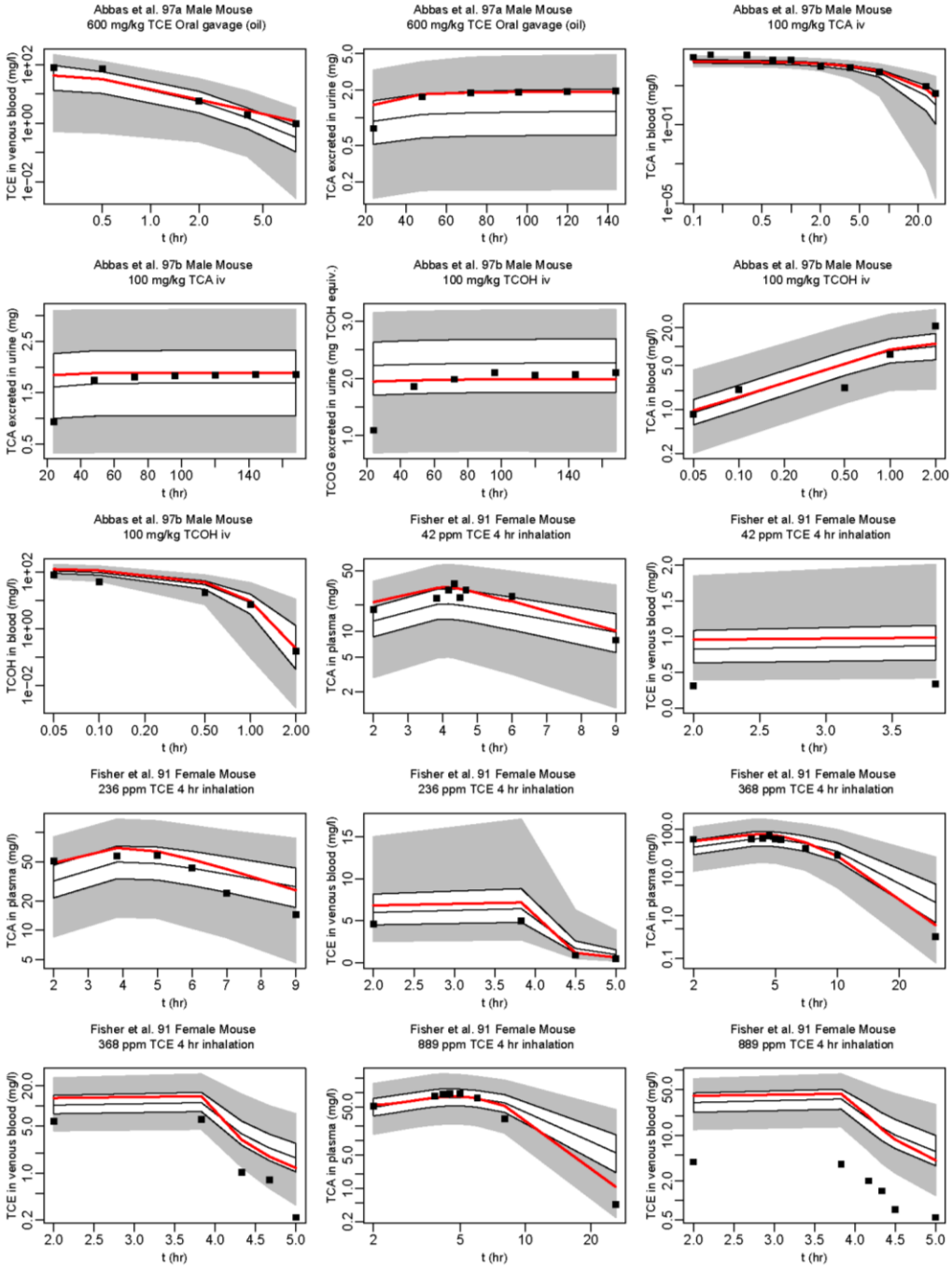

Figure A-31. Comparison of mouse calibration data (boxes) and PBPK model predictions (red line: using the posterior mean of the subject-specific parameters; + with error bars: single data points; or shaded regions: 2.5, 25, 50, 75, and 97.5% population-based predictions) (continued).

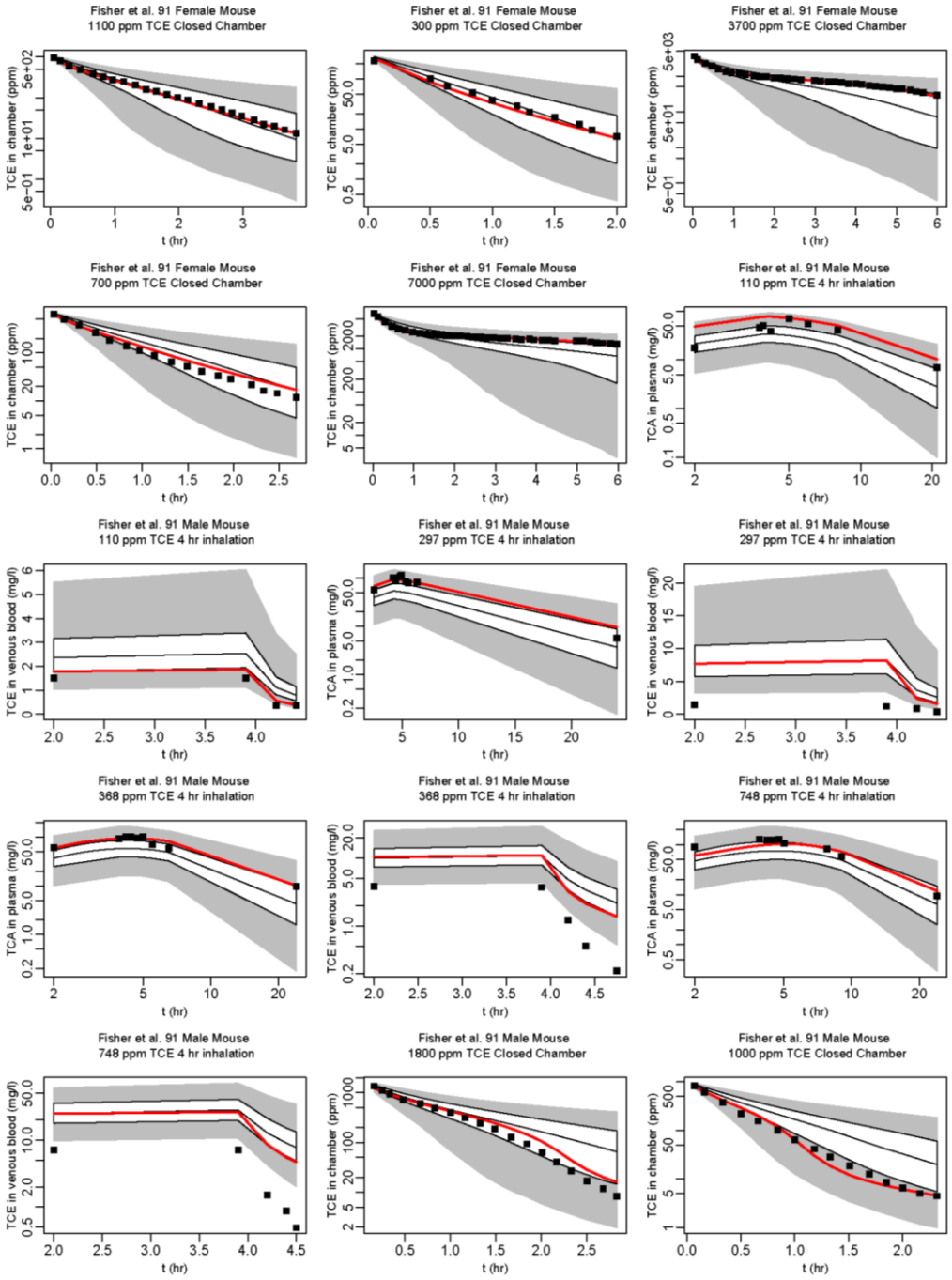

Figure A-31. Comparison of mouse calibration data (boxes) and PBPK model predictions (red line: using the posterior mean of the subject-specific parameters; + with error bars: single data points; or shaded regions: 2.5, 25, 50, 75, and 97.5% population-based predictions) (continued).

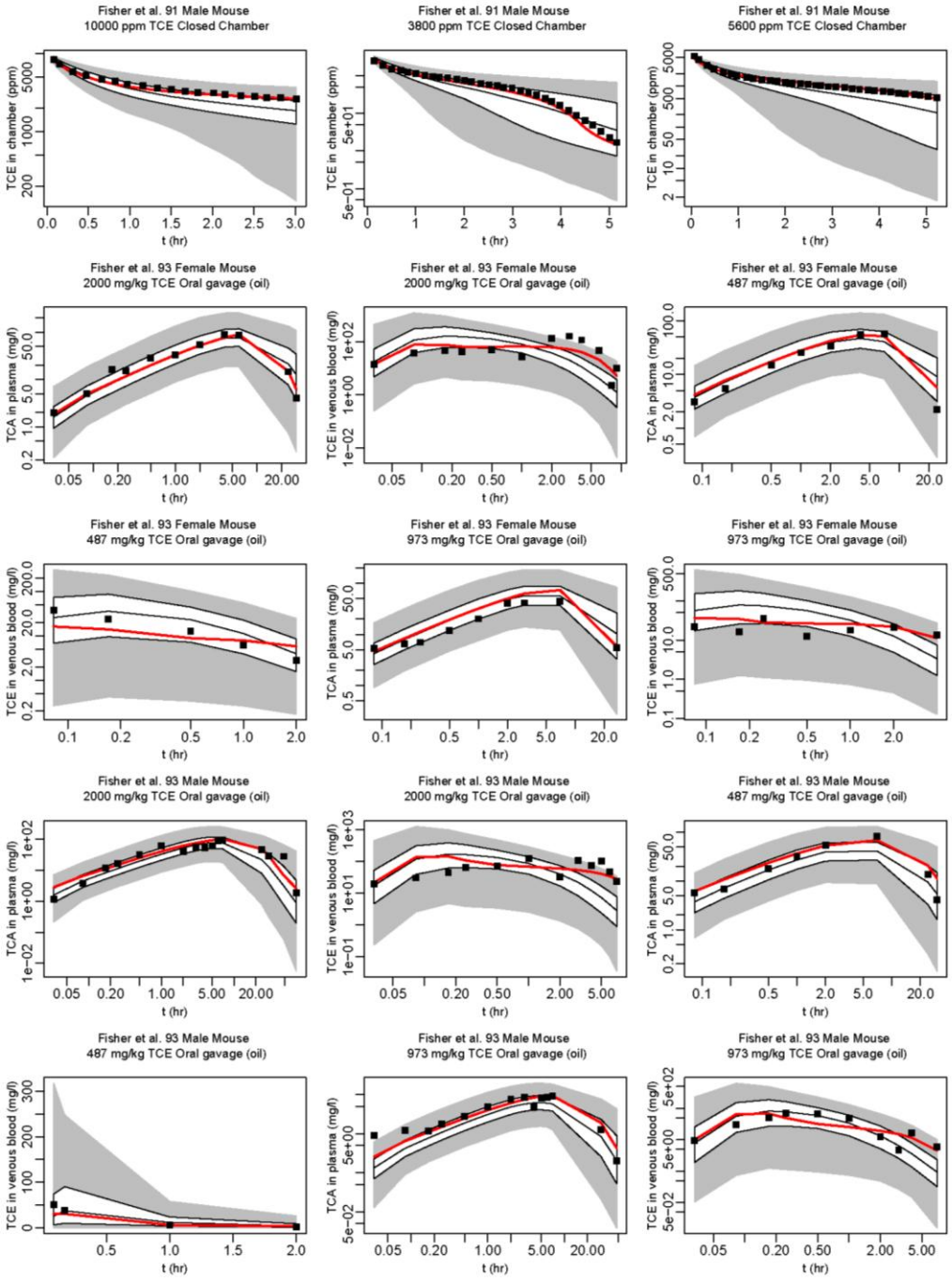

Figure A-31. Comparison of mouse calibration data (boxes) and PBPK model predictions (red line: using the posterior mean of the subject-specific parameters; + with error bars: single data points; or shaded regions: 2.5, 25, 50, 75, and 97.5% population-based predictions) (continued).

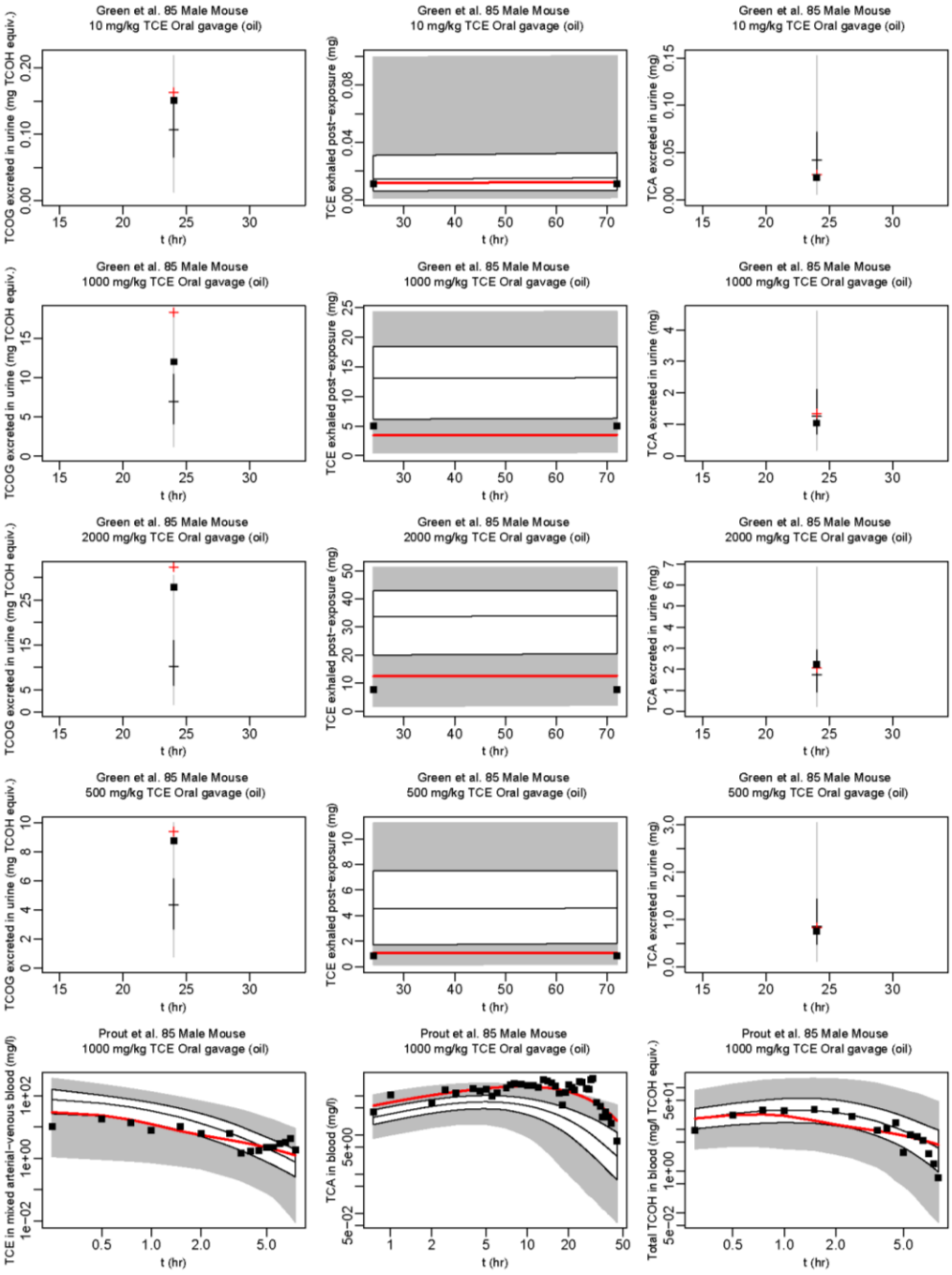

Figure A-31. Comparison of mouse calibration data (boxes) and PBPK model predictions (red line: using the posterior mean of the subject-specific parameters; + with error bars: single data points; or shaded regions: 2.5, 25, 50, 75, and 97.5% population-based predictions) (continued).

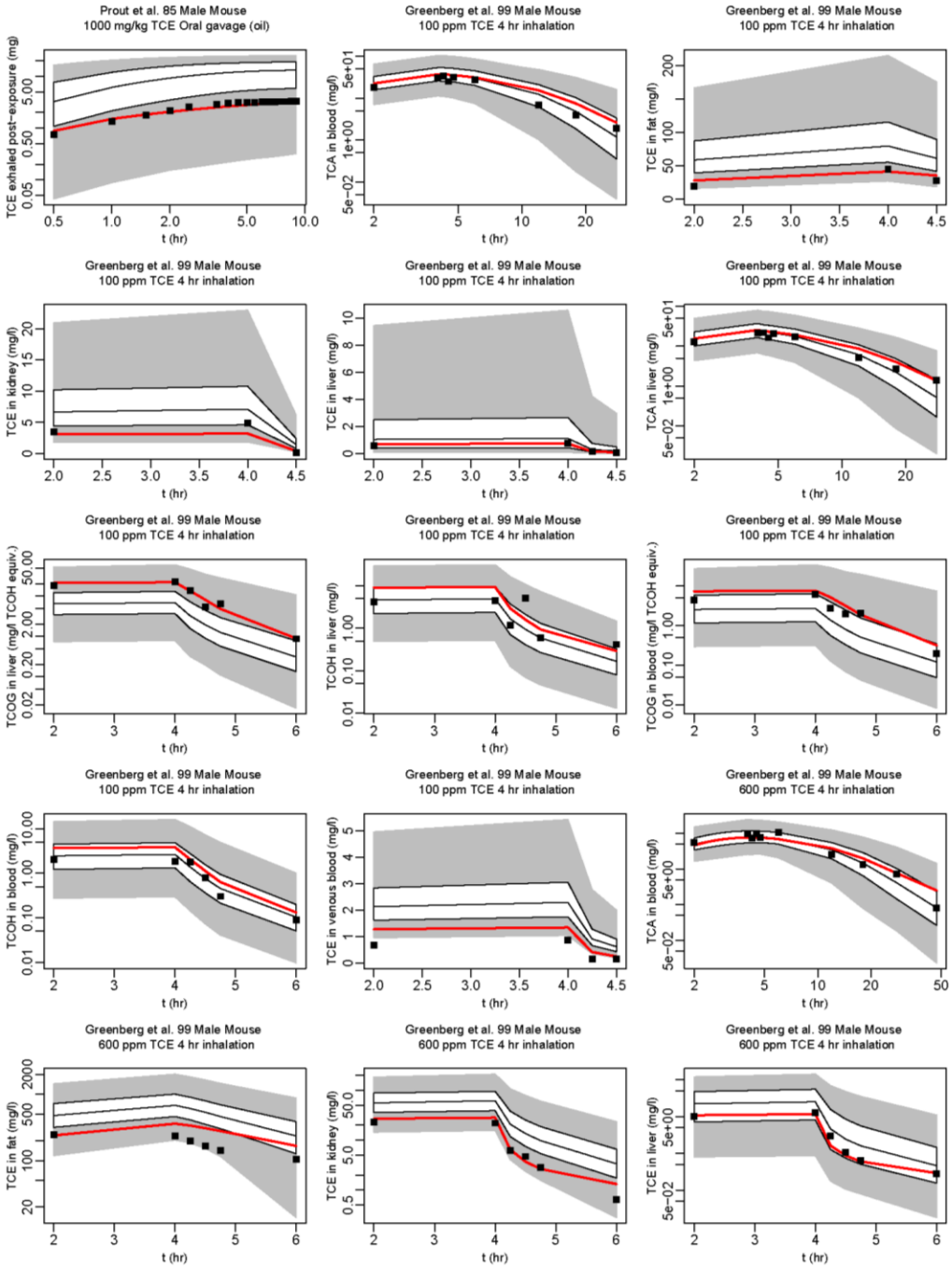

Figure A-31. Comparison of mouse calibration data (boxes) and PBPK model predictions (red line: using the posterior mean of the subject-specific parameters; + with error bars: single data points; or shaded regions: 2.5, 25, 50, 75, and 97.5% population-based predictions) (continued).

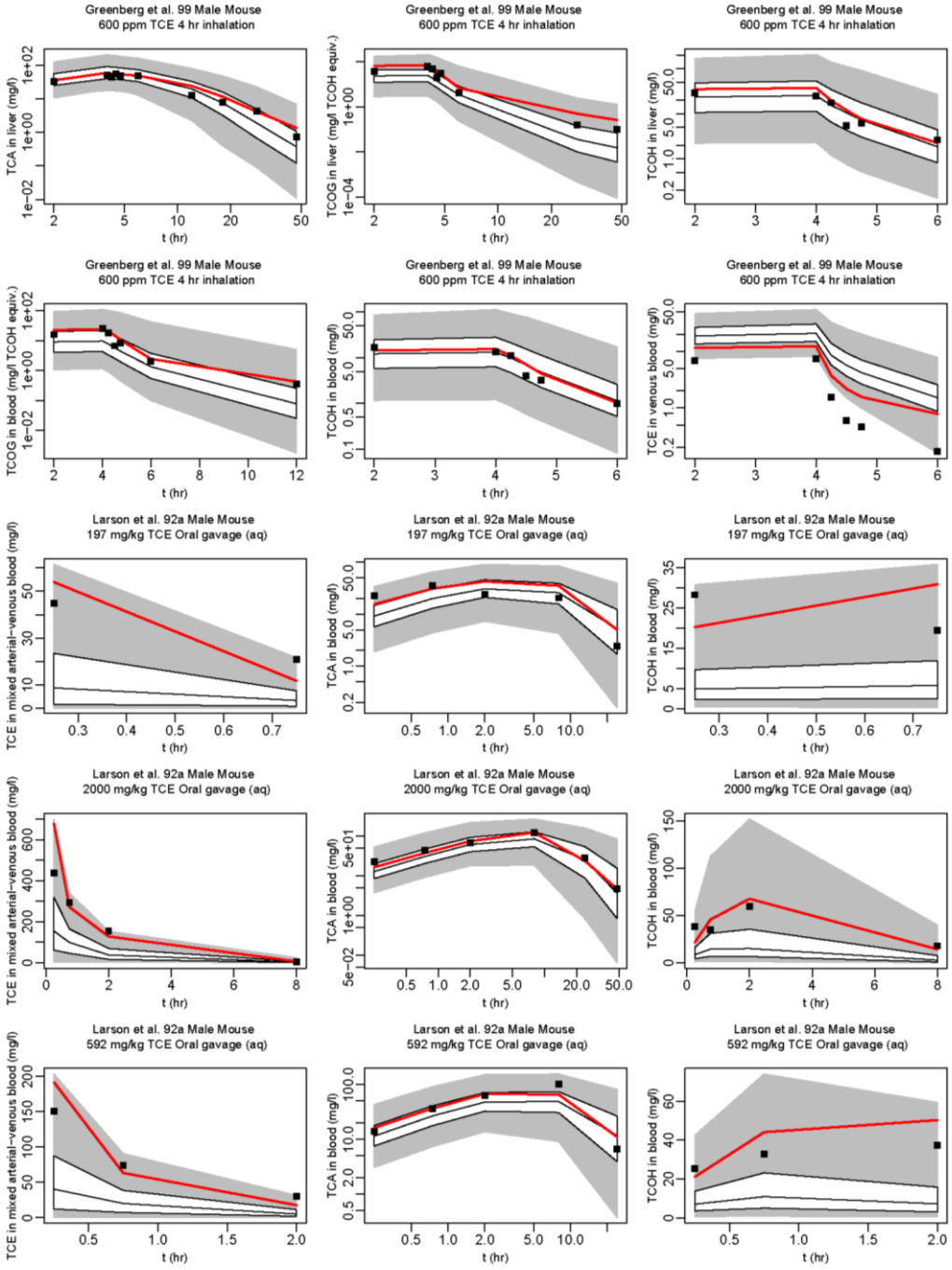

Figure A-31. Comparison of mouse calibration data (boxes) and PBPK model predictions (red line: using the posterior mean of the subject-specific parameters; + with error bars: single data points; or shaded regions: 2.5, 25, 50, 75, and 97.5% population-based predictions) (continued).

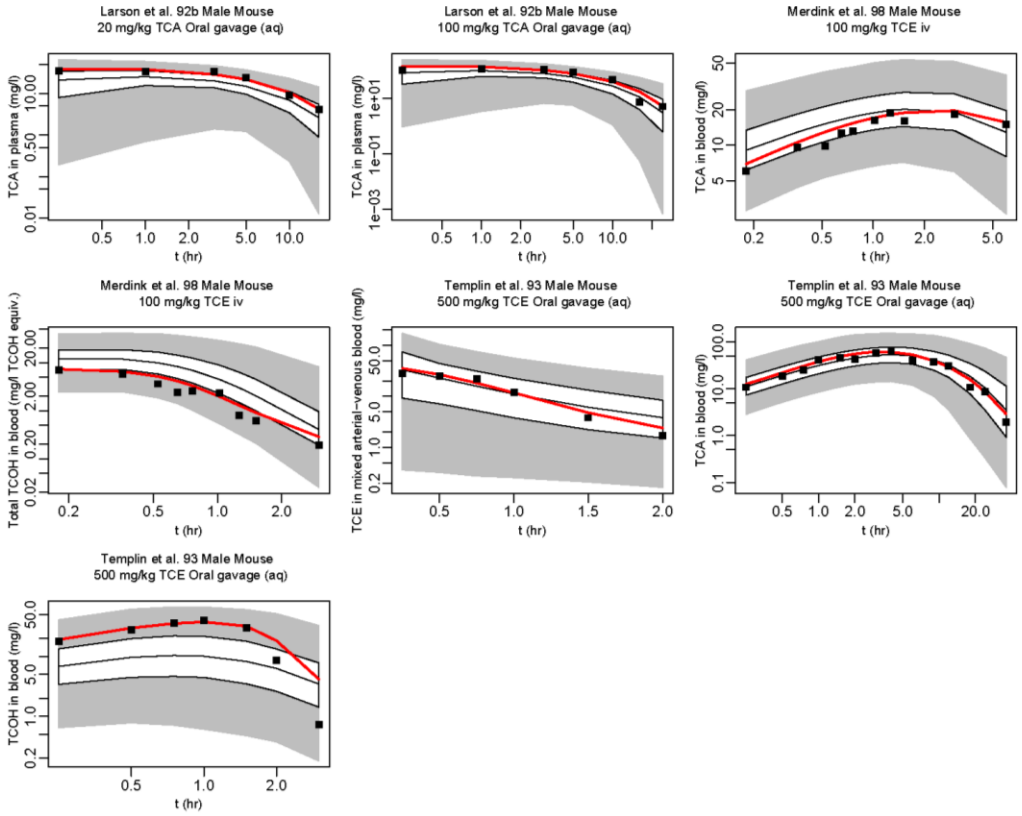

Figure A-31. Comparison of mouse calibration data (boxes) and PBPK model predictions (red line: using the posterior mean of the subject-specific parameters; + with error bars: single data points; or shaded regions: 2.5, 25, 50, 75, and 97.5% population-based predictions) (continued).

A.5.2.2. Rat Data and Model Predictions

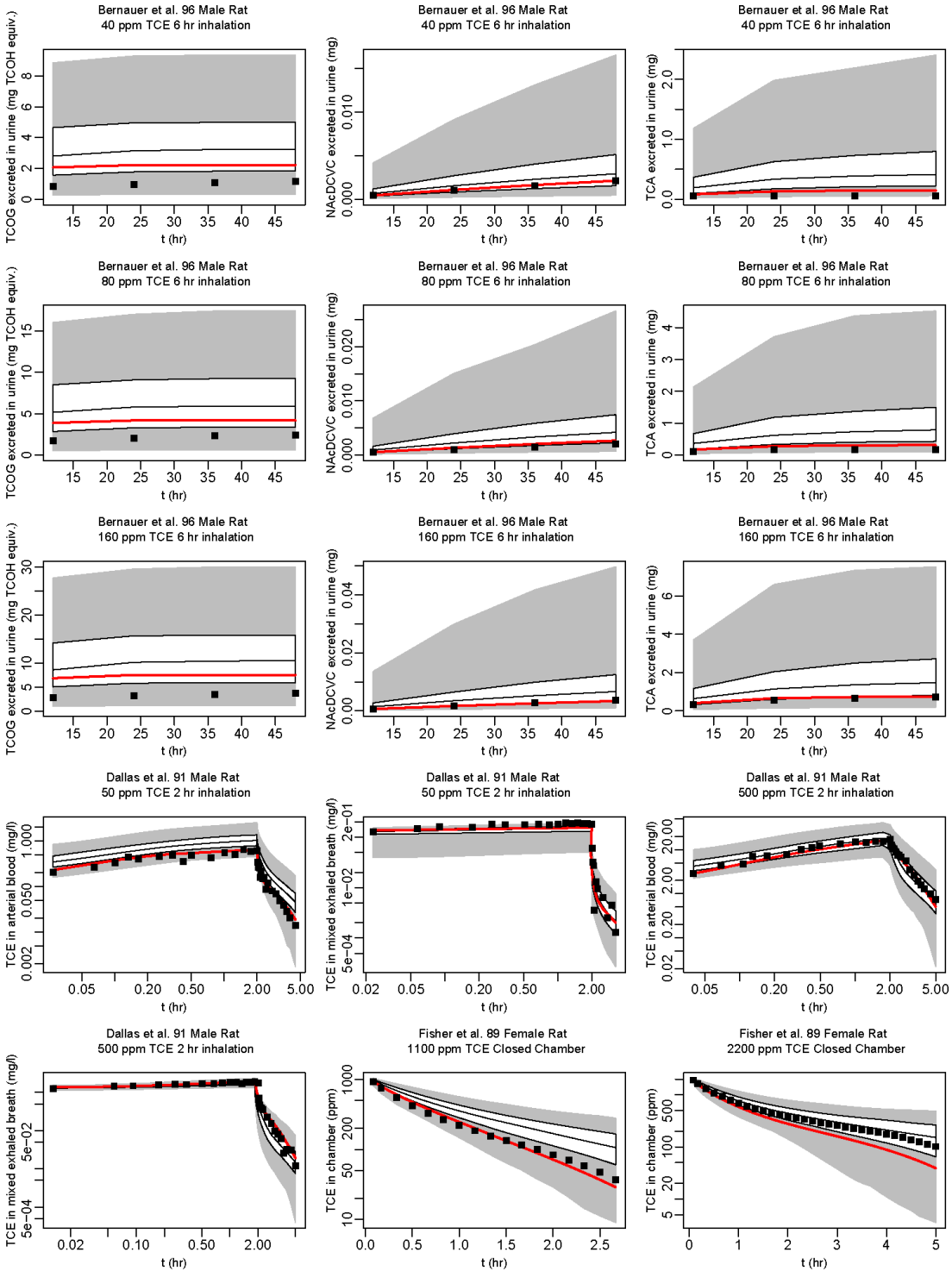

Figure A-32. Comparison of rat calibration data (boxes) and PBPK model predictions (red line: using the posterior mean of the subject-specific parameters; + with error bars: single data points; or shaded regions: 2.5, 25, 50, 75, and 97.5% population-based predictions).

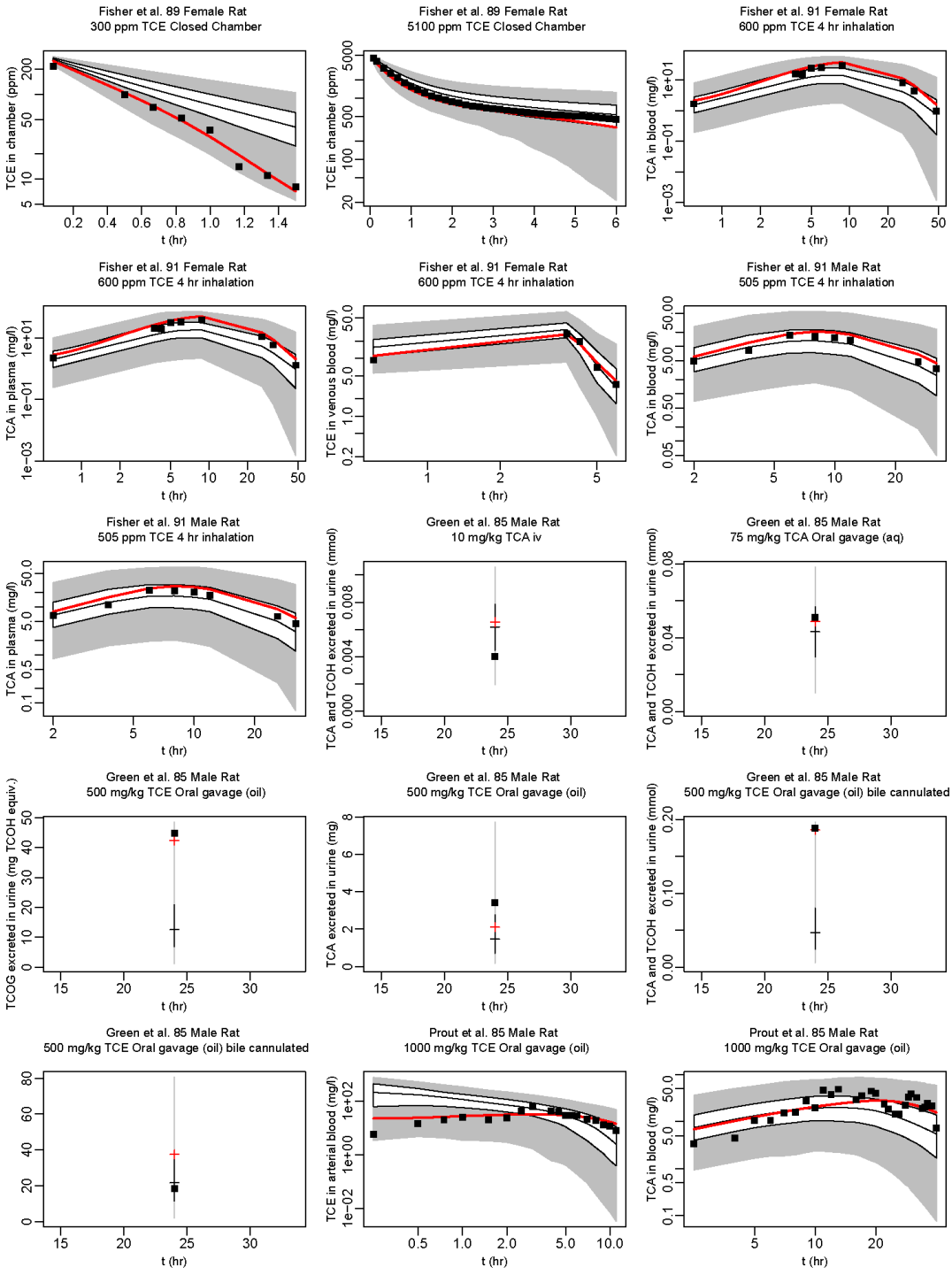

Figure A-32. Comparison of rat calibration data (boxes) and PBPK model predictions (red line: using the posterior mean of the subject-specific parameters; + with error bars: single data points; or shaded regions: 2.5, 25, 50, 75, and 97.5% population-based predictions) (continued).

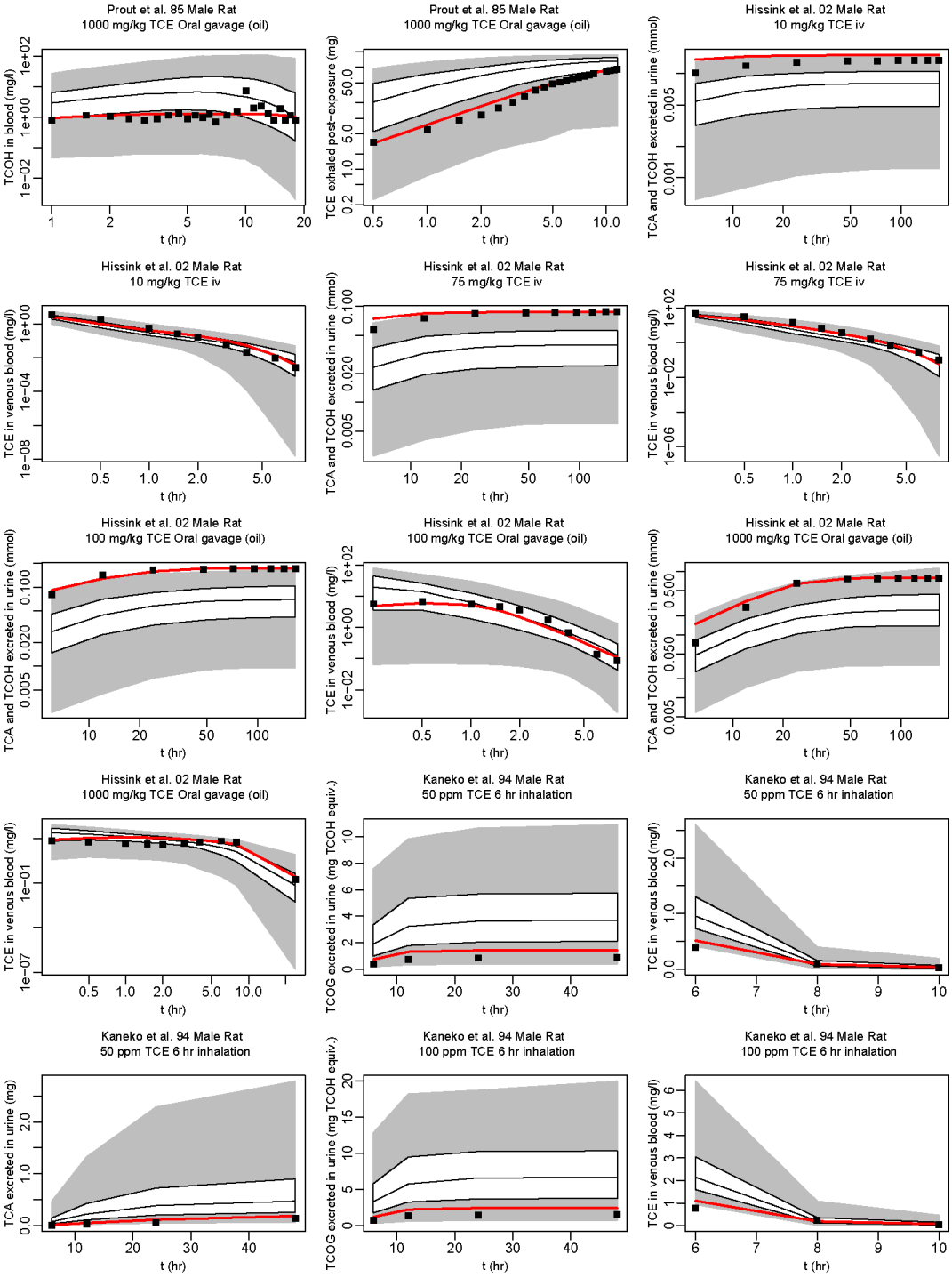

Figure A-32. Comparison of rat calibration data (boxes) and PBPK model predictions (red line: using the posterior mean of the subject-specific parameters; + with error bars: single data points; or shaded regions: 2.5, 25, 50, 75, and 97.5% population-based predictions) (continued).

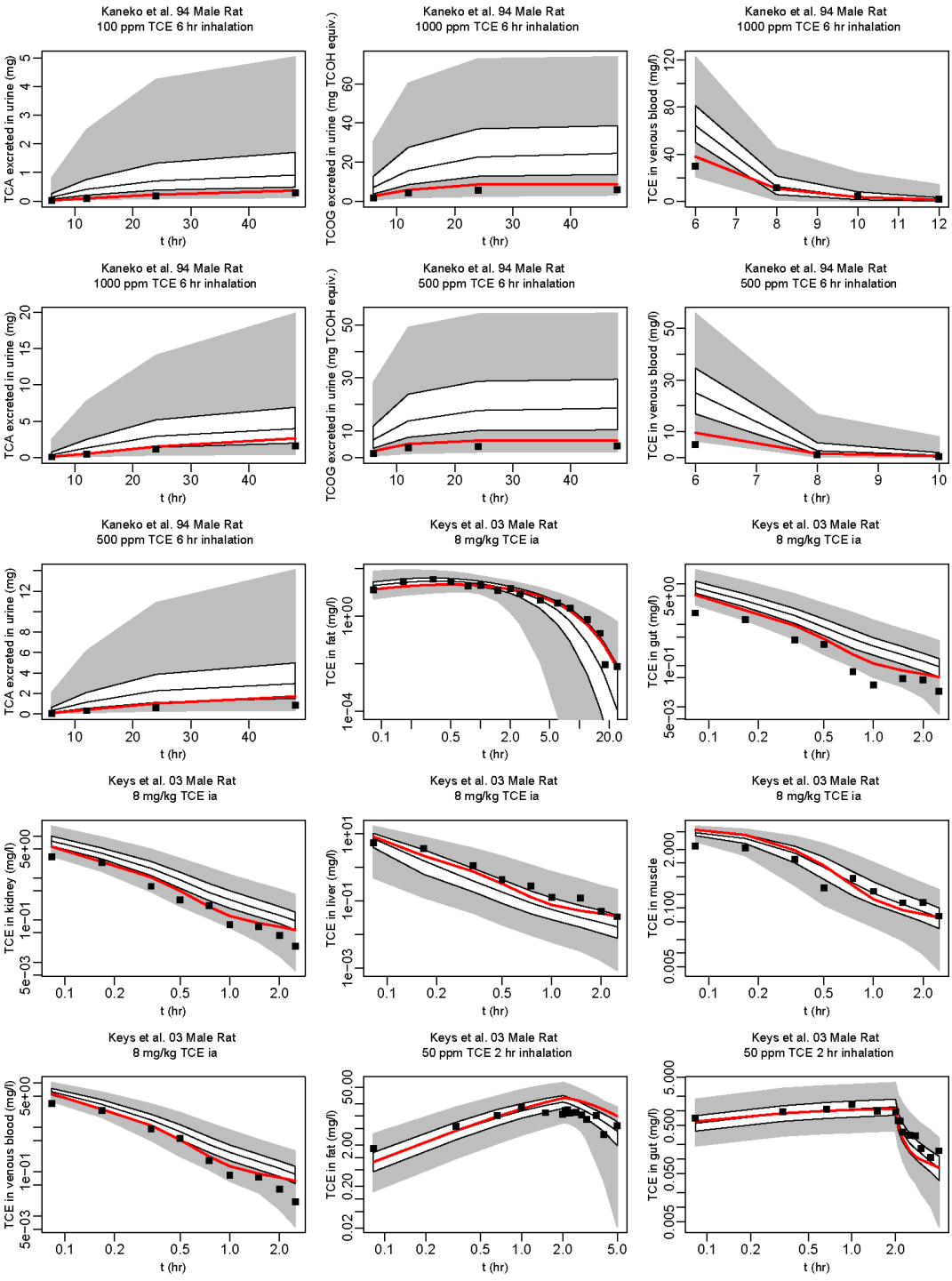

Figure A-32. (Comparison of rat calibration data (boxes) and PBPK model predictions (red line: using the posterior mean of the subject-specific parameters; + with error bars: single data points; or shaded regions: 2.5, 25 50 75, and 97.5% population-based predictions) (continued).

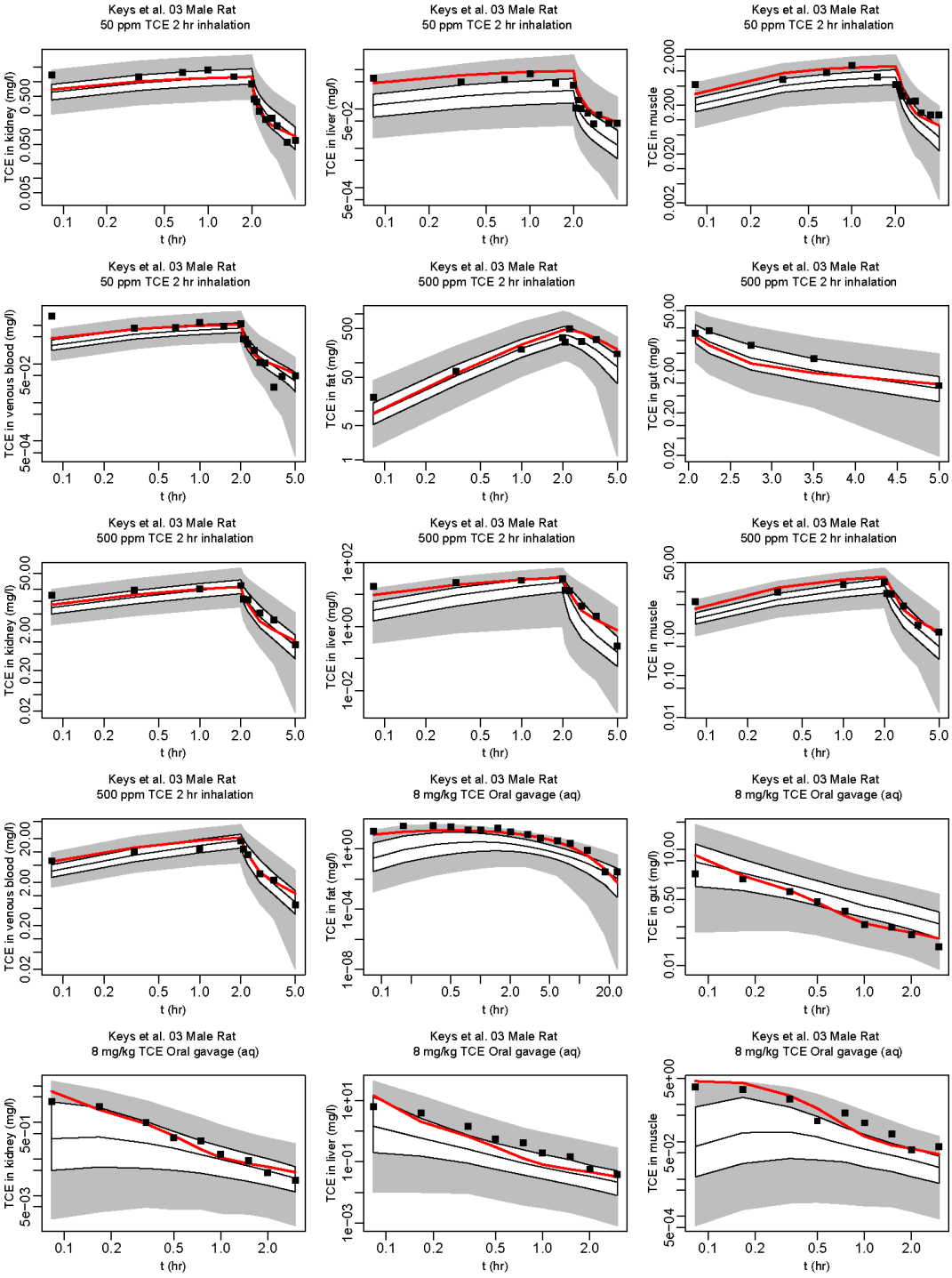

Figure A-32. Comparison of rat calibration data (boxes) and PBPK model predictions (red line: using the posterior mean of the subject-specific parameters; + with error bars: single data points; or shaded regions: 2.5, 25, 50, 75, and 97.5% population-based predictions) (continued).

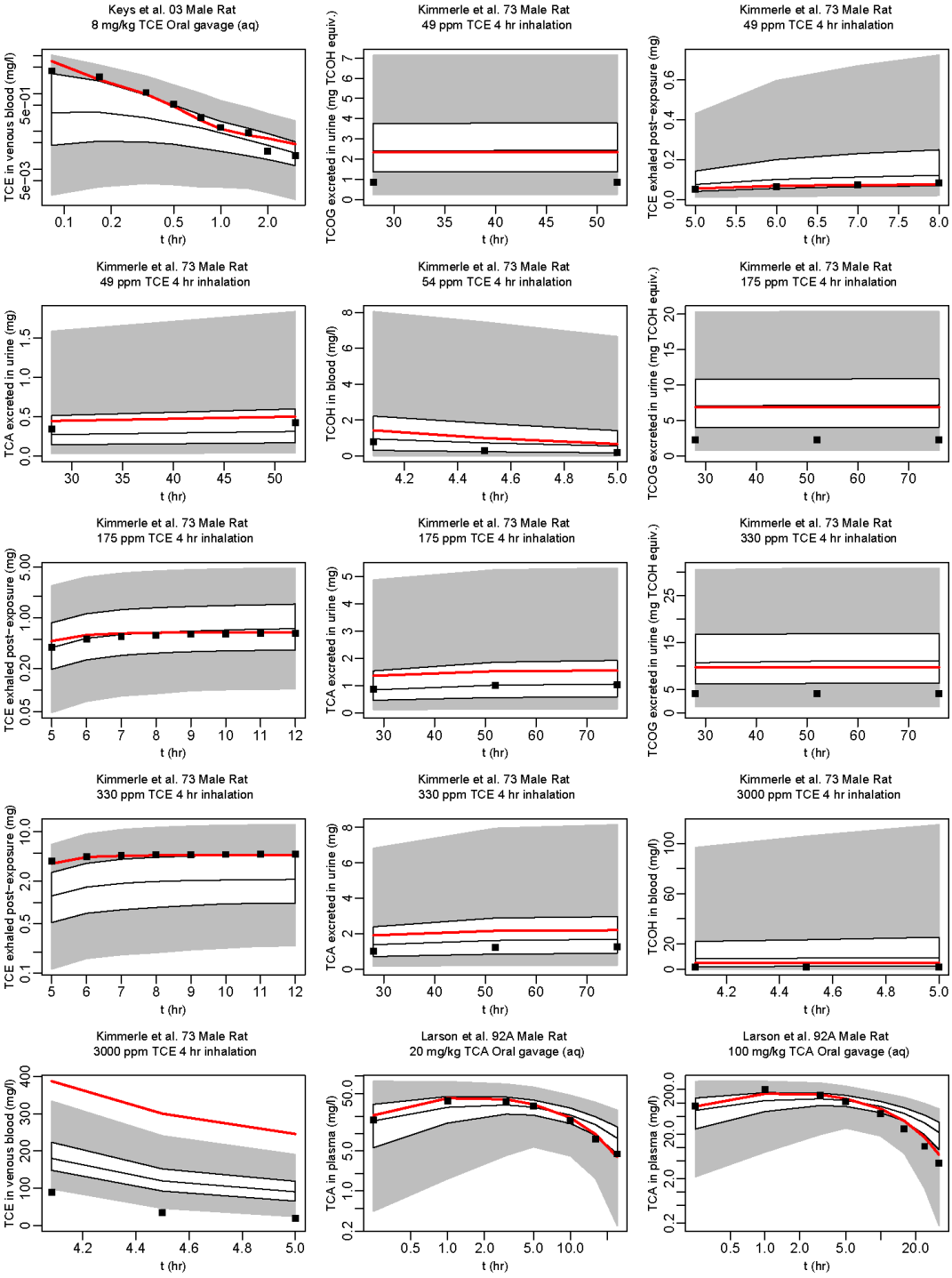

Figure A-32. Comparison of rat calibration data (boxes) and PBPK model predictions (red line: using the posterior mean of the subject-specific parameters; + with error bars: single data points; or shaded regions: 2.5, 25, 50, 75, and 97.5% population-based predictions) (continued).

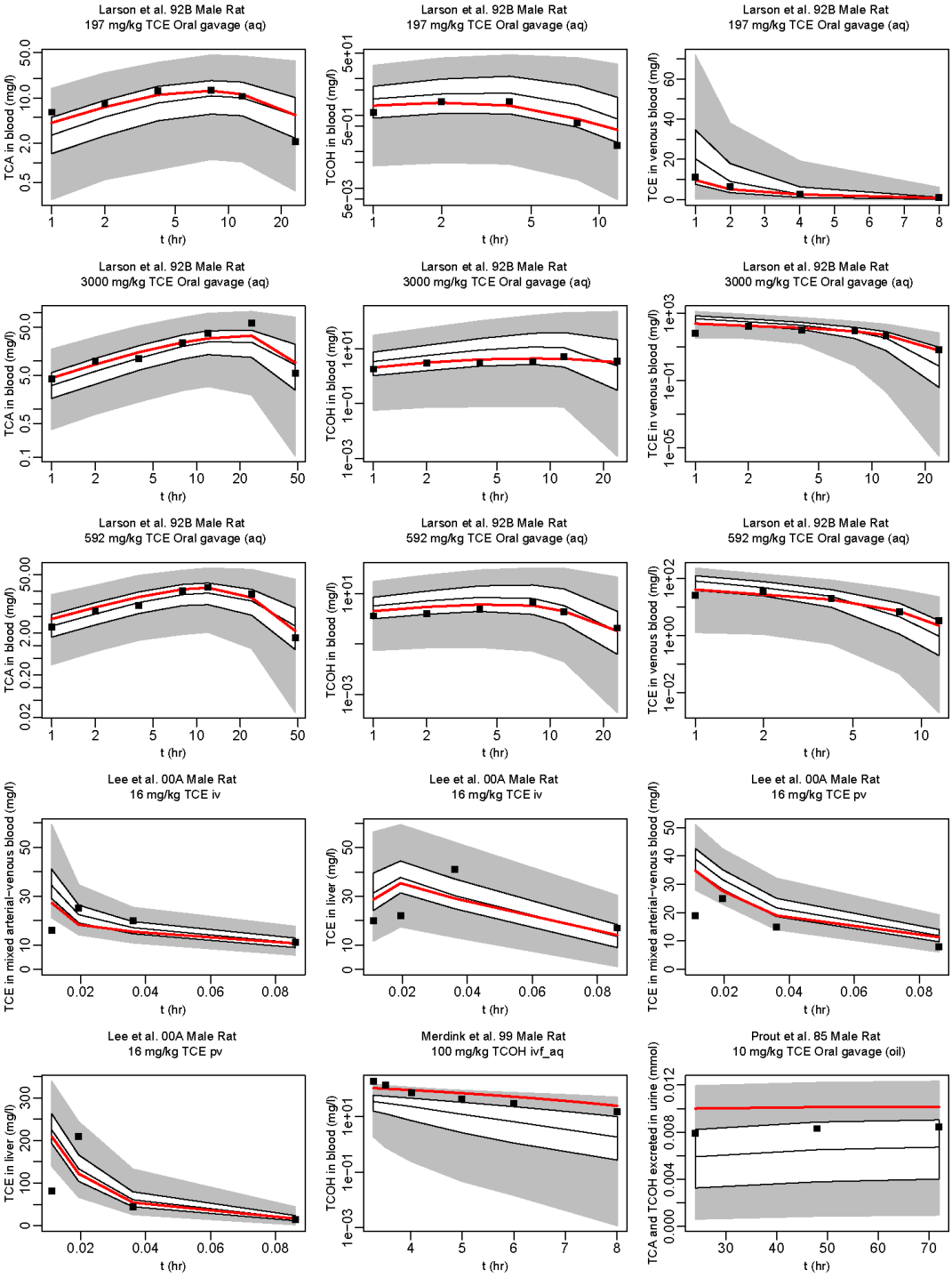

Figure A-32 Comparison of rat calibration data (boxes) and PBPK model predictions (red line: using the posterior mean of the subject-specific parameters; + with error bars: single data points; or shaded regions: 2.5, 25, 50, 75, and 97.5% population-based predictions) (continued).

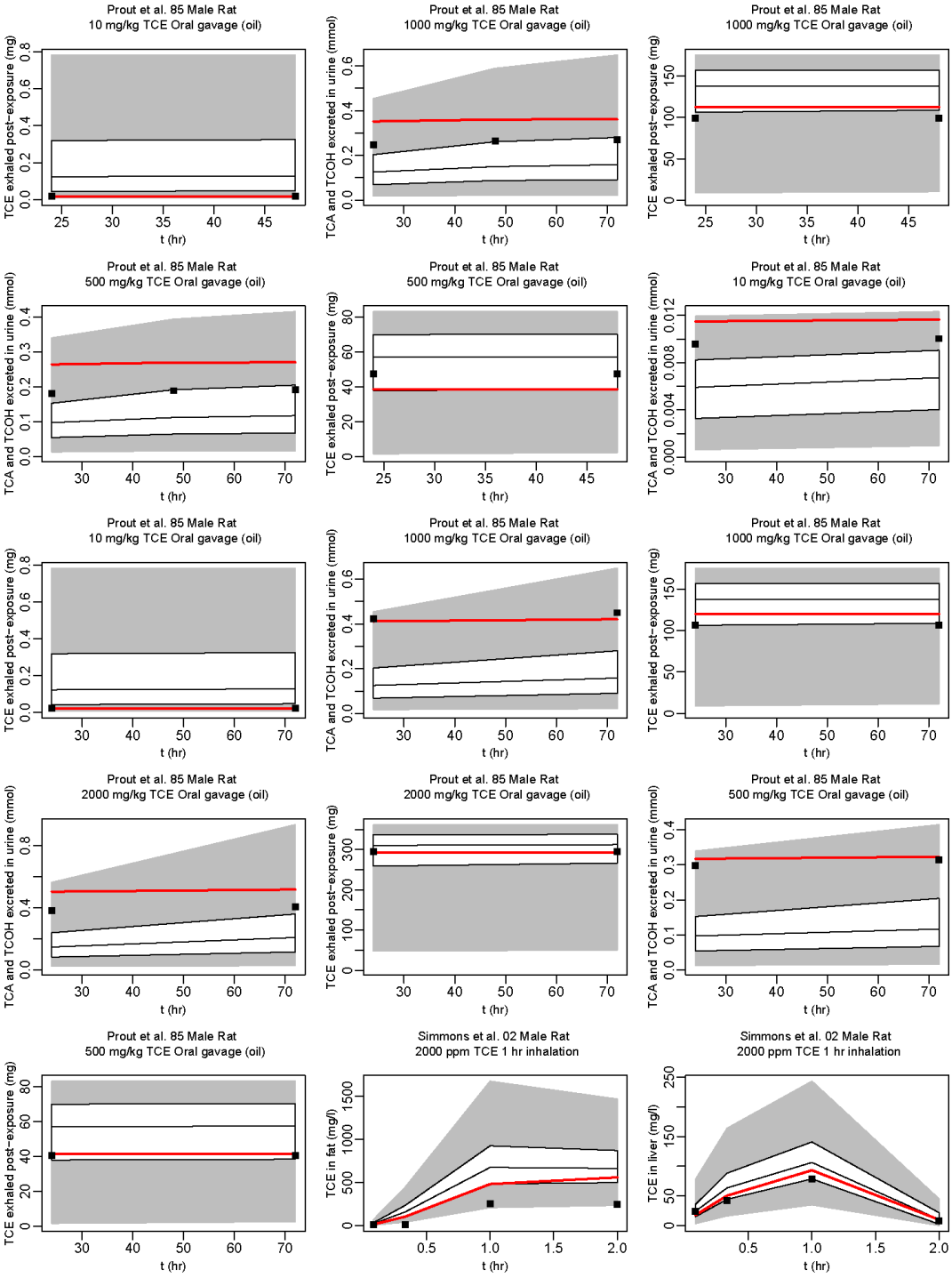

Figure A-32 Comparison of rat calibration data (boxes) and PBPK model predictions (red line: using the posterior mean of the subject-specific parameters; + with error bars: single data points; or shaded regions: 2.5, 25, 50, 75, and 97.5% population-based predictions) (continued).

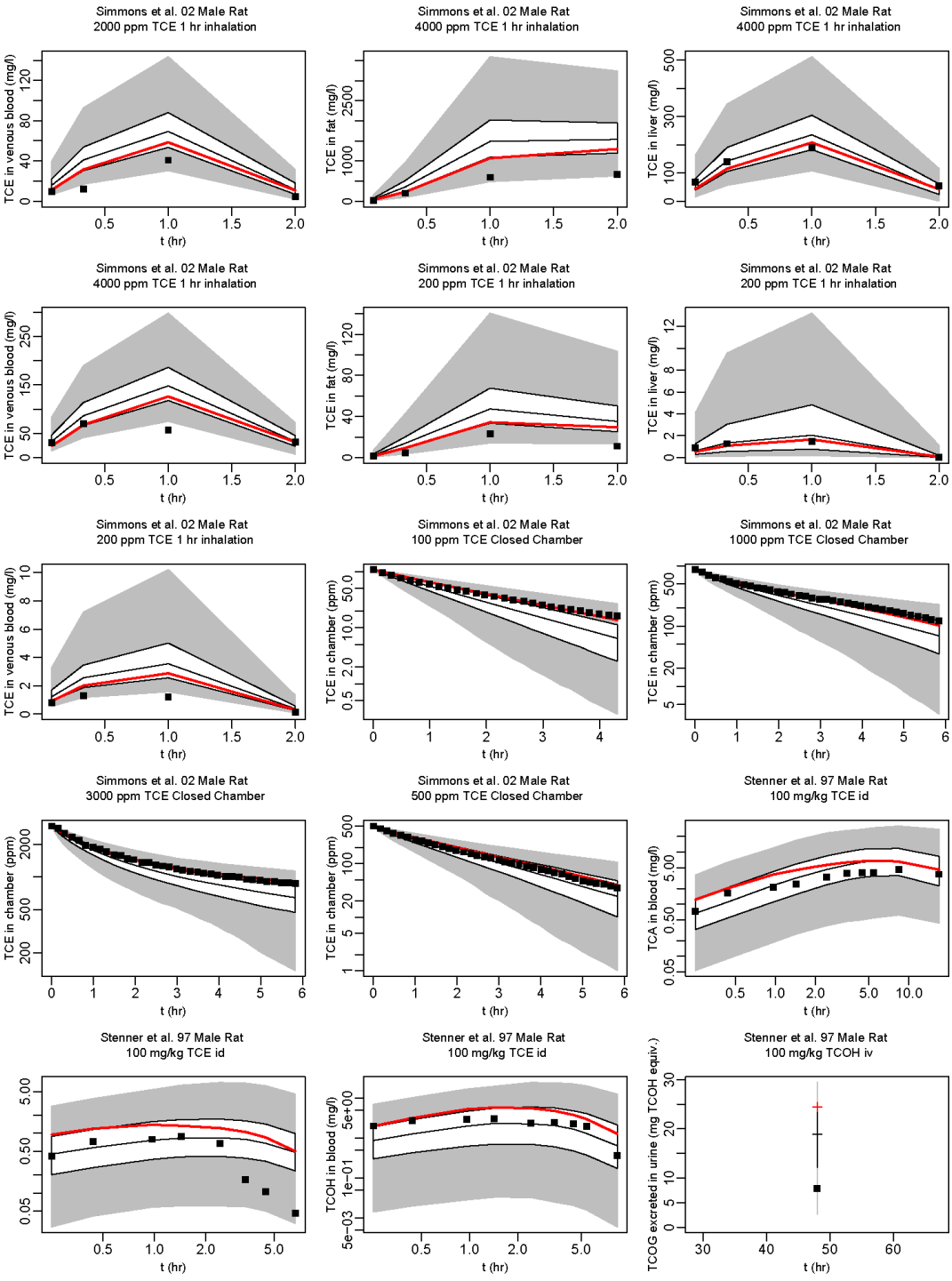

Figure A-32 Comparison of rat calibration data (boxes) and PBPK model predictions (red line: using the posterior mean of the subject-specific parameters; + with error bars: single data points; or shaded regions: 2.5, 25, 50, 75, and 97.5% population-based predictions) (continued).

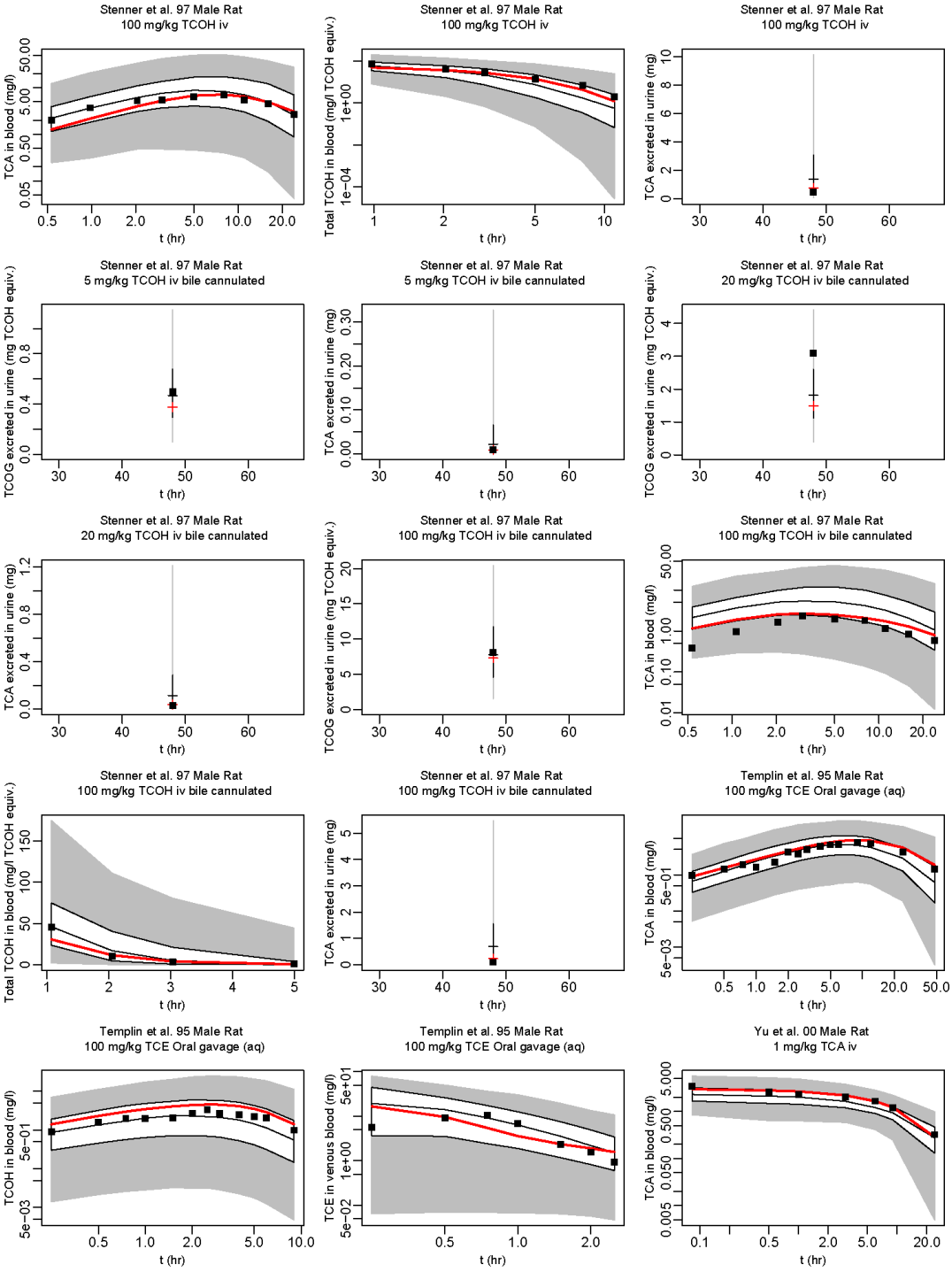

Figure A-32. Comparison of rat calibration data (boxes) and PBPK model predictions (red line: using the posterior mean of the subject-specific parameters; + with error bars: single data points; or shaded regions: 2.5, 25, 50, 75, and 97.5% population-based predictions) (continued).

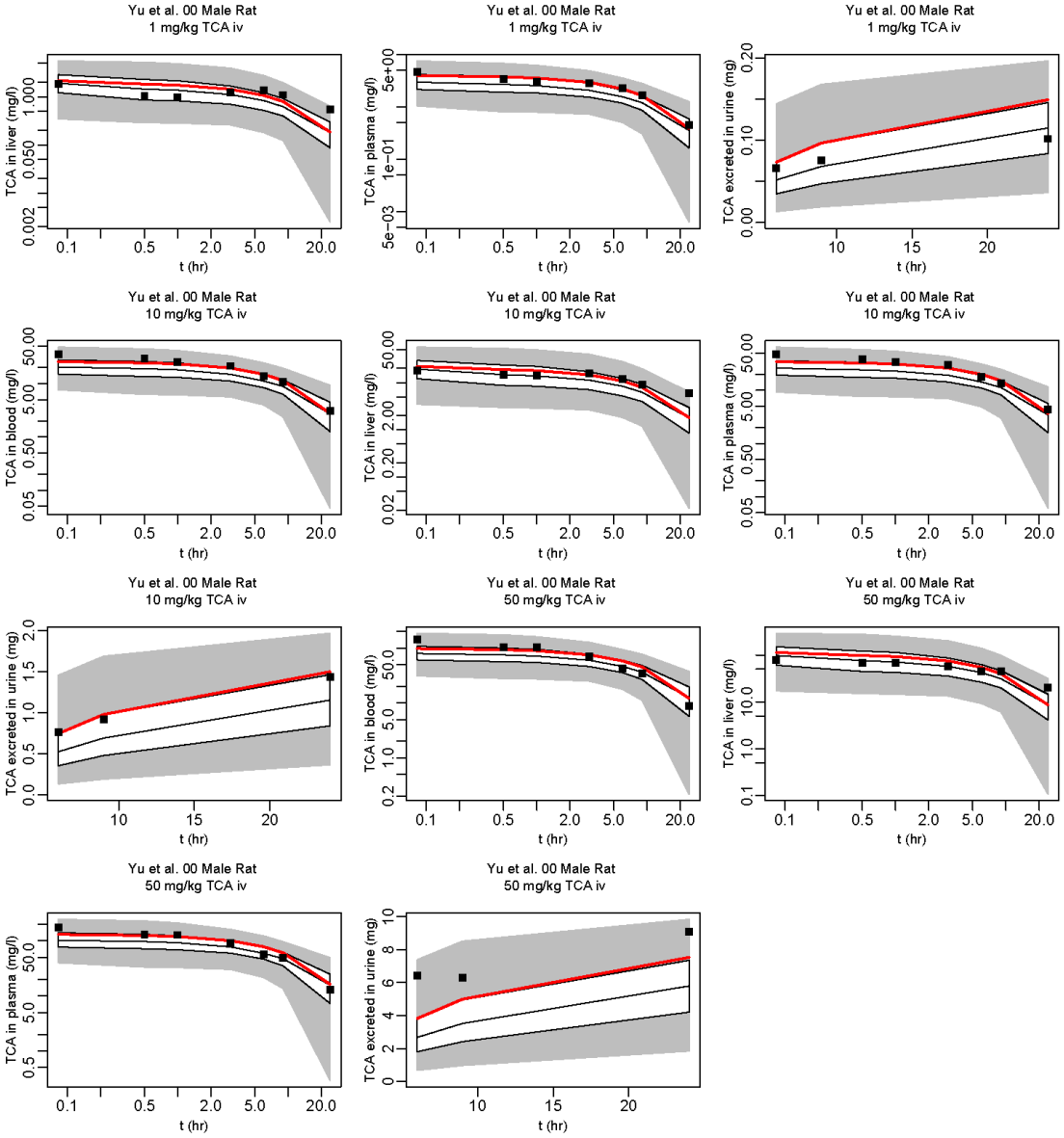

Figure A-32. Comparison of rat calibration data (boxes) and PBPK model predictions (red line: using the posterior mean of the subject-specific parameters; + with error bars: single data points; or shaded regions: 2.5, 25, 50, 75, and 97.5% population-based predictions) (continued).

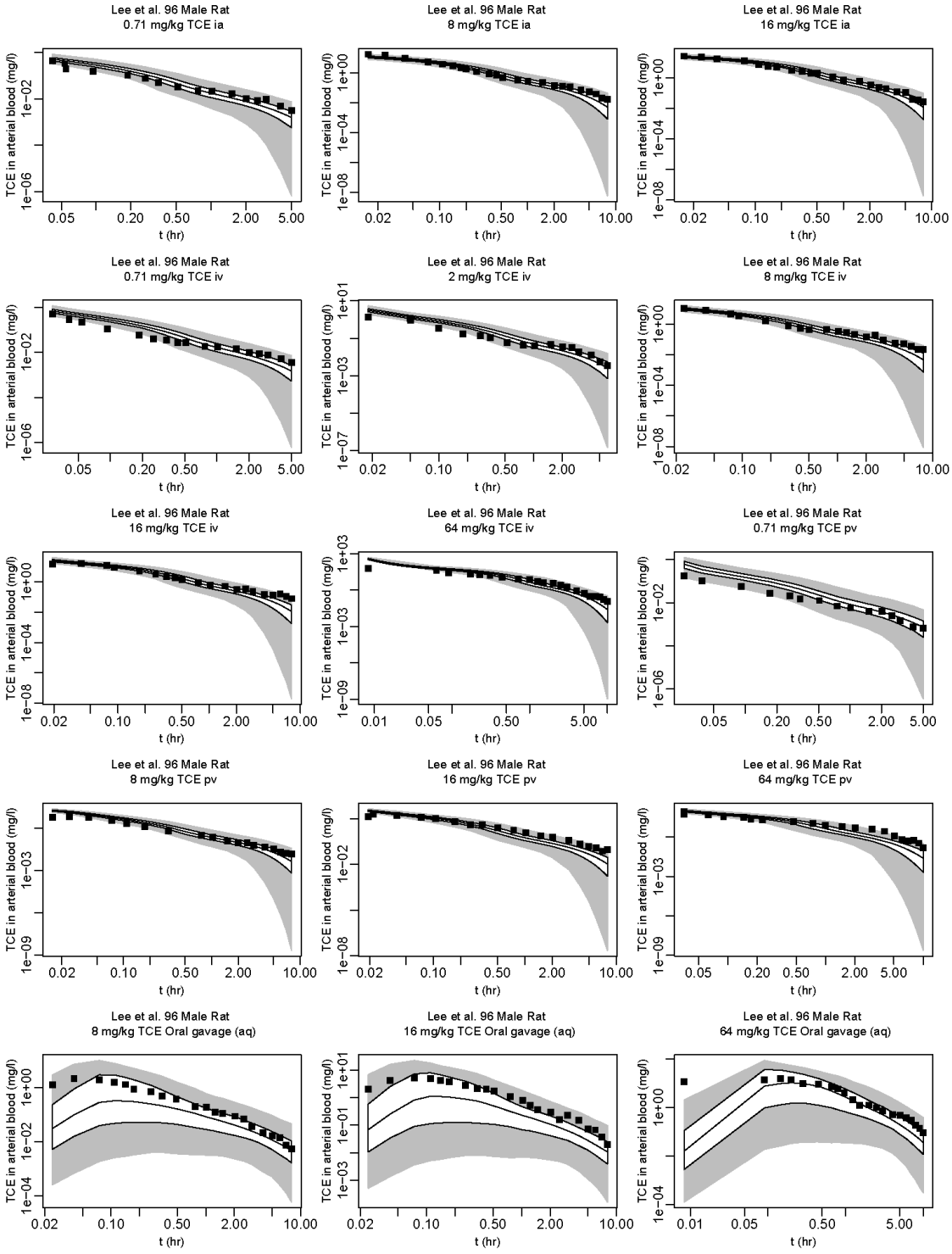

Figure A-33. Comparison of rat evaluation data (boxes) and PBPK model predictions (+ with error bars: single data points or shaded regions: 2.5, 25, 50, 75, and 97.5% population-based predictions).

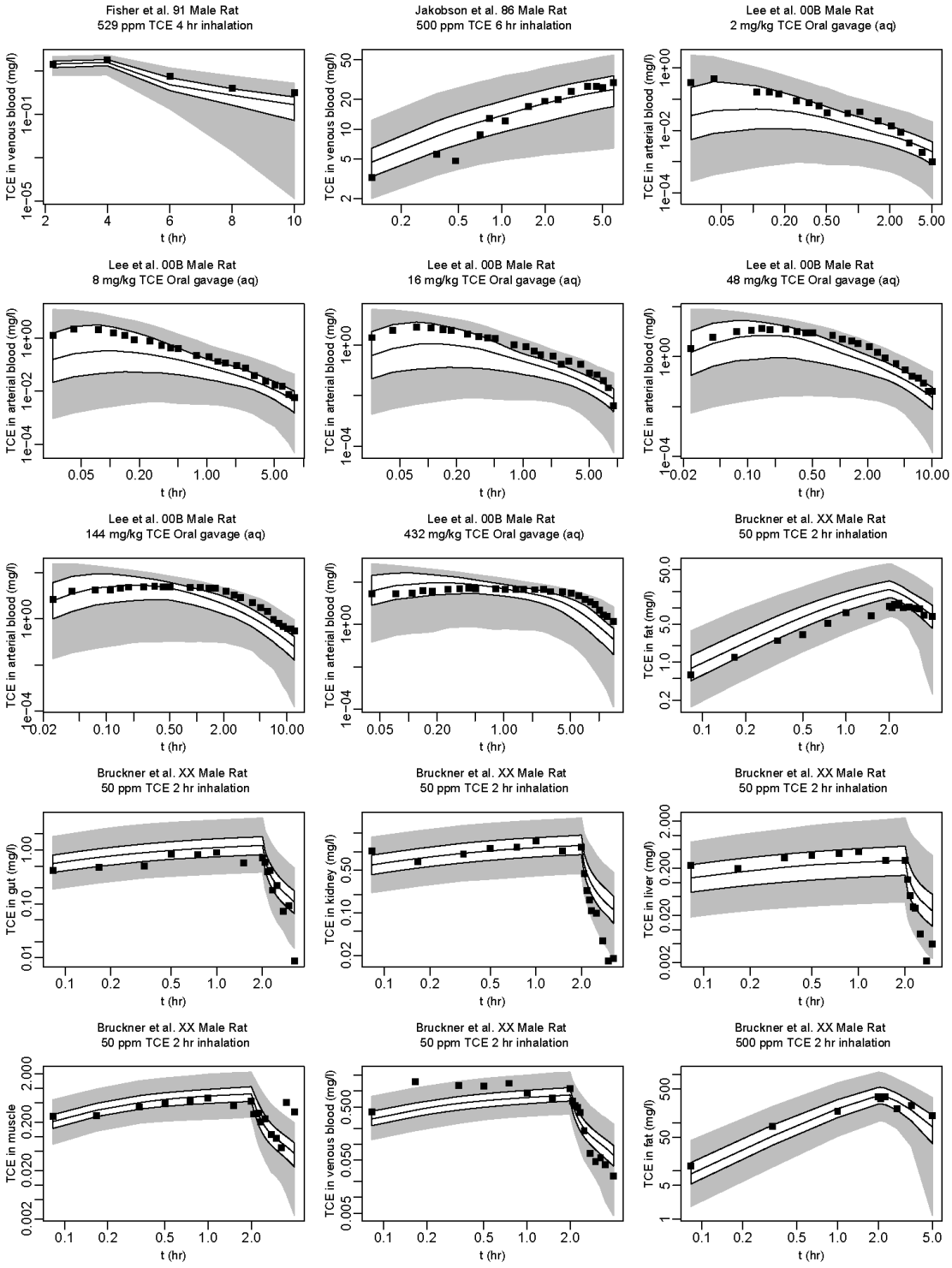

Figure A-33. Comparison of rat evaluation data (boxes) and PBPK model predictions (+ with error bars: single data points or shaded regions: 2.5, 25, 50, 75, and 97.5% population-based predictions) (continued).

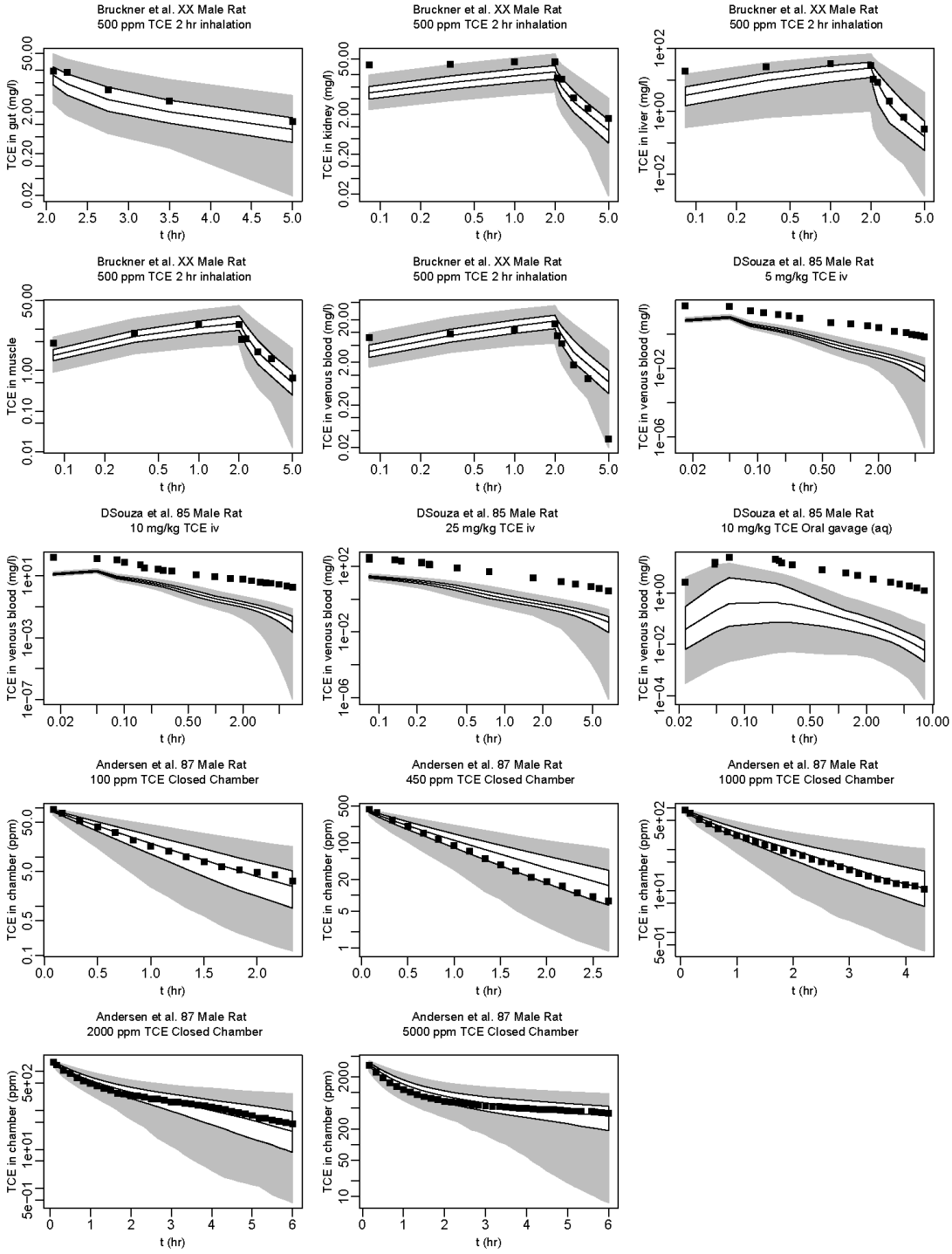

Figure A-33. Comparison of rat evaluation data (boxes) and PBPK model predictions (+ with error bars: single data points or shaded regions: 2.5, 25, 50, 75, and 97.5% population-based predictions) (continued).

A.5.2.3. Human Data and Model Predictions

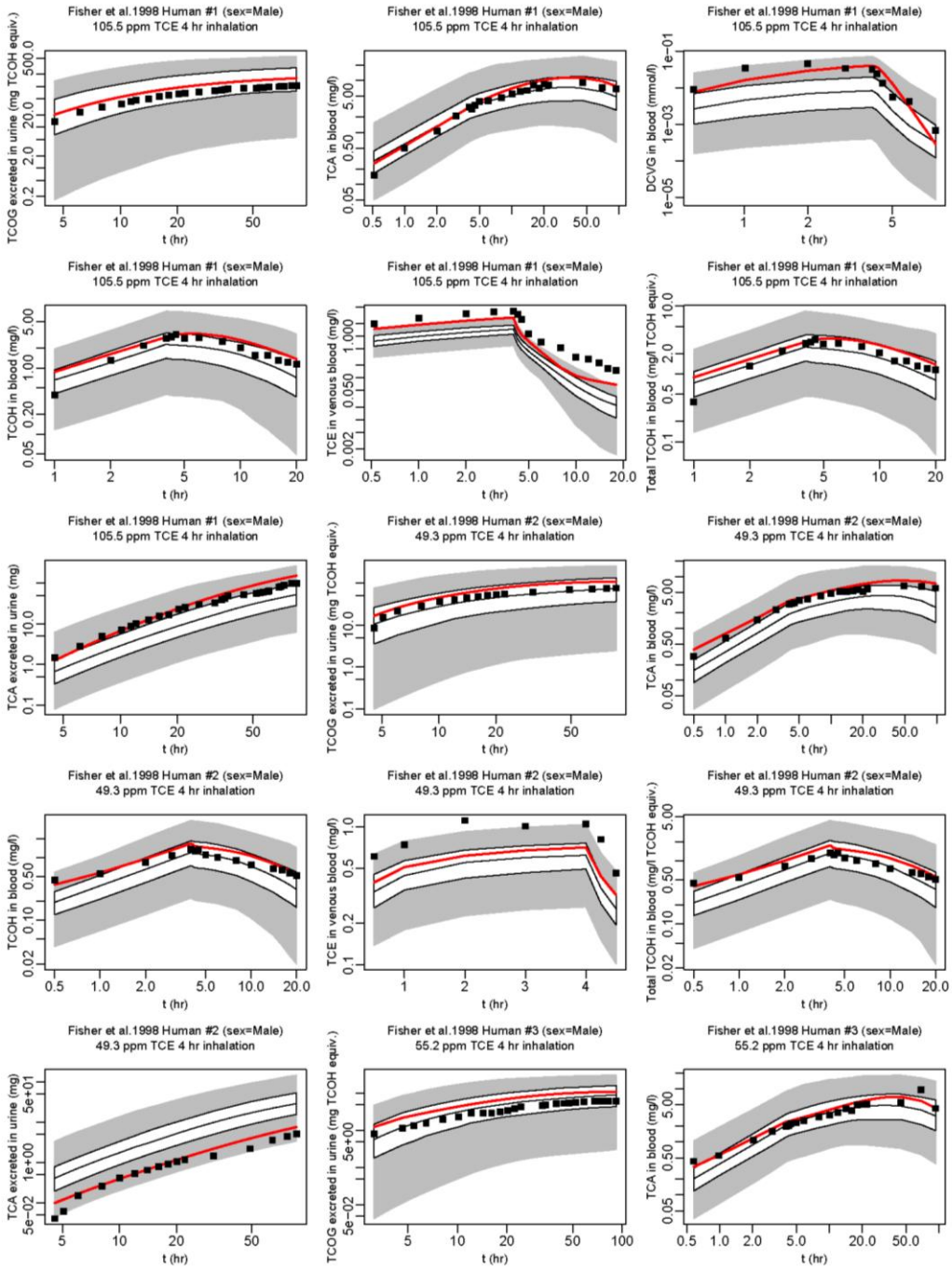

Figure A-34. Comparison of human calibration data (boxes) and PBPK model predictions (red line: using the posterior mean of the subject-specific parameters; + with error bars: single data points; or shaded regions: 2.5, 25, 50, 75, and 97.5% population-based predictions).

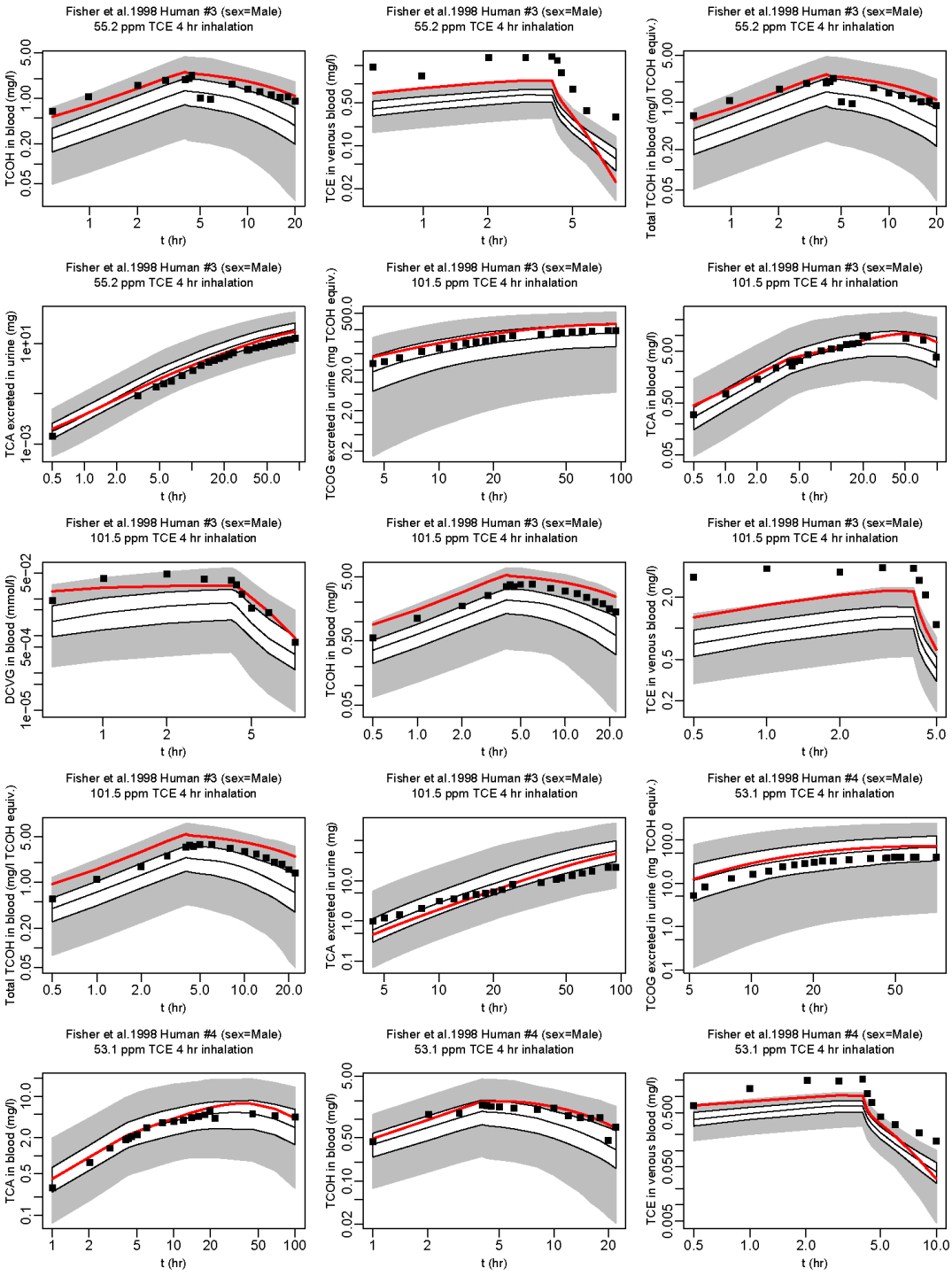

Figure A-34. Comparison of human calibration data (boxes) and PBPK model predictions (red line: using the posterior mean of the subject-specific parameters; + with error bars: single data points; or shaded regions: 2.5, 25, 50, 75, and 97.5% population-based predictions) (continued).

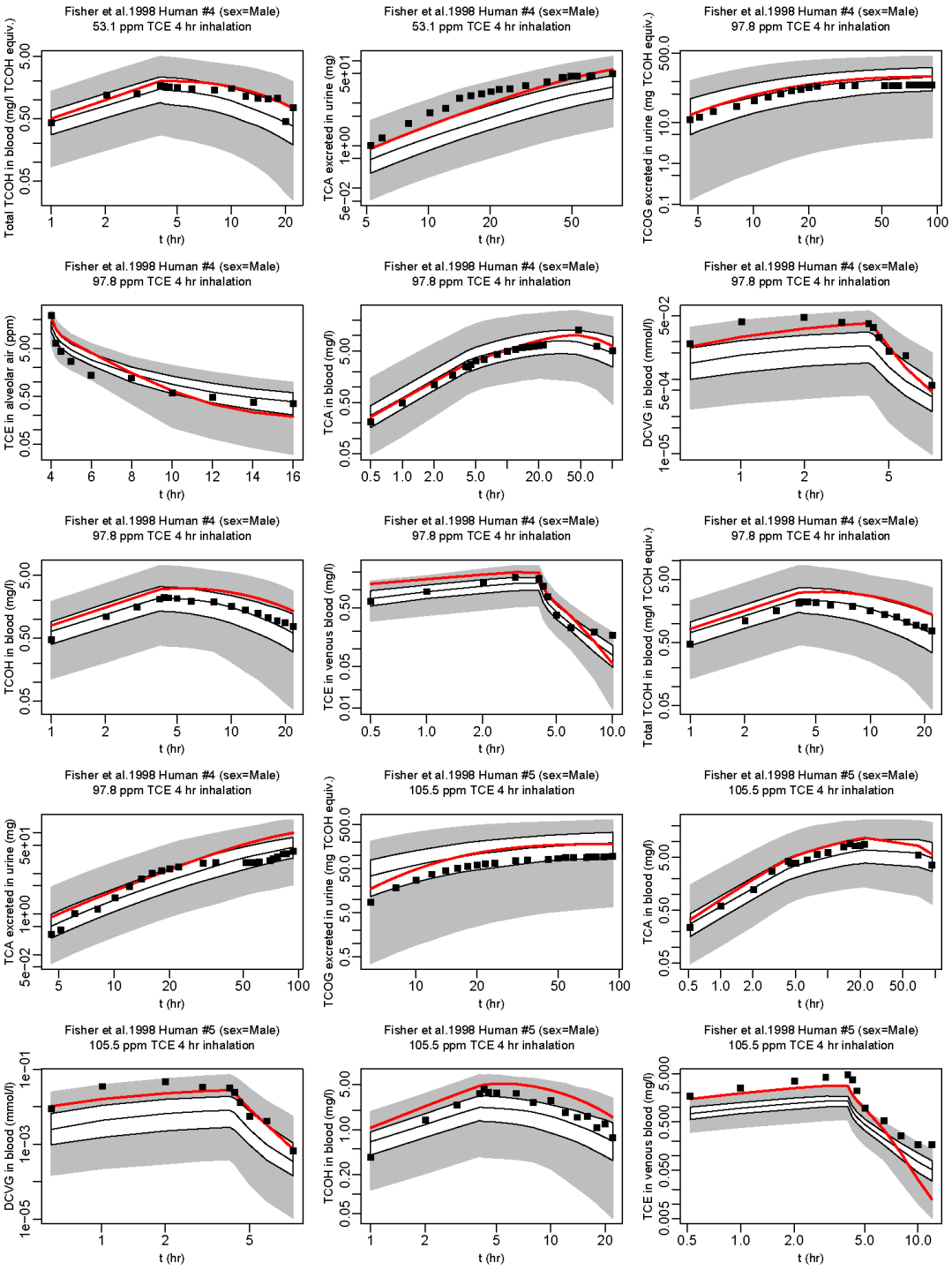

Figure A-34. Comparison of human calibration data (boxes) and PBPK model predictions (red line: using the posterior mean of the subject-specific parameters; + with error bars: single data points; or shaded regions: 2.5, 25, 50, 75, and 97.5% population-based predictions) (continued).

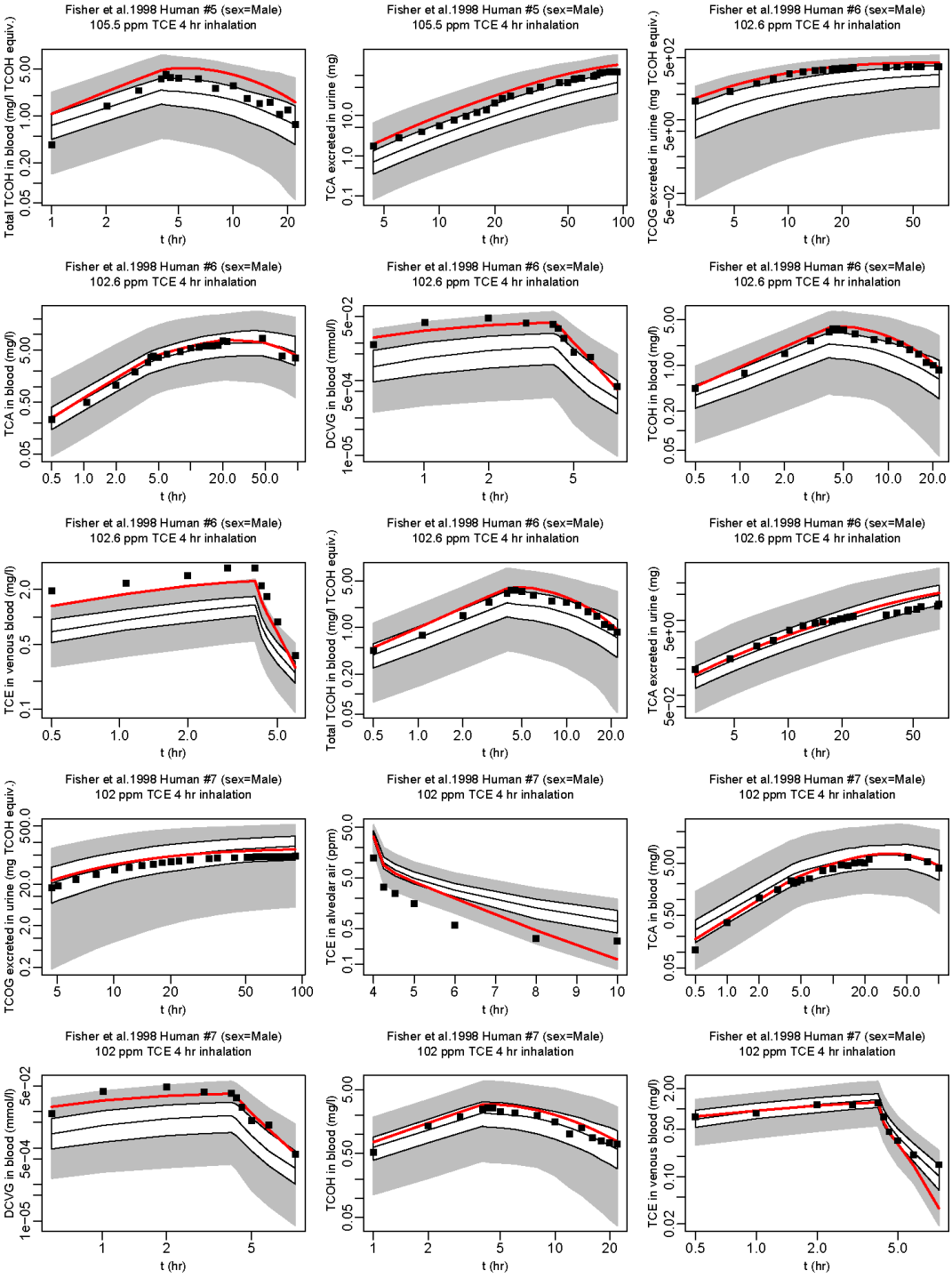

Figure A-34. Comparison of human calibration data (boxes) and PBPK model predictions (red line: using the posterior mean of the subject-specific parameters; + with error bars: single data points; or shaded regions: 2.5, 25, 50, 75, and 97.5% population-based predictions) (continued).

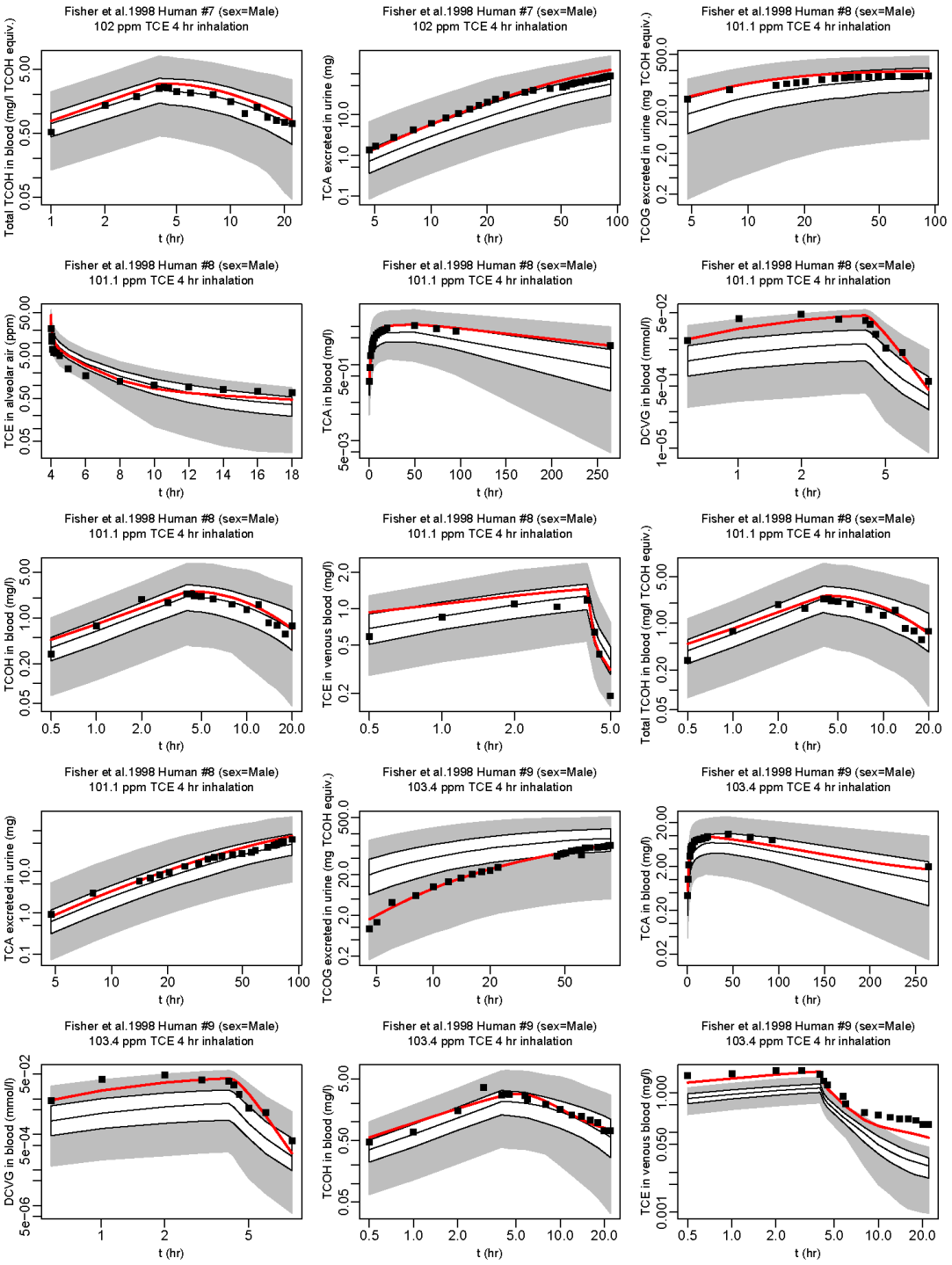

Figure A-34. Comparison of human calibration data (boxes) and PBPK model predictions (red line: using the posterior mean of the subject-specific parameters; + with error bars: single data points; or shaded regions: 2.5, 25, 50, 75, and 97.5% population-based predictions) (continued).

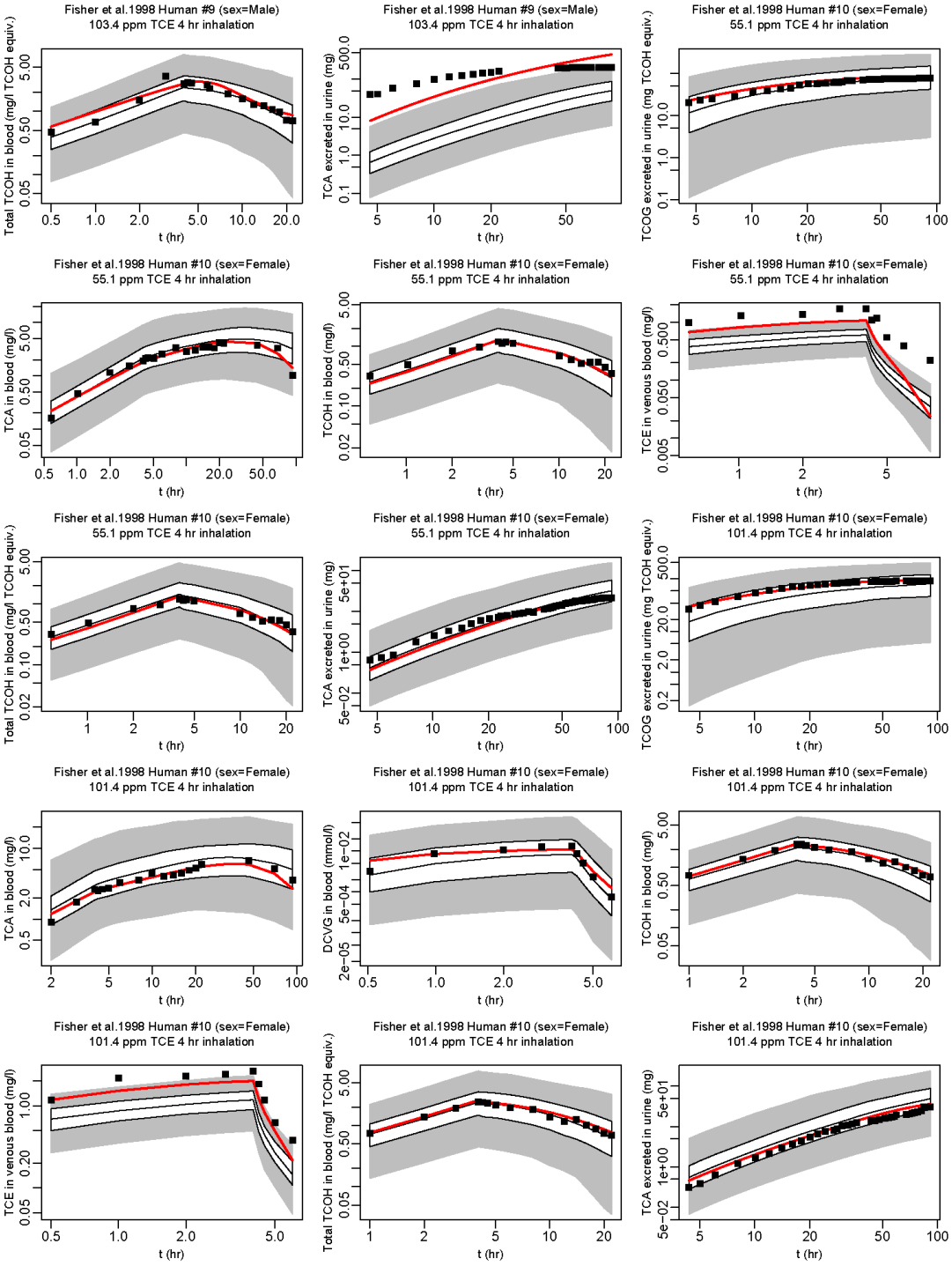

Figure A-34. Comparison of human calibration data (boxes) and PBPK model predictions (red line: using the posterior mean of the subject-specific parameters; + with error bars: single data points; or shaded regions: 2.5, 25, 50, 75, and 97.5% population-based predictions) (continued).

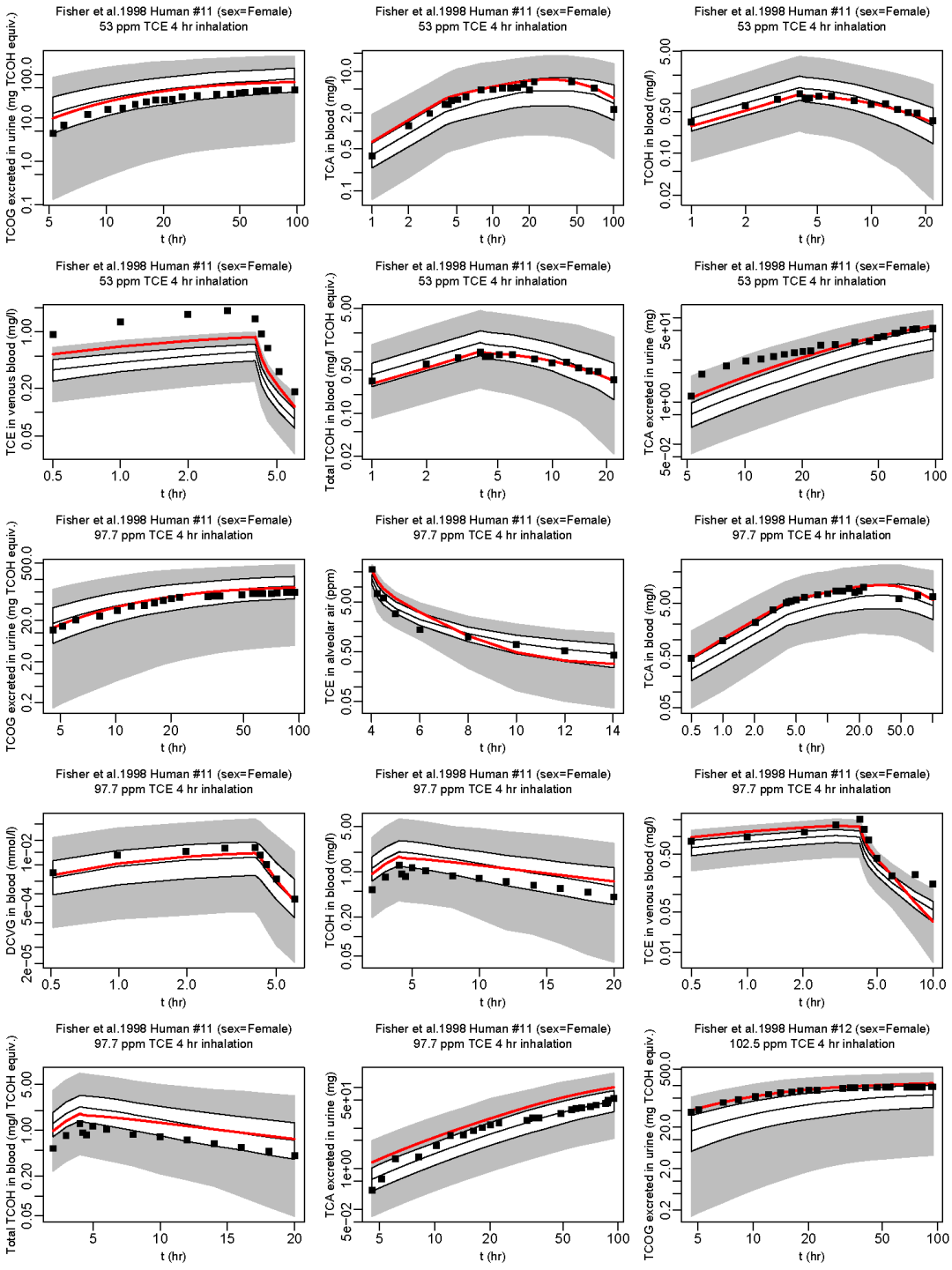

Figure A-34. Comparison of human calibration data (boxes) and PBPK model predictions (red line: using the posterior mean of the subject-specific parameters; + with error bars: single data points; or shaded regions: 2.5, 25, 50, 75, and 97.5% population-based predictions) (continued).

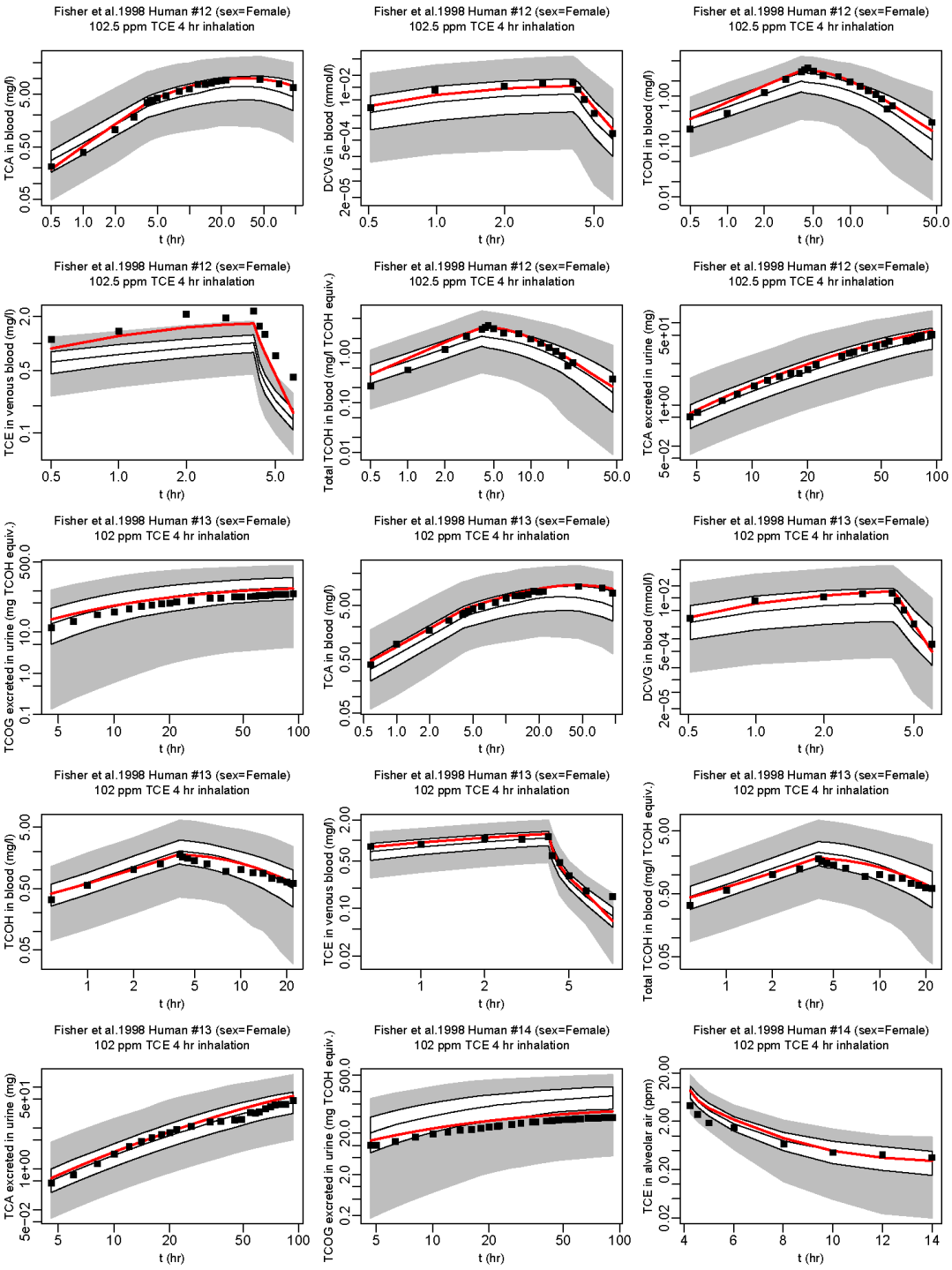

Figure A-34. Comparison of human calibration data (boxes) and PBPK model predictions (red line: using the posterior mean of the subject-specific parameters; + with error bars: single data points; or shaded regions: 2.5, 25, 50, 75, and 97.5% population-based predictions) (continued).

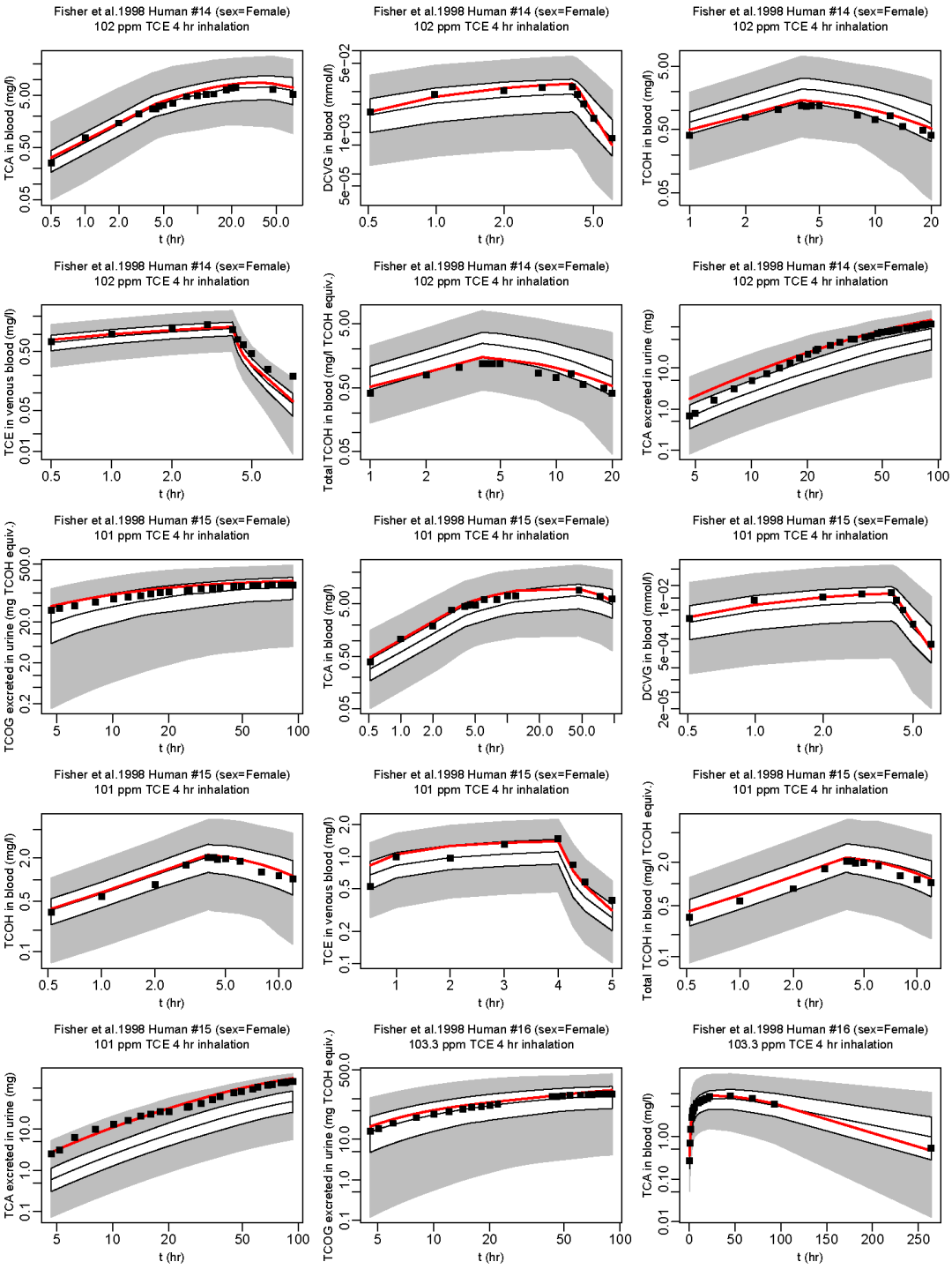

Figure A-34. Comparison of human calibration data (boxes) and PBPK model predictions (red line: using the posterior mean of the subject-specific parameters; + with error bars: single data points; or shaded regions: 2.5, 25, 50, 75, and 97.5% population-based predictions) (continued).

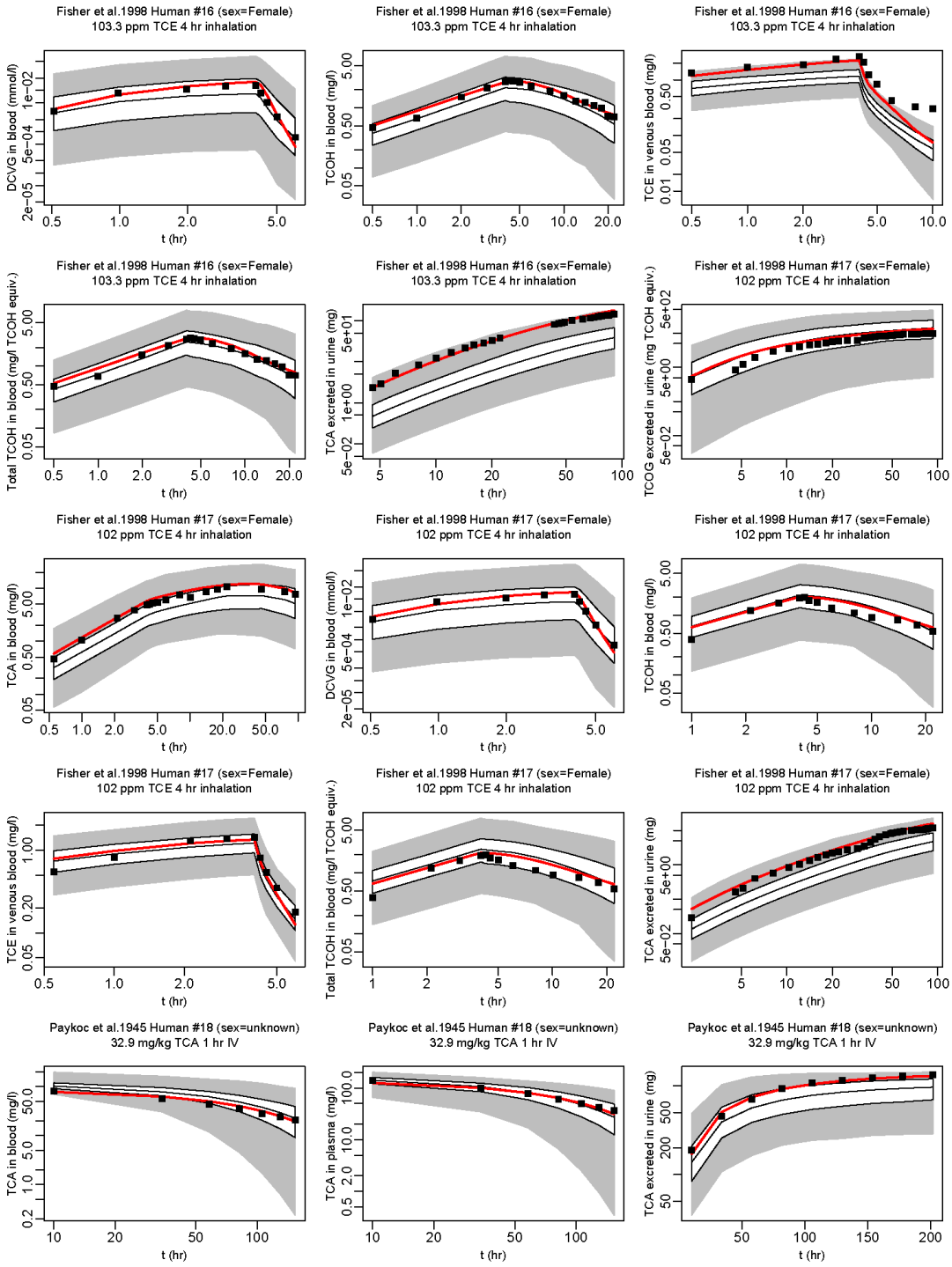

Figure A-34. Comparison of human calibration data (boxes) and PBPK model predictions (red line: using the posterior mean of the subject-specific parameters; + with error bars: single data points; or shaded regions: 2.5, 25, 50, 75, and 97.5% population-based predictions) (continued).

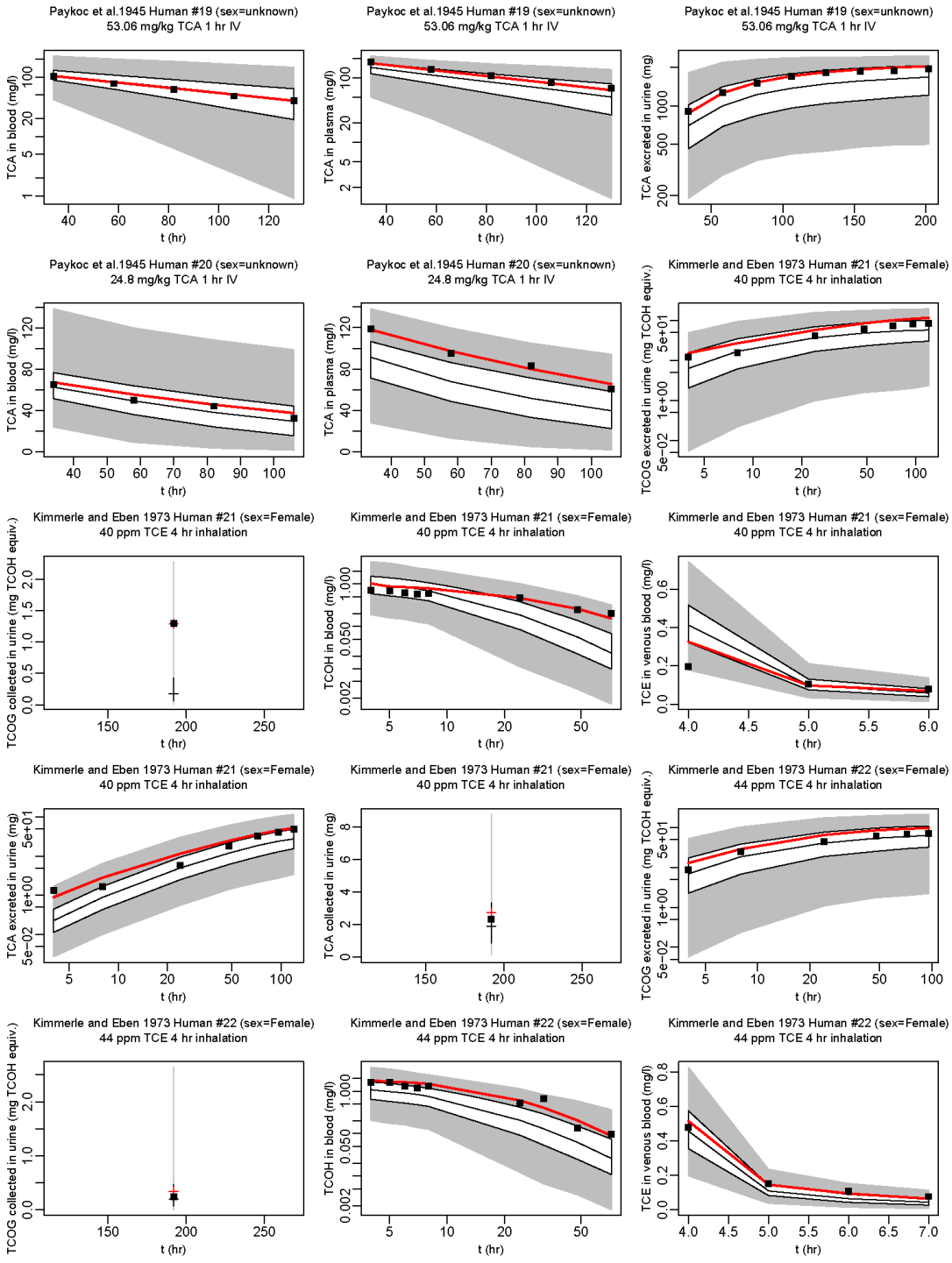

Figure A-34. Comparison of human calibration data (boxes) and PBPK model predictions (red line: using the posterior mean of the subject-specific parameters; + with error bars: single data points; or shaded regions: 2.5, 25, 50, 75, and 97.5% population-based predictions) (continued).

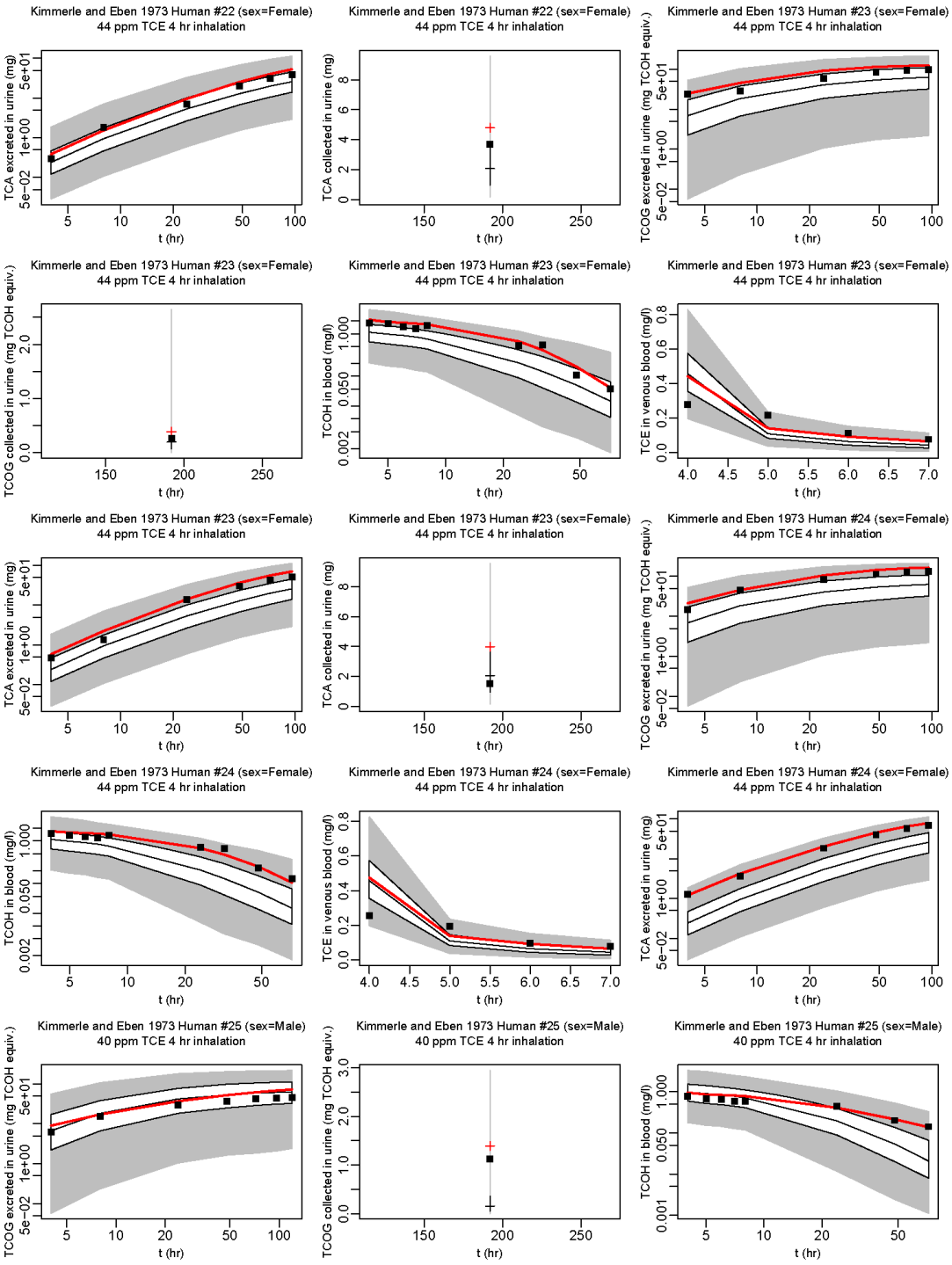

Figure A-34. Comparison of human calibration data (boxes) and PBPK model predictions (red line: using the posterior mean of the subject-specific parameters; + with error bars: single data points; or shaded regions: 2.5, 25, 50, 75, and 97.5% population-based predictions) (continued).

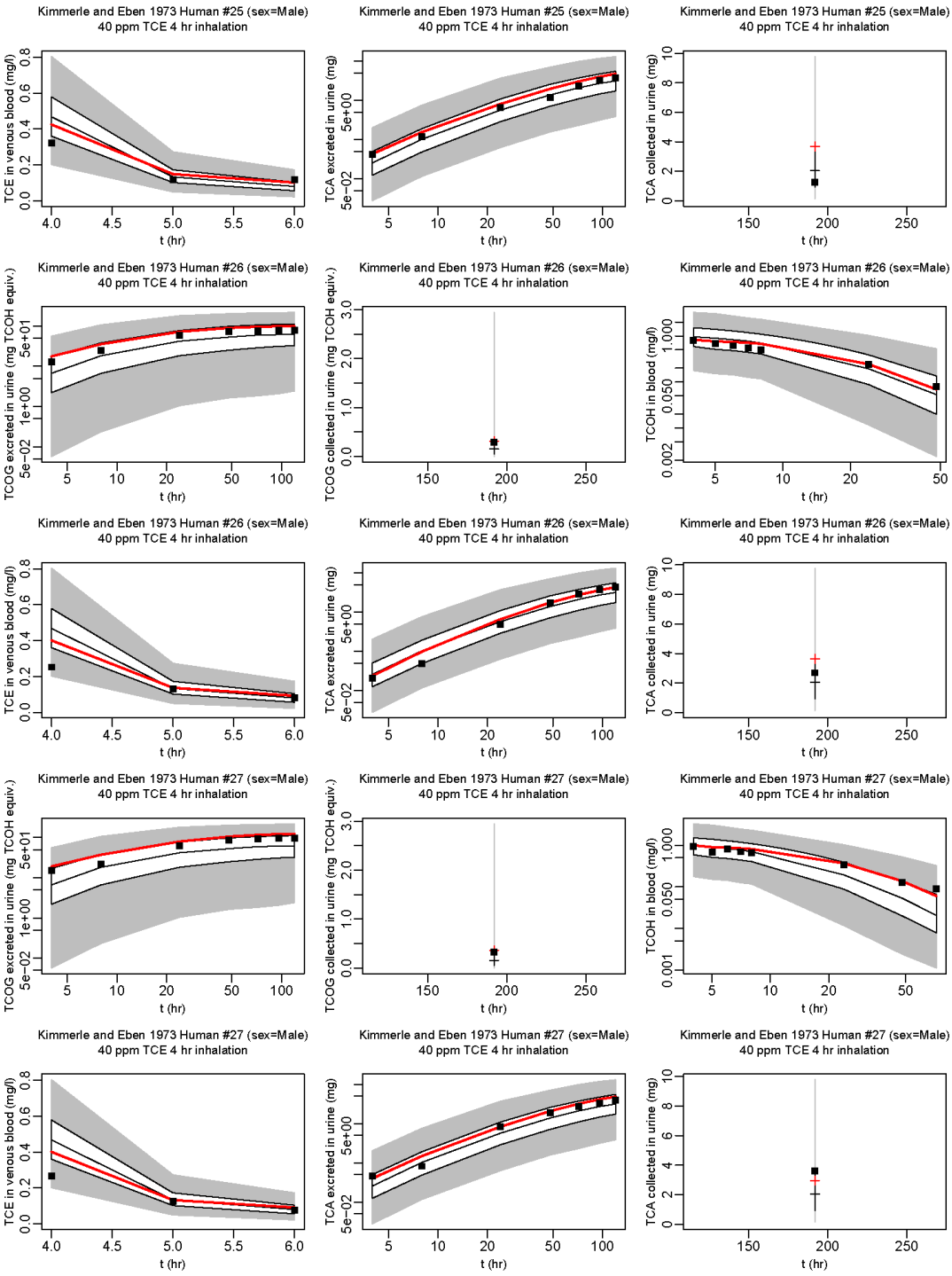

Figure A-34. Comparison of human calibration data (boxes) and PBPK model predictions (red line: using the posterior mean of the subject-specific parameters; + with error bars: single data points; or shaded regions: 2.5, 25, 50, 75, and 97.5% population-based predictions) (continued).

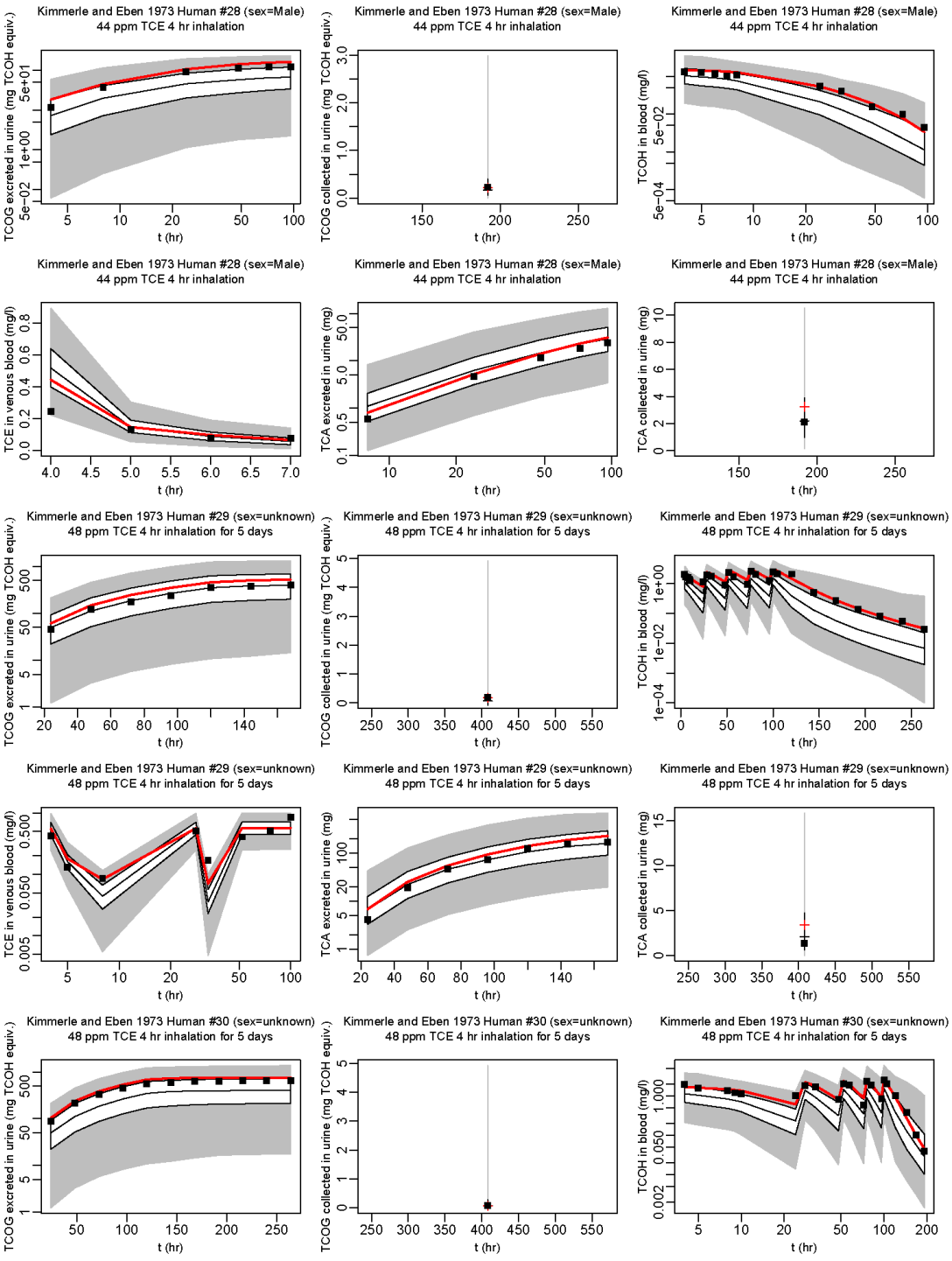

Figure A-34. Comparison of human calibration data (boxes) and PBPK model predictions (red line: using the posterior mean of the subject-specific parameters; + with error bars: single data points; or shaded regions: 2.5, 25, 50, 75, and 97.5% population-based predictions) (continued).

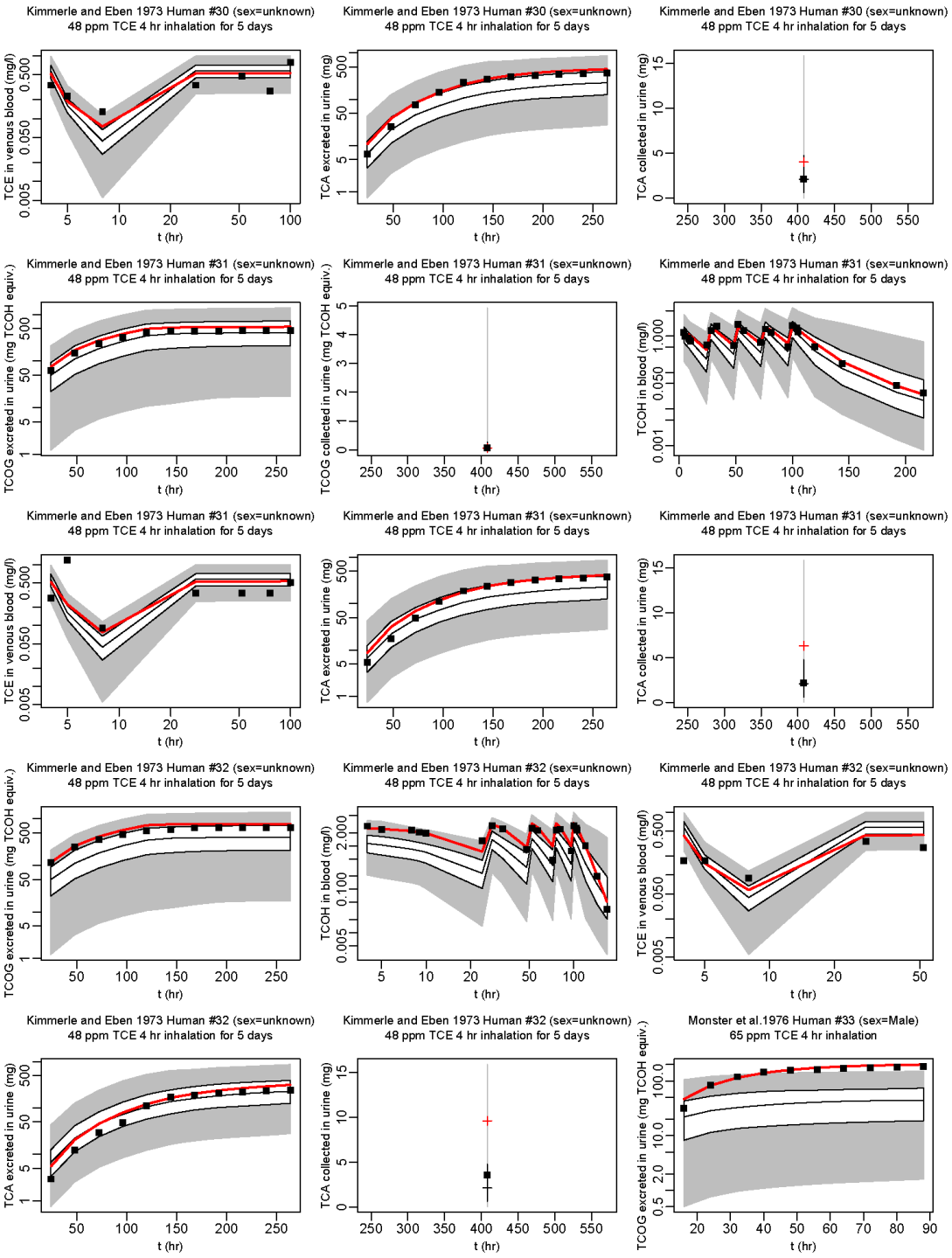

Figure A-34. Comparison of human calibration data (boxes) and PBPK model predictions (red line: using the posterior mean of the subject-specific parameters; + with error bars: single data points; or shaded regions: 2.5, 25, 50, 75, and 97.5% population-based predictions) (continued).

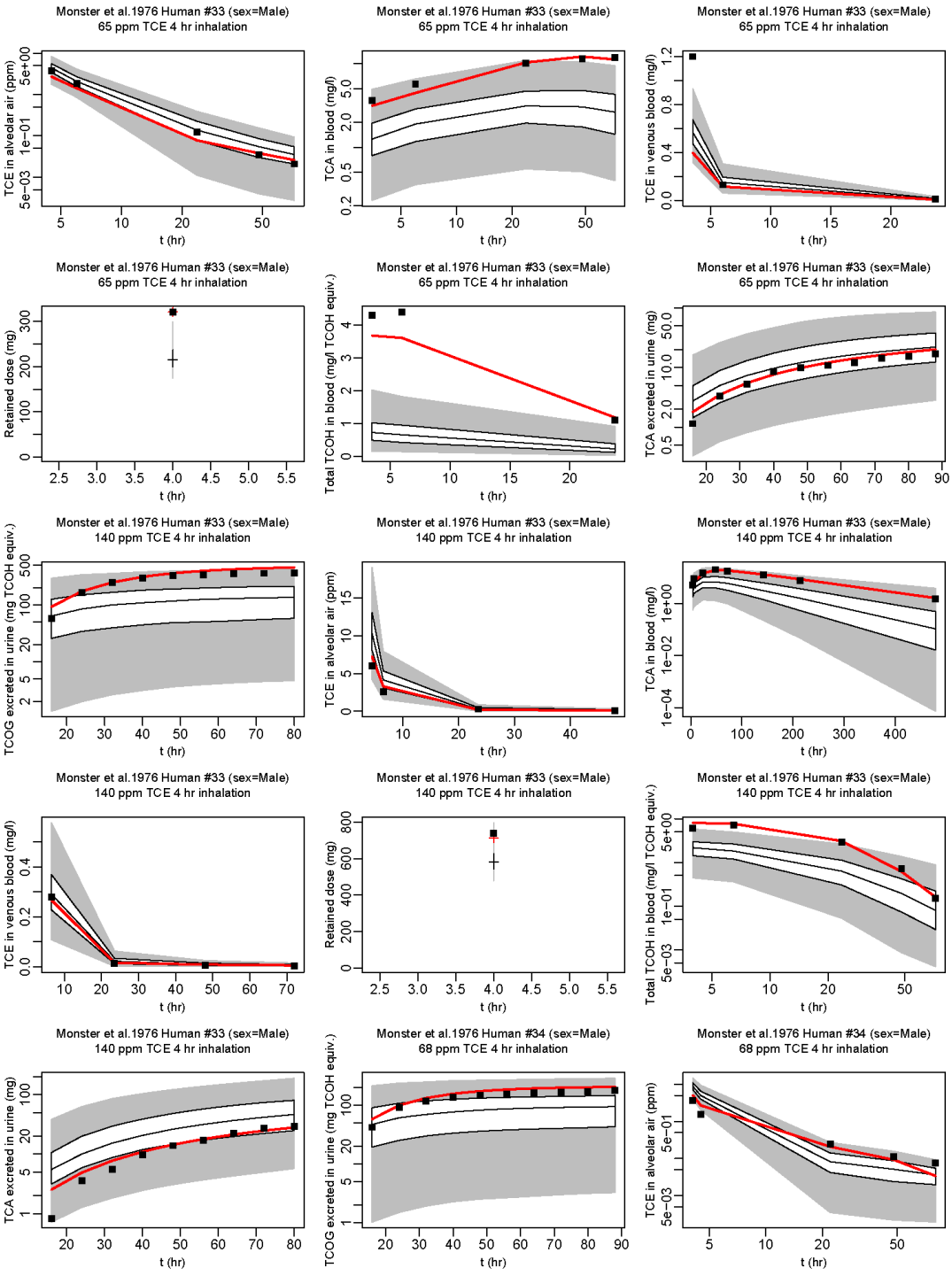

Figure A-34. Comparison of human calibration data (boxes) and PBPK model predictions (red line: using the posterior mean of the subject-specific parameters; + with error bars: single data points; or shaded regions: 2.5, 25, 50, 75, and 97.5% population-based predictions) (continued).

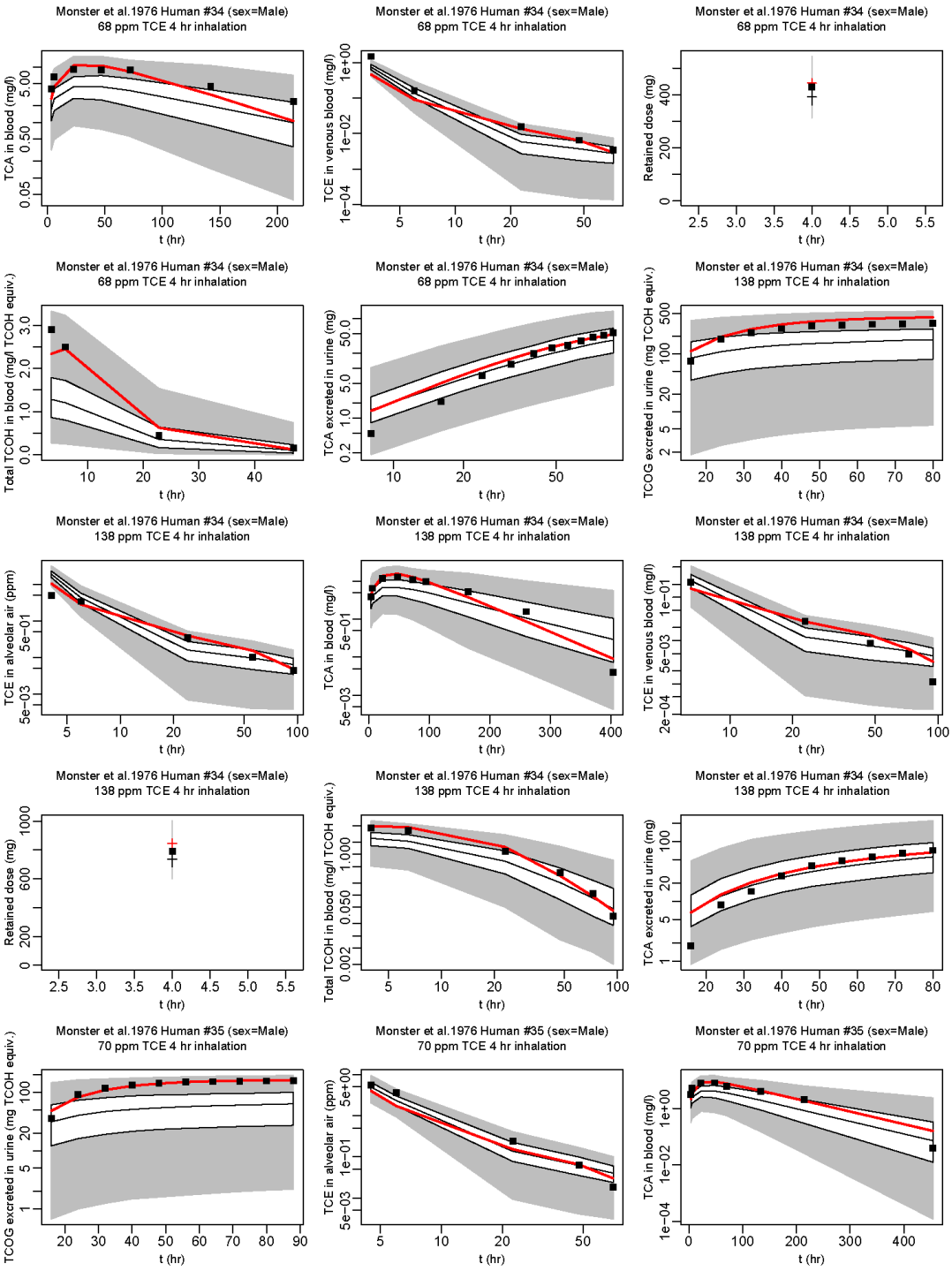

Figure A-34. Comparison of human calibration data (boxes) and PBPK model predictions (red line: using the posterior mean of the subject-specific parameters; + with error bars: single data points; or shaded regions: 2.5, 25, 50, 75, and 97.5% population-based predictions) (continued).

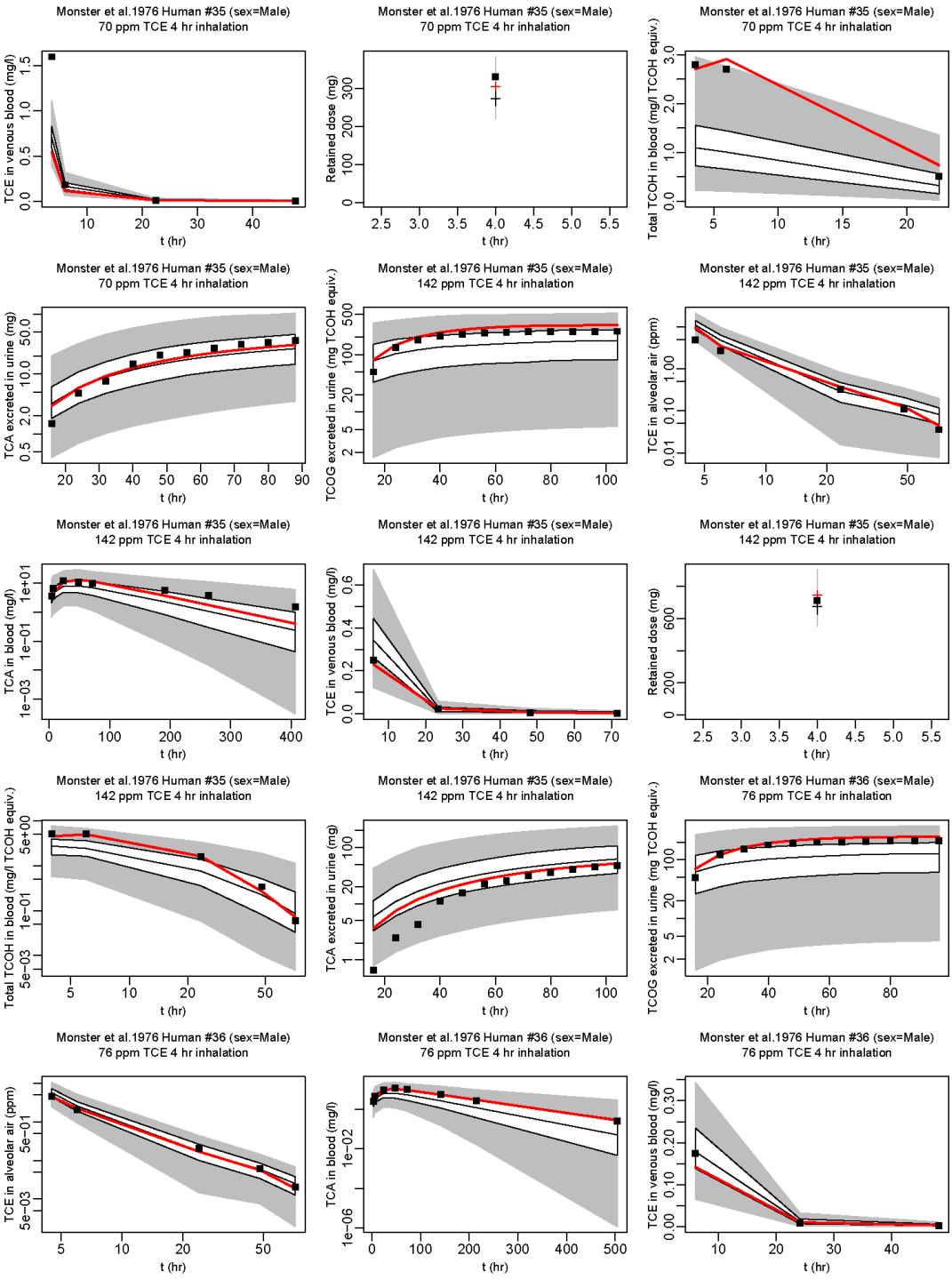

Figure A-34. Comparison of human calibration data (boxes) and PBPK model predictions (red line: using the posterior mean of the subject-specific parameters; + with error bars: single data points; or shaded regions: 2.5, 25, 50, 75, and 97.5% population-based predictions) (continued).

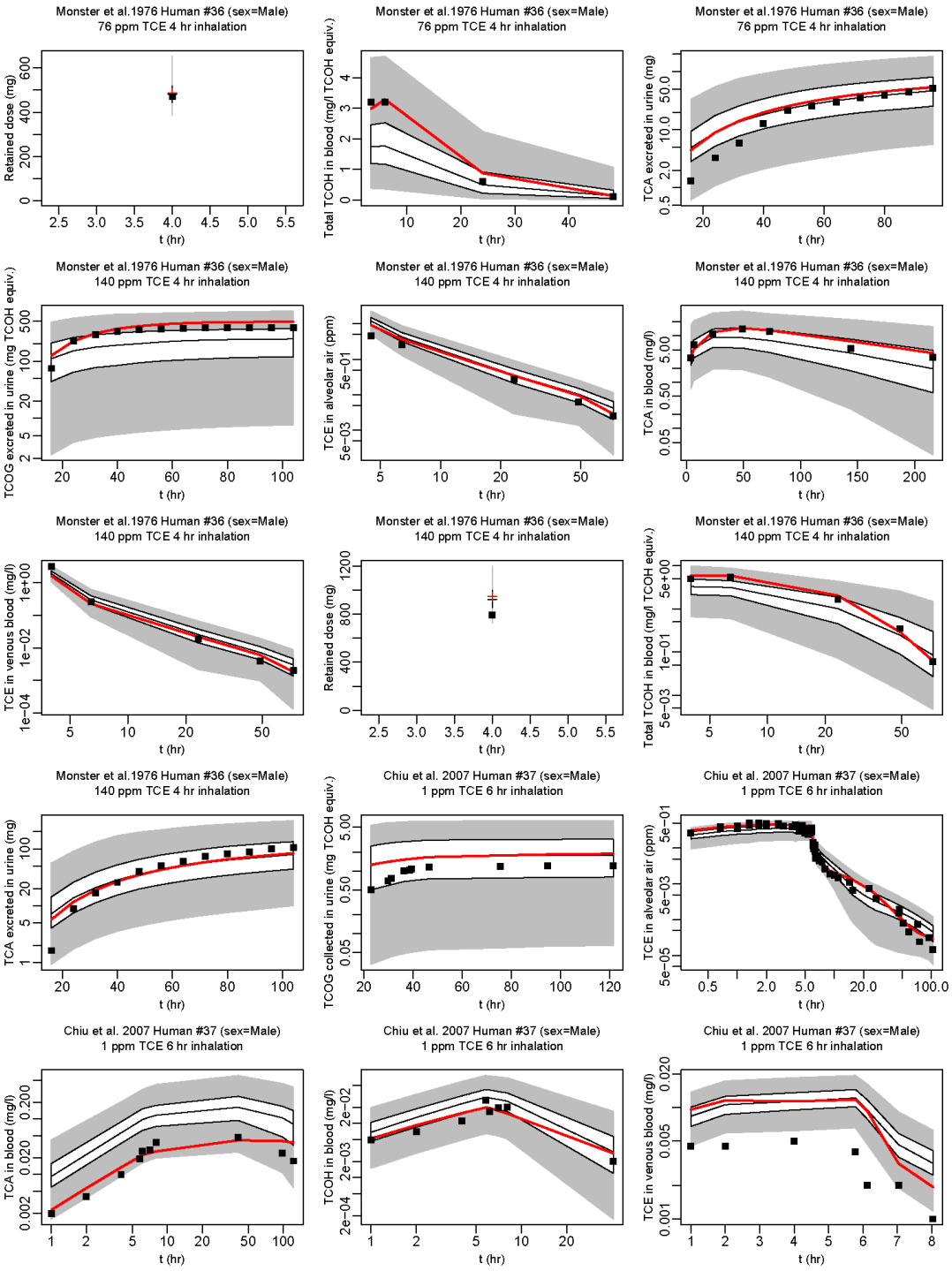

Figure A-34. Comparison of human calibration data (boxes) and PBPK model predictions (red line: using the posterior mean of the subject-specific parameters; + with error bars: single data points; or shaded regions: 2.5, 25, 50, 75, and 97.5% population-based predictions) (continued).

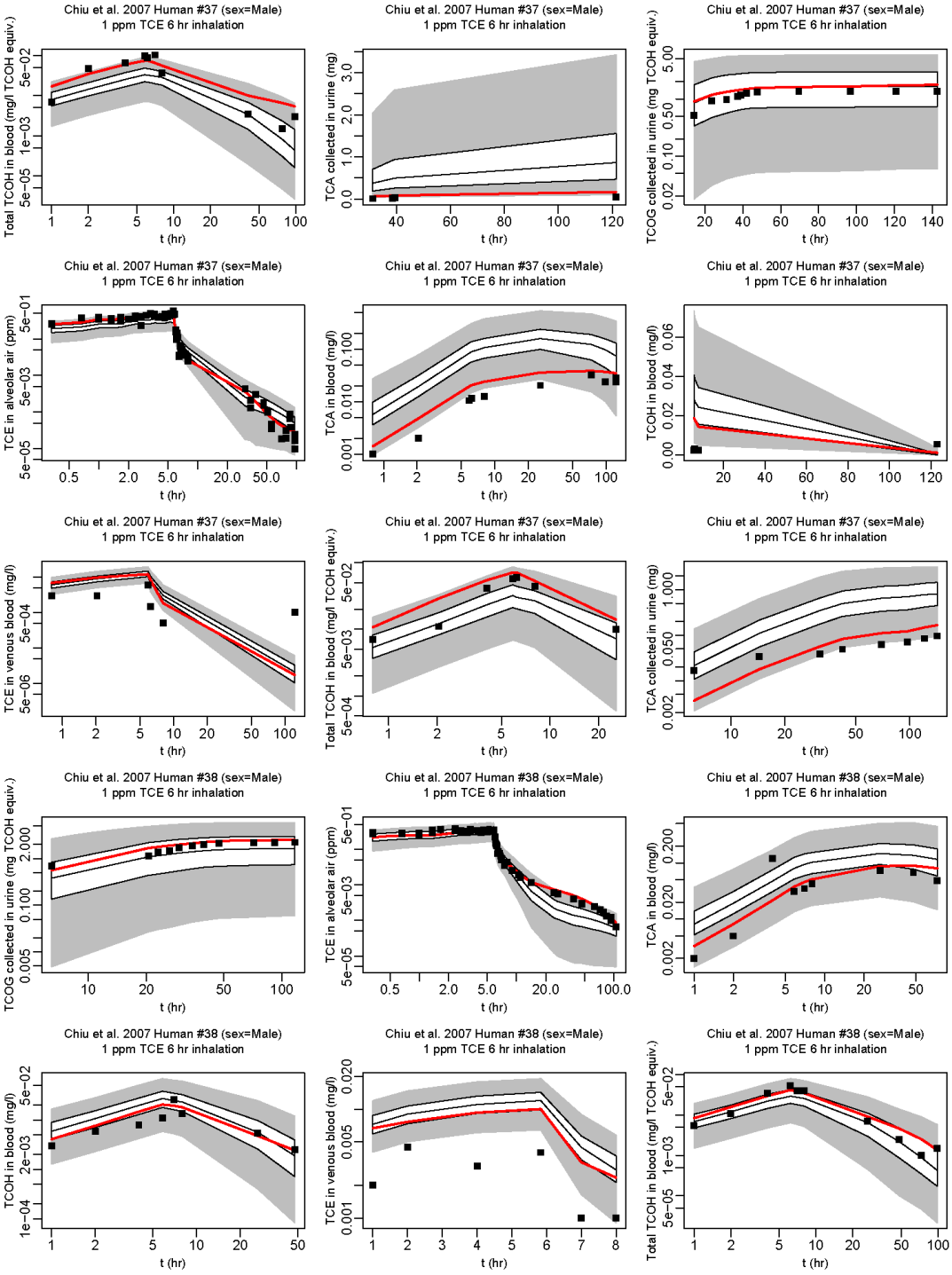

Figure A-34. Comparison of human calibration data (boxes) and PBPK model predictions (red line: using the posterior mean of the subject-specific parameters; + with error bars: single data points; or shaded regions: 2.5, 25, 50, 75, and 97.5% population-based predictions) (continued).

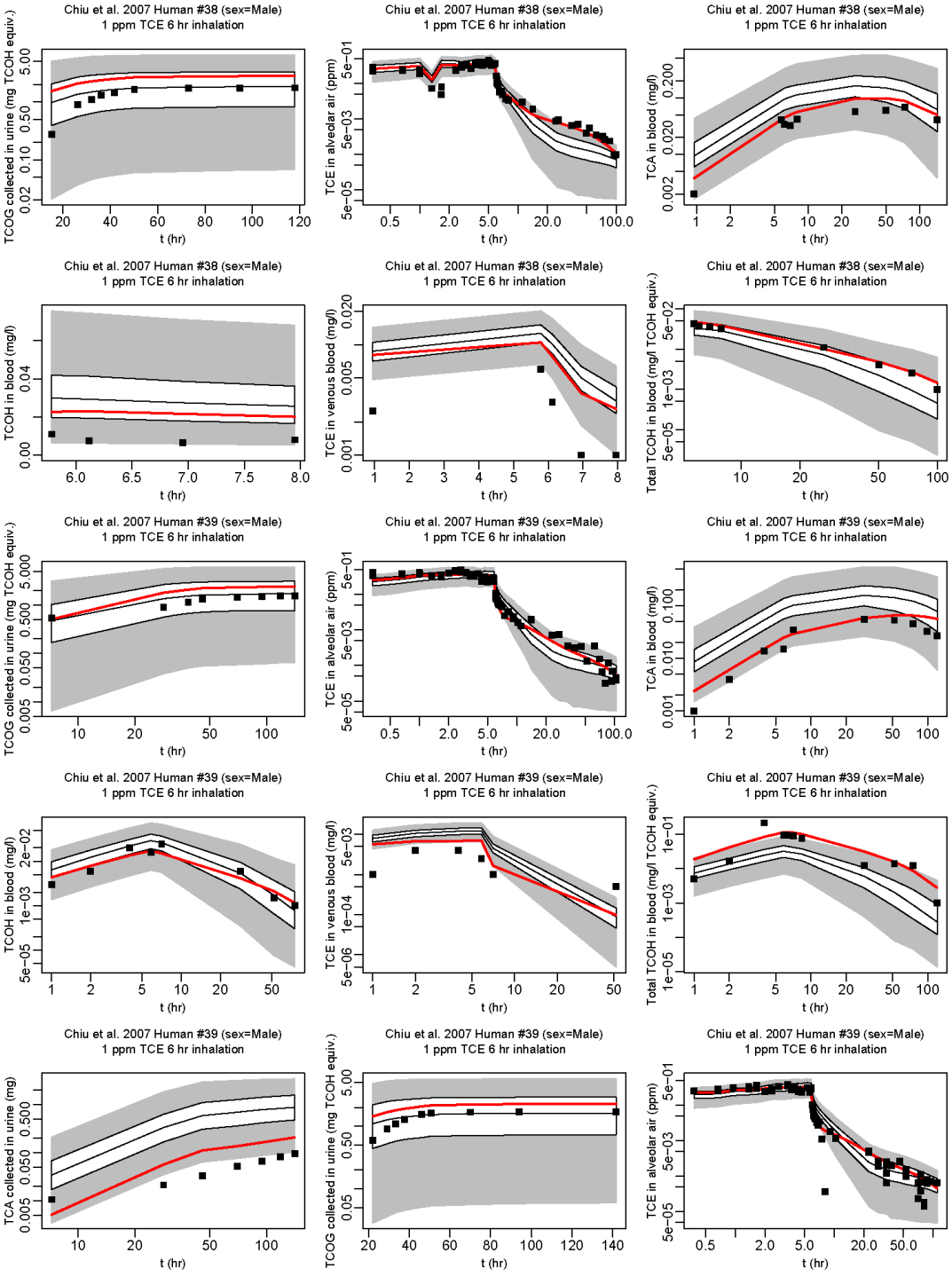

Figure A-34. Comparison of human calibration data (boxes) and PBPK model predictions (red line: using the posterior mean of the subject-specific parameters; + with error bars: single data points; or shaded regions: 2.5, 25, 50, 75, and 97.5% population-based predictions) (continued).

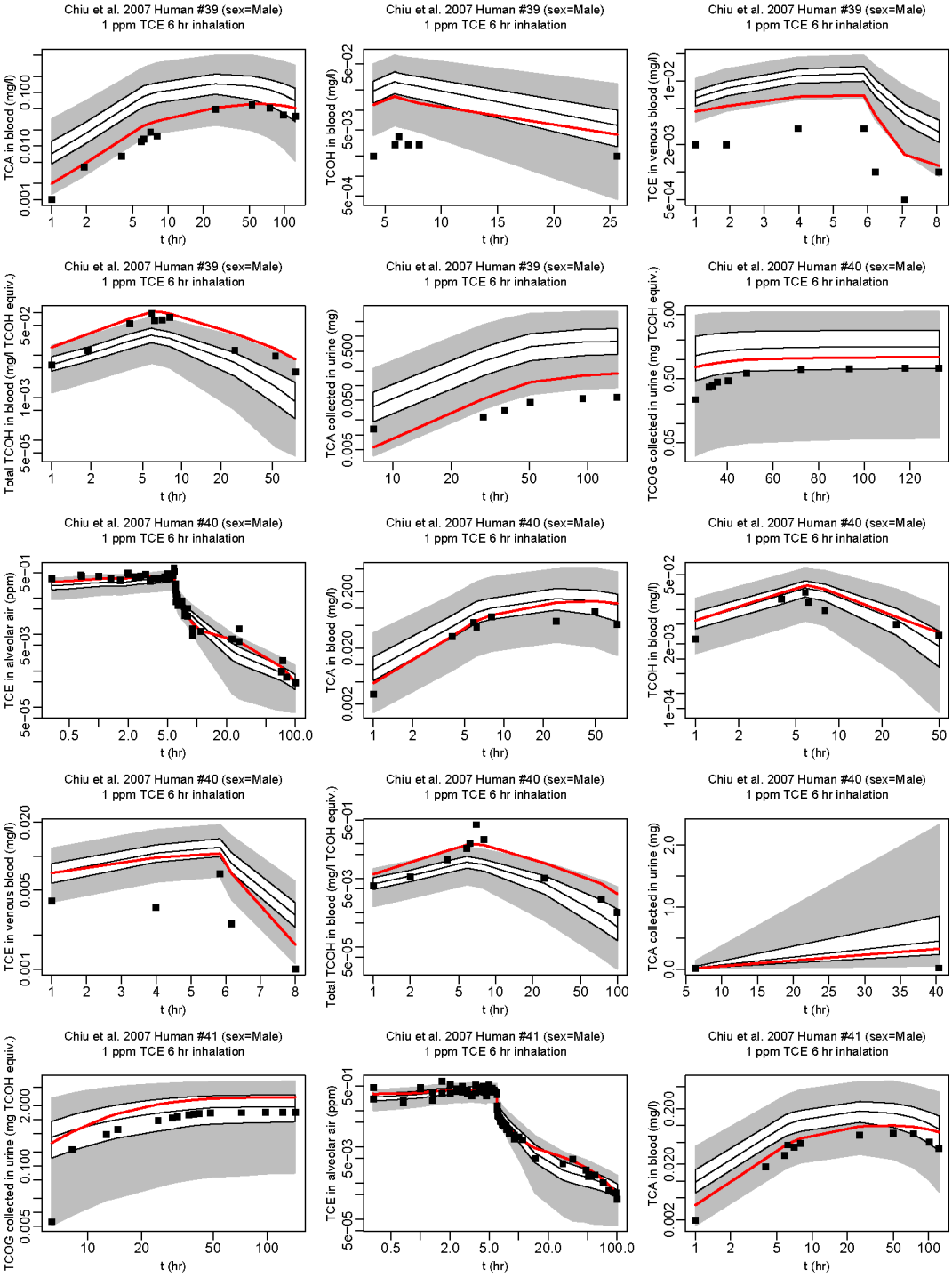

Figure A-34. Comparison of human calibration data (boxes) and PBPK model predictions (red line: using the posterior mean of the subject-specific parameters; + with error bars: single data points; or shaded regions: 2.5, 25, 50, 75, and 97.5% population-based predictions) (continued).

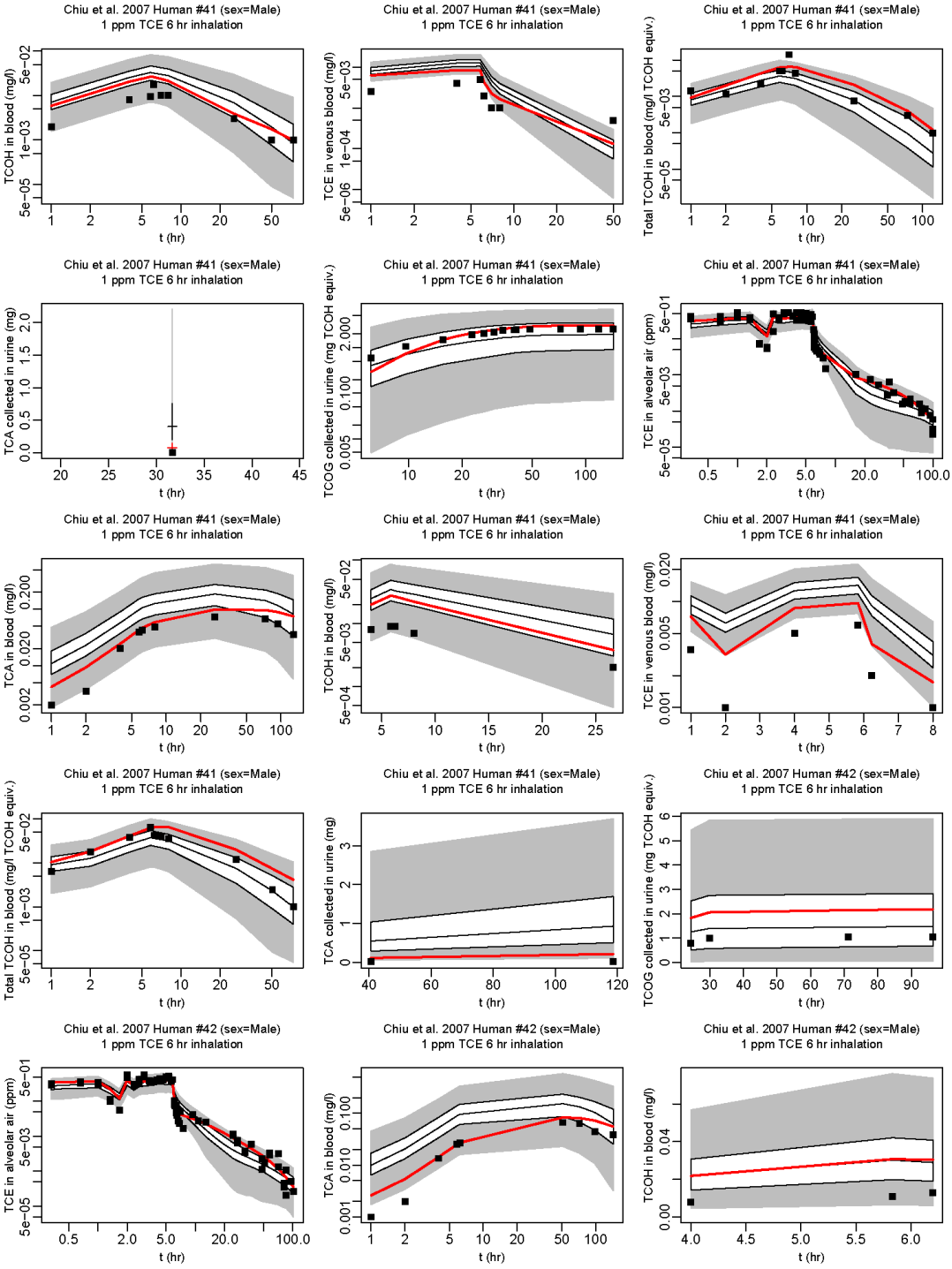

Figure A-34. Comparison of human calibration data (boxes) and PBPK model predictions (red line: using the posterior mean of the subject-specific parameters; + with error bars: single data points; or shaded regions: 2.5, 25, 50, 75, and 97.5% population-based predictions) (continued).

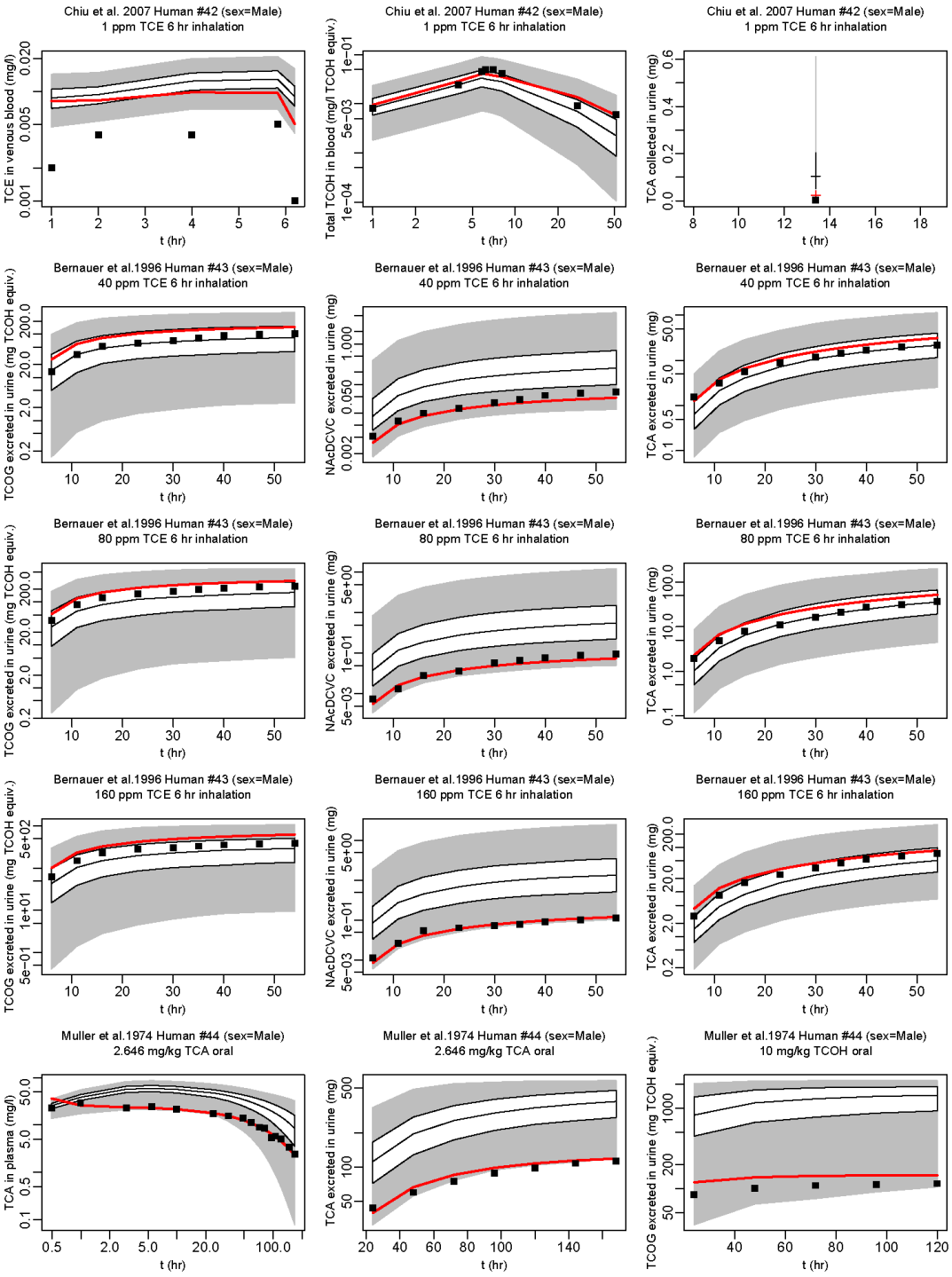

Figure A-34. Comparison of human calibration data (boxes) and PBPK model predictions (red line: using the posterior mean of the subject-specific parameters; + with error bars: single data points; or shaded regions: 2.5, 25, 50, 75, and 97.5% population-based predictions) (continued).

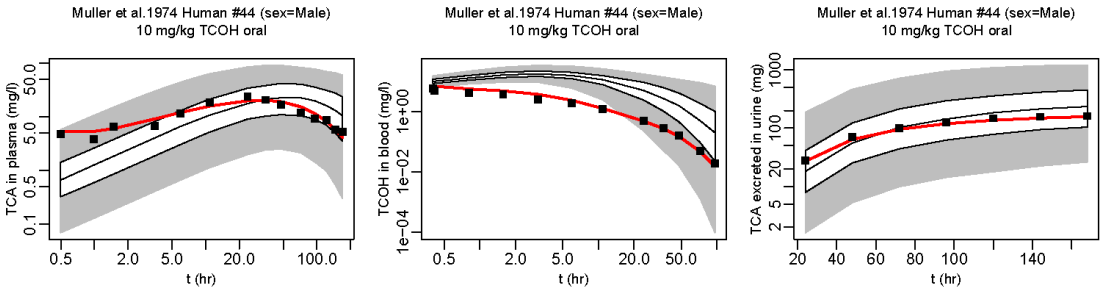

Figure A-34. Comparison of human calibration data (boxes) and PBPK model predictions (red line: using the posterior mean of the subject-specific parameters; + with error bars: single data points; or shaded regions: 2.5, 25, 50, 75, and 97.5% population-based predictions) (continued).

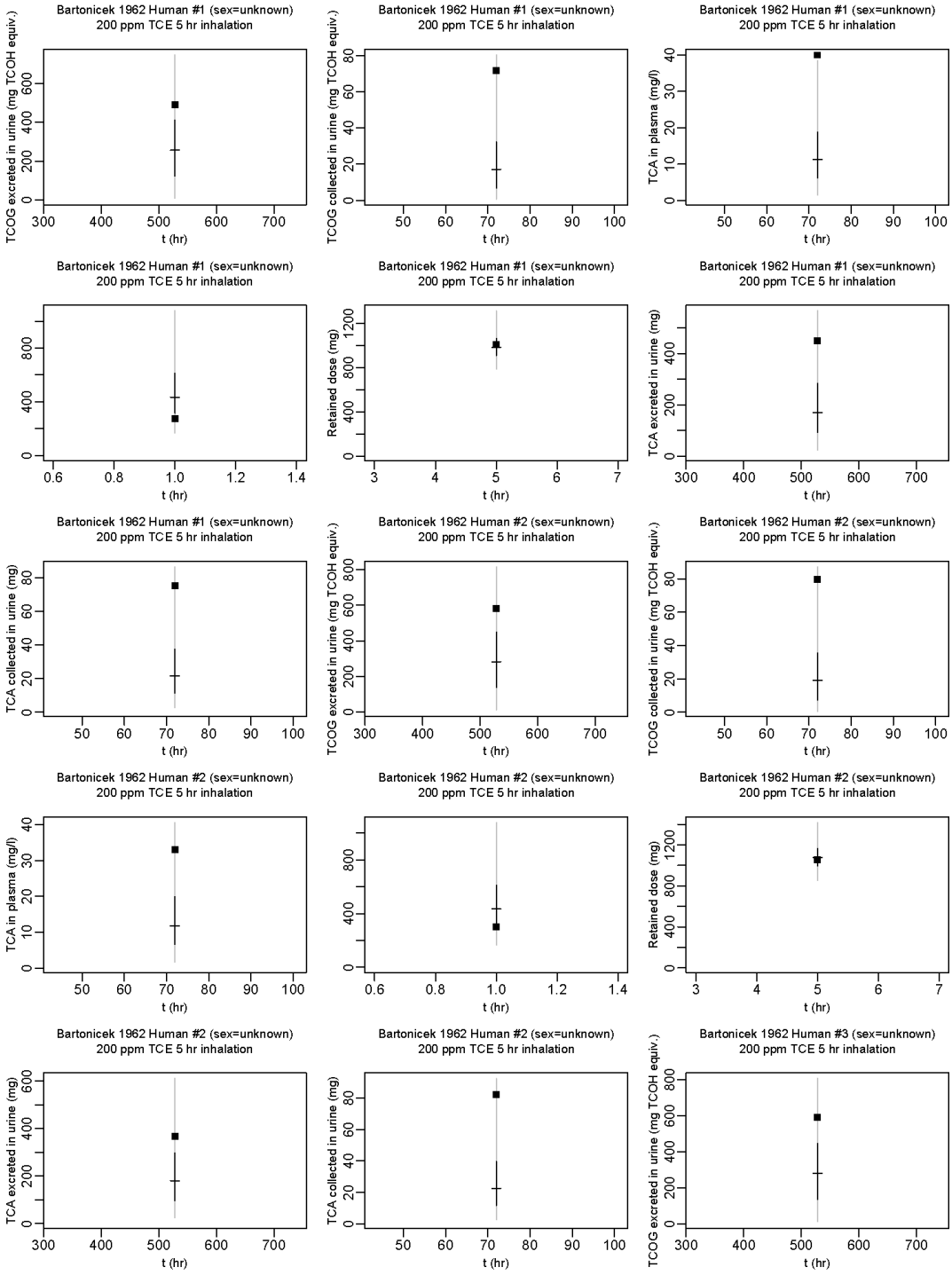

Figure A-35. Comparison of human evaluation data (boxes) and PBPK model predictions (+ with error bars: single data points or shaded regions: 2.5, 25, 50, 75, and 97.5% population-based predictions).

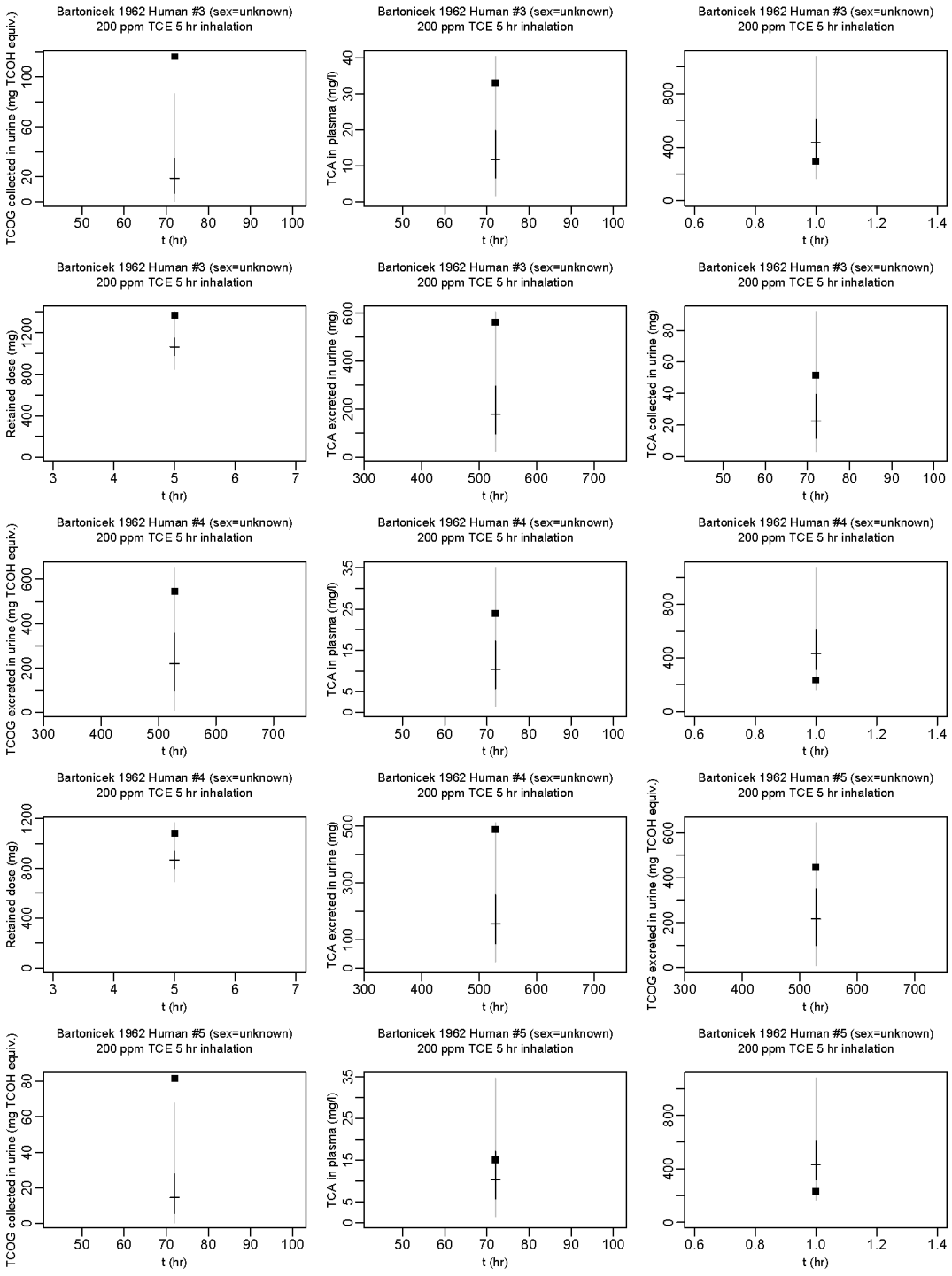

Figure A-35. Comparison of human evaluation data (boxes) and PBPK model predictions (+ with error bars: single data points or shaded regions: 2.5, 25, 50, 75, and 97.5% population-based predictions) (continued).

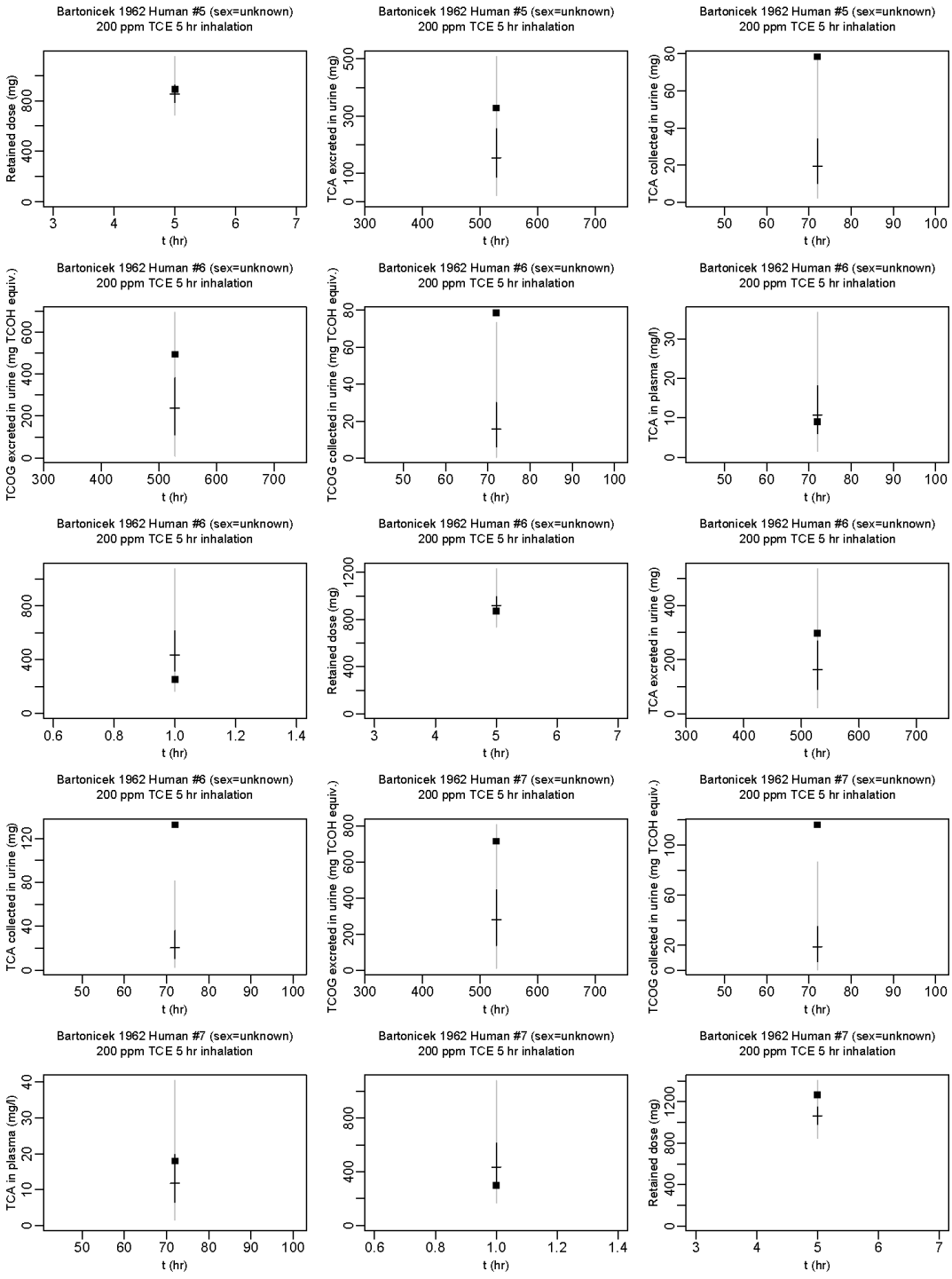

Figure A-35 Comparison of human evaluation data (boxes) and PBPK model predictions (+ with error bars: single data points or shaded regions: 2.5, 25, 50, 75, and 97.5% population-based predictions) (continued).

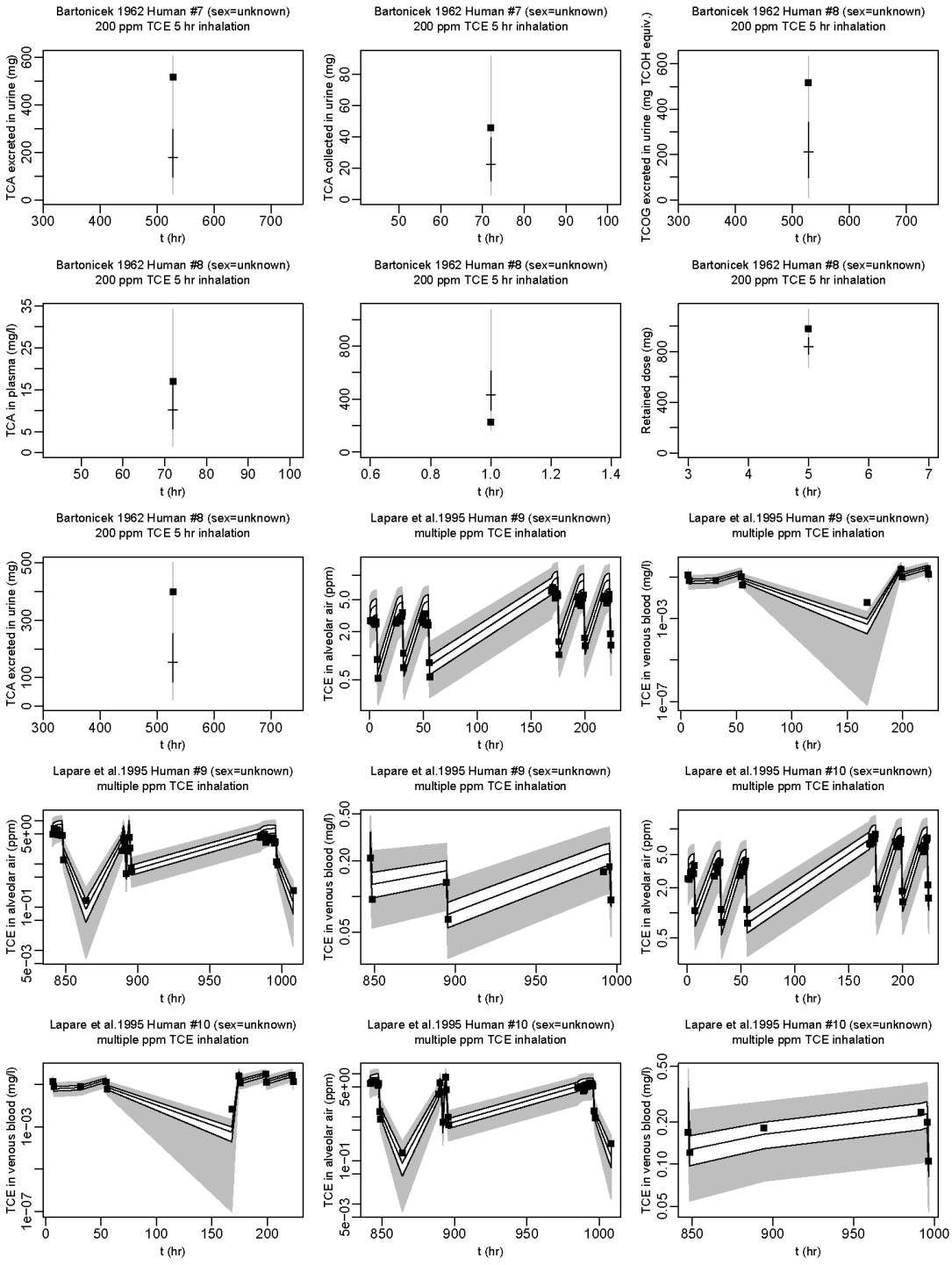

Figure A-35. Comparison of human evaluation data (boxes) and PBPK model predictions (+ with error bars: single data points or shaded regions: 2.5, 25, 50, 75, and 97.5% population-based predictions) (continued).

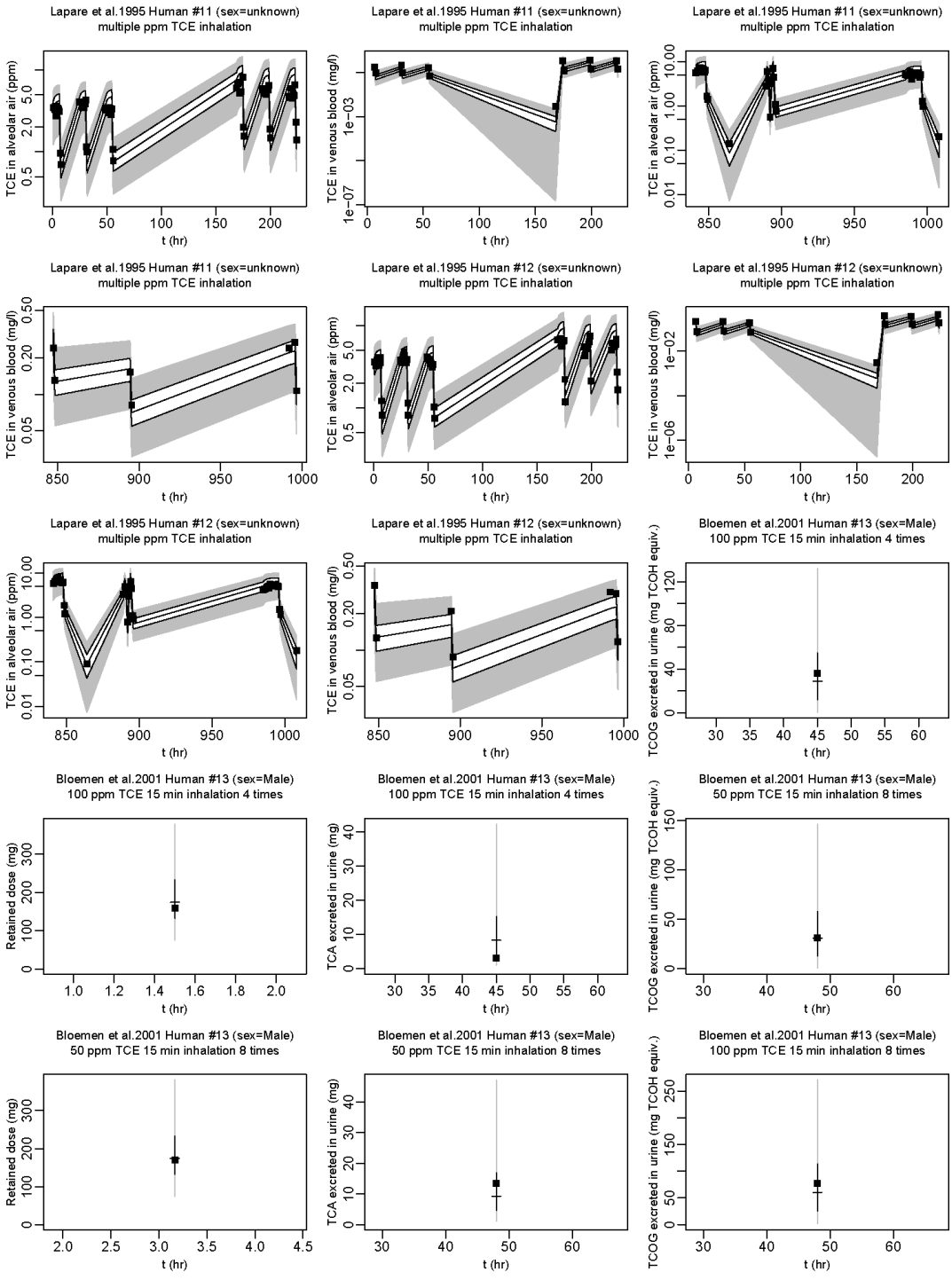

Figure A-35. Comparison of human evaluation data (boxes) and PBPK model predictions (+ with error bars: single data points or shaded regions: 2.5, 25, 50, 75, and 97.5% population-based predictions) (continued).

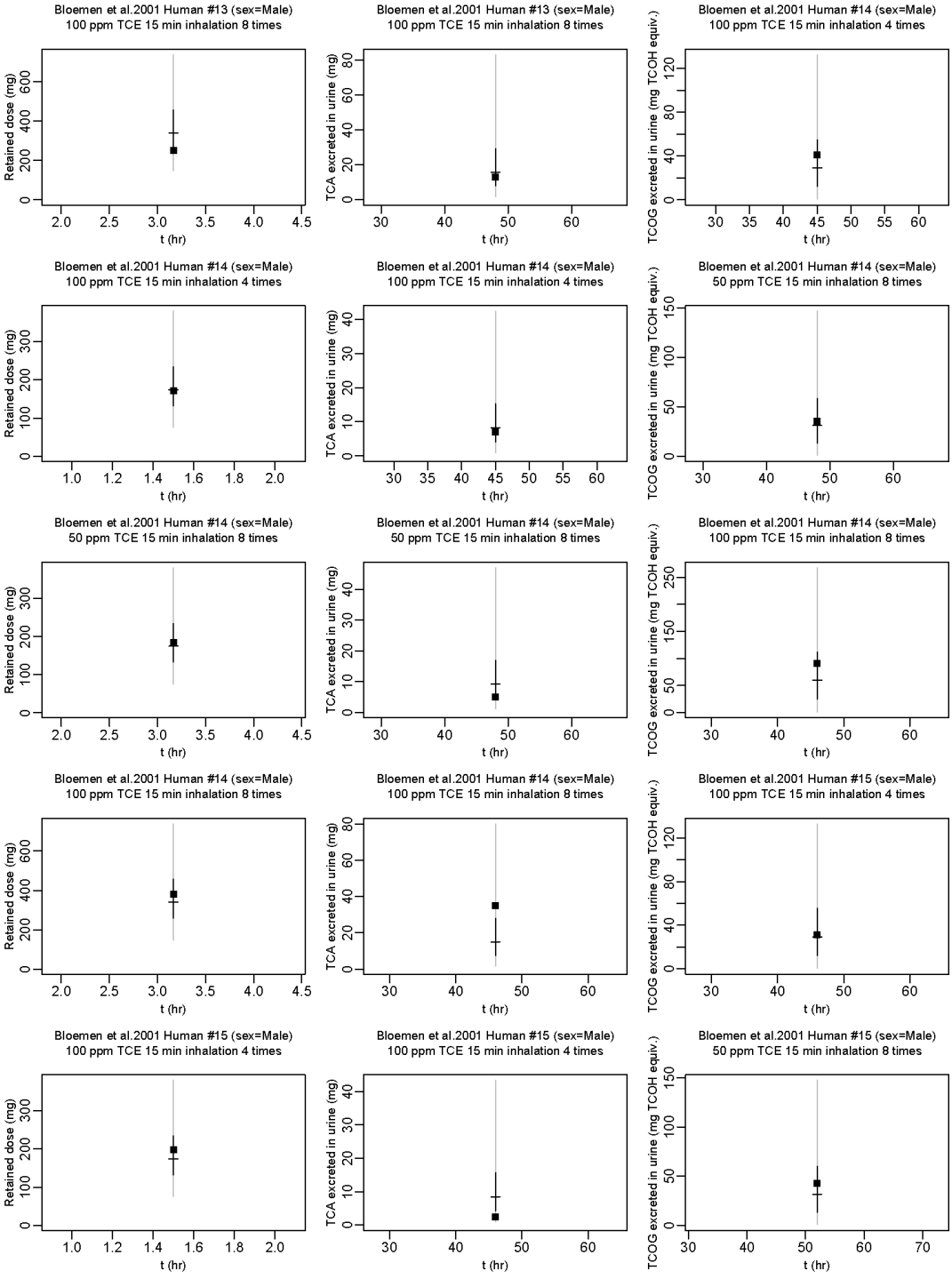

Figure A-35. Comparison of human evaluation data (boxes) and PBPK model predictions (+ with error bars: single data points or shaded regions: 2.5, 25, 50, 75, and 97.5% population-based predictions) (continued).

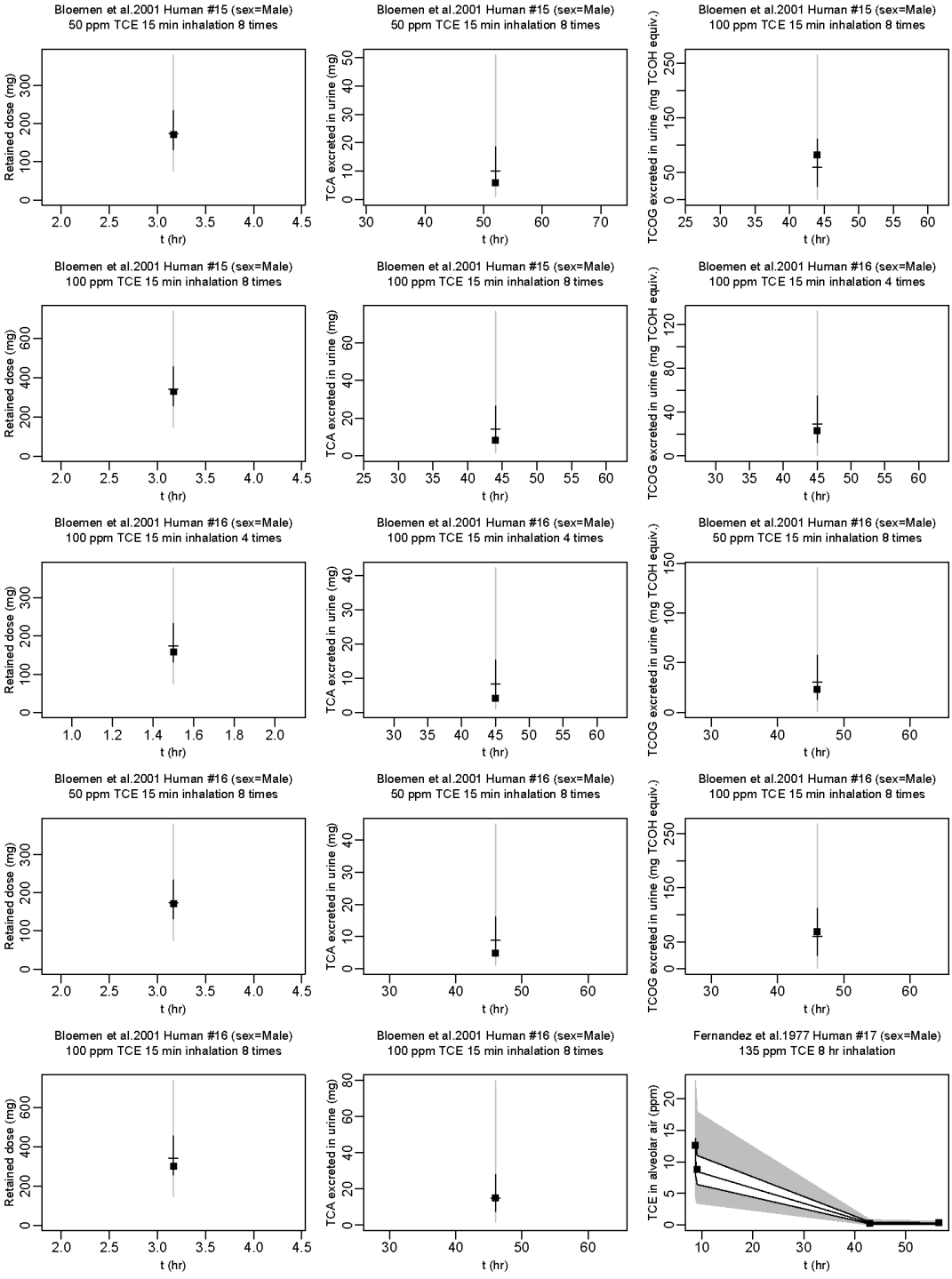

Figure A-35. Comparison of human evaluation data (boxes) and PBPK model predictions (+ with error bars: single data points or shaded regions: 2.5, 25, 50, 75, and 97.5% population-based predictions) (continued).

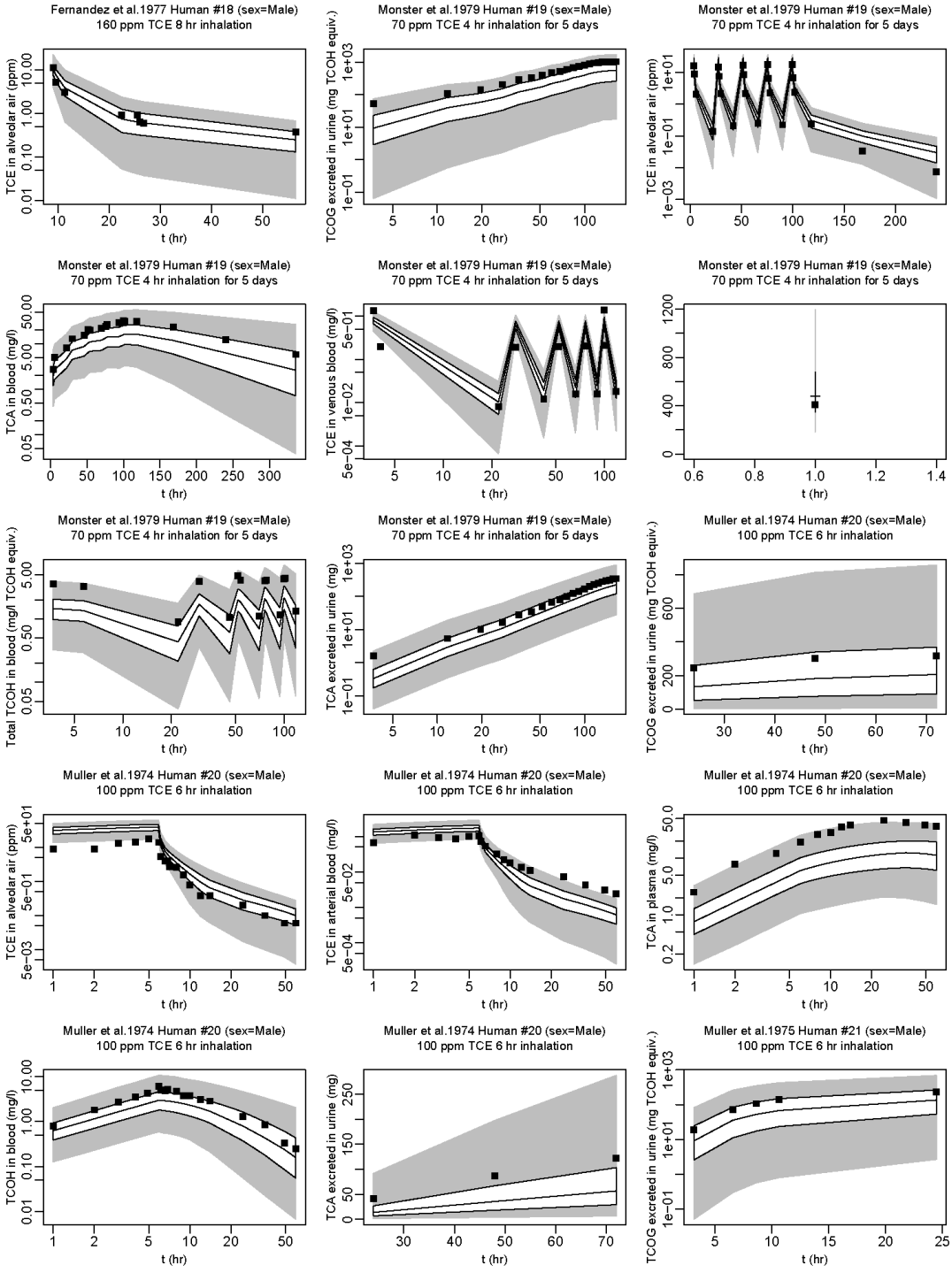

Figure A-35. Comparison of human evaluation data (boxes) and PBPK model predictions (+ with error bars: single data points or shaded regions: 2.5, 25, 50, 75, and 97.5% population-based predictions) (continued).

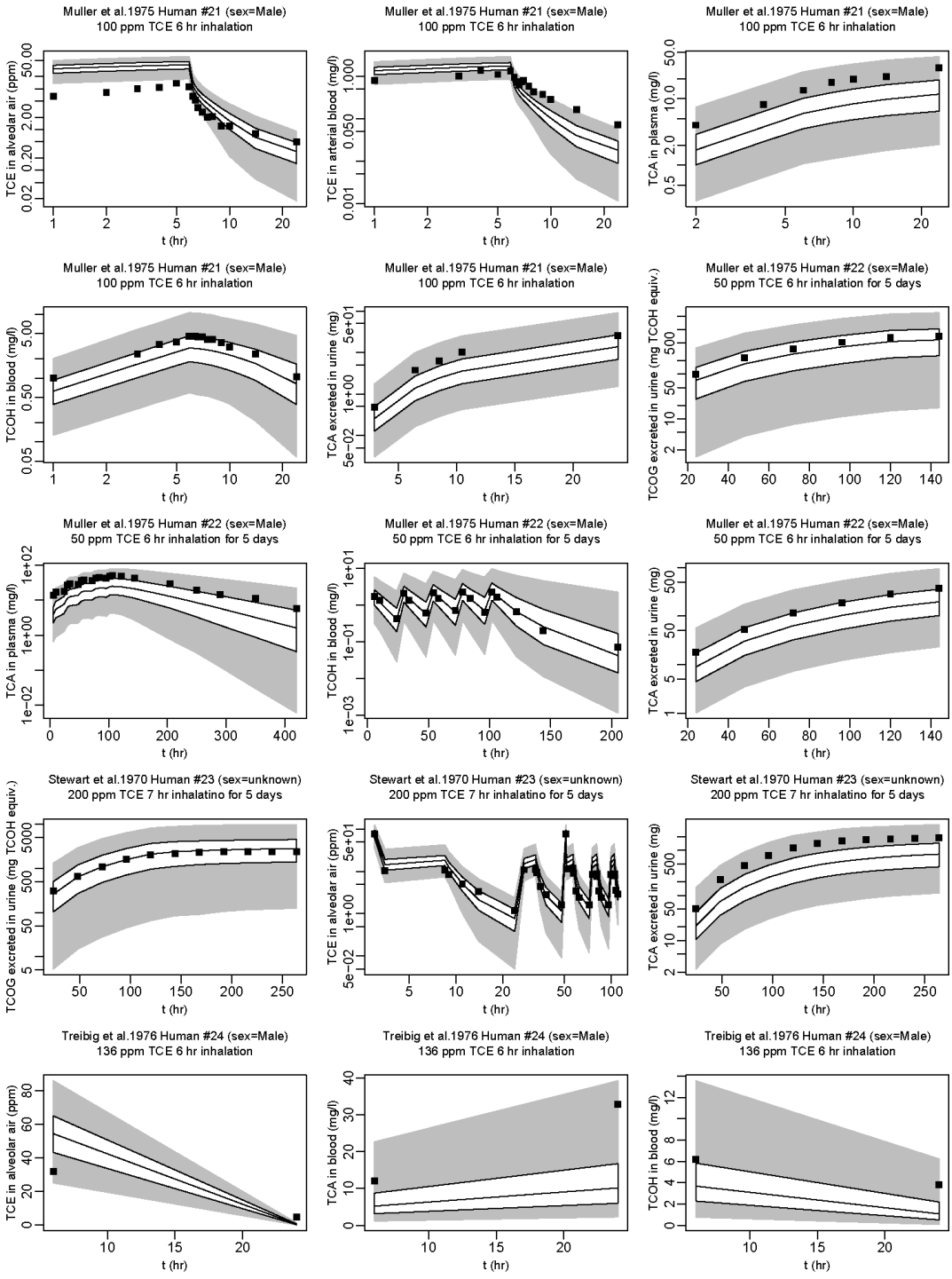

Figure A-35. Comparison of human evaluation data (boxes) and PBPK model predictions (+ with error bars: single data points or shaded regions: 2.5, 25, 50, 75, and 97.5% population-based predictions) (continued).

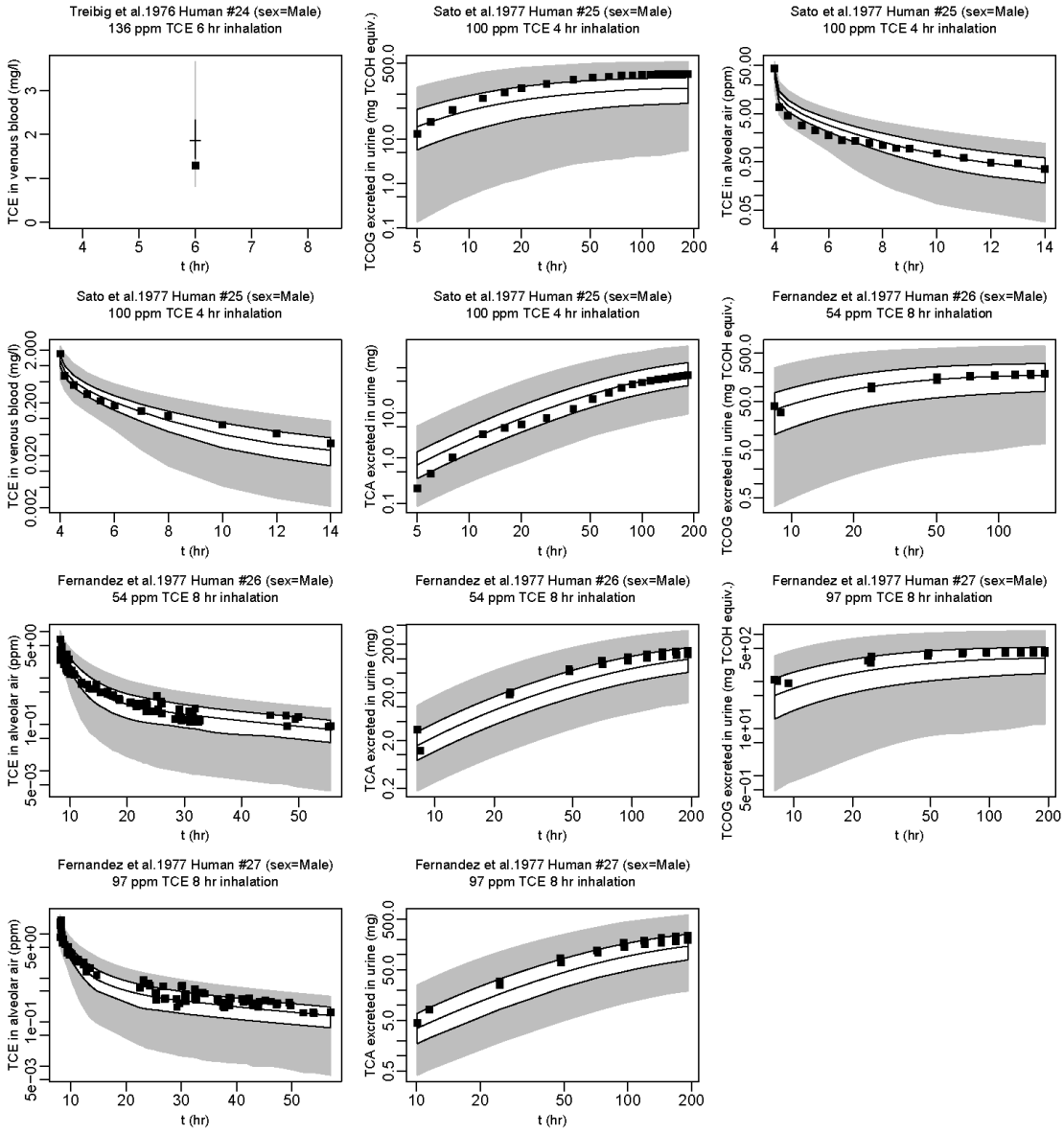

Figure A-35. Comparison of human evaluation data (boxes) and PBPK model predictions (+ with error bars: single data points or shaded regions: 2.5, 25, 50, 75, and 97.5% population-based predictions) (continued).

A.6. EVALUATION OF RECENTLY PUBLISHED TOXICOKINETIC DATA

Several in vivo toxicokinetic studies were published or became available during internal EPA review and Interagency Consultation, and were not evaluated as part of the originally planned analyses. Preliminary analyses of these data are summarized here. The general approach is the same as that used for the evaluation data in the primary analysis—population predictions from the PBPK model are compared visually with the toxicokinetic data.

A.6.1. TCE Metabolite Toxicokinetics in Mice: Kim et al. (2009)

Kim et al. (2009) measured TCA, DCA, DCVG, and DCVC in blood of male B6C3F$_1$ mice following a single gavage dose of 2,140 mg/kg. Of these data, only TCA and DCVG blood concentrations are predicted by the updated PBPK model, so only those data are compared with PBPK model predictions (prior values for the distribution volume and elimination rate constant of DCVG were used, as there were no calibration data informing those parameters). The TCA data were within the interquartile region of the PBPK model population predictions, as shown in Figure A-36. The DCVG data were at the lower end of the PBPK model population predictions, but within the 95% range.

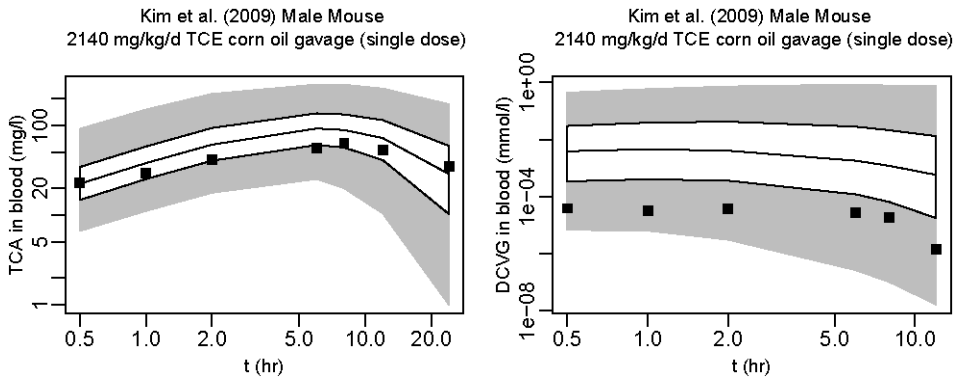

Figure A-36. Comparison of Kim et al. (2009) mouse data (boxes) and PBPK model predictions (+ with error bars: single data points or shaded regions: 2.5, 25, 50, 75, and 97.5% population-based predictions).

An assessment was made as to whether these data are informative as to the flux of GSH conjugation in mice. First, the best fitting parameter sample (least squares on TCA and DCVG in blood, weighted by inverse of the observed variance, Figures A-37 and A-38) from the posterior distribution was selected out of 50,000 samples generated by Monte Carlo (see Figures A-13 and A-14 for the comparison with predictions with data). This parameter sample was then used to calculate the fraction of intake that is predicted by the PBPK model to undergo GSH metabolism for continuous oral and continuous inhalation exposure, and this point estimate was compared to the full posterior distribution (see Figures A-15 and A-16). The predictions for this "best fitting" parameter set was similar (within threefold) of the median of the full posterior distribution (see Figures A-39 and A-40). While a formal assessment of the impact of these new data (i.e., including its uncertainty and variability) would require a rerunning of the Bayesian analysis, it appears that the median estimates for the mouse GSH conjugation dose-metric used in the dose-response assessment (see Chapter 5) are reasonably consistent with the Kim et al. (2009) data.

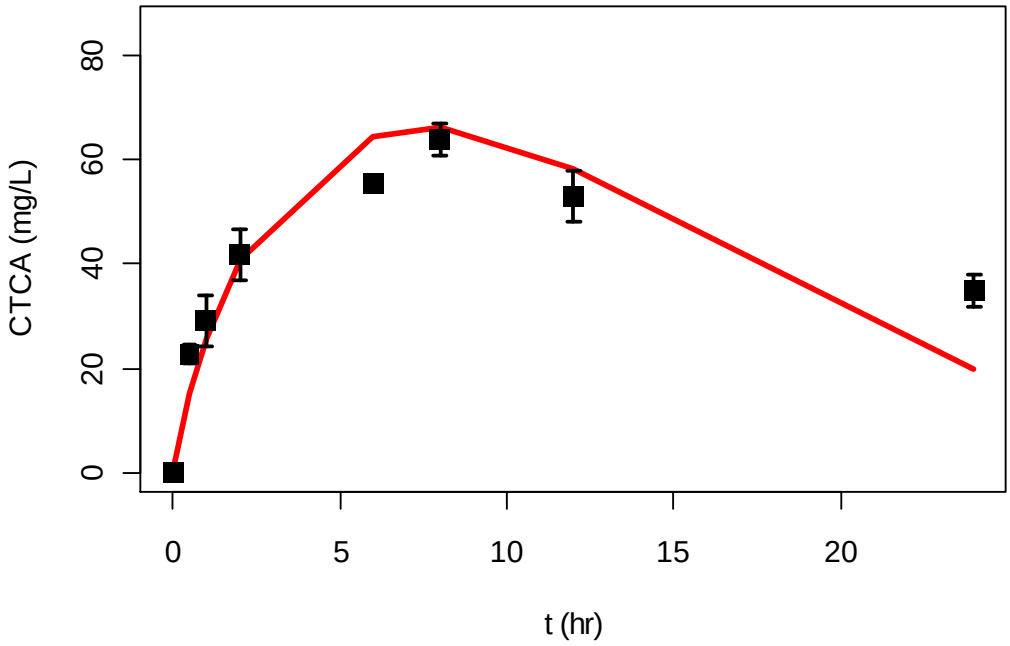

Figure A-37. Comparison of best-fitting (out of 50,000 posterior samples) PBPK model prediction and Kim et al. (2009) TCA blood concentration data for mice gavaged with 2,140 mg/kg TCE.

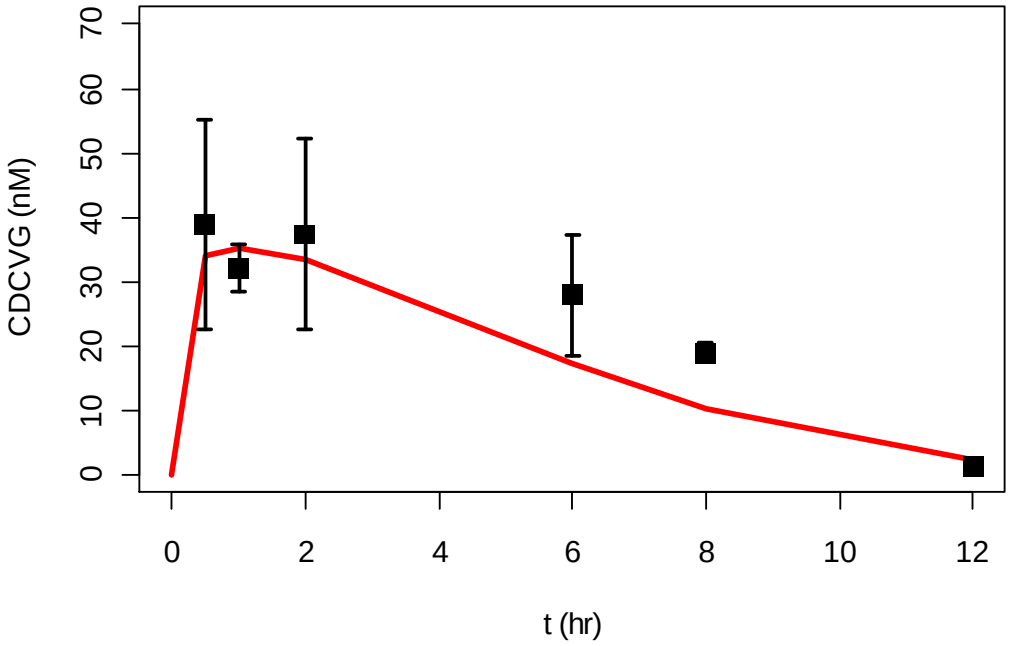

Figure A-38. Comparison of best-fitting (out of 50,000 posterior samples) PBPK model prediction and Kim et al. (2009) DCVG blood concentration data for mice gavaged with 2,140 mg/kg TCE.

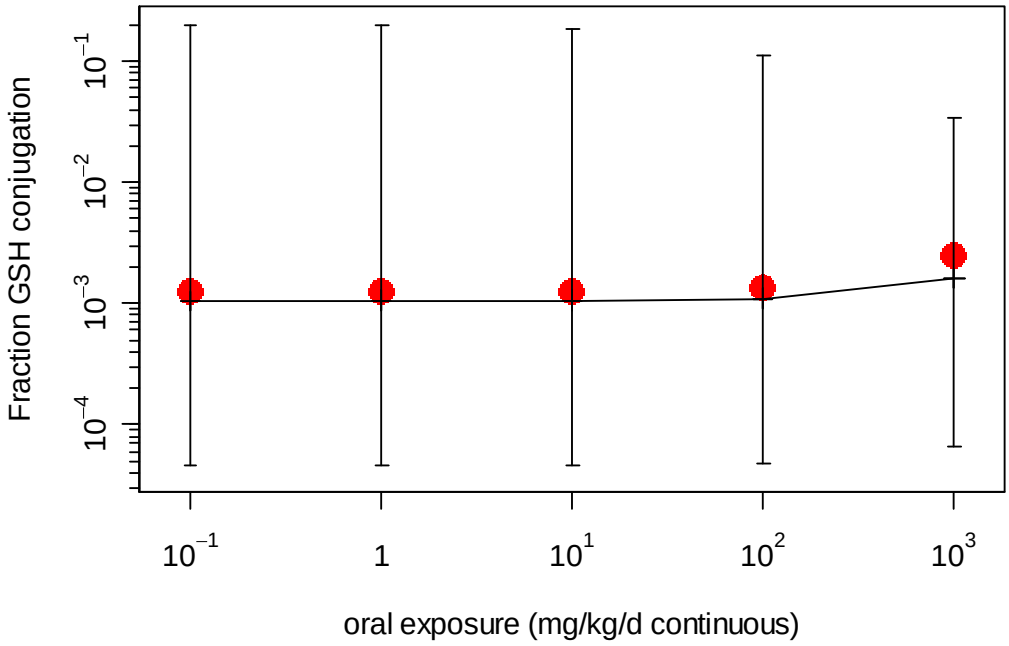

Lines and error bars represent the median and 95th percentile CI for the posterior predictions, respectively (also reported in Section 3.5.7.3.1). Filled circles represent the predictions from the sample (out of 50,000 total posterior samples) which provides the best fit to the Kim et al. (2009) TCA and DCVG blood concentration data for mice gavaged with 2,140 mg/kg TCE.

Figure A-39. PBPK model predictions for the fraction of intake undergoing GSH conjugation in mice continuously exposed orally to TCE.

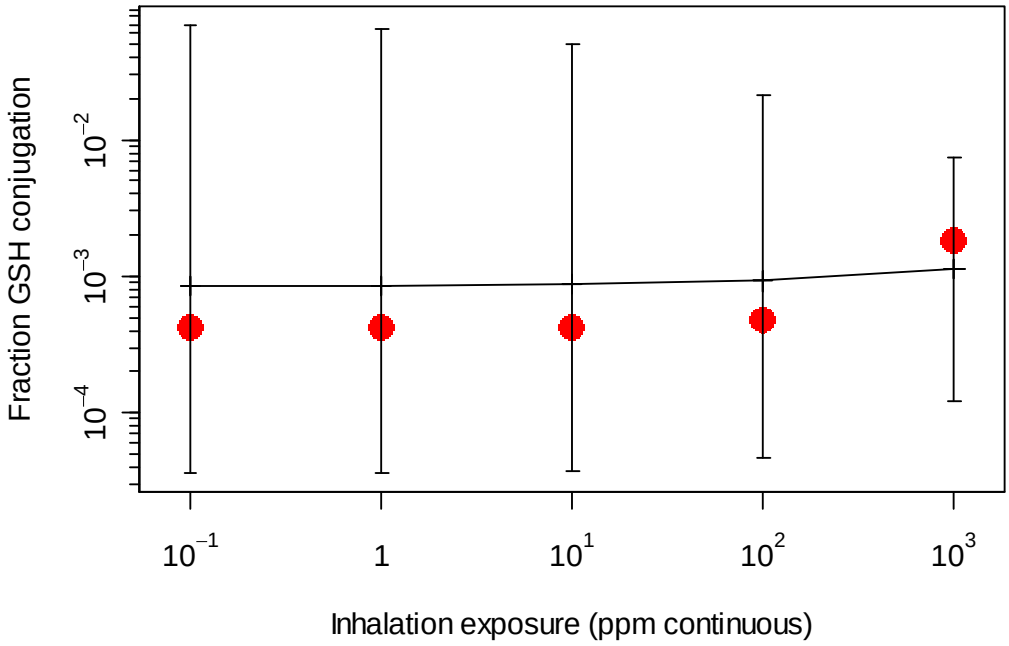

Lines and error bars represent the median and 95th percentile CI for the posterior predictions, respectively (also reported in Section 3.5.7.3.1). Filled circles represent the predictions from the sample (out of 50,000 total posterior samples) which provides the best fit to the Kim et al. (2009) TCA and DCVG blood concentration data for mice gavaged with 2,140 mg/kg TCE.

Figure A-40. PBPK model predictions for the fraction of intake undergoing GSH conjugation in mice continuously exposed via inhalation to TCE.

An additional note of interest from the Kim et al. (2009) data is the interstudy variability in TCA kinetics. In particular, the TCA blood concentrations reported by Kim et al. (2009) are twofold lower than those reported by Abbas and Fisher (1997) in the same sex and strain of mouse, with a very similar corn oil gavage dose of 2,000 mg/kg [as compared to 2,140 mg/kg used in Kim et al. (2009)].

A.6.2. TCE Toxicokinetics in Rats: Liu et al. (2009)

Liu et al. (2009) measured TCE in blood of male rats after treatment with TCE by i.v. injection (0.1, 1.0, or 2.5 mg/kg) or aqueous gavage (0.0001, 0.001, 0.01, 0.1, 1, 2.5, 5, or 10 mg/kg). Almost all of the data from gavage exposures were within the interquartile region of the PBPK model population predictions, with all of it within the 95% CI, as shown in Figure A-41. For i.v. exposures, the data at 1 and 2.5 mg/kg were well simulated, but the time-course data at 0.1 mg/kg were substantially different in shape from that predicted by the PBPK model, with a

lower initial concentration and longer half-life. The slower elimination rat at 0.1 mg/kg was noted by the study authors through use of noncompartamental analysis. There is no clear explanation for this discrepancy, particularly since the gavage data at this and even lower doses were well predicted by the PBPK model.

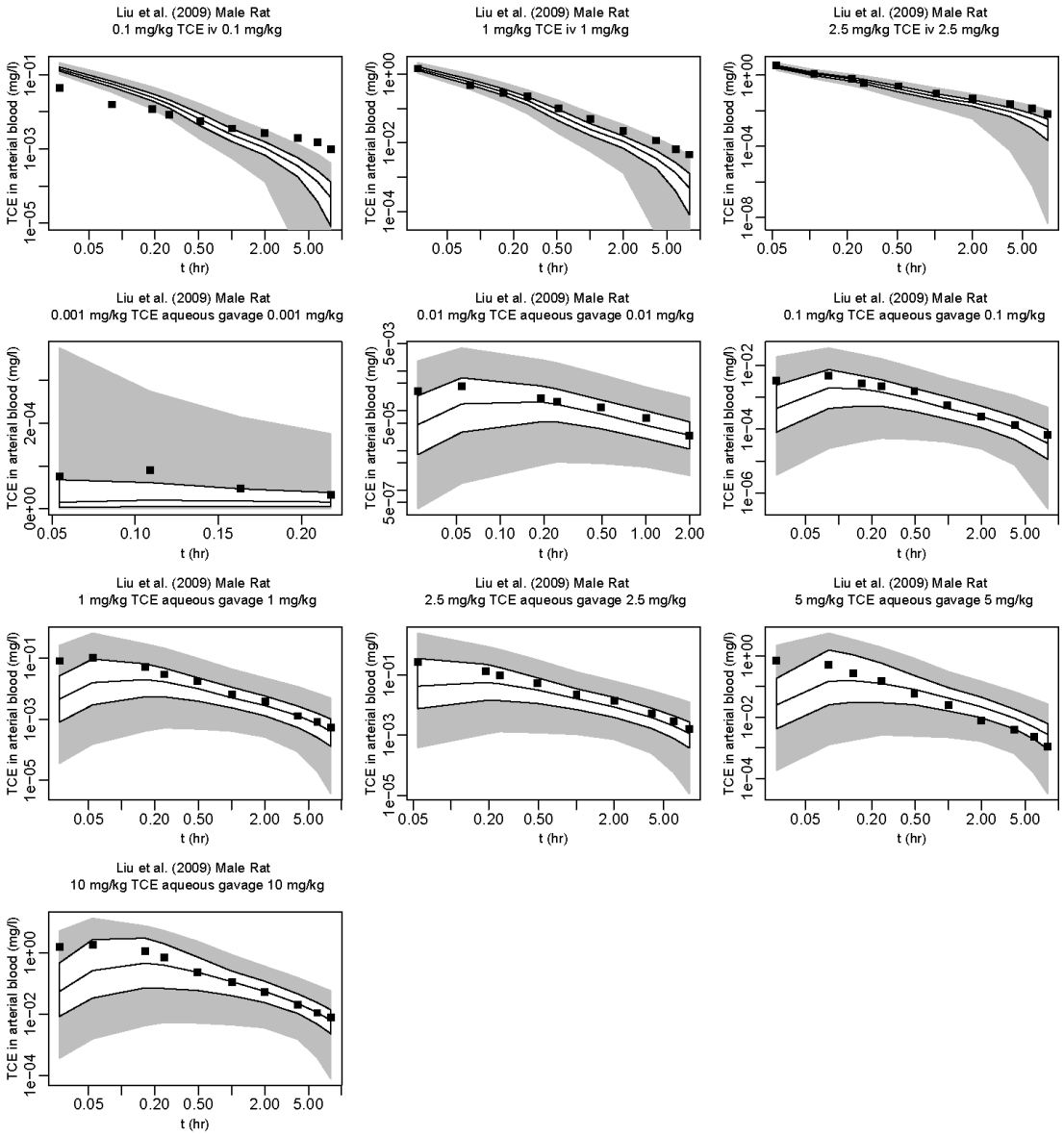

Figure A-41. Comparison of Liu et al. (2009) rat data (boxes) and PBPK model predictions (+ with error bars: single data points or shaded regions: 2.5, 25, 50, 75, and 97.5% population-based predictions).

A.6.3. TCA Toxicokinetics in Mice and Rats: Mahle et al. (1999) and Green (2003a, 2003b)

Three technical reports (Green, 2003b, a; Mahle et al., 1999) described by Sweeney et al. (2009) contained data on TCA toxicokinetics in mice and rats exposed to TCA in drinking water. These technical reports were provided to EPA by the Sweeney et al. (2009) authors.

A.6.3.1. Analysis Using Evans et al. (2009) and Chiu et al. (2009) PBPK Model

TCA blood and liver concentrations were reported by Mahle et al. (1999) for male B6C3F$_1$ mice and male F344 rats exposed to 0.1 g/L to 2 g/L TCA in drinking water for 3 or 14 days (12–270 mg/kg-day in mice and 7–150 mg/kg-day in rats). For mice, these data were all within the 95% CI of PBPK model population predictions, with about half of these data within the interquartile region. For rats, all of these data, except those for the 3-day exposure at 0.1 g/L, were within the 95% CI of the PBPK model predictions. In addition, the median rat predictions were consistently higher than the data, although this could be explained by interstudy (strain, lot, etc.) variability.

TCA blood concentrations were reported by Green (2003a) for male and female B6C3F$_1$ mice exposed to 0.5–2.5 g/L TCA in drinking water for 5 days (130–600 mg/kg-day in males and 160–750 mg/kg-day in females). Notably, these animals consumed around twice as much water per day as compared to the mice reported by Mahle et al. (1999), and therefore, received comparatively higher doses of TCA for the same TCE concentration in drinking water.

In male mice, the data at the lower two doses (130 and 250 mg/kg-day) were within the interquartile region of the PBPK model predictions. The data for male mice at the highest dose (600 mg/kg-day) were below the interquartile region, but within the 95% CI of the PBPK model predictions. In females, the data at the lower two doses (160 and 360 mg/kg-day) were mostly below the interquartile region, but within the 95% CI of the PBPK model predictions, while about half of the data at the highest dose were just below the 95% CI.

TCA blood, plasma, and liver concentrations were reported by Green (2003b) for male PPARα-null mice, male 129/sv mice (the background strain of the PPARα-null mice), and male and female B6C3F$_1$ mice, exposed to 1.0 or 2.5 g/L TCA in drinking water for 5 days (male B6C3F$_1$ only) to 14 days.[2] In male PPARα-null mice, plasma and blood concentrations were within the interquartile region of the PBPK model predictions, while liver concentrations were below the interquartile region but within the 95% CI. In male 129/sv mice, the plasma concentrations were within the interquartile region of the PBPK model predictions, while blood and liver concentrations were below the interquartile region but within the 95% CI. In male B6C3F$_1$ mice, all data were within the 95% CIs of the PBPK model predictions, with about half within the interquartile region, and the rest above (plasma concentrations at the lower dose) or below (liver concentrations at all but the lowest dose at 5 days). In female B6C3F$_1$ mice, plasma concentrations were below the interquartile region but within the 95% confidence region, while liver and blood concentrations were at or below the lower 95% confidence bound.

[2]Sweeney et al. (2009) reported that blood concentrations in Green (2003b) were incorrect due to an arithmetic error owing to a change in chemical analytic methodology, and should have been multiplied by 2. This correction was included in the present analysis.

Overall, the predictions of the TCA submodel of the updated TCE PBPK model appear consistent with these data on the toxicokinetics of TCA after drinking water exposure in male rats and male mice. In female mice, the reported concentrations tends to be at the low end of or lower than those predicted by the PBPK model. Importantly, the data used for calibrating the mouse PBPK model parameters were predominantly in males, with only Fisher et al. (1991) and Fisher and Allen (1993) reporting TCA plasma levels in female mice after TCE exposure. In addition, median PBPK model predictions at higher doses (>300 mg/kg-day), even in males, tended to be higher than the concentrations reported. While TCA kinetics after TCE exposure includes predicted internal production at these higher levels, previously published data on TCA kinetics alone only included doses up to 100 mg/kg, and only in males. Therefore, these results suggest that the median predictions of the TCA submodel of the updated TCE PBPK model are somewhat less accurate for female mice and for higher doses of TCA (>300 mg/kg-day) in mice, though the 95% CIs still cover the majority of the reported data. Finally, the ratio of blood to liver concentrations of ~1.4 reported in the mouse experiments in Mahle et al. (1999) were significantly different from the ratios of ~2.3 reported by Green (2003b), a difference for which there is no clear explanation given the similar experimental designs and common use the $B6C3F_1$ mouse strain. Because median PBPK model predictions for the blood to liver concentration ratio for these studies are ~1.3, they are more consistent with the Mahle et al. (1999) data than with the Green (2003b) data.

A.6.3.2. Summary of Results From Chiu of Bayesian Updating of Evans et al. (2009) and Chiu et al. (2009) Model Using TCA Drinking Water Data

Sweeney et al. (2009) also suggested that the available data, in conjunction with deterministic modeling using the TCA portion of the Hack et al. (2006) TCE PBPK model, supported a hypothesis that the bioavailability of TCA in drinking water in mice is substantially <100%. Classically, oral bioavailability is assessed by comparing blood concentration profiles from oral and i.v. dosing experiments, because blood concentration data from oral dosing alone cannot distinguish fractional uptake from metabolism. Schultz et al. (1999) made this comparison in rats at a single dose of 82 mg/kg, and reported an empirical bioavailability of 116%, consistent with complete absorption. A priori, there would not seem to be a strong reason to suspect that oral absorption in mice would be significantly different from that in rats. As discussed above in the evaluation of Hack et al. (2006) model, available data strongly support clearance of TCA in addition to urinary excretion, based on the finding of <100% recovery in urine after i.v. dosing. In addition, as the current TCE PBPK model assumes 100% absorption for orally-administered TCA, and the PBPK model predictions are consistent with these data, it is likely that the limited bioavailability determined by Sweeney et al. (2009) was confounded by this additional clearance pathway unaccounted for by Hack et al. (2006). Therefore, Chiu

conducted a Bayesian reanalysis of the TCE mouse PBPK model, the results of which are summarized here.

In brief, the TCA submodel from Evans et al. (2009) and Chiu et al. (2009) is augmented by the addition of a fractional absorption parameter for drinking water exposures and parameters reestimated by adding the newly available TCA drinking water kinetic studies in mice. Being nocturnal animals, rodents do not have a steady pattern of drinking water consumption throughout the day. It has been suggested that a 90/10%-split between dark-cycle (night time)/light-cycle (day time) drinking water consumption is a reasonable approximation (Yuan, 1995), and that pattern is assumed here. Most analyses assume something similar (e.g., Sweeney et al., 2009, assumed 100% consumption during the dark cycle).

However, TCA kinetics from drinking water exposures also depends on the relationship between the times of the light/dark cycle and the times of specimen collection (i.e., at what time during the cycle did exposure begin [when is "t = 0"])? These data are not specified in any of the available technical reports cited by Sweeney et al. (2009). Therefore, in the present analysis, three different assumptions that represent a range of possibilities were made, and the results of each were carried through the analysis. These patterns are shown in Figure A-42 and designated low-12/high-12 (LH), low-6/high-12/low-6 (LHL), and high-12/low-12 (HL). In the first, it is assumed that the start of exposure coincided exactly with the start of the light cycle; in the second, it is assumed that the start of exposure was exactly in the middle of the light cycle; and in the last case, it is assumed that the start of exposure was exactly at the end of the light cycle. A priori, one of the first two patterns (LH and LHL) would appear to be most likely, but the last pattern (HL) was included for completeness. Sweeney et al. (2009) assumed drinking water intake was most similar to the LH pattern.

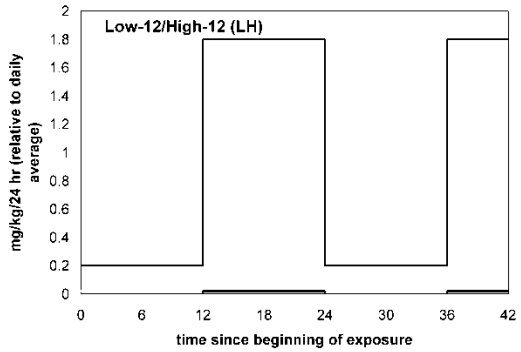

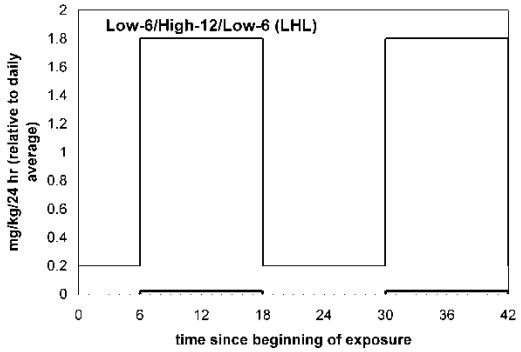

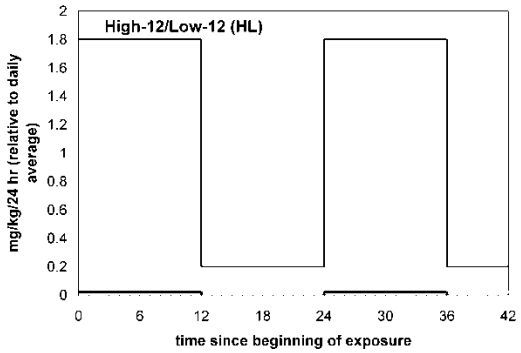

The upper left panel (LH) assumes that t = 0 is at the beginning of the "light" part of the "light/dark" cycle (light is dashed grey line at the bottom, dark is thick black line at the bottom). The upper right panel (LHL) assumes that t = 0 is in the middle of the "light" part of the cycle. The lower left panel (HL) assumes that t = 0 is at the end of the "light" part of the cycle.

Figure A-42. Assumed drinking water patterns as a function of time since beginning of exposure.

As was done by Evans et al. (2009) and Chiu et al. (2009), the PBPK parameter estimation is performed in a hierarchical Bayesian population statistical framework, with calculations performed using MCMC, using posteriors from the earlier analysis as priors for the reanalysis. A total of six different model runs were made using the "harmonized" PBPK model, as shown in Table A-18, using different assumptions for fractional absorption and for drinking water intake patterns. Comparisons between different modeling assumptions (i.e., fixing or estimating fractional absorption; assumed drinking water patterns) were made using the deviance information criterion (DIC) (Spiegelhalter et al., 2002). The DIC is a Bayesian analogue to the AIC and is used in a similar manner, with smaller values indicating better model fits. As with the AIC, "small" differences in DIC (e.g., <5, as suggested by the WinBUGS "DIC page" [http://www.mrc-bsu.cam.ac.uk/bugs/winbugs/dicpage.shtml]) are not likely to be important, but much lower values suggest substantially better fitting models. Results of these comparison are also shown in Table A-18. Adding the fractional absorption parameter decreases the DIC by about 100 units, which strongly supports inclusion of the parameter. In addition, in both cases of fixed and fitted fractional absorption, the lowest DIC was for the LHL drinking water intake pattern, with the second lowest DIC for the LH pattern, with a difference of 33 units in DIC. Given that these model runs are highly favored relative to the others, the rest of this summary reports the results for the "LHL.fitted" run (see Chiu, 2011, for additional details).

Table A-18. Summary characteristics of model runs

Run designation	Drinking water pattern	Fractional absorption		Convergence	DIC
		Fixed	Fitted		
LH.fixed	Low-12/high-12	√		$R \leq 1.04$	895
LHL.fixed	Low-6/high-12/low-6	√		$R \leq 1.09$	877
HL.fixed	High-12/low-12	√		$R \leq 1.05$	897
LH.fitted	Low-12/high-12		√	$R \leq 1.05$	764
LHL.fitted	Low-6/high-12/low-6		√	$R \leq 1.11$	731
HL.fitted	High-12/low-12		√	$R \leq 1.12$	781

Posterior model fits for the LHL.fitted runs are shown in Figures A-43 and A-44, using a representative sample from the converged MCMC chain. A dose-dependent fractional absorption can account for the less-than-proportional increase in TCA blood concentrations between the middle and high dose groups observed in Mahle et al. (1999) (see Figure A-43) and among all of the dose groups observed in Green (2003a, 2003b) (see Figure A-44).

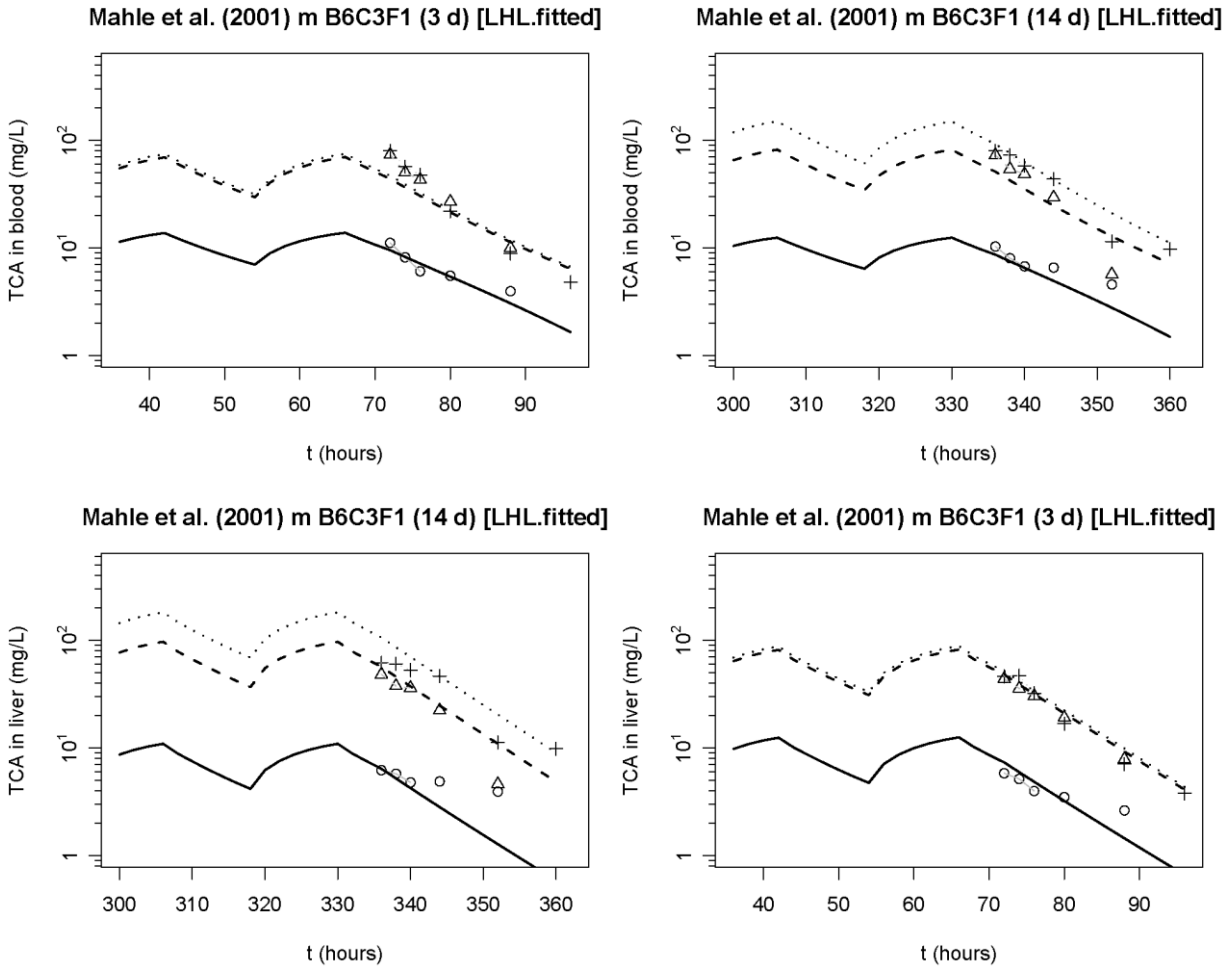

Three- and 14-day exposures to 0.08 (data: open circles, predictions: solid line), 0.8 (data: open triangle, predictions: dashed line), and 2 g/L TCA in drinking water (data: crosses, predictions: dotted line). Predictions use a representative parameter sample from the converged MCMC chain for the LHL drinking water intake pattern.

Figure A-43. PBPK model predictions for TCA in blood and liver of male B6C3F$_1$ mice from Mahle et al. (1999).

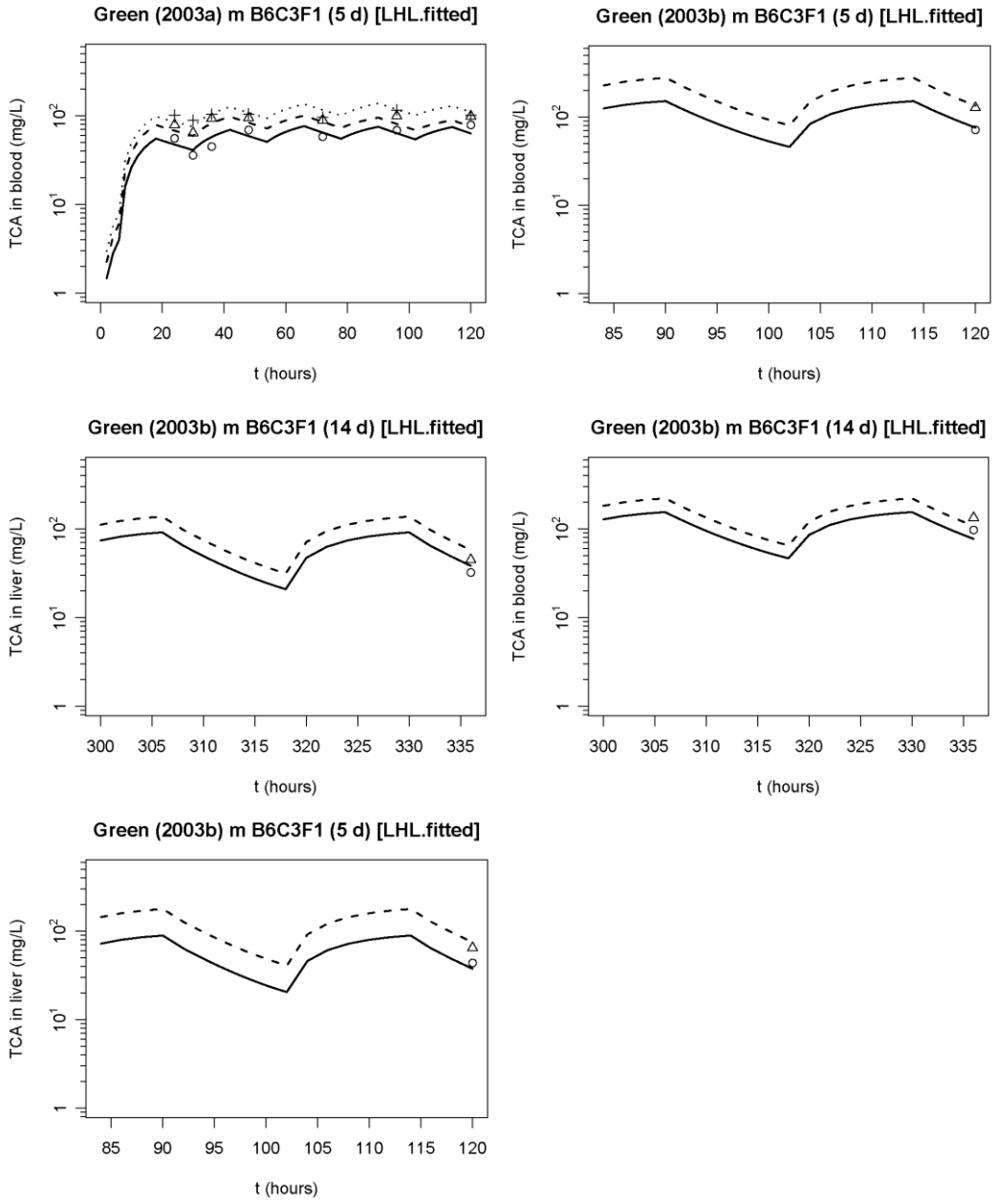

Green (2003a): 5-day drinking water exposures to 0.5 (data: open circle; predictions: solid line), 1 (data: open triangle; predictions: dashed line), and 2.5 g/L TCA (data: crosses; predictions: dotted lines). Green (2003b): 5- and 14-day drinking water exposures to 1 (data: open circle; predictions: solid line) and 2.5 g/L TCA (data: open triangle; predictions: dashed line). Predictions use a representative parameter sample from the converged MCMC chain for the LHL drinking water intake pattern.

Figure A-44. PBPK model predictions for TCA in blood and liver of male B6C3F$_1$ mice from Green (2003a, 2003b).

As was done by Sweeney et al. (2009), fractional absorption is separately estimated for each drinking water dose group, and the results are fit to a parametric model, shown in Figure A-45. Several features of the data and analysis are worth noting. First, there is a general trend for decrease in fractional absorption with increasing concentration, evident even within studies. Second, there appears to be substantial interstudy and intrastudy variability in the apparent fractional absorption. This is particularly evident across strains in Green (2003b)—the PPARα-null and 129/sv mice appear to have substantially higher fractional absorption than the $B6C3F_1$ mice, even though in all strains, there appeared to be a decreasing trend with increasing TCA concentration. Third, the fractional absorption estimates increase as the "start of exposure" is assumed to be later and later in the "light" cycle. Fourth, the estimated fractional absorption at low concentrations is fairly high, at >80%. Finally, the estimates for fractional absorption from the current analysis are 3–4 times greater than those reported by Sweeney et al. (2009). Because hepatic clearance was not included in the previous Hack et al. (2006) version of the TCE model used by Sweeney et al. (2009), and this could partially explain why they found a very low fractional absorption to be necessary to provide a fit to the observed data from drinking water exposures.

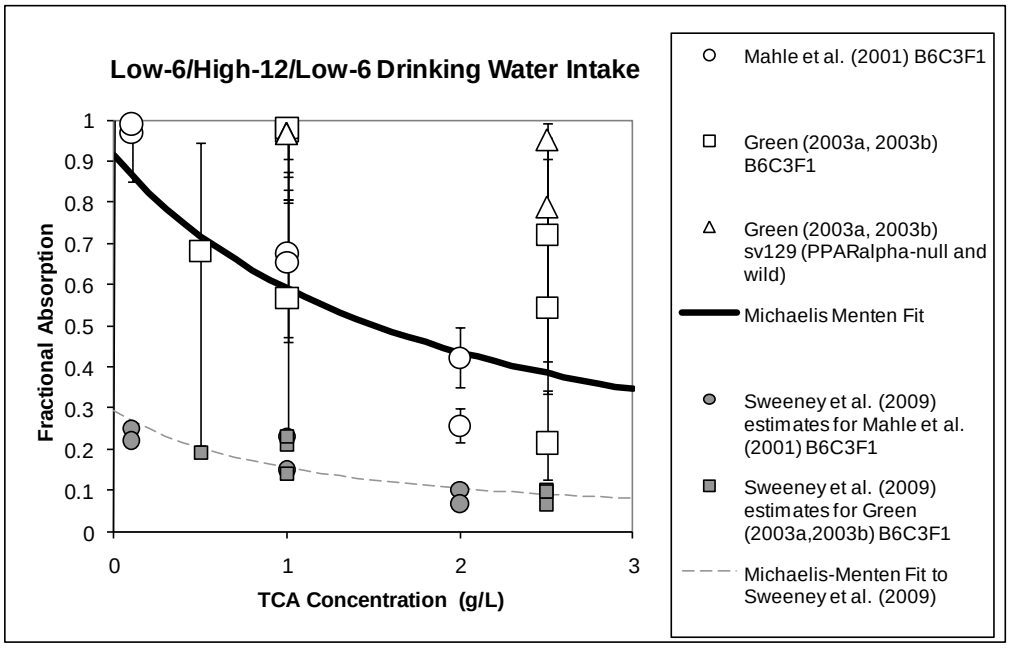

Fits are to a Michaelis-Menten function for "effective" concentration $C_{eff} = C_{max} \times C/(C_{½} + C)$, so that the fractional absorption $Fabs = C_{eff}/C = C_{max}/(C_{½} + C)$. Sweeney et al. (2009) estimates of Fabs, along with a Michaelis-Menten fit, are included for comparison. The ratio $C_{max}/C_{½}$ gives the fractional uptake at low concentrations.

Figure A-45. Distribution of fractional absorption fit to each TCA drinking water kinetic study group in mice, using LHL drinking water intake patterns.

In sum, comparing model results with complete- and less-than-complete-fractional absorption, it is evident (e.g., through the much lower DIC) that including a concentration-dependent fractional absorption substantially improves model fits. Thus, these data are consistent with reduced bioavailability from drinking water, particularly at higher TCA drinking water concentrations. However, the estimates of fractional absorption are three- to fourfold higher than those estimated by Sweeney et al. (2009). In addition, there appeared to be substantial inter- and intrastudy variability, with the fractional absorption for some mouse strains estimated to be nearly complete even at the higher TCA drinking water concentrations. Thus, on the whole, adding a fractional absorption parameter substantially improves the PBPK model predictions, though the degree of absorption is greater than that reported by Sweeney et al. (2009) and appears to be variable between studies and mouse strains. Data are lacking as to a mechanistic basis for reduced absorption of TCA at higher doses. Biliary excretion is a possibility, though data from rats suggest that the degree of biliary excretion of TCA is rather modest (Stenner et al., 1997). It is also possible that the nonlinearity in TCA kinetics reflects a difference in clearance processes, such as saturation of renal reabsorption, which would lead to increased urinary clearance and reduced internal dose. This could be tested experimentally by simultaneously measuring blood and urinary kinetics of TCA at different doses. However, this would not explain differences between drinking water and gavage dosing.

The degree of interexperimental variability raises the question of whether the apparent fractional absorption may be due, in part, to experimental factors, such as analytical errors due to incomplete/inadequate procedures to prevent TCA degradation or experimental losses in estimating drinking water consumption rates. With respect to TCA degradation, Mahle et al. (1999) appeared to be specifically aware of the issue and froze biological samples prior to analysis in order to address it. However, lacking any external validation, the extent to which this was completely successful is unclear. On the other hand, Green (2003a, 2003b) did not appear to have any particular procedure designed to address TCA degradation. Thus, the extent and impact of TCA degradation is not clear, though it may be a plausible explanation for the degree of variability observed across data sets. With respect to drinking water consumption, experimental variance is notable with respect to reported drinking water consumption rates, with Green (2003a) > Green (2003b) > Mahle et al. (1999) > other TCA drinking water studies. One may hypothesize that the *actual* drinking water consumption rates are roughly equal, with differences in *reported* values reflecting experimental losses. However, in this case, reported drinking water consumption would inversely correlate with fractional absorption, and no such correlation is evident. In addition, this does not explain the consistent dose-related trends within a study or data set, even if the slope of the trend varies between experiments.

Overall, then, it may be more accurate to characterize the fractional absorption as an empirical parameter reflecting unaccounted-for biological processes as well as experimental variation.

A.7. UPDATED PBPK MODEL CODE

The following pages contain the updated PBPK model code for the MCSim software (version 5.0.0). Additional details on baseline parameter derivations are included as inline documentation. Example simulation files containing prior distributions and experimental calibration data are available electronically:

- Mouse ("Supplementary data for TCE assessment: Mouse population example," 2011)
- Rat ("Supplementary data for TCE assessment: Rat population example," 2011)
- Human ("Supplementary data for TCE assessment: Human population example," 2011)

```
# TCE.risk.1.2.3.3.pop.model -- Updated TCE Risk Assessment Model
#
#### HISTORY OF HACK ET AL. (2006) MODEL
# Model code to correspond to the block diagram version of the model
# Edited by Deborah Keys to incorporate Lapare et al. 1995 data
# Last edited: August 6, 2004
# Translated into MCSim from acslXtreme CSL file by Eric Hack, started 31Aug2004
# Removed nonessential differential equations (i.e., AUCCBld) for MCMC runs.
# Changed QRap and QSlw calculations and added QTot to scale fractional flows
# back to 1 after sampling.
# Finished translating and verifying results on 15Sep2004.
# Changed QSlw calculation and removed QTot 21Sep2004.
# Removed diffusion-limited fat uptake 24Sep2004.
#### HISTORY OF U.S. EPA (2009) MODEL (CHIU ET AL., 2009)
# Extensively revised by U.S. EPA June 2007-June 2008
#         - Fixed hepatic plasma flow for TCA-submodel to include
#           portal vein (i.e., QGutLivPlas -- originally was just
#           QLivPlas, which was only hepatic artery).
#         - Clearer coding and in-line documentation
#         - Single model for 3 species
#         - Revised physiological parameters, with discussion of
#                 uncertainty and variability,
#         - In vitro data used for default metabolism parameters,
#                 with discussion of uncertainty and variability
#         - added TCE blood compartment
#         - added TCE kidney compartment, with GSH metabolism
#         - added DCVG compartment
#         - added additional outputs available from in vivo data
#         - removed DCA compartment
#         - added IA and PV dosing (for rats)
#         - Version 1.1 -- fixed urinary parameter scaling
#                         -- fixed VBod in kUrnTCOG (should be VBodTCOH)
#         - Version 1.1.1 -- changed some truncation limits (in commments only)
#         - Version 1.2 --
#                 -- removed TB compartment as currently coded
#                 -- added respiratory oxidative metabolism:
#                         3 states: AInhResp, AResp, AExhResp
#                 -- removed clearance from respiratory metabolism
#         - Version 1.2.1 -- changed oral dosing to be similar to IV
#         - Version 1.2.2 -- fixed default lung metabolism (additional
#                         scaling by lung/liver weight ratio)
#         - Version 1.2.3 -- fixed FracKidDCVC scaling
#         - Version 1.2.3.1 -- added output CDCVG_ND (no new dynamics)
#                 for non-detects of DCVG in blood
#         - Version 1.2.3.2 -- Exact version of non-detects likelihood
#         - Version 1.2.3.3 -- Error variances changed to "Ve_xxx"
#         NOTE -- lines with comment "(vrisk)" are used only for
#                 calculating dose metrics, and are commented out
#                 when doing MCMC runs.
#*****************************************************************************
#***                  State Variable Specifications                        ***
#*****************************************************************************

States = {
##-- TCE uptake
          AStom,              # Amount of TCE in stomach
          ADuod,              # oral gavage absorption -- mice and rats only
          AExc,               #(vrisk) excreted in feces from gavage (currently 0)
          AO,                 #(vrisk) total absorbed
          InhDose,  # Amount inhaled
##-- TCE in the body
          ARap,               # Amount in rapidly perfused tissues
          ASlw,               # Amount in slowly perfused tissues
          AFat,               # Amount in fat
          AGut,               # Amount in gut
          ALiv,               # Amount in liver
          AKid,               # Amount in Kidney -- previously in Rap tissue
          ABld,               # Amount in Blood -- previously in Rap tissue
          AInhResp, # Amount in respiratory lumen during inhalation
          AResp,              # Amount in respiratory tissue
          AExhResp, # Amount in respiratory lumen during exhalation
##-- TCA in the body
          AOTCA,              #(vrisk)
          AStomTCA, # Amount of TCA in stomach
          APlasTCA, # Amount of TCA in plasma #comment out for
          ABodTCA,  # Amount of TCA in lumped body compartment
          ALivTCA,  # Amount of TCA in liver
##-- TCA metabolized
          AUrnTCA,  # Cumulative Amount of TCA excreted in urine
          AUrnTCA_sat,        # Amount of TCA excreted that during times that had
                              # saturated measurements (for lower bounds)
          AUrnTCA_collect,# Cumulative Amount of TCA excreted in urine during
                              # collection times (for intermittent collection)
##-- TCOH in body
          AOTCOH,             #(vrisk)
          AStomTCOH,          # Amount of TCOH in stomach
          ABodTCOH,           # Amount of TCOH in lumped body compartment
          ALivTCOH,           # Amount of TCOH in liver
##-- TCOG in body
          ABodTCOG,           # Amount of TCOG in lumped body compartment
          ALivTCOG,           # Amount of TCOG in liver
          ABileTCOG,          # Amount of TCOG in bile (incl. gut)
          ARecircTCOG,        #(vrisk)
##-- TCOG excreted
          AUrnTCOG, # Amount of TCOG excreted in urine
          AUrnTCOG_sat,       # Amount of TCOG excreted that during times that had
                              # saturated measurements (for lower bounds)
          AUrnTCOG_collect,# Cumulative Amount of TCA excreted in urine during
                              # collection times (for intermittent collection)
##-- DCVG in body
          ADCVGIn,  #(vrisk)
          ADCVGmol, # Amount of DCVG in body in mmoles
          AMetDCVG, #(vrisk)
##-- DCVC in body
          ADCVCIn,  #(vrisk)
        ADCVC,                # Amount of DCVC in body
          ABioactDCVC,        #(vrisk)
##-- NAcDCVC excreted
          AUrnNDCVC,          # Amount of NAcDCVC excreted
##-- Other states for TCE
          ACh,                # Amount in closed chamber -- mice and rats only
          AExh,               # Amount exhaled
          AExhExp,  # Amount exhaled during expos  [to calc. retention]
##-- Metabolism
```

```
          AMetLiv1, #(vrisk) Amount metabolized by P450 in liver
          AMetLiv2, #(vrisk) Amount metabolized by GSH conjugation in liver
          AMetLng,  #(vrisk) Amount metabolized in the lung
          AMetKid,  #(vrisk)
          AMetTCOHTCA,        #(vrisk) Amount of TCOH metabolized to TCA
          AMetTCOHGluc,       #(vrisk) Amount of TCOH glucuronidated
          AMetTCOHOther,      #(vrisk)
          AMetTCA,  #(vrisk) Amount of TCA metabolized
##-- Other Dose metrics
          AUCCBld,  #(vrisk)
          AUCCLiv,  #(vrisk)
          AUCCKid,  #(vrisk)
          AUCCRap,  #(vrisk)
          AUCCTCOH, #(vrisk)
          AUCCBodTCOH,        #(vrisk)
          AUCTotCTCOH,        #(vrisk)
          AUCPlasTCAFree,     #(vrisk)
          AUCPlasTCA,         #(vrisk)
          AUCLivTCA,          #(vrisk)
          AUCCDCVG  #(vrisk)
};

#*****************************************************************************
#***                  Input Variable Specifications                        ***
#*****************************************************************************

Inputs = {
##-- TCE dosing
          Conc,               # Inhalation exposure conc. (ppm)
          IVDose,             # IV dose (mg/kg)
          PDose,              # Oral gavage dose (mg/kg)
          Drink,              # Drinking water dose (mg/kg-day)
          IADose,                       # Inter-arterial
          PVDose,                       # Portal Vein
##-- TCA dosing
          IVDoseTCA,          # IV dose (mg/kg) of TCA
          PODoseTCA,          # Oral dose (mg/kg) of TCA
##-- TCOH dosing
          IVDoseTCOH,         # IV dose (mg/kg) of TCOH
          PODoseTCOH,         # Oral dose (mg/kg) of TCOH
##-- Potentially time-varying parameters
          QPmeas,             # Measured value of Alveolar ventilation QP
          TCAUrnSat,          # Flag for saturated TCA urine
          TCOGUrnSat,         # Flag for saturated TCOG urine
          UrnMissing          # Flag for missing urine collection times
};

#*****************************************************************************
#***                  Output Variable Specifications                       ***
#*****************************************************************************
Outputs = {
#*****************************************************************************
#*** Outputs for mass balance check
MassBalTCE,
TotDose,
TotTissue,
MassBalTCOH,
TotTCOHIn,
TotTCOHDose,
TotTissueTCOH,
TotMetabTCOH,
MassBalTCA,
TotTCAIn,
TotTissueTCA,
MassBalTCOG,
TotTCOGIn,
TotTissueTCOG,
MassBalDCVG,
MassBalDCVC,
AUrnNDCVCequiv,

#*****************************************************************************
#*** Outputs that are potential dose metrics
          TotMetab, #(vrisk) Total metabolism
          TotMetabBW34, #(vrisk) Total metabolism/BW^3/4
          ATotMetLiv, #(vrisk) Total metabolism in liver
          AMetLiv1Liv, #(vrisk) Total oxidation in liver/liver volume
          AMetLivOther, #(vrisk) Total "other" oxidation in liver
          AMetLivOtherLiv, #(vrisk) Total "other" oxidation in liver/liver vol
          AMetLngResp, #(vrisk) oxiation in lung/respiratory tissue volume
          AMetGSH, #(vrisk) total GSH conjugation
          AMetGSHBW34, #(vrisk) total GSH conjugation/BW^3/4
          ABioactDCVCKid,     #(vrisk) Amount of DCVC bioactivated/kidney volume
# NEW
          TotDoseBW34, #(vrisk) mg intake / BW^3/4
          AMetLiv1BW34, #(vrisk) mg hepatic oxidative metabolism / BW^3/4
          TotOxMetabBW34, #(vrisk) mg oxidative metabolism / BW^3/4
          TotTCAInBW, #(vrisk) TCA production / BW
          AMetLngBW34, #(vrisk) oxiation in lung/BW^3/4
          ABioactDCVCBW34, #(vrisk) Amount of DCVC bioactivated/BW^3/4
          AMetLivOtherBW34, #(vrisk) Total "other" oxidation in liver/BW^3/4
#*****************************************************************************
#*** Outputs for comparison to in vivo data
# TCE
RetDose,  # human - = (InhDose - AExhExp)
CAlv,     # needed for CAlvPPM
CAlvPPM,  # human
CInhPPM,  # mouse, rat
CInh,     # needed for CMixExh
CMixExh,  # rat - Mixed exhaled breath (mg/l)
CArt,     # rat, human - Arterial blood concentration
CVen,     # mouse, rat, human
CBldMix,  # rat - Concentration in mixed arterial+venous blood
                    # (used for cardiac puncture)
CFat,     # mouse, rat - Concentration in fat
CGut,     # rat
CRap,     # needed for unlumped tissues
CSlw,     # needed for unlumped tissues
CHrt,     # rat - Concentration in heart tissue [use CRap]
CKid,     # mouse, rat -  Concentration in kidney
CLiv,     # mouse, rat - Concentration in liver
CLung,    # mouse, rat - Concentration in lung [use CRap]
CMus,     # rat - Concentration in muscle [use CSlw]
CSpl,     # rat - Concentration in spleen [use CRap]
```

```
CBrn,     # rat - Concentration in brain [use CRap]
zAExh,    # mouse
zAExhpost,          # rat - Amount exhaled post-exposure (mg)

# TCOH
CTCOH,    # mouse, rat, human - TCOH concentration in blood
CKidTCOH, # mouse - TCOH concentration in kidney
CLivTCOH, # mouse - TCOH concentration in liver
CLungTCOH,          # mouse - TCOH concentration in lung

# TCA
CPlasTCA, # mouse, rat, human - TCA concentration in plasma
CBldTCA,  # mouse, rat, human - TCA concentration in blood
CBodTCA,  # needed for CKidTCA and CLungTCA
CKidTCA,  # mouse - TCA concentration in kidney
CLivTCA,  # mouse, rat - TCA concentration in liver
CLungTCA, # mouse - TCA concentration in lung
zAUrnTCA, # mouse, rat, human - Cumulative Urinary TCA
zAUrnTCA_collect,   # human - TCA measurements for intermittent collection
zAUrnTCA_sat,       # human - Saturated TCA measurements

# TCOG
zABileTCOG,         # rat - Amount of TCOG in bile (mg)
CTCOG,    # needed for CTCOGTCOH
CTCOGTCOH,          # mouse - TCOG concentration in blood (in TCOH-equiv)
CKidTCOGTCOH,       # mouse - TCOG concentration in kidney (in TCOH-equiv)
CLivTCOGTCOH,       # mouse - TCOG concentration in liver (in TCOH-equiv)
CLungTCOGTCOH,      # mouse - TCOG concentration in lung (in TCOH-equiv)
AUrnTCOGTCOH,       # mouse, rat, human - Cumulative Urinary TCOG (in TCOH-equiv)
AUrnTCOGTCOH_collect,         # human - TCOG (in TCOH-equiv) measurements for
                              # intermittent collection
AUrnTCOGTCOH_sat,   # human - Saturated TCOG (in TCOH-equiv) measurements

# Other
CDCVGmol,           # concentration of DCVG (mmol/l)
CDCVGmol0,          # Dummy variable without likelihood (for plotting)#(v1.2.3.1)
CDCVG_ND, # Non-detect of DCVG (<0.05 pmol/ml= 5e-5 mmol/l )#(v1.2.3.1)
                    # Output -ln(likelihood)#(v1.2.3.1)
zAUrnNDCVC,         # rat, human - Cumulative urinary NAcDCVC
AUrnTCTotMole,      # rat, human - Cumulative urinary TCOH+TCA in mmoles
TotCTCOH, # mouse, human - TCOH+TCOG Concentration (in TCOH-equiv)
TotCTCOHcomp,       # ONLY FOR COMPARISON WITH HACK
ATCOG,              # ONLY FOR COMPARISON WITH HACK
QPsamp,   # human - sampled value of alveolar ventilation rate

## PARAMETERS #(vrisk)

  QCnow, # (vrisk) #Cardiac output (L/hr)
  QP, # (vrisk) #Alveolar ventilation (L/hr)
  QFatCtmp, # (vrisk) #Scaled fat blood flow
  QGutCtmp, # (vrisk) #Scaled gut blood flow
  QLivCtmp, # (vrisk) #Scaled liver blood flow
  QSlwCtmp, # (vrisk) #Scaled slowly perfused blood flow
  QRapCtmp, # (vrisk) #Scaled rapidly perfused blood flow
  QKidCtmp, # (vrisk) #Scaled kidney blood flow
  DResp, # (vrisk) #Respiratory lumen:tissue diffusive clearance rate
  VFatCtmp, # (vrisk) #Fat fractional compartment volume
  VGutCtmp, # (vrisk) #Gut fractional compartment volume
  VLivCtmp, # (vrisk) #Liver fractional compartment volume
  VRapCtmp, # (vrisk) #Rapidly perfused fractional compartment volume
  VRespLumCtmp, # (vrisk) # Fractional volume of respiratory lumen
  VRespEffCtmp, # (vrisk) #Effective fractional volume of respiratory tissue
  VKidCtmp, # (vrisk) #Kidney fractional compartment volume
  VBldCtmp, # (vrisk) #Blood fractional compartment volume
  VSlwCtmp, # (vrisk) #Slowly perfused fractional compartment volume
  VPlasCtmp, # (vrisk) #Plasma fractional compartment volume
  VBodCtmp, # (vrisk) #TCA Body fractional compartment volume [not incl.
blood+liver]
  VBodTCOHCtmp, # (vrisk) #TCOH/G Body fractional compartment volume [not incl.
liver]
  PB, # (vrisk) #TCE Blood/air partition coefficient
  PFat, # (vrisk) #TCE Fat/Blood partition coefficient
  PGut, # (vrisk) #TCE Gut/Blood partition coefficient
  PLiv, # (vrisk) #TCE Liver/Blood partition coefficient
  PRap, # (vrisk) #TCE Rapidly perfused/Blood partition coefficient
  PResp, # (vrisk) #TCE Respiratory tissue:air partition coefficient
  PKid, # (vrisk) #TCE Kidney/Blood partition coefficient
  PSlw, # (vrisk) #TCE Slowly perfused/Blood partition coefficient
  TCAPlas, # (vrisk) #TCA blood/plasma concentration ratio
  PBodTCA, # (vrisk) #Free TCA Body/blood plasma partition coefficient
  PLivTCA, # (vrisk) #Free TCA Liver/blood plasma partition coefficient
  kDissoc, # (vrisk) #Protein/TCA dissociation constant (umole/L)
  BMax, # (vrisk) #Maximum binding concentration (umole/L)
  PBodTCOH, # (vrisk) #TCOH body/blood partition coefficient
  PLivTCOH, # (vrisk) #TCOH liver/body partition coefficient
  PBodTCOG, # (vrisk) #TCOG body/blood partition coefficient
  PLivTCOG, # (vrisk) #TCOG liver/body partition coefficient
  VDCVG, # (vrisk) #DCVG effective volume of distribution
  kAS, # (vrisk) #TCE Stomach absorption coefficient (/hr)
  kTSD, # (vrisk) #TCE Stomach-duodenum transfer coefficient (/hr)
  kAD, # (vrisk) #TCE Duodenum absorption coefficient (/hr)
  kTD, # (vrisk) #TCE Duodenum-feces transfer coefficient (/hr)
  kASTCA, # (vrisk) #TCA Stomach absorption coefficient (/hr)
  kASTCOH, # (vrisk) #TCOH Stomach absorption coefficient (/hr)
  VMAX, # (vrisk) #VMAX for hepatic TCE oxidation (mg/hr)
  KM, # (vrisk) #KM for hepatic TCE oxidation (mg/L)
  FracOther, # (vrisk) #Fraction of hepatic TCE oxidation not to TCA+TCOH
  FracTCA, # (vrisk) #Fraction of hepatic TCE oxidation to TCA
  VMAXDCVG, # (vrisk) #VMAX for hepatic TCE GSH conjugation (mg/hr)
  KMDCVG, # (vrisk) #KM for hepatic TCE GSH conjugation (mg/L)
  VMAXKidDCVG, # (vrisk) #VMAX for renal TCE GSH conjugation (mg/hr)
  KMKidDCVG, # (vrisk) #KM for renal TCE GSH conjugation (mg/L)
  FracKidDCVC, # (vrisk) #Fraction of renal TCE GSH conj. "directly" to DCVC
               # (vrisk) #(i.e., via first pass)
  VMAXClara, # (vrisk) #VMAX for Tracheo-bronchial TCE oxidation (mg/hr)
  KMClara, # (vrisk) #KM for Tracheo-bronchial TCE oxidation (mg/L)
  FracLungSys, # (vrisk) #Fraction of respiratory metabolism to systemic circ.
  VMAXTCOH, # (vrisk) #VMAX for hepatic TCOH->TCA (mg/hr)
  KMTCOH, # (vrisk) #KM for hepatic TCOH->TCA (mg/L)
  VMAXGluc, # (vrisk) #VMAX for hepatic TCOH->TCOG (mg/hr)
  KMGluc, # (vrisk) #KM for hepatic TCOH->TCOG (mg/L)
  kMetTCOH, # (vrisk) #Rate constant for hepatic TCOH->other (/hr)
  kUrnTCA, # (vrisk) #Rate constant for TCA plasma->urine (/hr)
  kMetTCA, # (vrisk) #Rate constant for hepatic TCA->other (/hr)
```

```
  kBile, # (vrisk) #Rate constant for TCOG liver->bile (/hr)
  kEHR, # (vrisk) #Lumped rate constant for TCOG bile->TCOH liver (/hr)
  kUrnTCOG, # (vrisk) #Rate constant for TCOG->urine (/hr)
  kDCVG, # (vrisk) #Rate constant for hepatic DCVG->DCVC (/hr)
  kNAT, # (vrisk) #Lumped rate constant for DCVC->Urinary NAcDCVC (/hr)
  kKidBioact, # (vrisk) #Rate constant for DCVC bioactivation (/hr)

## Misc
  RUrnTCA, #(vrisk)
  RUrnTCOGTCOH, #(vrisk)
  RUrnNDCVC, #(vrisk)
  RAO,
  CVenMole,
  CPlasTCAMole,
  CPlasTCAFreeMole
};

#*****************************************************************************
#***                  Global Constants                                     ***
#*****************************************************************************

# Molecular Weights
        MWTCE = 131.39;        # TCE
        MWDCA = 129.0;         # DCA
       MWDCVC = 216.1;         # DCVC
        MWTCA = 163.5;         # TCA
      MWChlor = 147.5;         # Chloral
       MWTCOH = 149.5;         # TCOH
   MWTCOHGluc = 325.53;        # TCOH-Gluc
     MWNADCVC = 258.8;         # N Acetyl DCVC

# Stoichiometry
 StochChlorTCE = MWChlor / MWTCE;
   StochTCATCE = MWTCA / MWTCE;
  StochTCATCOH = MWTCA / MWTCOH;
  StochTCOHTCE = MWTCOH / MWTCE;
 StochGlucTCOH = MWTCOHGluc / MWTCOH;
 StochTCOHGluc = MWTCOH / MWTCOHGluc;
  StochTCEGluc = MWTCE / MWTCOHGluc;
  StochDCVCTCE = MWDCVC / MWTCE;
       StochN = MWNADCVC / MWDCVC;
   StochDCATCE = MWDCA / MWTCE;

#*****************************************************************************
#***                  Global Model Parameters                              ***
#*****************************************************************************
# These are the actual model parameters used in "dynamics."
# Values that are assigned in the "initialize" section,
# are all set to 1 to avoid confusion.

#*****************************************************************************
# Flows
QC        = 1;      # Cardiac output (L/hr)
QPsamp    = 1;      # Alveolar ventilation (L/hr)
VPR       = 1;      # Alveolar ventilation-perfusion ratio
QFatCtmp  = 1;      # Scaled fat blood flow
QGutCtmp  = 1;      # Scaled gut blood flow
QLivCtmp  = 1;      # Scaled liver blood flow
QSlwCtmp  = 1;      # Scaled slowly perfused blood flow
DResptmp  = 1;      # Respiratory lumen:tissue diffusive clearance rate (L/hr)
[scaled to QP]
QKidCtmp  = 1;      # Scaled kidney blood flow
FracPlas  = 1;      # Fraction of blood that is plasma (1-hematocrit)
#*****************************************************************************
# Volumes
VFat      = 1;      # Fat compartment volume (L)
VGut      = 1;      # Gut compartment volume (L)
VLiv      = 1;      # Liver compartment volume (L)
VRap      = 1;      # Rapidly perfused compartment volume (L)
VRespLum  = 1;      # Volume of respiratory lumen (L air)
VRespEfftmp         = 1;      #(vrisk) volume for respiratory tissue (L)
VRespEff  = 1;      # Effective volume for respiratory tissue (L air) = V(tissue) *
Resp:Air partition coefficient
VKid      = 1;      # Kidney compartment volume (L)
VBld      = 1;      # Blood compartment volume (L)
VSlw      = 1;      # Slowly perfused compartment volume (L)
VPlas     = 1;      # Plasma compartment volume [fraction of blood] (L)
VBod      = 1;      # TCA Body compartment volume [not incl. blood+liver] (L)
VBodTCOH  = 1;      # TCOH/G Body compartment volume [not incl. liver] (L)
#*****************************************************************************
# Distribution/partitioning
PB        = 1;      # TCE Blood/air partition coefficient
PFat      = 1;      # TCE Fat/Blood partition coefficient
PGut      = 1;      # TCE Gut/Blood partition coefficient
PLiv      = 1;      # TCE Liver/Blood partition coefficient
PRap      = 1;      # TCE Rapidly perfused/Blood partition coefficient
PResp     = 1;      # TCE Respiratory tissue:air partition coefficient
PKid      = 1;      # TCE Kidney/Blood partition coefficient
PSlw      = 1;      # TCE Slowly perfused/Blood partition coefficient
TCAPlas   = 1;      # TCA blood/plasma concentration ratio
PBodTCA   = 1;      # Free TCA Body/blood plasma partition coefficient
PLivTCA   = 1;      # Free TCA Liver/blood plasma partition coefficient
kDissoc   = 1;      # Protein/TCA dissociation constant (umole/L)
BMax      = 1;      # Protein concentration (UNITS?)
PBodTCOH  = 1;      # TCOH body/blood partition coefficient
PLivTCOH  = 1;      # TCOH liver/body partition coefficient
PBodTCOG  = 1;      # TCOG body/blood partition coefficient
PLivTCOG  = 1;      # TCOG liver/body partition coefficient
VDCVG     = 1;      # DCVG effective volume of distribution
#*****************************************************************************
# Oral absorption
kTSD      = 1.4;    # TCE Stomach-duodenum transfer coefficient (/hr)
kAS       = 1.4;    # TCE Stomach absorption coefficient (/hr)
kTD       = 0.1;    # TCE Duodenum-feces transfer coefficient (/hr)
kAD       = 0.75;   # TCE Duodenum absorption coefficient (/hr)
kASTCA    = 0.75;   # TCA Stomach absorption coefficient (/hr)
kASTCOH   = 0.75;   # TCOH Stomach absorption coefficient (/hr)
#*****************************************************************************
# TCE Metabolism
VMAX      = 1;      # VMAX for hepatic TCE oxidation (mg/hr)
KM        = 1;      # KM for hepatic TCE oxidation (mg/L)
FracOther = 1;      # Fraction of hepatic TCE oxidation not to TCA+TCOH
FracTCA   = 1;      # Fraction of hepatic TCE oxidation to TCA
VMAXDCVG  = 1;      # VMAX for hepatic TCE GSH conjugation (mg/hr)
```

```
KMDCVG    = 1;      # KM for hepatic TCE GSH conjugation (mg/L)
VMAXKidDCVG         = 1;      # VMAX for renal TCE GSH conjugation (mg/hr)
KMKidDCVG = 1;      # KM for renal TCE GSH conjugation (mg/L)
VMAXClara = 1;      # VMAX for Tracheo-bronchial TCE oxidation (mg/hr)
KMClara   = 1;      # KM for Tracheo-bronchial TCE oxidation (mg/L)
                    # but in units of air concentration
FracLungSys         = 1;      # Fraction of respiratory oxidative metabolism that
enters systemic circulation

#*******************************************************************************
# TCOH metabolism
VMAXTCOH  = 1;      # VMAX for hepatic TCOH->TCA (mg/hr)
KMTCOH    = 1;      # KM for hepatic TCOH->TCA (mg/L)
VMAXGluc  = 1;      # VMAX for hepatic TCOH->TCOG (mg/hr)
KMGluc    = 1;      # KM for hepatic TCOH->TCOG (mg/L)
kMetTCOH  = 1;      # Rate constant for hepatic TCOH->other (/hr)
#*******************************************************************************
# TCA metabolism/clearance
kUrnTCA   = 1;      # Rate constant for TCA plasma->urine (/hr)
kMetTCA   = 1;      # Rate constant for hepatic TCA->other (/hr)
#*******************************************************************************
# TCOG metabolism/clearance
kBile     = 1;      # Rate constant for TCOG liver->bile (/hr)
kEHR      = 1;      # Lumped rate constant for TCOG bile->TCOH liver (/hr)
kUrnTCOG  = 1;      # Rate constant for TCOG->urine (/hr)
#*******************************************************************************
# DCVG metabolism
kDCVG     = 1;      # Rate constant for hepatic DCVG->DCVC (/hr)
FracKidDCVC         = 1;      # Fraction of renal TCE GSH conj. "directly" to DCVC
(i.e., via first pass)
#*******************************************************************************
# DCVC metabolism/clearance
kNAT      = 1;      # Lumped rate constant for DCVC->Urinary NAcDCVC (/hr)
kKidBioact          = 1;      # Rate constant for DCVC bioactivation (/hr)
#*******************************************************************************
# Closed chamber and other exposure parameters
Rodents   = 1;      # Number of rodents in closed chamber data
VCh       = 1;      # Chamber volume for closed chamber data
kLoss     = 1;      # Rate constant for closed chamber air loss
CC        = 0.0;    # Initial chamber concentration (ppm)
TChng     = 0.003;  # IV infusion duration (hour)
#*******************************************************************************
## Flag for species, sex -- these are global parameters
BW        = 0.0;  # Species-specific defaults during initialization
BW75      = 0.0;    #(vrisk) Variable for BW^3/4
Male      = 1.0;    # 1 = male, 0 = female
Species   = 1.0;    # 1 = human, 2 = rat, 3 = mouse

#*******************************************************************************
#***                  Potentially measured covariates (constants)           ***
#*******************************************************************************
BWmeas    = 0.0;    # Body weight
VFatCmeas = 0.0; # Fractional volume fat
PBmeas    = 0.0;    # Measured blood-air partition coefficient
Hematocritmeas = 0.0; # Measured hematocrit -- used for FracPlas = 1 - HCt
CDCVGmolLD = 5e-5; # Detection limit of CDCVGmol#(v1.2.3.1)
```

```
#*******************************************************************************
#***                  Global Sampling Parameters                             ***
#*******************************************************************************
# These parameters are potentially sampled/calibrated in the MCMC or MC
# analyses.  The default values here are used if no sampled value is given.
# M_ indicates population mean parameters used only in MC sampling
# V_ indicates a population variance parameter used in MC and MCMC sampling

# Flow Rates
lnQCC     = 0.0;    # Scaled by BW^0.75 and species-specific central estimates
lnVPRC    = 0.0;    # Scaled to species-specific central estimates

# Fractional Blood Flows to Tissues (fraction of cardiac output)
QFatC     = 1.0;    # Scaled to species-specific central estimates
QGutC     = 1.0;    # Scaled to species-specific central estimates
QLivC     = 1.0;    # Scaled to species-specific central estimates
QSlwC     = 1.0;    # Scaled to species-specific central estimates
QKidC     = 1.0;    # Scaled to species-specific central estimates
FracPlasC = 1.0;    # Scaled to species-specific central estimates
lnDRespC  = 0.0;    # Scaled to alveolar ventilation rate in dynamics

# Fractional Tissue Volumes (fraction of BW)
VFatC     = 1.0;    # Scaled to species-specific central estimates
VGutC     = 1.0;    # Scaled to species-specific central estimates
VLivC     = 1.0;    # Scaled to species-specific central estimates
VRapC     = 1.0;    # Scaled to species-specific central estimates
VRespLumC = 1.0;    # Scaled to species-specific central estimates
VRespEffC = 1.0;    # Scaled to species-specific central estimates

VKidC     = 1.0;    # Scaled to species-specific central estimates
VBldC     = 1.0;    # Scaled to species-specific central estimate

# Partition Coefficients for TCE
lnPBC     = 0.0;    # Scaled to species-specific central estimates
lnPFatC   = 0.0;    # Scaled to species-specific central estimates
lnPGutC   = 0.0;    # Scaled to species-specific central estimates
lnPLivC   = 0.0;    # Scaled to species-specific central estimates
lnPRapC   = 0.0;    # Scaled to species-specific central estimates
lnPRespC  = 0.0;    # Scaled to species-specific central estimates
lnPKidC   = 0.0;    # Scaled to species-specific central estimates
lnPSlwC   = 0.0;    # Scaled to species-specific central estimates

# Partition Coefficients for TCA
lnPRBCPlasTCAC      = 0.0;    # Scaled to species-specific central estimates
lnPBodTCAC          = 0.0;    # Scaled to species-specific central estimates
lnPLivTCAC          = 0.0;    # Scaled to species-specific central estimates

# Plasma Binding for TCA
lnkDissocC          = 0.0;    # Scaled to species-specific central estimates
lnBMaxkDC = 0.0;    # Scaled to species-specific central estimates

# Partition Coefficients for TCOH and TCOG
lnPBodTCOHC         = 0.0;    # Scaled to species-specific central estimates
lnPLivTCOHC         = 0.0;    # Scaled to species-specific central estimates
lnPBodTCOGC         = 0.0;    # Scaled to species-specific central estimates
lnPLivTCOGC         = 0.0;    # Scaled to species-specific central estimates
lnPeffDCVG          = 0.0;    # Scaled to species-specific central estimates
```

```
# Oral Absorption rates
lnkTSD    = 0.336;
lnkAS     = 0.336;
lnkTD     = -2.303;
lnkAD     = -0.288;
lnkASTCA  = -0.288;
lnkASTCOH = -0.288;

# TCE Metabolism
lnVMAXC   = 0.0;    # Scaled by liver weight and species-specific central estimates
lnKMC     = 0.0;    # Scaled to species-specific central estimates
lnClC     = 0.0;    # Scaled to species-specific central estimates
lnFracOtherC        = 0.0;    # Ratio of DCA to non-DCA
lnFracTCAC          = 0.0;    # Ratio of TCA to TCOH
lnVMAXDCVGC         = 0.0;    # Scaled by liver weight and species-specific central
estimates
lnClDCVGC = 0.0;    # Scaled to species-specific central estimates
lnKMDCVGC = 0.0;    # Scaled to species-specific central estimates
lnVMAXKidDCVGC      = 0.0;    # Scaled by kidney weight and species-specific central
estimates
lnClKidDCVGC        = 0.0;    # Scaled to species-specific central estimates
lnKMKidDCVGC        = 0.0;    # Scaled to species-specific central estimates
lnVMAXLungLivC      = 0.0;    # Ratio of lung VMAX to liver VMAX,
                              # Scaled to species-specific central estimates
lnKMClara = 0.0;    # now in units of air concentration

# Clearance in lung
lnFracLungSysC      = 0.0;    # ratio of systemic to local clearance of lung
oxidation

# TCOH Metabolism
lnVMAXTCOHC         = 0.0;    # Scaled by BW^0.75
lnClTCOHC = 0.0;    # Scaled by BW^0.75
lnKMTCOH  = 0.0;    #
lnVMAXGlucC         = 0.0;    # Scaled by BW^0.75
lnClGlucC = 0.0;    # Scaled by BW^0.75
lnKMGluc  = 0.0;    #
lnkMetTCOHC         = 0.0;    # Scaled by BW^-0.25

# TCA Metabolism/clearance
lnkUrnTCAC          = 0.0;    # Scaled by (plasma volume)^-1 and species-specific
central estimates
lnkMetTCAC          = 0.0;    # Scaled by BW^-0.25

# TCOG excretion and reabsorption
lnkBileC  = 0.0;    # Scaled by BW^-0.25
lnkEHRC   = 0.0;    # Scaled by BW^-0.25
lnkUrnTCOGC         = 0.0;    # Scaled by (blood volume)^-1 and species-specific
central estimates

# DCVG metabolism
lnFracKidDCVCC      = 0.0;    # Ratio of "directly" to DCVC to systemic DCVG
lnkDCVGC  = 0.0;    # Scaled by BW^-0.25

# DCVC metabolism
lnkNATC   = 0.0;    # Scaled by BW^-0.25
lnkKidBioactC       = 0.0;    # Scaled by BW^-0.25

# Closed chamber parameters
NRodents  = 1;      #
VChC      = 1;      #
lnkLossC  = 0;      #

#*****************************************************************************
# Population means
#
# These are given truncated normal or uniform distributions, depending on
#         what prior information is available.  Note that these distributions
#         reflect uncertainty in the population mean, not inter-individual
#         variability.  Normal distributions are truncated at 2, 3, or 4 SD.
#                   For fractional volumes and flows, 2xSD
#                   For plasma fraction, 3xSD
#                   For cardiac output and ventilation-perfusion ratio, 4xSD
#                   For all others, 3xSD
#         For uniform distributions, range of 1e2 to 1e8 fold, centered on
#                   central estimate.
#
M_lnQCC   = 1.0;
M_lnVPRC  = 1.0;
M_QFatC   = 1.0;
M_QGutC   = 1.0;
M_QLivC   = 1.0;
M_QSlwC   = 1.0;
M_QKidC   = 1.0;
M_FracPlasC         = 1.0;
M_lnDRespC = 1.0;
M_VFatC   = 1.0;
M_VGutC   = 1.0;
M_VLivC   = 1.0;
M_VRapC   = 1.0;
M_VRespLumC = 1.0;
M_VRespEffC = 1.0;
M_VKidC   = 1.0;
M_VBldC   = 1.0;
M_lnPBC   = 1.0;
M_lnPFatC = 1.0;
M_lnPGutC = 1.0;
M_lnPLivC = 1.0;
M_lnPRapC = 1.0;
M_lnPRespC          = 1.0;
M_lnPKidC = 1.0;
M_lnPSlwC = 1.0;
M_lnPRBCPlasTCAC    = 1.0;
M_lnPBodTCAC        = 1.0;
M_lnPLivTCAC        = 1.0;
M_lnkDissocC        = 1.0;
M_lnBMaxkDC         = 1.0;
M_lnPBodTCOHC       = 1.0;
M_lnPLivTCOHC       = 1.0;
M_lnPBodTCOGC       = 1.0;
M_lnPLivTCOGC       = 1.0;
M_lnPeffDCVG        = 1.0;
M_lnkTSD  = 1.0;
```

```
M_lnkAS   = 1.0;
M_lnkTD   = 1.0;
M_lnkAD   = 1.0;
M_lnkASTCA          = 1.0;
M_lnkASTCOH         = 1.0;
M_lnVMAXC = 1.0;
M_lnKMC   = 1.0;
M_lnClC   = 1.0;
M_lnFracOtherC      = 1.0;
M_lnFracTCAC        = 1.0;
M_lnVMAXDCVGC       = 1.0;
M_lnClDCVGC         = 1.0;
M_lnKMDCVGC         = 1.0;
M_lnVMAXKidDCVGC    = 1.0;
M_lnClKidDCVGC      = 1.0;
M_lnKMKidDCVGC      = 1.0;
M_lnVMAXLungLivC    = 1.0;
M_lnKMClara         = 1.0;
M_lnFracLungSysC    = 1.0;
M_lnVMAXTCOHC       = 1.0;
M_lnClTCOHC         = 1.0;
M_lnKMTCOH          = 1.0;
M_lnVMAXGlucC       = 1.0;
M_lnClGlucC         = 1.0;
M_lnKMGluc          = 1.0;
M_lnkMetTCOHC       = 1.0;
M_lnkUrnTCAC        = 1.0;
M_lnkMetTCAC        = 1.0;
M_lnkBileC          = 1.0;
M_lnkEHRC = 1.0;
M_lnkUrnTCOGC       = 1.0;
M_lnFracKidDCVCC    = 1.0;
M_lnkDCVGC          = 1.0;
M_lnkNATC = 1.0;
M_lnkKidBioactC     = 1.0;


#*****************************************************************************
# Population Variances
#
# These are given InvGamma(alpha,beta) distributions.  The parameterization
#         for alpha and beta is given by:
#                   alpha = (n-1)/2
#                   beta = s^2*(n-1)/2
#         where n = number of data points, and s^2 is the sample variance
#         Sum(x_i^2)/n - <x>^2.
# Generally, for parameters for which there is no direct data, assume a
#         value of n = 5 (alpha = 2).  For a sample variance s^2, this gives
#         an expected value for the standard deviation <sigma> = 0.9*s,
#         a median [2.5%,97.5%] of 1.1*s [0.6*s,2.9*s].
#
V_lnQCC   = 1.0;
V_lnVPRC  = 1.0;
V_QFatC   = 1.0;
V_QGutC   = 1.0;
V_QLivC   = 1.0;
V_QSlwC   = 1.0;
V_QKidC   = 1.0;
V_FracPlasC         = 1.0;
V_lnDRespC = 1.0;
V_VFatC   = 1.0;
V_VGutC   = 1.0;
V_VLivC   = 1.0;
V_VRapC   = 1.0;
V_VRespLumC = 1.0;
V_VRespEffC = 1.0;
V_VKidC   = 1.0;
V_VBldC   = 1.0;
V_lnPBC   = 1.0;
V_lnPFatC = 1.0;
V_lnPGutC = 1.0;
V_lnPLivC = 1.0;
V_lnPRapC = 1.0;
V_lnPRespC          = 1.0;
V_lnPKidC = 1.0;
V_lnPSlwC = 1.0;
V_lnPRBCPlasTCAC    = 1.0;
V_lnPBodTCAC        = 1.0;
V_lnPLivTCAC        = 1.0;
V_lnkDissocC        = 1.0;
V_lnBMaxkDC         = 1.0;
V_lnPBodTCOHC       = 1.0;
V_lnPLivTCOHC       = 1.0;
V_lnPBodTCOGC       = 1.0;
V_lnPLivTCOGC       = 1.0;
V_lnPeffDCVG        = 1.0;
V_lnkTSD  = 1.0;
V_lnkAS   = 1.0;
V_lnkTD   = 1.0;
V_lnkAD   = 1.0;
V_lnkASTCA          = 1.0;
V_lnkASTCOH         = 1.0;
V_lnVMAXC = 1.0;
V_lnKMC   = 1.0;
V_lnClC   = 1.0;
V_lnFracOtherC      = 1.0;
V_lnFracTCAC        = 1.0;
V_lnVMAXDCVGC       = 1.0;
V_lnClDCVGC         = 1.0;
V_lnKMDCVGC         = 1.0;
V_lnVMAXKidDCVGC    = 1.0;
V_lnClKidDCVGC      = 1.0;
V_lnKMKidDCVGC      = 1.0;
V_lnVMAXLungLivC    = 1.0;
V_lnKMClara         = 1.0;
V_lnFracLungSysC    = 1.0;
V_lnVMAXTCOHC       = 1.0;
V_lnClTCOHC         = 1.0;
V_lnKMTCOH          = 1.0;
V_lnVMAXGlucC       = 1.0;
V_lnClGlucC         = 1.0;
V_lnKMGluc          = 1.0;
V_lnkMetTCOHC       = 1.0;
V_lnkUrnTCAC        = 1.0;
```

```
V_lnkMetTCAC        = 1.0;
V_lnkBileC          = 1.0;
V_lnkEHRC = 1.0;
V_lnkUrnTCOGC       = 1.0;
V_lnFracKidDCVCC    = 1.0;
V_lnkDCVGC          = 1.0;
V_lnkNATC = 1.0;
V_lnkKidBioactC     = 1.0;

#*****************************************************************************
# Measurement error variances for output

Ve_RetDose          = 1;
Ve_CAlv   = 1;
Ve_CAlvPPM          = 1;
Ve_CInhPPM          = 1;
Ve_CInh   = 1;
Ve_CMixExh          = 1;
Ve_CArt   = 1;
Ve_CVen   = 1;
Ve_CBldMix          = 1;

Ve_CFat   = 1;
Ve_CGut   = 1;
Ve_CRap   = 1;
Ve_CSlw   = 1;
Ve_CHrt   = 1;
Ve_CKid   = 1;
Ve_CLiv   = 1;
Ve_CLung  = 1;
Ve_CMus   = 1;
Ve_CSpl   = 1;
Ve_CBrn   = 1;
Ve_zAExh  = 1;
Ve_zAExhpost        = 1;


Ve_CTCOH  = 1;
Ve_CKidTCOH         = 1;
Ve_CLivTCOH         = 1;
Ve_CLungTCOH        = 1;


Ve_CPlasTCA         = 1;
Ve_CBldTCA          = 1;
Ve_CBodTCA          = 1;
Ve_CKidTCA          = 1;
Ve_CLivTCA          = 1;
Ve_CLungTCA         = 1;
Ve_zAUrnTCA         = 1;
Ve_zAUrnTCA_collect = 1;
Ve_zAUrnTCA_sat     = 1;


Ve_zABileTCOG       = 1;
Ve_CTCOG  = 1;
Ve_CTCOGTCOH        = 1;

Ve_CKidTCOGTCOH     = 1;
Ve_CLivTCOGTCOH     = 1;
Ve_CLungTCOGTCOH    = 1;
Ve_AUrnTCOGTCOH     = 1;
Ve_AUrnTCOGTCOH_collect       = 1;

Ve_AUrnTCOGTCOH_sat = 1;


Ve_CDCVGmol         = 1;
Ve_zAUrnNDCVC       = 1;
Ve_AUrnTCTotMole    = 1;
Ve_TotCTCOH         = 1;
Ve_QPsamp = 1;

#*****************************************************************************
#***                  Defaults for input parameters                        ***
#*****************************************************************************
##-- TCE dosing
          Conc = 0.0;         # Inhalation exposure conc. (ppm)
          IVDose = 0.0;       # IV dose (mg/kg)
          PDose = 0.0;        # Oral gavage dose (mg/kg)
          Drink = 0.0;        # Drinking water dose (mg/kg-day)
          IADose = 0.0;       # Intraarterial dose (mg/kg)
          PVDose = 0.0;       # Portal vein dose (mg/kg)
##-- TCA dosing
          IVDoseTCA = 0.0;# IV dose (mg/kg) of TCA
          PODoseTCA = 0.0;# Oral dose (mg/kg) of TCA
##-- TCOH dosing
          IVDoseTCOH = 0.0;# IV dose (mg/kg) of TCOH
          PODoseTCOH = 0.0;# Oral dose (mg/kg) of TCOH
##-- Potentially time-varying parameters
          QPmeas = 0.0;       # Measured value of Alveolar ventilation QP
          TCAUrnSat = 0.0;# Flag for saturated TCA urine
          TCOGUrnSat = 0.0;# Flag for saturated TCOG urine
          UrnMissing = 0.0;# Flag for missing urine collection times

Initialize {

#*****************************************************************************
#***                  Parameter Initialization and Scaling                 ***
#*****************************************************************************
# Model Parameters (used in dynamics):
#         QC                  Cardiac output (L/hr)
#         VPR                 Ventilation-perfusion ratio
#         QPsamp              Alveolar ventilation (L/hr)
#         QFatCtmp  Scaled fat blood flow
#         QGutCtmp  Scaled gut blood flow
#         QLivCtmp  Scaled liver blood flow
#         QSlwCtmp  Scaled slowly perfused blood flow
#         DResptmp  Respiratory lumen:tissue diffusive clearance rate
#         QKidCtmp  Scaled kidney blood flow
#         FracPlas  Fraction of blood that is plasma (1-hematocrit)
#         VFat                Fat compartment volume (L)
#         VGut                Gut compartment volume (L)
#         VLiv                Liver compartment volume (L)
#         VRap                Rapidly perfused compartment volume (L)
```

```
#         VRespLum  Volume of respiratory lumen (L air)
#         VRespEff  Effective volume of respiratory tissue (L air)
#         VKid              Kidney compartment volume (L)
#         VBld              Blood compartment volume (L)
#         VSlw              Slowly perfused compartment volume (L)
#         VPlas             Plasma compartment volume [fraction of blood] (L)
#         VBod              TCA Body compartment volume [not incl. blood+liver]
(L)
#         VBodTCOH  TCOH/G Body compartment volume [not incl. liver] (L)
#         PB                TCE Blood/air partition coefficient
#         PFat              TCE Fat/Blood partition coefficient
#         PGut              TCE Gut/Blood partition coefficient
#         PLiv              TCE Liver/Blood partition coefficient
#         PRap              TCE Rapidly perfused/Blood partition coefficient
#         PResp             TCE Respiratory tissue:air partition coefficient
#         PKid              TCE Kidney/Blood partition coefficient
#         PSlw              TCE Slowly perfused/Blood partition coefficient
#         TCAPlas           TCA blood/plasma concentration ratio
#         PBodTCA           Free TCA Body/blood plasma partition coefficient
#         PLivTCA           Free TCA Liver/blood plasma partition coefficient
#         kDissoc           Protein/TCA dissociation constant (umole/L)
#         BMax              Maximum binding concentration (umole/L)
#         PBodTCOH  TCOH body/blood partition coefficient
#         PLivTCOH  TCOH liver/body partition coefficient
#         PBodTCOG  TCOG body/blood partition coefficient
#         PLivTCOG  TCOG liver/body partition coefficient
#         kAS               TCE Stomach absorption coefficient (/hr)
#         kTSD              TCE Stomach-duodenum transfer coefficient (/hr)
#         kAD               TCE Duodenum absorption coefficient (/hr)
#         kTD               TCE Duodenum-feces transfer coefficient (/hr)
#         kASTCA            TCA Stomach absorption coefficient (/hr)
#         kASTCOH           TCOH Stomach absorption coefficient (/hr)
#         VMAX              VMAX for hepatic TCE oxidation (mg/hr)
#         KM                KM for hepatic TCE oxidation (mg/L)
#         FracOther Fraction of hepatic TCE oxidation not to TCA+TCOH
#         FracTCA           Fraction of hepatic TCE oxidation to TCA
#         VMAXDCVG  VMAX for hepatic TCE GSH conjugation (mg/hr)
#         KMDCVG            KM for hepatic TCE GSH conjugation (mg/L)
#         VMAXKidDCVG       VMAX for renal TCE GSH conjugation (mg/hr)
#         KMKidDCVG KM for renal TCE GSH conjugation (mg/L)
#         VMAXClara VMAX for Tracheo-bronchial TCE oxidation (mg/hr)
#         KMClara           KM for Tracheo-bronchial TCE oxidation (mg/L)
#         FracLungSys       Fraction of respiratory metabolism to systemic circ.
#         VMAXTCOH  VMAX for hepatic TCOH->TCA (mg/hr)
#         KMTCOH            KM for hepatic TCOH->TCA (mg/L)
#         VMAXGluc  VMAX for hepatic TCOH->TCOG (mg/hr)
#         KMGluc            KM for hepatic TCOH->TCOG (mg/L)
#         kMetTCOH  Rate constant for hepatic TCOH->other (/hr)
#         kUrnTCA           Rate constant for TCA plasma->urine (/hr)
#         kMetTCA           Rate constant for hepatic TCA->other (/hr)
#         kBile             Rate constant for TCOG liver->bile (/hr)
#         kEHR              Lumped rate constant for TCOG bile->TCOH liver (/hr)
#         kUrnTCOG  Rate constant for TCOG->urine (/hr)
#         kDCVG             Rate constant for hepatic DCVG->DCVC (/hr)
#         FracKidDCVC       Fraction of renal TCE GSH conj. "directly" to DCVC
#                           (i.e., via first pass)
#         VDCVG             DCVG effective volume of distribution
#         kNAT              Lumped rate constant for DCVC->Urinary NAcDCVC (/hr)
#         kKidBioact        Rate constant for DCVC bioactivation (/hr)
#         Rodents           Number of rodents in closed chamber data
#         VCh               Chamber volume for closed chamber data
#         kLoss             Rate constant for closed chamber air loss
# Parameters used (not assigned here)
#         BW                Body weight in kg
#         Species           1 = human (default), 2 = rat, 3 = mouse
#         Male              0 = female, 1 (default) = male
#         CC                Closed chamber initial concentration
# Sampling/scaling parameters (assigned or sampled)
#         lnQCC
#         lnVPRC
#         lnDRespC
#         QFatC
#         QGutC
#         QLivC
#         QSlwC
#         QKidC
#         FracPlasC
#         VFatC
#         VGutC
#         VLivC
#         VRapC
#         VRespLumC
#         VRespEffC
#         VKidC
#         VBldC
#         lnPBC
#         lnPFatC
#         lnPGutC
#         lnPLivC
#         lnPRapC
#         lnPSlwC
#         lnPRespC
#         lnPKidC
#         lnPRBCPlasTCAC
#         lnPBodTCAC
#         lnPLivTCAC
#         lnkDissocC
#         lnBMaxkDC
#         lnPBodTCOHC
#         lnPLivTCOHC
#         lnPBodTCOGC
#         lnPLivTCOGC
#         lnPeffDCVG
#         lnkTSD
#         lnkAS
#         lnkTD
#         lnkAD
#         lnkASTCA
#         lnkASTCOH
#         lnVMAXC
#         lnKMC
#         lnClC
#         lnFracOtherC
#         lnFracTCAC
```

```
#         lnVMAXDCVGC
#         lnClDCVGC
#         lnKMDCVGC
#         lnVMAXKidDCVGC
#         lnClKidDCVGC
#         lnKMKidDCVGC
#         lnVMAXLungLivC
#         lnKMClara
#         lnFracLungSysC
#         lnVMAXTCOHC
#         lnClTCOHC
#         lnKMTCOH
#         lnVMAXGlucC
#         lnClGlucC
#         lnKMGluc
#         lnkMetTCOHC
#         lnkUrnTCAC
#         lnkMetTCAC
#         lnkBileC
#         lnkEHRC
#         lnkUrnTCOGC
#         lnFracKidDCVCC
#         lnkDCVGC
#         lnkNATC
#         lnkKidBioactC
#         NRodents
#         VChC
#         lnkLossC
# Input parameters
#         none
# Notes:
#*****************************************************************************
          # use measured value of > 0, otherwise use 0.03 for mouse,
          #         0.3 for rat, 60 for female human, 70 for male human
          BW = (BWmeas > 0.0 ? BWmeas : (Species == 3 ? 0.03 : (Species == 2 ? 0.3 :
(Male == 0 ? 60.0 : 70.0) )));

          BW75 = pow(BW, 0.75);
          BW25 = pow(BW, 0.25);

# Cardiac Output and alveolar ventilation (L/hr)
          QC = exp(lnQCC) * BW75 *      # Mouse, Rat, Human (default)
                    (Species == 3 ? 11.6 : (Species == 2 ? 13.3 : 16.0 ));
          # Mouse: CO=13.98 +/- 2.85 ml/min, BW=30 g (Brown et al. 1997, Tab. 22)
          #         Uncertainty CV is 0.20
          # Rat: CO=110.4 ml/min +/- 15.6, BW=396 g (Brown et al. 1997, Tab. 22,
          #         p 441).  Uncertainty CV is 0.14.
          # Human: Average of Male CO=6.5 l/min, BW=73 kg
          #         and female CO= 5.9 l/min, BW=60 kg (ICRP #89, sitting at rest)
          #         From Price et al. 2003, estimates of human perfusion rate were
          #         4.7~6.5 for females and 5.5~7.1 l/min for males (note
          #         portal blood was double-counted, and subtracted off here)
          #         Thus for uncertainty use CV of 0.2, truncated at 4xCV
          #         Variability from Price et al. (2003) had CV of 0.14~0.20,
          #         so use 0.2 as central estimate
          VPR = exp(lnVPRC)*
                    (Species == 3 ? 2.5 : (Species == 2 ? 1.9 : 0.96 ));
          # Mouse: QP/BW=116.5 ml/min/100 g (Brown et al. 1997, Tab. 31), VPR=2.5
          #         Assume uncertainty CV of 0.2 similar to QC, truncated at 4xCV
          #         Consistent with range of QP in Tab. 31
          # Rat: QP/BW=52.9 ml/min/100 g (Brown et al. 1997, Tab. 31), VPR=1.9
          #         Assume uncertainty CV of 0.3 similar to QC, truncated at 4xCV
          #         Used larger CV because Tab. 31 shows a very large range of QP
          # Human: Average of Male VE=9 l/min, resp. rate=12 /min,
          #         dead space=0.15 l (QP=7.2 l/min), and Female
          #         VE=6.5 l/min, resp. rate=14 /min, dead space=0.12 l
          #         (QP=4.8 l/min), VPR = 0.96
          #         Assume uncertainty CV of 0.2 similar to QC, truncated at 4xCV
          #         Consistent with range of QP in Tab. 31
          QPsamp = QC*VPR;

#         Respiratory diffusion flow rate
#         Will be scaled by QP in dynamics
#         Use log-uniform distribution from 1e-5 to 10
          DResptmp = exp(lnDRespC);

# Fractional Flows scaled to the appropriate species
# Fat = Adipose only
# Gut = GI tract + pancreas + spleen (all drain to portal vein)
# Liv = Liver, hepatic artery
# Slw = Muscle + Skin
# Kid = Kidney
# Rap = Rapidly perfused (rest of organs, plus bone marrow, lymph, etc.),
#         derived by difference in dynamics
#
# Mouse and rat data from Brown et al. (1997).  Human data from
#         ICRP-89 (2002), and is sex-specific.

          QFatCtmp = QFatC*
          (Species == 3 ? 0.07 : (Species == 2 ? 0.07 : (Male == 0 ? 0.085 : 0.05)
));
          QGutCtmp = QGutC*
          (Species == 3 ? 0.141 : (Species == 2 ? 0.153 : (Male == 0 ? 0.21 : 0.19)
));
          QLivCtmp = QLivC*
          (Species == 3 ? 0.02 : (Species == 2 ? 0.021 : 0.065 ));
          QSlwCtmp = QSlwC*
          (Species == 3 ? 0.217 : (Species == 2 ? 0.336 : (Male == 0 ? 0.17 : 0.22)
));
          QKidCtmp = QKidC*
                    (Species == 3 ? 0.091 : (Species == 2 ? 0.141 : (Male == 0 ?
0.17 : 0.19) ));

# Plasma Flows to Tissues (L/hr)
## Mice and rats from Hejtmancik et al. 2002,
##        control F344 rats and B6C3F1 mice at 19 weeks of age
## However, there appear to be significant strain differences in rodents, so
##        assume uncertainty CV=0.2 and variability CV=0.2.
## Human central estimate from ICRP.  Well measured in humans, from Price et al.,
##        human SD in hematocrit was 0.029 in females, 0.027 in males,
##        corresponding to FracPlas CV of 0.047 in females and
##        0.048 in males.  Use rounded CV = 0.05 for both uncertainty and
variability
## Use measured 1-hematocrit if available
```

```
## Truncate distributions at 3xCV to encompass clinical "normal range"
         FracPlas = (Hematocritmeas > 0.0 ? (1-Hematocritmeas) : (FracPlasC *
         (Species == 3 ? 0.52 : (Species == 2 ? 0.53 : (Male == 0 ? 0.615 :
0.567)))));

# Tissue Volumes (L)
# Fat = Adipose only
# Gut = GI tract (not contents) + pancreas + spleen (all drain to portal vein)
# Liv = Liver
# Rap = Brain + Heart + (Lungs-TB) + Bone marrow + "Rest of the body"
# VResp = Tracheobroncial region (trachea+broncial basal+
#                   broncial secretory+bronchiolar)
# Kid = Kidney
# Bld = Blood
# Slw = Muscle + Skin, derived by difference
# residual (assumed unperfused) = (Bone-Marrow)+GI contents+other
#
# Mouse and rat data from Brown et al. (1997).  Human data from
#         ICRP-89 (2002), and is sex-specific.

       VFat = BW * (VFatCmeas > 0.0 ? VFatCmeas : (VFatC * (Species == 3 ? 0.07 :
(Species == 2 ? 0.07 : (Male == 0 ? 0.317 : 0.199)  ))));
       VGut = VGutC * BW *
         (Species == 3 ? 0.049 : (Species == 2 ? 0.032 : (Male == 0 ? 0.022 :
0.020) ));
       VLiv = VLivC * BW *
         (Species == 3 ? 0.055 : (Species == 2 ? 0.034 : (Male == 0 ? 0.023 :
0.025) ));
       VRap = VRapC * BW *
         (Species == 3 ? 0.100 : (Species == 2 ? 0.088 : (Male == 0 ? 0.093 :
0.088) ));
         VRespLum = VRespLumC * BW *
         (Species == 3 ? (0.00014/0.03) : (Species == 2 ? (0.0014/0.3) : (0.167/70)
)); # Lumenal volumes from Styrene model (Sarangapani et al. 2002)
         VRespEfftmp = VRespEffC * BW *
         (Species == 3 ? 0.0007 : (Species == 2 ? 0.0005 : 0.00018 ));
         # Respiratory tract volume is TB region
         # will be multiplied by partition coef. below
         VKid = VKidC * BW *
         (Species == 3 ? 0.017 : (Species == 2 ? 0.007 : (Male == 0 ? 0.0046 :
0.0043) ));
       VBld = VBldC * BW *
         (Species == 3 ? 0.049 : (Species == 2 ? 0.074 : (Male == 0 ? 0.068 :
0.077) ));
       VSlw = (Species == 3 ? 0.8897 : (Species == 2 ? 0.8995 : (Male == 0 ?
0.85778 : 0.856))) * BW
                  - VFat - VGut - VLiv - VRap - VRespEfftmp - VKid - VBld;
# Slowly perfused:
# Baseline mouse: 0.8897-0.049-0.017-0.0007-0.1-0.055-0.049-0.07= 0.549
# Baseline rat: 0.8995 -0.074-0.007-0.0005-0.088-0.034-0.032-0.07= 0.594
# Baseline human F: 0.85778-0.068-0.0046-0.00018-0.093-0.023-0.022-0.317= 0.33
# Baseline human M: 0.856-0.077-0.0043-0.00018-0.088-0.025-0.02-0.199= 0.4425

      VPlas = FracPlas * VBld;
         VBod = VFat + VGut + VRap + VRespEfftmp + VKid + VSlw; # For TCA
         VBodTCOH = VBod + VBld;       # for TCOH and TCOG -- body without liver

# Partition coefficients
      PB = (PBmeas > 0.0 ? PBmeas : (exp(lnPBC) * (Species == 3 ? 15. : (Species ==
2 ? 22. : 9.5 )))); # Blood-air
         # Mice: pooling Abbas and Fisher 1997, Fisher et al. 1991
         #         each a single measurement, with overall CV = 0.07.
         #         Given small number of measurements, and variability
         #         in rat, use CV of 0.25 for uncertainty and variability.
         # Rats: pooling Sato et al. 1977, Gargas et al. 1989,
         #         Barton et al. 1995, Simmons et al. 2002, Koizumi 1989,
         #         Fisher et al. 1989.  Fisher et al. measurement substantially
         #         smaller than others (15 vs. 21~26).  Recent article
         #         by Rodriguez et al. 2007 shows significant change with
         #         age (13.1 at PND10, 17.5 at adult, 21.8 at aged), also seems
         #         to favor lower values than previously reported.  Therefore
         #         use CV = 0.25 for uncertainty and variability.
         # Humans: pooling Sato and Nakajima 1979, Sato et al. 1977,
         #         Gargas et al. 1989, Fiserova-Bergerova et al. 1984,
         #         Fisher et al. 1998, Koizumi 1989
         #         Overall variability CV = 0.185.  Consistent with
         #         within study inter-individual variability CV = 0.07~0.22.
         #         Study-to-study, sex-specific means range 8.1~11, so
         #         uncertainty CV = 0.2.
       PFat = exp(lnPFatC) *           # Fat/blood
                  (Species == 3 ? 36. : (Species == 2 ? 27. : 67. ));
         # Mice: Abbas and Fisher 1997.  Single measurement.  Use
         #         rat uncertainty of CV = 0.3.
         # Rats: Pooling Barton et al. 1995, Sato et al. 1977,
         #         Fisher et al. 1989.  Recent article by Rodriguez et al.
         #         (2007) shows higher value of 36., so assume uncertainty
         #         CV of 0.3.
         # Humans: Pooling Fiserova-Bergerova et al. 1984, Fisher et al. 1998,
         #         Sato et al. 1977.  Variability in Fat:Air has CV = 0.07.
         #         For uncertainty, dominated by PB uncertainty CV = 0.2
         #         For variability, add CVs in quadrature for
         #         sqrt(0.07^2+0.185^2)=0.20
       PGut = exp(lnPGutC) *           # Gut/blood
                  (Species == 3 ? 1.9 : (Species == 2 ? 1.4 : 2.6 ));
         # Mice: Geometric mean of liver, kidney
         # Rats: Geometric mean of liver, kidney
         # Humans: Geometric mean of liver, kidney
         #         Uncertainty of CV = 0.4 due to tissue extrapolation
       PLiv = exp(lnPLivC) *           # Liver/blood
                  (Species == 3 ? 1.7 : (Species == 2 ? 1.5 : 4.1 ));
         # Mice: Fisher et al. 1991, single datum, so assumed uncert CV = 0.4
         # Rats: Pooling Barton et al. 1995, Sato et al. 1977,
         #         Fisher et al. 1989, with little variation (range 1.3~1.7).
         #         Recent article by Rodriguez et al.reports 1.34.  Use
         #         uncertainty CV = 0.15.
         # Humans: Pooling Fiserova-Bergerova et al. 1984, Fisher et al. 1998
         #         almost 2-fold difference in Liver:Air values, so uncertainty
         #         CV = 0.4
       PRap = exp(lnPRapC) *           # Rapidly perfused/blood
                  (Species == 3 ? 1.9 : (Species == 2 ? 1.3 : 2.6 ));
         # Mice: Similar to liver, kidney.  Uncertainty CV = 0.4 due to
         #         tissue extrapolation
         # Rats: Use brain values Sato et al. 1977.  Recent article by
         #         Rodriguez et al. (2007) reports 0.99 for brain.  Uncertainty
```

```
          #         CV of 0.4 due to tissue extrapolation.
          # Humans: Use brain from Fiserova-Bergerova et al. 1984
          #         Uncertainty of CV = 0.4 due to tissue extrapolation
        PResp = exp(lnPRespC) *                    # Resp/blood =
                  (Species == 3 ? 2.6 : (Species == 2 ? 1.0 : 1.3 ));
          # Mice: Abbas and Fisher 1997, single datum, so assumed uncert CV = 0.4
          # Rats: Sato et al. 1977, single datum, so assumed uncert CV = 0.4
          # Humans: Pooling Fiserova-Bergerova et al. 1984, Fisher et al. 1998
          #         > 2-fold difference in lung:air values, so uncertainty
          #         CV = 0.4
        VRespEff = VRespEfftmp * PResp * PB; # Effective air volume
        PKid = exp(lnPKidC) *            # Slowly perfused/blood
                  (Species == 3 ? 2.1 : (Species == 2 ? 1.3 : 1.6 ));
          # Mice: Abbas and Fisher 1997, single datum, so assumed uncert CV = 0.4
          # Rats: Pooling Barton et al. 1995, Sato et al. 1977.  Recent article
          #         by Rodriguez et al. (2007) reports 1.01, so use uncertainty
          #         CV of 0.3.  Pooled variability CV = 0.39.
          # Humans: Pooling Fiserova-Bergerova et al. 1984, Fisher et al. 1998
          #         For uncertainty, dominated by PB uncertainty CV = 0.2
          #         Variability in kidney:air CV = 0.23, so add to PB variability
          #         in quadrature       sqrt(0.23^2+0.185^2)=0.30
        PSlw = exp(lnPSlwC) *            # Slowly perfused/blood
                  (Species == 3 ? 2.4 : (Species == 2 ? 0.58 : 2.1 ));
          # Mice: Muscle - Abbas and Fisher 1997, single datum, so assumed
          #         uncert CV = 0.4
          # Rats: Pooling Barton et al. 1995, Sato et al. 1977,
          #         Fisher et al. 1989.  Recent article by Rodriguez et al. (2007)
          #         reported 0.72, so use uncertainty CV of 0.25.  Variability
          #         in Muscle:air and muscle:blood ~ CV = 0.3
          # Humans: Pooling Fiserova-Bergerova et al. 1984, Fisher et al. 1998
          #         Range of values 1.4~2.4, so uncertainty CV = 0.3
          #         Variability in muscle:air CV = 0.3, so add to PB variability
          #         in quadrature sqrt(0.3^2+0.185^2)=0.35

# TCA partitioning
    TCAPlas = FracPlas + (1 - FracPlas) * 0.5 * exp(lnPRBCPlasTCAC);
          #         Blood/Plasma concentration ratio.  Note dependence
          #         on fraction of blood that is plasma.  Here
          #         exp(lnPRBCPlasTCA) = partition coefficient
          #                   C(blood minus plasma)/C(plasma)
          #         Default of 0.5, corresponding to Blood/Plasma
          #                   concentration ratio of 0.76 in
          #                   rats (Schultz et al 1999)
          #         For rats, Normal uncertainty with GSD = 1.4
          #         For mice and humans, diffuse prior uncertainty of
          #         100-fold up/down
    PBodTCA = TCAPlas * exp(lnPBodTCAC) *
                  (Species == 3 ? 0.88 : (Species == 2 ? 0.88 : 0.52 ));
          # Note -- these were done at 10~20 microg/ml (Abbas and Fisher 1997),
          #         which is 1.635-3.27 mmol/ml (1.635-3.27 x 10^6 microM).
          #         At this high concentration, plasma binding should be
          #         saturated -- e.g., plasma albumin concentration was
          #         measured to be P=190-239 microM in mouse, rat, and human
          #         plasma by Lumpkin et al. 2003, or > 6800 molecules of
          #         TCA per molecule of albumin.  So the measured partition
          #         coefficients should reflect free blood-tissue partitioning.
          # Used muscle values, multiplied by blood:plasma ratio to get
          #         Body:Plasma partition coefficient
          # Rats = mice from Abbas and Fisher 1997
          # Humans from Fisher et al. 1998
          #         Uncertainty in mice, humans GSD = 1.4
          #         For rats, GSD = 2.0, based on difference between mice
          #         and humans.
        PLivTCA = TCAPlas * exp(lnPLivTCAC) *
                  (Species == 3 ? 1.18 : (Species == 2 ? 1.18 : 0.66 ));
          # Multiplied by blood:plasma ratio to get Liver:Plasma
          # Rats = mice from Abbas and Fisher 1997
          # Humans from Fisher et al. 1998
          #         Uncertainty in mice, humans GSD = 1.4
          #         For rats, GSD = 2.0, based on difference between mice
          #         and humans.

# Binding Parameters for TCA
          # GM of Lumpkin et al. 2003; Schultz et al. 1999;
          #         Templin et al. 1993, 1995; Yu et al. 2000
          # Protein/TCA dissociation constant (umole/L)
          #         note - GSD = 3.29, 1.84, and 1.062 for mouse, rat, human
          kDissoc = exp(lnkDissocC) *
                  (Species == 3 ? 107. : (Species == 2 ? 275. : 182. ));
          # BMax = NSites * Protein concentration.  Sampled parameter is
          #         BMax/kD (determines binding at low concentrations)
          #         note - GSD = 1.64, 1.60, 1.20 for mouse, rat, human
          BMax = kDissoc * exp(lnBMaxkDC) *
                  (Species == 3 ? 0.88 : (Species == 2 ? 1.22 : 4.62 ));

# TCOH partitioning
          # Data from Abbas and Fisher 1997 (mouse) and Fisher et al.
          #         1998 (human).  For rat, used mouse values.
          #         Uncertainty in mice, humans GSD = 1.4
          #         For rats, GSD = 2.0, based on difference between mice
          #         and humans.

        PBodTCOH = exp(lnPBodTCOHC) *
                  (Species == 3 ? 1.11 : (Species == 2 ? 1.11 : 0.91 ));
        PLivTCOH = exp(lnPLivTCOHC) *
                  (Species == 3 ? 1.3 : (Species == 2 ? 1.3 : 0.59 ));

# TCOG partitioning
          # Use TCOH as a proxy, but uncertainty much greater
          # (e.g., use uniform prior, 100-fold up/down)
        PBodTCOG = exp(lnPBodTCOGC) *
                  (Species == 3 ? 1.11 : (Species == 2 ? 1.11 : 0.91 ));
        PLivTCOG = exp(lnPLivTCOGC) *
                  (Species == 3 ? 1.3 : (Species == 2 ? 1.3 : 0.59 ));

# DCVG distribution volume
          # exp(lnPeffDCVG) is the effective partition coefficient for
          # the "body" (non-blood) compartment
          # Diffuse prior distribution: loguniform 1e-3 to 1e3
          VDCVG = VBld +      # blood plus body (with "effective" PC)
          exp(lnPeffDCVG) * (VBod + VLiv);

# Absorption Rate Constants (/hr)
          # All priors are diffuse (log)uniform distributions
```

```
          # transfer from stomach centered on 1.4/hr, range up or down 100-fold,
          #         based on human stomach half-time of 0.5 hr.
        kTSD = exp(lnkTSD);
          # stomach absorption centered on 1.4/hr, range up or down 1000-fold
          kAS = exp(lnkAS);
          # assume no fecal excretion -- 100% absorption
          kTD = 0.0 * exp(lnkTD);
          # intestinal absorption centered on 0.75/hr, range up or down
          #         1000-fold, based on human transit time of small intestine
          #         of 4 hr   (95% throughput in 4 hr)
          kAD = exp(lnkAD);
          kASTCA = exp(lnkASTCA);
          kASTCOH = exp(lnkASTCOH);

# TCE Oxidative Metabolism Constants
# For rodents, in vitro microsomal data define priors (pooled).
# For human, combined in vitro microsomoal+hepatocellular individual data
#         define priors.
# All data from Elfarra et al. 1998; Lipscomb et al. 1997, 1998a,b
# For VMAX, scaling from in vitro data were (Barter et al. 2007):
#         32 mg microsomal protein/g liver
#         99 x 1e6 hepatocytes/g liver
#         Here, human data assumed representative of mouse and rats.
# For KM, two different scaling methods were used for microsomes:
#         Assume microsomal concentration = liver concentration, and
#                 use central estimate of liver:blood PC (see above)
#         Use measured microsome:air partition coefficient (1.78) and
#                 central estimate of blood:air PC (see above)
# For human KM from hepatocytes, used measured human hepatocyte:air
#         partition coefficient (21.62, Lipscomb et al. 1998), and
#         central estimate of blood:air PC.
#         Note that to that the hepatocyte:air PC is similar to that
#         found in liver homogenates (human: 29.4+/-5.1 from Fiserova-
#         Bergerova et al. 1984, and 54 for Fisher et al. 1998; rat:
#         27.2+/-3.4 from Gargas et al. 1989, 62.7 from Koisumi 1989,
#         43.6 from Sato et al. 1977; mouse: 23.2 from Fisher et al. 1991).
# For humans, sampled parameters are VMAX and ClC (VMAX/KM), due to
#         improved convergence.  VMAX is kept as a parameter because it
#         appears less uncertain (i.e., more consistent across microsomal
#         and hepatocyte data).

          # Central estimate of VMAX is 342, 76.2, and 32.3 (micromol/min/
          #         kg liver) for mouse, rat, human.  Converting to /hr by
          #         * (60 min/hr * 0.1314 mg/micromol) gives
          #         2700, 600, and 255 mg/hr/kg liver
          # Observed variability of about 2-fold GSD.  Assume 2-fold GSD for
          #         both uncertainty and variability
        VMAX = VLiv*exp(lnVMAXC)*
                  (Species == 3 ? 2700. : (Species == 2 ? 600. : 255.));

          # For mouse and rat central estimates for KM are 0.068~1.088 and
          #         0.039~0.679 mmol/l in blood, depending on the scaling
          #         method used.  Taking the geometric mean, and converting
          #         to mg/l by 131.4 mg/mmol gives 36. and 21. mg/l in blood.
          # For human, central estimate
          #         for Cl are 0.306~3.95 l/min/kg liver.  Taking the geometric
          #         mean and converting to /hr gives a central estimate of
          #         66. l/hr/kg.
          #         KM is then derived from KM = VMAX/(Cl*Vliv) (central estimate
          #         of
          # Note uncertainty due to scaling is about 4-fold.
          #         Variability is about 3-fold in mice, 1.3-fold in rats, and
          #         2- to 4- fold in humans (depending on scaling).
        KM = (Species == 3 ? 36.*exp(lnKMC) : (Species == 2 ? 21.*exp(lnKMC) :
VMAX/(VLiv*66.*exp(lnClC))));

# Oxidative metabolism splits
          # Fractional split of TCE to DCA
          # exp(lnFracOtherC) = ratio of DCA to non-DCA
          # Diffuse prior distribution: loguniform 1e-4 to 1e2
          FracOther = exp(lnFracOtherC)/(1+exp(lnFracOtherC));
          # Fractional split of TCE to TCA
          # exp(lnFracTCAC) = ratio of TCA to TCOH
          # TCA/TCOH = 0.1 from Lipscomb et al. 1998 using fresh hepatocytes,
          # but TCA/TCOH ~ 1 from Bronley-DeLancey et al 2006
          # GM = 0.32, GSD = 3.2
          FracTCA = 0.32*exp(lnFracTCAC)*(1-FracOther)/(1+0.32*exp(lnFracTCAC));

# TCE GSH Metabolism Constants
# Human in vitro data from Lash et al. 1999, define human priors.
#                             VMAX (nmol/min/     KM (mM)             CLeff (ml/min/
#                                   g tissue)                             g tissue)
#                         ---------------------------------------------
#                             [high affinity pathway only]  [total]
# Human liver cytosol:        ~423                0.0055~0.023        21.2~87.0
# Human liver cytosol+        ~211                --                  --
#         microsomes
#                             [total]             [total]             [total]
# Human hepatocytes*          12~30**             0.012~0.039***      0.2~0.5****
# Human kidney cytosol:       81                  0.0164~0.0263       3.08~4.93
#         * estimated visually from Fig 1, Lash et al. 1999
#         ** Fig 1A, data from 50~500 ppm headspace at 60 min
#                 and Fig 1B, data at 100~5000 ppm in headspace for 120 min
#         *** Fig 1B, 30~100 ppm headspace, converted to blood concentration
#                 using blood:air PC of 9.5
#         **** Fig 1A, data at 50 ppm headspace at 120 min and Fig 1B, data at
#                 25 and 50 ppm headspace at 120 min.
# Overall, human liver hepatocytes are probably most like the
#         intact liver (e.g., accounting for the competition between
#         GSH conjugation and oxidation).  So central estimates based
#         on those: CLeff ~ 0.32 ml/min/g tissue, KM ~ 0.022 mM in blood.
#         CLeff converted to 19 l/hr/kg; KM converted to 2.9 mg/l in blood
#         However, uncertainty in CLeff is large (values in cytosol
#         ~100-fold larger).  Moreover, Green et al. 1997 reported
#         DCVG formation in cytosol that was ~30,000-fold smaller
#         than Lash et al. (1998) in cytosol, which would be a VMAX
#         ~300-fold smaller than Lash et al. (1998) in hepatocytes.
#         Uncertainty in KM appears smaller (~4-fold)
#         CLC: GM = 19., GSD = 100; KM: GM = 2.9., GSD = 4.
#         In addition, at a single concentration, the variability
#         in human liver cytosol samples had a GSD=1.3.
# For the human kidney, the kidney cytosol values are used, with the same
#         uncertainty as for the liver.  Note that the DCVG formation rates
#         in rat kidney cortical cells and rat cytosol are quite similar
```

```
#         (see below).
#         CLC: GM = 230., GSD = 100; KM: GM = 2.7., GSD = 4.
# Rat and mouse in vitro data from Lash et al. 1995,1998 define rat and mouse
#         priors.  However, rats and mice are only assayed at 1 and 2 mM
#         providing only a bound on VMAX and very little data on KM.
#                              Rate at 2 mM        Equivalent          CLeff
#                                                  blood conc.         at 2 mM
#                              (nmol/min/          (mM)                (ml/min/
#                              g tissue)                       g tissue)
#                         ---------------------------------------------
# Rat     hepatocytes:         4.4~16              2.0                 0.0022~0.0079
#         liver cytosol:       8.0~12              1.7~2.0             0.0040~0.0072
#         kidney cells:        0.79~1.1  2.2                 0.00036~0.00049
#         kidney cytosol:      0.53~0.75 1.1~2.0             0.00027~0.00068
# Mouse   liver cytosol:       36~40               1.1~2.0             0.018~0.036
#         kidney cytosol:      6.2~9.3             0.91~2.0  0.0031~0.0102
#
# In most cases, rates were increased over the same sex/species at 1 mM,
#         indicating VMAX has not yet been reached.  The values between cells
#         and cytosol are more much consistent that in the human data.
#         These data therefore put a lower bound on VMAX and a lower bound
#         on CLC.  To account for in vitro-in vivo uncertainty, the lower
#         bound of the prior distribution is set 100-fold below the central
#         estimate of the measurements here.  In addition, Green et al.
#         (1997) found values 100-fold smaller than Lash et al. 1995, 1998.
#         Therefore diffuse prior distributions set to 1e-2~1e4.
# Rat liver: Bound on VMAX of 4.4~16, with GM of 8.4.  Converting to
#         mg/hr/kg tissue (* 131.4 ng/nmol * 60 min/hr * 1e3 g/kg / 1e6 mg/ng)
#         gives a central estimate of 66. mg/hr/kg tissue.  Bound on CL of
#         0.0022~0.0079, with GM of 0.0042.  Converting to l/hr/kg tissue
#         (* 60 min/hr) gives 0.25 l/hr/kg tissue.
# Rat kidney: Bound on VMAX of 0.53~1.1, with GM of 0.76.  Converting
#         to mg/hr/kg tissue gives a central estimate of 6.0 mg/hr/kg.
#         Bound on CL of 0.00027~0.00068, with GM of 0.00043.  Converting
#         to l/hr/kg tissue gives 0.026 l/hr/kg tissue.
# Mouse liver: Bound on VMAX of 36~40, with GM of 38.  Converting
#         to mg/hr/kg tissue gives a central estimate of 300. mg/hr/kg.
#         Bound on CL of 0.018~0.036, with GM of 0.025.  Converting
#         to l/hr/kg tissue gives 1.53 l/hr/kg tissue.
# Mouse kidney: Bound on VMAX of 6.2~9.3, with GM of 7.6.  Converting
#         to mg/hr/kg tissue gives a central estimate of 60. mg/hr/kg.
#         Bound on CL of 0.0031~0.0102, with GM of 0.0056.  Converting
#         to l/hr/kg tissue gives 0.34 l/hr/kg tissue.

         VMAXDCVG = VLiv*(Species == 3 ? (300.*exp(lnVMAXDCVGC)) : (Species == 2 ?
(66.*exp(lnVMAXDCVGC)) : (2.9*19.*exp(lnClDCVGC+lnKMDCVGC))));
       KMDCVG = (Species == 3 ? (VMAXDCVG/(VLiv*1.53*exp(lnClDCVGC))) : (Species ==
2 ? (VMAXDCVG/(VLiv*0.25*exp(lnClDCVGC))) : 2.9*exp(lnKMDCVGC)));
         VMAXKidDCVG = VKid*(Species == 3 ? (60.*exp(lnVMAXKidDCVGC)) : (Species ==
2 ? (6.0*exp(lnVMAXKidDCVGC)) : (2.7*230.*exp(lnClKidDCVGC+lnKMKidDCVGC))));
       KMKidDCVG = (Species == 3 ? (VMAXKidDCVG/(VKid*0.34*exp(lnClKidDCVGC))) :
(Species == 2 ? (VMAXKidDCVG/(VKid*0.026*exp(lnClKidDCVGC))) :
2.7*exp(lnKMKidDCVGC)));

# TCE Metabolism Constants for Chloral Kinetics in Lung (mg/hr)
#         Scaled to liver VMAX using data from Green et al. (1997)
#         in microsomal preparations (nmol/min/mg protein) at ~1 mM.
#         For humans, used detection limit of 0.03
#         Additional scaling by lung/liver weight ratio
#         from Brown et al. Table 21 (mouse and rat) or
#         ICRP Pub 89 Table 2.8 (Human female and male)
#         Uncertainty ~ 3-fold truncated at 3 GSD
   VMAXClara = exp(lnVMAXLungLivC) * VMAX *
         (Species == 3 ? (1.03/1.87*0.7/5.5):(Species == 2 ?
(0.08/0.82*0.5/3.4):(0.03/0.33*(Male == 0 ? (0.42/1.4) : (0.5/1.8)))));
   KMClara = exp(lnKMClara);
# Fraction of Respiratory Metabolism that goes to system circulation
# (translocated to the liver)
   FracLungSys = exp(lnFracLungSysC)/(1 + exp(lnFracLungSysC));

# TCOH Metabolism Constants (mg/hr)
         # No in vitro data.  So use diffuse priors of
         #         1e-4 to 1e4 mg/hr/kg^0.75 for VMAX
         #                  (4e-5 to 4000 mg/hr for rat),
         #         1e-4 to 1e4 mg/l for KM,
         #         and 1e-5 to 1e3 l/hr/kg^0.75 for Cl
         #                  (2e-4 to 2.4e4 l/hr for human)
         VMAXTCOH = BW75*
                  (Species == 3 ? (exp(lnVMAXTCOHC)) : (Species == 2 ?
(exp(lnVMAXTCOHC)) : (exp(lnClTCOHC+lnKMTCOH))));
         KMTCOH = exp(lnKMTCOH);
         VMAXGluc = BW75*
                  (Species == 3 ? (exp(lnVMAXGlucC)) : (Species == 2 ?
(exp(lnVMAXGlucC)) : (exp(lnClGlucC+lnKMGluc))));
         KMGluc = exp(lnKMGluc);
         # No in vitro data.  So use diffuse priors of
         #         1e-5 to 1e3 kg^0.25/hr (3.5e-6/hr to 3.5e2/hr for human)
         kMetTCOH = exp(lnkMetTCOHC) / BW25;

# TCA kinetic parameters
         # Central estimate based on GFR clearance per unit body weight
         #         10.0, 8.7, 1.8 ml/min/kg for mouse, rat, human
         #         (= 0.6, 0.522, 0.108 l/hr/kg) from Lin 1995.
         #         = CL_GFR / BW (BW=0.02 for mouse, 0.265 for rat, 70 for human)
         #         kUrn = CL_GFR / VPlas
         #         Diffuse prior with uncertainty of up,down 100-fold
         kUrnTCA = exp(lnkUrnTCAC) * BW / VPlas *
                  (Species == 3 ? 0.6 : (Species == 2 ? 0.522 : 0.108));
         # No in vitro data.  So use diffuse priors of
         #         1e-4 to 1e2 /hr/kg^0.25 (0.3/hr to 35/hr for human)
         kMetTCA = exp(lnkMetTCAC) / BW25;

# TCOG kinetic parameters
         # No in vitro data.  So use diffuse priors of
         #         1e-4 to 1e2 /hr/kg^0.25 (0.3/hr to 35/hr for human)
         kBile = exp(lnkBileC) / BW25;
       kEHR = exp(lnkEHRC) / BW25;
         # Central estimate based on GFR clearance per unit body weight
         #         10.0, 8.7, 1.8 ml/min/kg for mouse, rat, human
         #         (= 0.6, 0.522, 0.108 l/hr/kg) from Lin 1995.
         #         = CL_GFR / BW (BW=0.02 for mouse, 0.265 for rat, 70 for human)
         #         kUrn = CL_GFR / VBld
         #         Diffuse prior with Uncertainty of up,down 1000-fold
         kUrnTCOG = exp(lnkUrnTCOGC) * BW / (VBodTCOH * PBodTCOG) *
```

```
                    (Species == 3 ? 0.6 : (Species == 2 ? 0.522 : 0.108));

# DCVG Kinetics (/hr)
          # Fraction of renal TCE GSH conj. "directly" to DCVC via "first pass"
          # exp(lnFracOtherCC) = ratio of direct/non-direct
          # Diffuse prior distribution: loguniform 1e-3 to 1e3
          # FIXED in v1.2.3
          # In ".in" files, set to 1, so that all kidney GSH conjugation
          # is assumed to directly produce DCVC (model lacks identifiability
          # otherwise).
          FracKidDCVC = exp(lnFracKidDCVCC)/(1 + exp(lnFracKidDCVCC));
          # No in vitro data.  So use diffuse priors of
          #         1e-4 to 1e2 /hr/kg^0.25 (0.3/hr to 35/hr for human)
          kDCVG = exp(lnkDCVGC) / BW25;

# DCVC Kinetics in Kidney (/hr)
          # No in vitro data.  So use diffuse priors of
          #         1e-4 to 1e2 /hr/kg^0.25 (0.3/hr to 35/hr for human)
          kNAT = exp(lnkNATC) / BW25;
          kKidBioact = exp(lnkKidBioactC) / BW25;

# CC data initialization
          Rodents = (CC > 0 ? NRodents : 0.0); # Closed chamber simulation
          VCh = (CC > 0 ? VChC - (Rodents * BW) : 1.0);
                    # Calculate net chamber volume
          kLoss = (CC > 0 ? exp(lnkLossC) : 0.0);

#*****************************************************************************
#***                   State Variable Initialization and Scaling           ***
#*****************************************************************************
# NOTE: All State Variables are automatically set to 0 initially,
# unless re-initialized here

          ACh = (CC * VCh * MWTCE) / 24450.0;    # Initial amount in chamber

};
###################### End of Initialization ########################

Dynamics{

#*****************************************************************************
#***                        Dynamic physiological parameter scaling          ***
#*****************************************************************************
# State Variables with dynamics:
#         none
# Input Variables:
#         QPmeas
# Other State Variables and Global Parameters:
#         QC
#         VPR
#         DResptmp
#         QPsamp
#         QFatCtmp
#         QGutCtmp
#         QLivCtmp
#         QSlwCtmp
#         QKidCtmp
#         FracPlas
# Temporary variables used:
#         none
# Temporary variables assigned:
#         QP
#         DResp
#         QCnow
#         QFat
#         QGut
#         QLiv
#         QSlw
#         QKid
#         QGutLiv
#         QRap
#         QCPlas
#         QBodPlas
#         QGutLivPlas
# Notes:
#*****************************************************************************

# QP uses QPmeas if value is > 0, otherwise uses sampled value
          QP = (QPmeas > 0 ? QPmeas : QPsamp);
          DResp = DResptmp * QP;

# QCnow uses QPmeas/VPR if QPmeas > 0, otherwise uses sampled value
          QCnow = (QPmeas > 0 ? QPmeas/VPR : QC);

# These done here in dynamics in case QCnow changes
# Blood Flows to Tissues (L/hr)
        QFat = (QFatCtmp) * QCnow; #
        QGut = (QGutCtmp) * QCnow; #
        QLiv = (QLivCtmp) * QCnow; #
        QSlw = (QSlwCtmp) * QCnow; #

        QKid = (QKidCtmp) * QCnow; #
     QGutLiv = QGut + QLiv; #
          QRap = QCnow - QFat - QGut - QLiv - QSlw - QKid;
          QRapCtmp = QRap/QCnow; #(vrisk)
          QBod = QCnow - QGutLiv;

# Plasma Flows to Tissues (L/hr)
      QCPlas = FracPlas * QCnow; #
    QBodPlas = FracPlas * QBod; #
    QGutLivPlas = FracPlas * QGutLiv; #

#*****************************************************************************
#***                  Exposure and Absorption calculations                 ***
#*****************************************************************************
# State Variables with dynamics:
#         AStom
#         ADuod
#         AStomTCA
#         AStomTCOH
# Input Variables:
#         IVDose
#         PDose
#         Drink
```

```
#         Conc
#         IVDoseTCA
#         PODoseTCA
#         IVDoseTCOH
#         PODoseTCOH
# Other State Variables and Global Parameters:
#         ACh
#         CC
#         VCh
#         MWTCE
#         BW
#         TChng
#         kAS
#         kTSD
#         kAD
#         kTD
#         kASTCA
#         kASTCOH
# Temporary variables used:
#         none
# Temporary variables assigned:
#         kIV - rate into CVen
#         kIA - rate into CArt
#         kPV - rate into portal vein
#         kStom - rate into stomach
#         kDrink - incorporated into RAO
#         RAO - rate into gut (oral absorption - both gavage and drinking water)
#         CInh - inhalation exposure concentration
#         kIVTCA - rate into blood
#         kStomTCA - rate into stomach
#         kPOTCA - rate into liver (oral absorption)
#         kIVTCOH - rate into blood
#         kStomTCOH - rate into stomach
#         kPOTCOH - rate into liver (oral absorption)
# Notes:
# For oral dosing, using "Spikes" for instantaneous inputs
# Inhalation Concentration (mg/L)
#         CInh uses Conc when open chamber (CC=0) and
#         ACh/VCh when closed chamber CC>0.
#*******************************************************************************

#### TCE DOSING
## IV route
    kIV = (IVDose * BW) / TChng;# IV infusion rate (mg/hr)
                                    # (IVDose constant for duration TChng)
    kIA = (IADose * BW) / TChng;        # IA infusion rate (mg/hr)
    kPV = (PVDose * BW) / TChng;        # PV infusion rate (mg/hr)
    kStom = (PDose * BW) / TChng;# PO dose rate (into stomach) (mg/hr)

## Oral route
# Amount of TCE in stomach -- for oral dosing only (mg)
    dt(AStom) = kStom - AStom * (kAS + kTSD);

# Amount of TCE in duodenum -- for oral dosing only (mg)
    dt(ADuod) = (kTSD * AStom) - (kAD + kTD) * ADuod;
# Rate of absorption from drinking water
    kDrink = (Drink * BW) / 24.0; #Ingestion rate via drinking water (mg/hr)

# Total rate of absorption including gavage and drinking water
    RAO = kDrink + (kAS * AStom) + (kAD * ADuod);
## Inhalation route
    CInh = (CC > 0 ? ACh/VCh : Conc*MWTCE/24450.0); # in mg/l

#### TCA Dosing
          kIVTCA = (IVDoseTCA * BW) / TChng;  # TCA IV infusion rate (mg/hr)
          kStomTCA = (PODoseTCA * BW) / TChng; # TCA PO dose rate into stomach
          dt(AStomTCA) = kStomTCA - AStomTCA * kASTCA;
          kPOTCA = AStomTCA * kASTCA;  # TCA oral absorption rate (mg/hr)

#### TCOH Dosing
          kIVTCOH = (IVDoseTCOH * BW) / TChng;#TCOH IV infusion rate (mg/hr)
          kStomTCOH = (PODoseTCOH * BW) / TChng; # TCOH PO dose rate into stomach
    dt(AStomTCOH) = kStomTCOH - AStomTCOH * kASTCOH;
          kPOTCOH = AStomTCOH * kASTCOH;# TCOH oral absorption rate (mg/hr)

#*******************************************************************************
#***                          TCE Model                                      ***
#*******************************************************************************
# State Variables with dynamics:
#         ARap,               # Amount in rapidly perfused tissues
#         ASlw,               # Amount in slowly perfused tissues
#         AFat,               # Amount in fat
#         AGut,               # Amount in gut
#         ALiv,               # Amount in liver
#         AInhResp,
#         AResp,
#         AExhResp,
#         AKid,               # Amount in Kidney -- currently in Rap tissue
#         ABld,               # Amount in Blood -- currently in Rap tissue
#         ACh,                # Amount of TCE in closed chamber
# Input Variables:
#         none
# Other State Variables and Global Parameters:
#         VRap
#         PRap
#         VSlw
#         PSlw
#         VFat
#         PFat
#         VGut
#         PGut
#         VLiv
#         PLiv
#         VRespLum
#         VRespEff
#         FracLungSys
#         VKid
#         PKid
#         VBld
#         VMAXClara
#         KMClara
#         PB
#         Rodents
#         VCh
#         kLoss
```

```
#         VMAX
#         KM
#         VMAXDCVG
#         KMDCVG
#         VMAXKidDCVG
#         KMKidDCVG
# Temporary variables used:
#         QM
#         QFat
#         QGutLiv
#         QSlw
#         QRap
#         QKid
#         kIV
#         QCnow
#         CInh
#         QP
#         RAO
# Temporary variables assigned:
#         QM
#         CRap
#         CSlw
#         CFat
#         CGut
#         CLiv
#         CInhResp
#         CResp
#         CExhResp
#         ExhFactor
#         CMixExh
#         CKid
#         CVRap
#         CVSlw
#         CVFat
#         CVGut
#         CVLiv
#         CVTB
#         CVKid
#         CVen
#         RAMetLng
#         CArt_tmp
#         CArt
#         CAlv
#         RAMetLiv1
#         RAMetLiv2
#         RAMetKid
# Notes:
#*******************************************************************************
#

#****Blood (venous)*************************************************************
# Tissue Concentrations (mg/L)
          CRap = ARap/VRap;
          CSlw = ASlw/VSlw;
          CFat = AFat/VFat;
          CGut = AGut/VGut;
          CLiv = ALiv/VLiv;
          CKid = AKid/VKid;
# Venous Concentrations (mg/L)
          CVRap = CRap / PRap;
          CVSlw = CSlw / PSlw;
          CVFat = CFat / PFat;
          CVGut = CGut / PGut;
          CVLiv = CLiv / PLiv;
          CVKid = CKid / PKid;
# Concentration of TCE in mixed venous blood (mg/L)
          CVen = ABld/VBld;
# Dynamics for blood
    dt(ABld) = (QFat*CVFat + QGutLiv*CVLiv + QSlw*CVSlw +
                    QRap*CVRap + QKid*CVKid + kIV) - CVen * QCnow;

#****Gas exchange and Respiratory Metabolism************************************
#
    QM = QP/0.7;    # Minute-volume
    CInhResp = AInhResp/VRespLum;
    CResp = AResp/VRespEff;
    CExhResp = AExhResp/VRespLum;
    dt(AInhResp) = (QM*CInh + DResp*(CResp-CInhResp) - QM*CInhResp);
    RAMetLng = VMAXClara * CResp/(KMClara + CResp);
    dt(AResp) = (DResp*(CInhResp + CExhResp - 2*CResp) - RAMetLng);
    CArt_tmp = (QCnow*CVen + QP*CInhResp)/(QCnow + (QP/PB));
    dt(AExhResp) = (QM*(CInhResp-CExhResp) + QP*(CArt_tmp/PB-CInhResp) +
                    DResp*(CResp-CExhResp));
    CMixExh = (CExhResp > 0 ? CExhResp : 1e-15); # mixed exhaled breath

# Concentration in alveolar air (mg/L)
          # Correction factor for exhaled air to account for
          # absorption/desorption/metabolism in respiratory tissue
          # = 1 if DResp = 0
          ExhFactor_den = (QP * CArt_tmp / PB + (QM-QP)*CInhResp);
          ExhFactor = (ExhFactor_den > 0) ? (
                    QM * CMixExh / ExhFactor_den) : 1;
          # End-exhaled breath (corrected for absorption/
          #         desorption/metabolism in respiratory tissue)
          CAlv = CArt_tmp / PB * ExhFactor;
# Concentration in arterial blood entering circulation (mg/L)
          CArt = CArt_tmp + kIA/QCnow;  # add inter-arterial dose

#****Other dynamics for inhalation/exhalation ***********************************
# Dynamics for amount of TCE in closed chamber
    dt(ACh) = (Rodents * (QM * CMixExh - QM * ACh/VCh)) - (kLoss * ACh);

#**** Non-metabolizing tissues *************************************************
# Amount of TCE in rapidly perfused tissues (mg)
    dt(ARap) = QRap * (CArt - CVRap);
# Amount of TCE in slowly perfused tissues
    dt(ASlw) = QSlw * (CArt - CVSlw);
# Amount of TCE in fat tissue (mg)
    dt(AFat) = QFat*(CArt - CVFat);
# Amount of TCE in gut compartment (mg)
    dt(AGut) = (QGut * (CArt - CVGut)) + RAO;

#**** Liver ********************************************************************
# Rate of TCE oxidation by P450 to TCA, TCOH, and other (DCA) in liver (mg/hr)
```

```
          RAMetLiv1 = (VMAX * CVLiv) / (KM + CVLiv);
# Rate of TCE metabolized to DCVG in liver (mg)
          RAMetLiv2 = (VMAXDCVG * CVLiv) / (KMDCVG + CVLiv);
# Dynamics for amount of TCE in liver (mg)
    dt(ALiv) = (QLiv * (CArt - CVLiv)) + (QGut * (CVGut - CVLiv))
                              - RAMetLiv1 - RAMetLiv2 + kPV; # added PV dose

#**** Kidney ********************************************************************
# Rate of TCE metabolized to DCVG in kidney (mg) #
          RAMetKid = (VMAXKidDCVG * CVKid) / (KMKidDCVG + CVKid);
# Amount of TCE in kidney compartment (mg)
    dt(AKid) = (QKid * (CArt - CVKid)) - RAMetKid;

#*******************************************************************************
#***                       TCOH Sub-model                                    ***
#*******************************************************************************
# State Variables with dynamics:
#          ABodTCOH
#          ALivTCOH
# Input Variables:
#          none
# Other State Variables and Global Parameters:
#          ABileTCOG
#          kEHR
#          VBodTCOH
#          PBodTCOH
#          VLiv
#          PLivTCOH
#          VMAXTCOH
#          KMTCOH
#          VMAXGluc
#          KMGluc
#          kMetTCOH - hepatic metabolism of TCOH (e.g., to DCA)
#          FracOther
#          FracTCA
#          StochTCOHTCE
#          StochTCOHGluc
#          FracLungSys
# Temporary variables used:
#          QBod
#          QGutLiv
#          QCnow
#          kPOTCOH
#          RAMetLiv1
#          RAMetLng
# Temporary variables assigned:
#          CVBodTCOH
#          CVLivTCOH
#          CTCOH
#          RAMetTCOHTCA
#          RAMetTCOHGluc
#          RAMetTCOH
#          RARecircTCOG
# Notes:
#*******************************************************************************
#**** Blood (venous=arterial) ****************************************************
# Venous Concentrations (mg/L)
          CVBodTCOH = ABodTCOH / VBodTCOH / PBodTCOH;
          CVLivTCOH = ALivTCOH / VLiv / PLivTCOH;
          CTCOH = (QBod * CVBodTCOH + QGutLiv * CVLivTCOH + kIVTCOH)/QCnow;

#**** Body **********************************************************************
# Amount of TCOH in body
    dt(ABodTCOH) = QBod * (CTCOH - CVBodTCOH);

#**** Liver *********************************************************************

# Rate of oxidation of TCOH to TCA (mg/hr)
          RAMetTCOHTCA = (VMAXTCOH * CVLivTCOH) / (KMTCOH + CVLivTCOH);
# Amount of glucuronidation to TCOG (mg/hr)
          RAMetTCOHGluc = (VMAXGluc * CVLivTCOH) / (KMGluc + CVLivTCOH);
# Amount of TCOH metabolized to other (e.g., DCA)
          RAMetTCOH = kMetTCOH * ALivTCOH;
# Amount of TCOH-Gluc recirculated (mg)
          RARecircTCOG = kEHR * ABileTCOG;
# Amount of TCOH in liver (mg)
    dt(ALivTCOH) = kPOTCOH + QGutLiv * (CTCOH - CVLivTCOH)
                    - RAMetTCOH - RAMetTCOHTCA - RAMetTCOHGluc
                    + ((1.0 - FracOther - FracTCA) * StochTCOHTCE *
                    (RAMetLiv1 + FracLungSys*RAMetLng))
                    + (StochTCOHGluc * RARecircTCOG);

#*******************************************************************************
#***                       TCA Sub-model                                     ***
#*******************************************************************************
# State Variables with dynamics:
#          APlasTCA
#          ABodTCA
#          ALivTCA
#          AUrnTCA
#          AUrnTCA_sat
#          AUrnTCA_collect
# Input Variables:
#          TCAUrnSat
#          UrnMissing
# Other State Variables and Global Parameters:
#          VPlas
#          MWTCA
#          kDissoc
#          BMax
#          kMetTCA -- hepatic metabolism of TCA (e.g., to DCA)
#          VBod
#          PBodTCA
#          PLivTCA
#          kUrnTCA
#          FracTCA
#          StochTCATCE
#          StochTCATCOH
#          FracLungSys
# Temporary variables used:
#          kIVTCA
#          kPOTCA
#          QBodPlas
#          QGutLivPlas
```

```
#         QCPlas
#         RAMetLiv1
#         RAMetTCOHTCA
#         RAMetLng
# Temporary variables assigned:
#         CPlasTCA
#         CPLasTCAMole
#         a, b, c
#         CPlasTCAFreeMole
#         CPlasTCAFree
#         APlasTCAFree
#         CPlasTCABnd
#         CBodTCAFree
#         CLivTCAFree
#         CBodTCA
#         CLivTCA
#         CVBodTCA
#         CVLivTCA
#         RUrnTCA
#         RAMetTCA
# Notes:
#*************************************************************************
#**** Plasma *********************************************************
# Concentration of TCA in plasma (umoles/L)
          CPlasTCA = (APlasTCA<1.0e-15 ? 1.0e-15 : APlasTCA/VPlas);
# Concentration of free TCA in plasma in (umoles/L)
          CPlasTCAMole = (CPlasTCA / MWTCA) * 1000.0;
          a = kDissoc+BMax-CPlasTCAMole;
          b = 4.0*kDissoc*CPlasTCAMole;
          c = (b < 0.01*a*a ? b/2.0/a : sqrt(a*a+b)-a);
          CPlasTCAFreeMole = 0.5*c;
# Concentration of free TCA in plasma (mg/L)
          CPlasTCAFree = (CPlasTCAFreeMole * MWTCA) / 1000.0;
          APlasTCAFree = CPlasTCAFree * VPlas;
# Concentration of bound TCA in plasma (mg/L)
          CPlasTCABnd = (CPlasTCA<CPlasTCAFree ? 0 : CPlasTCA-CPlasTCAFree);
# Concentration in body and liver
          CBodTCA = (ABodTCA<0 ? 0 : ABodTCA/VBod);
          CLivTCA = (ALivTCA<1.0e-15 ? 1.0e-15 : ALivTCA/VLiv);
# Total concentration in venous plasma (free+bound)
          CVBodTCAFree = (CBodTCA / PBodTCA);     # free in equilibrium
          CVBodTCA = CPlasTCABnd + CVBodTCAFree;
          CVLivTCAFree = (CLivTCA / PLivTCA);
          CVLivTCA = CPlasTCABnd + CVLivTCAFree;  # free in equilibrium
# Rate of urinary excretion of TCA
          RUrnTCA = kUrnTCA * APlasTCAFree;
# Dynamics for amount of total (free+bound) TCA in plasma (mg)
    dt(APlasTCA) = kIVTCA + (QBodPlas*CVBodTCA) + (QGutLivPlas*CVLivTCA)
                          - (QCPlas * CPlasTCA) - RUrnTCA;

#**** Body ***********************************************************
# Dynamics for amount of TCA in the body (mg)
    dt(ABodTCA) = QBodPlas * (CPlasTCAFree - CVBodTCAFree);

#**** Liver **********************************************************
# Rate of metabolism of TCA
          RAMetTCA = kMetTCA * ALivTCA;

# Dynamics for amount of TCA in the liver (mg)
    dt(ALivTCA) = kPOTCA + QGutLivPlas*(CPlasTCAFree - CVLivTCAFree)
                         - RAMetTCA + (FracTCA * StochTCATCE *
                         (RAMetLiv1 + FracLungSys*RAMetLng))
                         + (StochTCATCOH * RAMetTCOHTCA);

#**** Urine **********************************************************
# Dynamics for amount of TCA in urine (mg)
    dt(AUrnTCA) = RUrnTCA;
    dt(AUrnTCA_sat) = TCAUrnSat*(1-UrnMissing)* RUrnTCA;
                    # Saturated, but not missing collection times
    dt(AUrnTCA_collect) = (1-TCAUrnSat)*(1-UrnMissing)*RUrnTCA;
                    # Not saturated and not missing collection times

#*************************************************************************
#***                        TCOG Sub-model                             ***
#*************************************************************************
# State Variables with dynamics:
#         ABodTCOG
#         ALivTCOG
#         ABileTCOG
#         AUrnTCOG
#         AUrnTCOG_sat
#         AUrnTCOG_collect
# Input Variables:
#         TCOGUrnSat
#         UrnMissing
# Other State Variables and Global Parameters:
#         VBodTCOH
#         VLiv
#         PBodTCOG
#         PLivTCOG
#         kUrnTCOG
#         kBile
#         StochGlucTCOH
# Temporary variables used:
#         QBod
#         QGutLiv
#         QCnow
#         RAMetTCOHGluc
#         RARecircTCOG
# Temporary variables assigned:
#         CVBodTCOG
#         CVLivTCOG
#         CTCOG
#         RUrnTCOG
#         RBileTCOG
# Notes:
#*************************************************************************
#**** Blood (venous=arterial) ****************************************
# Venous Concentrations (mg/L)
          CVBodTCOG = ABodTCOG / VBodTCOH / PBodTCOG;
          CVLivTCOG = ALivTCOG / VLiv / PLivTCOG;
          CTCOG = (QBod * CVBodTCOG + QGutLiv * CVLivTCOG)/QCnow;
#**** Body ***********************************************************
# Amount of TCOG in body
          RUrnTCOG = kUrnTCOG * ABodTCOG;
```

```
    dt(ABodTCOG) = QBod * (CTCOG - CVBodTCOG) - RUrnTCOG;
          RUrnTCOGTCOH = RUrnTCOG*StochTCOHGluc; #(vrisk)
#**** Liver ************************************************************************
# Amount of TCOG in liver (mg)
          RBileTCOG = kBile * ALivTCOG;
    dt(ALivTCOG) = QGutLiv * (CTCOG - CVLivTCOG)
                   + (StochGlucTCOH * RAMetTCOHGluc) - RBileTCOG;

#**** Bile *************************************************************************
# Amount of TCOH-Gluc excreted into bile (mg)
    dt(ABileTCOG) = RBileTCOG - RARecircTCOG;

#**** Urine ************************************************************************
# Amount of TCOH-Gluc excreted in urine (mg)
    dt(AUrnTCOG) = RUrnTCOG;
    dt(AUrnTCOG_sat) = TCOGUrnSat*(1-UrnMissing)*RUrnTCOG;
                   # Saturated, but not missing collection times
    dt(AUrnTCOG_collect) = (1-TCOGUrnSat)*(1-UrnMissing)*RUrnTCOG;
                   # Not saturated and not missing collection times

#************************************************************************************
#***                        DCVG Sub-model                                       ***
#************************************************************************************
# State Variables with dynamics:
#         ADCVGmol
# Input Variables:
#         none
# Other State Variables and Global Parameters:
#         kDCVG
#         FracKidDCVC         # Fraction of kidney DCVG going to DCVC in first pass
#         VDCVG
# Temporary variables used:
#         RAMetLiv2
#         RAMetKid
# Temporary variables assigned:
#         RAMetDCVGmol
#         CDCVGmol
# Notes:
#         Assume negligible GGT activity in liver as compared to kidney,
#         supported by in vitro data on GGT (even accounting for 5x
#         greater liver mass relative to kidney mass), as well as lack
#         of DCVC detected in blood.
#         "FracKidDCVC" Needed to account for "first pass" in
#         kidney (TCE->DCVG->DCVC without systemic circulation of DCVG).
#************************************************************************************
# Rate of metabolism of DCVG to DCVC
          RAMetDCVGmol = kDCVG * ADCVGmol;
# Dynamics for DCVG in blood
    dt(ADCVGmol) = (RAMetLiv2 + RAMetKid*(1-FracKidDCVC)) / MWTCE
                   - RAMetDCVGmol;
# Concentration of DCVG in blood (in mmoles/l)
          CDCVGmol = ADCVGmol / VDCVG;

#************************************************************************************
#***                        DCVC Sub-model                                       ***
#************************************************************************************
# State Variables with dynamics:
#         ADCVC
#         AUrnNDCVC
# Input Variables:
#         none
# Other State Variables and Global Parameters:
#         MWDCVC
#         FracKidDCVC
#         StochDCVCTCE
#         kNAT
#         kKidBioact
#         StochN
# Temporary variables used:
#         RAMetDCVGmol
#         RAMetKid
# Temporary variables assigned:
#         RAUrnDCVC
# Notes:
#         Cannot detect DCVC in blood, so assume all is locally generated
#         and excreted or bioactivated in kidney.
#************************************************************************************
# Amount of DCVC in kidney (mg)
    dt(ADCVC) = RAMetDCVGmol * MWDCVC
                   + RAMetKid * FracKidDCVC * StochDCVCTCE
                   - ((kNAT + kKidBioact) * ADCVC);
# Rate of NAcDCVC excretion into urine (mg)
          RAUrnDCVC = kNAT * ADCVC;
# Dynamics for amount of N Acetyl DCVC excreted (mg)
     dt(AUrnNDCVC) = StochN * RAUrnDCVC;
          RUrnNDCVC = StochN * RAUrnDCVC; #(vrisk)
#************************************************************************************
#***                        Total Mass Balance                                   ***
#************************************************************************************
#**** Mass Balance for TCE *********************************************************
# Total intake from inhalation (mg)
          RInhDose = QM * CInh;
    dt(InhDose) = RInhDose;
# Amount of TCE absorbed by non-inhalation routes (mg)
    dt(AO) = RAO + kIV + kIA + kPV; #(vrisk)
# Total dose
          TotDose = InhDose + AO; #(vrisk)
# Total in tissues
          TotTissue = #(vrisk)
                   ARap + ASlw + AFat + AGut + ALiv + AKid + ABld + #(vrisk)
                   AInhResp + AResp + AExhResp; #(vrisk)
# Total metabolized
    dt(AMetLng) = RAMetLng; #(vrisk)
    dt(AMetLiv1) = RAMetLiv1; #(vrisk)
    dt(AMetLiv2) = RAMetLiv2; #(vrisk)
    dt(AMetKid) = RAMetKid; #(vrisk)
          ATotMetLiv = AMetLiv1 + AMetLiv2; #(vrisk)
          TotMetab = AMetLng + ATotMetLiv + AMetKid; #(vrisk)
          AMetLivOther = AMetLiv1 * FracOther; #(vrisk)
          AMetGSH = AMetLiv2 + AMetKid; #(vrisk)
# Amount of TCE excreted in feces (mg)
          RAExc = kTD * ADuod; #(vrisk)
    dt(AExc) = RAExc; #(vrisk)
# Amount exhaled (mg)
```

```
          RAExh = QM * CMixExh;
    dt(AExh) = RAExh;
# Mass balance
          TCEDiff = TotDose - TotTissue - TotMetab; #(vrisk)
          MassBalTCE = TCEDiff - AExc - AExh; #(vrisk)

#**** Mass Balance for TCOH ******************************************************
# Total production/intake of TCOH
    dt(ARecircTCOG) = RARecircTCOG; #(vrisk)
    dt(AOTCOH) = kPOTCOH + kIVTCOH; #(vrisk)
          TotTCOHIn = AOTCOH + ((1.0 - FracOther - FracTCA) * #(vrisk)
                    StochTCOHTCE * (AMetLiv1 + FracLungSys*AMetLng)) + #(vrisk)
                    (StochTCOHGluc * ARecircTCOG); #(vrisk)
          TotTCOHDose = AOTCOH + ((1.0 - FracOther - FracTCA) * #(vrisk)
                    StochTCOHTCE * (AMetLiv1 + FracLungSys*AMetLng)); #(vrisk)
# Total in tissues
          TotTissueTCOH = ABodTCOH + ALivTCOH; #(vrisk)
# Total metabolism of TCOH
    dt(AMetTCOHTCA) = RAMetTCOHTCA; #(vrisk)
    dt(AMetTCOHGluc) = RAMetTCOHGluc; #(vrisk)
    dt(AMetTCOHOther) = RAMetTCOH; #(vrisk)
          TotMetabTCOH = AMetTCOHTCA + AMetTCOHGluc + AMetTCOHOther; #(vrisk)
# Mass balance
          MassBalTCOH = TotTCOHIn - TotTissueTCOH - TotMetabTCOH; #(vrisk)

#**** Mass Balance for TCA *******************************************************
# Total production/intake of TCA
    dt(AOTCA) = kPOTCA + kIVTCA; #(vrisk)
          TotTCAIn = AOTCA + (FracTCA*StochTCATCE*(AMetLiv1 + #(vrisk)
                    FracLungSys*AMetLng)) + (StochTCATCOH*AMetTCOHTCA); #(vrisk)
# Total in tissues
          TotTissueTCA = APlasTCA + ABodTCA + ALivTCA; #(vrisk)
# Total metabolism of TCA
    dt(AMetTCA) = RAMetTCA; #(vrisk)
# Mass balance
          TCADiff = TotTCAIn - TotTissueTCA - AMetTCA; #(vrisk)
          MassBalTCA = TCADiff - AUrnTCA; #(vrisk)

#**** Mass Balance for TCOG ******************************************************
# Total production of TCOG
          TotTCOGIn = StochGlucTCOH * AMetTCOHGluc; #(vrisk)
# Total in tissues
          TotTissueTCOG = ABodTCOG + ALivTCOG + ABileTCOG; #(vrisk)
# Mass balance
          MassBalTCOG = TotTCOGIn - TotTissueTCOG - #(vrisk)
                    ARecircTCOG - AUrnTCOG; #(vrisk)

#**** Mass Balance for DCVG ******************************************************
# Total production of DCVG
    dt(ADCVGIn) = (RAMetLiv2 + RAMetKid*(1-FracKidDCVC)) / MWTCE; #(vrisk)
# Metabolism of DCVG
    dt(AMetDCVG) = RAMetDCVGmol; #(vrisk)
# Mass balance
          MassBalDCVG = ADCVGIn - ADCVGmol - AMetDCVG; #(vrisk)

#**** Mass Balance for DCVC ******************************************************
# Total production of DCVC
    dt(ADCVCIn) = RAMetDCVGmol * MWDCVC  #(vrisk)
                + RAMetKid * FracKidDCVC * StochDCVCTCE;#(vrisk)
# Bioactivation of DCVC
    dt(ABioactDCVC) = (kKidBioact * ADCVC);#(vrisk)
# Mass balance
          AUrnNDCVCequiv = AUrnNDCVC/StochN;
          MassBalDCVC = ADCVCIn - ADCVC - ABioactDCVC - AUrnNDCVCequiv;#(vrisk)

#*******************************************************************************
#***                          Dynamic Outputs                                 ***
#*******************************************************************************
# Amount exhaled during exposure (mg)
    dt(AExhExp) = (CInh > 0 ? RAExh : 0);

#*******************************************************************************
#***                          Dose Metrics                                    ***
#*******************************************************************************
#**** AUCs in mg-hr/L unless otherwise noted **********************************
#AUC of TCE in arterial blood
    dt(AUCCBld) = CArt; #(vrisk)
#AUC of TCE in liver
    dt(AUCCLiv) = CLiv; #(vrisk)
#AUC of TCE in kidney
    dt(AUCCKid) = CKid; #(vrisk)
#AUC of TCE in rapidly perfused
    dt(AUCCRap) = CRap; #(vrisk)
#AUC of TCOH in blood
    dt(AUCCTCOH) = CTCOH; #(vrisk)
#AUC of TCOH in body
    dt(AUCCBodTCOH) = ABodTCOH / VBodTCOH; #(vrisk)
#AUC of free TCA in the plasma (mg/L * hr)
    dt(AUCPlasTCAFree) = CPlasTCAFree; #(vrisk)
#AUC of total TCA in plasma (mg/L * hr)
    dt(AUCPlasTCA) = CPlasTCA; #(vrisk)
#AUC of TCA in liver (mg/L * hr)
    dt(AUCLivTCA) = CLivTCA; #(vrisk)
#AUC of total TCOH (free+gluc) in TCOH-equiv in blood (mg/L * hr)
    dt(AUCTotCTCOH) = CTCOH + CTCOGTCOH; #(vrisk)
#AUC of DCVG in blood (mmol/L * hr) -- NOTE moles, not mg
    dt(AUCCDCVG) = CDCVGmol; #(vrisk)
};
################ End of Dynamics ####################################


CalcOutputs{

#**** Static outputs for comparison to data **************************************
# TCE
          RetDose = ((InhDose-AExhExp) > 0 ? (InhDose - AExhExp) : 1e-15);
          CAlvPPM = (CAlv < 1.0e-15 ? 1.0e-15 : CAlv * (24450.0 / MWTCE));
          CInhPPM = (ACh< 1.0e-15 ? 1.0e-15 : ACh/VCh*24450.0/MWTCE);
                    # CInhPPM Only used for CC inhalation
          CArt = (CArt < 1.0e-15 ? 1.0e-15 : CArt);
          CVen = (CVen < 1.0e-15 ? 1.0e-15 : CVen);
          CBldMix = (CArt+CVen)/2;
          CFat = (CFat < 1.0e-15 ? 1.0e-15 : CFat);
          CGut = (CGut < 1.0e-15 ? 1.0e-15 : CGut);
```

```
          CRap = (CRap < 1.0e-15 ? 1.0e-15 : CRap);
          CSlw = (CSlw < 1.0e-15 ? 1.0e-15 : CSlw);
          CHrt = CRap;
          CKid = (CKid < 1.0e-15 ? 1.0e-15 : CKid);
          CLiv = (CLiv < 1.0e-15 ? 1.0e-15 : CLiv);
          CLung = CRap;
          CMus = (CSlw < 1.0e-15 ? 1.0e-15 : CSlw);
          CSpl = CRap;
          CBrn = CRap;
          zAExh = (AExh < 1.0e-15 ? 1.0e-15 : AExh);
          zAExhpost = ((AExh - AExhExp) < 1.0e-15 ? 1.0e-15 : AExh - AExhExp);
# TCOH
          CTCOH = (CTCOH < 1.0e-15 ? 1.0e-15 : CTCOH);
          CBodTCOH = (ABodTCOH < 1.0e-15 ? 1.0e-15 : ABodTCOH/VBodTCOH);
          CKidTCOH = CBodTCOH;
          CLivTCOH = (ALivTCOH < 1.0e-15 ? 1.0e-15 : ALivTCOH/VLiv);
          CLungTCOH = CBodTCOH;
# TCA
          CPlasTCA = (CPlasTCA < 1.0e-15 ? 1.0e-15 : CPlasTCA);
          CBldTCA = CPlasTCA*TCAPlas;
          CBodTCA = (CBodTCA < 1.0e-15 ? 1.0e-15 : CBodTCA);
          CLivTCA = (CLivTCA < 1.0e-15 ? 1.0e-15 : CLivTCA);
          CKidTCA = CBodTCA;
          CLungTCA = CBodTCA;
          zAUrnTCA = (AUrnTCA < 1.0e-15 ? 1.0e-15 : AUrnTCA);
          zAUrnTCA_sat = (AUrnTCA_sat < 1.0e-15 ? 1.0e-15 : AUrnTCA_sat);
          zAUrnTCA_collect = (AUrnTCA_collect < 1.0e-15 ? 1.0e-15 :
AUrnTCA_collect);
# TCOG
          zABileTCOG = (ABileTCOG < 1.0e-15 ? 1.0e-15 : ABileTCOG);
          #  Concentrations are in TCOH-equivalents
          CTCOG = (CTCOG < 1.0e-15 ? 1.0e-15 : CTCOG);
          CTCOGTCOH = (CTCOG < 1.0e-15 ? 1.0e-15 : StochTCOHGluc*CTCOG);
          CBodTCOGTCOH = (ABodTCOG < 1.0e-15 ? 1.0e-15 :
StochTCOHGluc*ABodTCOG/VBodTCOH);
          CKidTCOGTCOH = CBodTCOGTCOH;
          CLivTCOGTCOH = (ALivTCOG < 1.0e-15 ? 1.0e-15 :
StochTCOHGluc*ALivTCOG/VLiv);
          CLungTCOGTCOH = CBodTCOGTCOH;
          AUrnTCOGTCOH = (AUrnTCOG < 1.0e-15 ? 1.0e-15 : StochTCOHGluc*AUrnTCOG);
          AUrnTCOGTCOH_sat = (AUrnTCOG_sat < 1.0e-15 ? 1.0e-15 :
StochTCOHGluc*AUrnTCOG_sat);
          AUrnTCOGTCOH_collect = (AUrnTCOG_collect < 1.0e-15 ? 1.0e-15 :
StochTCOHGluc*AUrnTCOG_collect);
# Other
          CDCVGmol = (CDCVGmol < 1.0e-15 ? 1.0e-15 : CDCVGmol);
          CDCVGmol0 = CDCVGmol; #(v1.2.3.2)
          CDCVG_NDtmp = CDFNormal(3*(1-CDCVGmol/CDCVGmolLD));
                    # Assuming LD = 3*sigma_blank, Normally distributed
          CDCVG_ND = ( CDCVG_NDtmp < 1.0 ? ( CDCVG_NDtmp >= 1e-100 ? -
log(CDCVG_NDtmp) : -log(1e-100)) : 1e-100 );
             #(v1.2.3.2)
          zAUrnNDCVC =(AUrnNDCVC < 1.0e-15 ? 1.0e-15 : AUrnNDCVC);
          AUrnTCTotMole = zAUrnTCA / MWTCA + AUrnTCOGTCOH / MWTCOH;
          TotCTCOH = CTCOH + CTCOGTCOH;
          TotCTCOHcomp = CTCOH + CTCOG; # ONLY FOR COMPARISON WITH HACK
          ATCOG = ABodTCOG + ALivTCOG; # ONLY FOR COMPARISON WITH HACK
# Misc
          CVenMole = CVen / MWTCE;
          CPlasTCAMole = (CPlasTCAMole < 1.0e-15 ? 1.0e-15 : CPlasTCAMole);
          CPlasTCAFreeMole = (CPlasTCAFreeMole < 1.0e-15 ? 1.0e-15 :
CPlasTCAFreeMole);

#**** Additional Dose Metrics ************************************************
#

          TotTCAInBW = TotTCAIn/BW;#(vrisk)

# Scaled by BW^3/4
          TotMetabBW34 = TotMetab/BW75;#(vrisk)
          AMetGSHBW34 = AMetGSH/BW75;#(vrisk)
          TotDoseBW34 = TotDose/BW75;#(vrisk)
          AMetLiv1BW34 = AMetLiv1/BW75;#(vrisk)
          TotOxMetabBW34 = (AMetLng+AMetLiv1)/BW75;#(vrisk)
          AMetLngBW34 = AMetLng/BW75; #(vrisk)
          ABioactDCVCBW34 = ABioactDCVC/BW75;#(vrisk)
          AMetLivOtherBW34 = AMetLivOther/BW75; #(vrisk)

# Scaled by tissue volume
          AMetLiv1Liv = AMetLiv1/VLiv; #(vrisk)
          AMetLivOtherLiv = AMetLivOther/VLiv; #(vrisk)
          AMetLngResp = AMetLng/VRespEfftmp; #(vrisk)
          ABioactDCVCKid = ABioactDCVC/VKid;#(vrisk)

#**** Fractional Volumes

          VFatCtmp = VFat/BW; #(vrisk)
          VGutCtmp = VGut/BW; #(vrisk)
          VLivCtmp = VLiv/BW; #(vrisk)
          VRapCtmp = VRap/BW; #(vrisk)
          VRespLumCtmp = VRespLum/BW; #(vrisk)
          VRespEffCtmp = VRespEfftmp/BW; #(vrisk)
          VKidCtmp = VKid/BW; #(vrisk)
          VBldCtmp = VBld/BW; #(vrisk)
          VSlwCtmp = VSlw/BW; #(vrisk)
          VPlasCtmp = VPlas/BW; #(vrisk)
          VBodCtmp = VBod/BW; #(vrisk)
          VBodTCOHCtmp = VBodTCOH/BW; #(vrisk)


};
```